IDENTIFICATION OF INTRACELLULAR SIGNALING PATHWAYS REGULATED BY THE TAO FAMILY OF MAMMALIAN STE20p KINASES

APPROVED BY SUPERVISORY COMMITTEE

Melanie H. Cobb, Ph.D.

Michael A. White, Ph.D.

Hongtao Yu, Ph.D.

Nicolai S.C. van Oers, Ph.D.

DEDICATED WITH LOVE TO APPUDU, AMMUDU, SHALU, MADHU, APPA, AMMA AND PULI

IDENTIFICATION OF INTRACELLULAR SIGNALING PATHWAYS REGULATED BY THE TAO FAMILY OF MAMMALIAN STE20p KINASES

by

MALAVIKA RAMAN

DISSERTATION

Presented to the Faculty of the Graduate School of Biomedical Sciences

The University of Texas Southwestern Medical Center at Dallas

In Partial Fulfillment of the Requirements

For the Degree of

DOCTOR OF PHILOSOPHY

The University of Texas Southwestern Medical Center at Dallas

Dallas, Texas

January 2006

ACKNOWLEDGEMENTS

I would like to thank my mentor Melanie Cobb for the past five years I have spent in this lab. Melanie has been incredibly supportive of both my academic and personal life. I have turned to her with many problems and she has always had help and advice to offer. She understood early on that I needed to be independent and work through problems myself. This often meant that I thought through and executed experiments in a round-about manner. She has patiently allowed me to learn from my mistakes but has always been there to offer an idea or word of advice that re-oriented me down the right path. The thing that I admire the most is her ability to mentor the individuals in the lab in a manner that is suited to their needs. It is a rare quality and is what sets her apart from everyone else. I have grown as both a scientist and a person by observing her.

I am incredibly grateful to my thesis committee: Michael White, Hongtao Yu and Nicolai S.C. van Oers. They taught me the importance of questioning the biological relevance of a problem at a time when I was perhaps too involved in minor and un-important details. This past year they have provided greater insight into my work and have offered ideas that helped me successfully complete my thesis. They have been inspirational and wonderful role models.

I owe thanks also to Dr. Elliott Ross and his wonderful technician Jimmy Woodson. I lived in Elliott's lab for practically a year when I was working on the G-protein story. Elliott and Jimmy taught me many of the difficult G protein assays, but perhaps the most important thing I learned was not to be afraid of trying a new technique. Before working in the Ross lab, I would try to find the easiest way of doing an experiment, but now I realize the

importance of determining the correct approach to solving a problem. I would also like to thank Dr. Ron Taussig and members of the Gilman lab especially Dr.Susanne Mumby, for many reagents and advice. I was very lucky to have their expertise.

I am deeply grateful to the members of my lab both past and present for creating a wonderful atmosphere to work in. I would especially like to thank members of the window-less Antarctica: Gray, Fred (Frodo), Wei (Chairman), Lee (Hooner) and Sveta. We spent long hours together talking science and Tolkien. I would like to finally apologize to Lee and Wei for all those dreadful pranks I played on them and thank them for putting up with me. I hope we remain friends for many years to come.

I would like to thank my friends both in and out of graduate school. Vidya, because of whom I joined Southwestern, Tony D. for making my skin thicker, and Tony A. for good taste in music and movies and perhaps more importantly for being inquisitive about everything. My friends at Asha: Ramesh, Sumit, Vasu, Nikhil and Manisha for a welcome respite from graduate school.

Finally, I would like to thank my family. Words cannot express my gratitude but here goes! My parents and sister have been so incredibly supportive of everything I have done and have always encouraged me to do my best. They have sacrificed a great deal to educate me and I hope I have made them proud. I would also like to thank my husband's parents for their love and support. I am blessed to have them in my life. There are too many things that I have to thank my husband Madhu for-I would never have made it so far without his love and support. He has made the worst times seem bearable and has made me laugh like no one else. I am a better person because of him. Finally, our dog Puli - for unconditional love.

IDENTIFICATION OF INTRACELLULAR SIGNALING PATHWAYS REGULATED BY THE TAO FAMILY OF MAMMALIAN STE20p KINASES

Publication No. _____

Malavika Raman Ph.D.

The University of Texas Southwestern Medical Center at Dallas, 2006

Supervising Professor: Melanie H. Cobb, Ph.D.

Abstract: TAO1, 2 and 3 are a sub-family of mammalian Ste20p protein kinases. They have been shown to regulate activation of p38 MAPK by phosphorylating and activating MEK3 and 6. Little is known about the precise cellular roles for these TAO protein kinases, or whether they function together or individually within the cell. Recently, genome-wide screens have identified these protein kinases as important mediators of vital cellular processes such as proliferation and apoptosis. Determining the mechanisms that govern the activity of these protein kinases and the pathways that utilize them is of utmost importance

for understanding important aspects of cell signaling. My research focused on determining physiological stimuli that activated TAO protein kinases and the consequence of this activation on downstream signaling. This approach, in conjunction with two-hybrid screening led to the elucidation of two pathways that utilized TAO kinases. TAO2 interacted with $G\alpha_s$ and $G_{\beta\gamma}$ subunits in yeast two-hybrid screens. TAO2 phosphorylated $G\alpha_s$ on threonine 9 in the N-terminus, and this phosphorylation was inhibited when the α subunit was activated by GTPγS. TAO2 also interacted with $G_{\beta\gamma}$ in detergent-soluble membrane extracts from cells. At present, the biological significance of this interaction is unclear. I also showed that TAO1, 2 and 3 are activated significantly by agents that damage DNA. The kinetics of activation mirrors that of p38 MAPK. I subsequently demonstrated that over-expression of kinase-deficient TAOs inhibited the activation of p38 by UV and hydroxyurea. The relative contribution of MEK3 and 6 in the activation of p38 by these agents was also determined. Knockdown of TAO 1-3 protein levels by siRNA oligonucleotides against these protein kinases also mimicked the dominant-negative results. TAO kinases interact with one another and p38 and this may be one manner in which signaling is made selective and efficient. The UV-induced G2/M checkpoint is diminished when TAO kinase expression levels are reduced by siRNA. Finally we show that TAOs may be substrates of the ataxia telangiectasia mutated (ATM) and ATM and Rad50-related (ATR) DNA damage kinases, as activation of TAO2 is diminished in cells from a patient with AT, which do not express ATM. These findings show that TAO kinases regulate critical events in cell-cycle arrest by DNA damage by acting as intermediates in p38 activation by ATM/ATR.

TABLE OF CONTENTS

PUBLICATIONS

Sridhar, N., Babu, R.J., Gupta, CNVHB., **Raman, M.**, Sai Priya, S., and Veeranjaneyulu, A. (2000) Morphine withdrawal induced diarrhea and acetic acid induced abdominal constriction: animal models for the evaluation of the 5-HT3 ligands in the treatment of irritable bowel syndrome, Journal of Pharmacy Pharmacology Communications, *6 (11)*, 513-516.

Robinson, F. L., Whitehurst, A. W., **Raman, M.**, and Cobb, M. H. (2002). Identification of novel point mutations in ERK2 that selectively disrupt binding to MEK1. J Biol Chem *277*, 14844-14852.

Chen, Z., **Raman, M.**, Chen, L., Lee, S. F., Gilman, A. G., and Cobb, M. H. (2003). TAO (thousand-and-one amino acid) protein kinases mediate signaling from carbachol to p38 mitogen-activated protein kinase and ternary complex factors. J Biol Chem *278*, 22278-22283.

Raman, M., and Cobb, M. H. (2003). MAP kinase modules: many roads home. Curr Biol *13*, R886-888.

Zhou, T., **Raman, M.**, Gao, Y., Earnest, S., Chen, Z., Machius, M., Cobb, M. H., and Goldsmith, E. J. (2004). Crystal structure of the TAO2 kinase domain: activation and specificity of a Ste20p MAP3K. Structure (Camb) *12*, 1891-1900.

Raman, M., Qin, J., and Cobb, M. (2006). TAO kinases are required for the p38 MAPK mediated G2/M DNA damage checkpoint. (in preparation).

LIST OF FIGURES

LIST OF TABLES

LIST OF ABBREVIATIONS

ADAM	A disintegrin and metalloprotease
AKAP	A-kinase anchoring protein
ASK	Apoptosis signal regulated kinase
ATM	Ataxia telangiectasia mutated
ATR	ATM and Rad50 related
BRCA1	Breast cancer 1 early onset
BRCT	BRCA C-terminal
Btk	Bruton's tyrosine kinase
CNK	Connecter enhancer of KSR
CRIB	Cdc42/Rac-interactive binding
CSK	COOH-terminal Src kinase
CSM	Complete synthetic medium
DDR	DNA damage response
DSB	Double-strand DNA breaks
DVD	Domain for versatile docking
EGF	Epidermal growth factor
FACS	Fluorescence activated cell sorting
FAK	Focal adhesion kinase
FDA	Food and drug administration
FHA	Forkhead associated
GCK	Germinal center kinase

GPCR	G protein coupled receptor
KSR	Kinase suppressor of Ras
MAPK	Mitogen activated protein kinase
MAP2K	MAPK kinase
MAP3K	MAP2K kinase
MAP4K	MAP3K kinase
MDC1	Mediator of DNA damage checkpoint 1
MLK	Mixed lineage kinase
MMS	Methyl methanesulfonate
NBS	Nijmegen breakage syndrome
NCI	National Cancer Institute
NHEJ	Non-homologous end joining
NGF	Nerve growth factor
OSR1	Osmotic stress-responsive 1
PAK	p21 Activated kinase
PHD	Plant homeodomain
PI3K	Phosphatidylinositol 3 kinase
PIKK	PI3K-related kinase
Pyk	Proline-rich tyrosine kinase
RGC	Receptor guanylate kinase
RTK	Receptor tyrosine kinase
SAPK/JNK	Stress activated protein kinase/c-Jun NH2-terminal kinase

SH2/3	Src homology 2/3
SUMO	Small ubiquitin-like modifier
TAB	TAK binding protein
TAK	TGFβ-activated kinase
TAO	Thousand and one amino acid
TGFβ	Transforming growth factor β
TLR	Toll-like receptor
TNFα	Tumor necrosis factor α
WNK	With no lysine (K)

CHAPTER 1. INTRODUCTION

I. Overview of signaling through protein kinases

A. The Kinome

Since the discovery nearly half a century ago that reversible protein phosphorylation was a means of regulating protein function, intense study has been focused on protein kinases- the enzymes that orchestrate this reaction (Krebs and Fischer, 1955). The completion of the human genome has allowed the complete cataloguing of the kinome. This effort has identified more than 700 phylogenetically related protein kinases (71 of which were not previously identified). This family constitutes slightly less than 2% of the human genome, making it one of the largest gene families in our genome, equivalent to the G protein coupled receptor (GPCR) super-family (Figure 1-1) (Manning et al., 2002).

Most signaling in the eukaryotic cell involves protein kinases. These enzymes participate in functions that are fundamental to every cell such as metabolism, transcription, proliferation and apoptosis as well as programs that are unique to certain cell types such as motility. In regulating these processes, protein kinases can act as initiators or intermediates in an intracellular relay system that allows the cell to fine-tune its physiological state from moment to moment by rapidly perceiving and responding to stimuli. Protein kinase signaling is often studied in isolation as a linear cascade where phospho-relays serve to amplify and propagate an extra- or intracellular cue, as is usually the case in mitogen activated protein kinase (MAPK) cascades. *In vivo* however, the cell is constantly bombarded with a multitude of signals at the same time. How then is this vast message space decoded and how are unique responses generated? Mechanisms have evolved to meet requirements of signaling fidelity

and encoding complexity by interconnecting a limited set of components into a dense network such that a small perturbation at one end of the network can be rapidly propagated to diverse pathways. A prime example of this cross-connectivity is the ability of G-protein coupled receptors (GPCRs) to transactivate receptor tyrosine kinases (RTKs) via the G protein-stimulated cleavage of an inactive membrane bound ligand for a RTK (Wetzker and Bohmer, 2003). A number of groups have begun to address how interconnected the signaling network is by carrying out genome-wide analyses of interconnectivity between proteins and signaling pathways in model organisms such as *C.elegans* and *S.cerevisiae* (Gavin et al., 2002; Li et al., 2004; Rual et al., 2005). These large datasets suggest that the network connectivity is not evenly distributed among all proteins, rather there exist "nodes" within the matrix where information flow is dense and other areas are sparsely connected. This indicates that a fraction of proteins are essential hubs for signal processing and eliminating them would have profound effects on cell viability. Similar studies have been carried out in mammalian systems with comparable conclusions (Stelzl et al., 2005) (Figure1-2). From these studies a more global picture of signaling cross-talk in the cell will become apparent.

B. Classification of protein kinases

In 1988, the first systematic classification of the eukaryotic protein kinase super-family based on all available sequences was undertaken (Hanks et al., 1988). Based solely on the amino acid sequence similarity between the protein kinase domains, four protein kinase families were created. These included the (a) AGC kinases so called for the cyclic-nucleotide family e.g., protein kinase A and G(PK**A** and PK**G**) and protein kinase C (PK**C**) as well as

the β-adrenergic receptor kinase family (βARK) and the ribosomal S6 kinases; (b) CaMK family consisting of kinases regulated by calcium and calmodulin as well as members of the AMPK family; (c) CMGC which included the **c**yclin-dependent kinases, **M**APK, **g**lycogen synthases, the **c**asein kinase II family and the Cdk-like (Clk) family; (d) TK including all conventional protein tyrosine kinases. A more recent analysis of the human genome led to the expansion of this classification to include four new families. This includes the (a) STE family consisting of all Ste7/MAP2ks, Ste11/MAP3Ks and Ste20p/MAP4Ks; (b) CK1 family consisting of CK1, tau tubulin kinase (TTBK) and vaccinia related kinase (VRK) families; (c) TKL (tyrosine kinase like) which includes both tyrosine and serine/threonine kinases such as mixed lineage kinase (MLK) etc; and finally (d) RGC (receptor guanylate cyclase) members that have kinase domains similar to tyrosine kinases (Manning et al., 2002) (Figure 1-1).

One of the key observations from the kinome data and human genome sequencing was the number of protein kinases that were associated with disease loci. A total of 164 protein kinases were found at tumor loci and an additional 80 were mapped to other disease-related loci. This begs the question, what functions do these protein kinases carry out in tumorigenesis and disease. Another surprising finding was that about 10% of human protein kinases may be catalytically inactive due the absence of one or more catalytically conserved residues. In such cases, it has been speculated that these proteins act as scaffolds or modulate in some manner the protein kinase activity of other proteins.

However this doesn't mean that all protein kinases missing catalytic residues are inactive. For example, with the with-no-lysine-K (WNK) family members, the important

catalytic residues are positioned differently. The catalytic lysine that coordinates ATP is replaced by a cysteine. Further studies showed that the catalytic lysine was positioned elsewhere in the kinase domain and resulted in a functionally competent enzyme (Xu et al., 2000). Hence in cases in which the sequence predicts that the protein kinase is catalytically deficient, further studies are necessary.

C. Kinomics, clinical implications and future prospects

The identification and cataloguing of the human kinome has provided a launching pad for the analysis of protein phosphorylation in normal and disease conditions. It is now possible to identify and quantify protein kinase expression and phosphorylation states and their substrates in a rapid and high-throughput fashion. New technology is being developed to mine the kinome to identify potential therapeutic targets. Microarrayed compound screening (μ-ARCS) is one of many high-throughput screening platforms that allows thousands of test compounds to be arrayed on matrices over which gels containing assay reagents are overlaid. This methodology was used to identify inhibitors of caspase 3 and could easily be used to screen for protein kinase inhibitors (Gopalakrishnan et al., 2002). Such technologies have led to the synthesis of novel p38 MAPK inhibitors, such as BIRB796. BIRB796 shows remarkable selectivity for all p38 isoforms but not other MAPKs such as ERK1/2 (Pargellis et al., 2002). The above techniques are being used in conjunction with protein kinase-specific siRNA library screening to identify protein kinases that enhance or repress proliferation or apoptosis in cancer models (MacKeigan et al., 2005; Morgan-Lappe et al., 2005). High-throughput screens such as those discussed above should help

speed the discovery of novel inhibitors for protein kinases. That aberrant signaling is the underlying cause of those diseases is undisputed, yet <1% of the marketed drugs are kinase inhibitors and <3% are now in Phase I clinical trials (Vieth et al., 2005) (Figure 1-3). These small numbers can be attributed to lack of specificity in the currently available inhibitors. Most kinase inhibitors target the active site that is conserved in many protein kinases. However, new inhibitors are being developed by exploiting small differences in protein kinase sequence and structure. For example, the Taunton group has designed highly selective inhibitors that target a cysteine following the highly conserved G-x-G-x-x-G motif in the kinase domain (Cohen et al., 2005). This residue is a valine in most protein kinases, but in about 11 kinases it is replaced by a cysteine. Additionally, the group looked for a threonine in the ATP binding site (called a "gatekeeper" residue). The gatekeeper residue is a selectivity filter for many protein kinase inhibitors. Small residues such as threonine allow large moieties in drugs to enter deep into the pocket and inhibit ATP binding; whereas larger residues such as phenylalanine prevent access to the ATP binding site. This allowed the group to synthesize selective inhibitors to protein kinases that had a cysteine as well as the threonine. Out of the 11 kinases, only RSK1, 2 and 4 had the optimal positioning of residues in these two filters, which allowed for the synthesis of small molecule inhibitors that were selective for these kinases against all others (Cohen et al., 2005).

The Food and Drug Administration (FDA) in collaboration with the National Cancer Institute (NCI) have formed the Clinical Proteomics Program that aims at characterizing the activation or lack thereof of signaling pathways in patients (http://ccr.ncifcrf.gov/tech_initiatives/clinical_proteomics.asp). Using laser-capture micro-

dissection they have profiled the expression levels and the activation state of multiple proteins in normal and tumor tissues (Dunn, 2002). These and other initiatives are leading the way towards individualized treatment regimens for patients.

II. Regulation of protein kinases

A. Structure of protein kinases

Inappropriate activation of protein kinases (i.e. at the wrong place or time) is an underlying theme in many cancers. The activity of these enzymes is under multiple layers of regulation ranging from interaction with allosteric effectors to modulation of their localization. All protein kinases have an easily recognizable kinase fold characterized by two globular domains. The small upper N-terminal domain is composed of five β-strands and one α helix (helix C). The lower and larger C-terminal domain is predominantly α helical (Figure 1-5A). Protein kinases are often compared to switches with structurally distinct "on" and "off" states. The "off" or structurally open state has minimal activity within the cell and upon stimulation of elements upstream of the kinase, the "on" or structurally closed active conformation is adopted which will modulate downstream signaling components (Knighton et al., 1991). In some kinases however, phosphorylation doesn't necessarily induce closing of the N- and C-terminal domains. For example, in the crystal structure of the dually phosphorylated ERK2 MAPK, domain closure is not as exaggerated as in PKA (Figure 1-4) (Canagarajah et al., 1997). A structure-based overlay of the available active structures of serine/threonine and tyrosine protein kinases showed remarkable overlap between the N-terminal and C-terminal domains of these kinases. Only the activation loop (the site of

regulatory phosphorylation) showed diverse orientations. This overlay stresses the many different ways in which activation of protein kinases can be accomplished (Figure 1-6) (Nolen et al., 2004).

The alteration of downstream signaling is carried out by an identical reaction in all protein kinases, the transfer of the γ-phosphate of ATP to the hydroxyl group of a serine, threonine or tyrosine residue in substrates. The interface between the two domains serves as the platform on which the enzymatic reaction is catalyzed. ATP is bound deep in the cleft between the two domains, whereas substrate peptides bind in an extended conformation such that they are positioned close to the γ-phosphoryl group of ATP for efficient nucleotide transfer. The ATP molecule is optimally positioned and stabilized by the glycines in the G-X-G-X-ϕ-G (ϕ=tyrosine or phenylalanine) motif in the phosphate binding loop (P loop). In the absence of ATP, the glycines residues render the P-loop highly flexible. The peptide substrate binds to the protein kinase core and is stabilized by a stretch of 20-30 residues known as the activation loop (Figure 1-7). This region is easily identified in primary sequence as the residues residing between conserved tripeptide motifs D(F/L)G…APE. In the on (active) state of protein kinases, this activation loop is phosphorylated, which allows for a conformation that supports extended substrate binding. It is the activation loop that is structurally the least stable between different kinases (Figure 1-5B). The ends of this loop have the conserved D(F/L)G and APE motifs which are anchor points for the activation loop. The N-terminal anchor point is composed of the magnesium binding loop and β9. The D(F/L)G motif lies within the magnesium binding loop. This catalytic aspartate is critical for chelating two magnesium ions that positions the phosphates in ATP for phosphotransfer. The

phenylalanine in this motif makes contacts with residues in helix C that allows for proper orientation of a catalytically important glutamate in helix C. The β9 strand C-terminal to DFG forms an antiparallel β-sheet with β6 via three hydrogen bonds and this interaction is characteristic of the active state. In inactive protein kinases, this antiparallel sheet is not formed, disordering magnesium binding and the position of helix C. Another critical and invariant residue in the protein kinase domain is the catalytic lysine in the N-terminal domain which makes contacts with the α- and β-phosphates of ATP orienting them properly for catalysis. This lysine is usually buried in the cleft between the domains and maintained in the correct orientation by interaction with the glutamate in helix C mentioned above (Nolen et al., 2004 and Huse and Kuriyan 2002). At the C-terminal end of the activation loop is the P+1 loop, named for the interaction it makes with the P+1 residue on the substrate peptide (where P is the phosphorylated residue) (Figure 1-5B). The P+1 loop makes multiple other interactions with the substrate peptide and as such is critical in governing substrate specificity for the protein kinase. The sequence diversity within the activation/P+1 loop is thought to have evolved so that the cell may use the common protein kinase fold to achieve multiple biological functions. While major structural features are conserved among protein kinases, subtle differences in sequence and tertiary structure do exist. The residues on PKA that interact with the P+1 of the substrates are usually two leucines and a glutamic acid. The P+1 pocket as these residues are called accommodate large side chains such as those found in the P+1 site of PKA substrates. In contrast, in ERK2 the residues in the P+1 pocket (an alanine and two arginine residues) contribute the side chains that make up the pocket. Hence

ERK2 substrates do not have a bulky hydrophobic side chain (proline is the P+1 residue) (Cobb et al., 1996)

Apart from changes arising in the activation loop and propagating to other regions of the protein kinase such as helix C, activity can also be modulated from sites distant from the protein kinase core. Substrates and activators of protein kinases bind not only to the activation loop but also to a number of other surfaces on the protein kinase. This has been demonstrated in MAPK cascades. These are three tier cascades - the first protein kinase in the cascade the MAP kinase kinase kinase (MAPKKK or MA3K or MEKK), once activated, will dually phosphorylate the MAP kinase kinase (MAPKK or MAK2K or MEK) on two sites within the activation loop. MEKs will then phosphorylate and activate the final protein kinase, the MAP kinase (MAPK). MAPKs have a docking groove and acidic common docking (CD) and Glu-Asp (ED) pockets which are distinct from their active sites (Chang et al., 2002; Tanoue et al., 2000). These regions are used as additional binding elements in interaction with regulators and substrates. Complementing these MAPK motifs, many of the proteins they interact with – MAPK substrates, MAP2Ks, phosphatases and scaffolds – have a docking (D) domain, composed of basic and hydrophobic residues (Yang et al., 1998) (Figure 1-8). The crystal structures of p38 MAPK bound to peptides, based on the D domains of the p38 activator MKK3b and a substrate MEF2A, show that both D domains bind to the same docking groove on p38. The binding of the D domain peptides causes distinct conformational changes in p38, leading to the hypothesis that activators and effectors use the same site on a MAPK to regulate the enzyme in different ways (Chang et al., 2002). A conserved docking site named the DVD domain (**d**omain for **v**ersatile **d**ocking) has been

identified in multiple MAP2Ks which is required for efficient binding of MAP2Ks with their upstream counterparts the MAP3Ks (Takekawa et al., 2005).

B. Post-translational modification of protein kinases

Protein kinase activity is regulated by multiple means, but the predominant mechanism is by phosphorylation of one or more residues in the activation loop. Phosphorylation causes large rearrangements of the loop and causes it to be oriented in a manner that enhances substrate binding. In some protein kinases, a secondary site of phosphorylation is also present either upstream or downstream of the primary site, and phosphorylation at this second site may have additional unique roles in regulation of activity depending on the kinase. For example, the MAPKs ERK1/2 are dually phosphorylated, and phosphorylation at the second site increases activity by up to 1000 fold compared to the singly phosphorylated form of the protein. The dually phosphorylated form of the protein is required for full kinase activity (Prowse and Lew, 2001; Robbins et al., 1993; Zhang et al., 1995). Phosphorylation not only enhances kinase activity but it also controls other regulatory mechanisms such as dimerization. For example, phosphorylation of ERK2 causes a conformational change in the C-terminal extension that is unique to these enzymes. The loop binds near the N-terminal domain close to helix C and exposes a hydrophobic surface that facilitates dimerization. Studies have shown that dimerization of active ERK2 enhances nuclear localization (Canagarajah et al., 1997; Khokhlatchev et al., 1998).

Another means by which protein kinase activation is regulated is through autoinhibition by a pseudosubstrate. A pseudosubstrate binds to the active form of the kinase

in a manner similar to the substrate (Figure 1-9A). A well studied protein kinase that is regulated by pseudosubstrate binding is the p21-activated kinase (PAK). A motif known as the inhibitory switch domain that resides N-terminal to the protein kinase domain binds to the active site cleft between the N- and C-terminal domains. This binding distorts the structure of the protein kinase domain and prevents nucleotide binding (Lei et al., 2000; Parrini et al., 2002). Pseudosubstrate inhibition is relieved by binding of an activated small G protein to PAK and causing disassociation of the inhibitory switch domain (Huse and Kuriyan 2002).

Perhaps the most direct way to inactivate most protein kinases is via protein phosphatases which dephosphorylate and return kinases to their inactive state. Protein phosphatases have looser substrate specificity than protein kinases in order to be able to regulate a greater number of substrates. Their function is governed by specific interaction partners, targeting subunits (e.g., the B subunit in protein phosphatase 2A [PP2A]), and subcellular localization. It is increasingly becoming apparent that phosphatases too are governed by many layers of regulation. Phosphatases themselves can be regulated by all the mechanisms that regulate protein kinases from phosphorylation to ubiquitin-mediated degradation.

The ubiquitin-proteasome system plays an important role in cellular homeostasis. Ubiquitination of signaling proteins is emerging as a powerful way in which kinase signaling can be manipulated as ubiquitination can control the duration of the signal, localization of molecules, and stability of signaling proteins (Figure 1-9B). For example, the role of ubiquitin modification in modulating the activity of the NF-κB pathway has been elucidated. Some protein kinases themselves act as E3 ligases- the molecules that conjugate ubiquitin on

to substrates demonstrating how multiple functionalities can be built into the protein directly. For example, the MAP3K (MEKK1) was demonstrated contains a PHD (plant homeodomain) domain in its N-terminus that bears strong sequence similarity to the canonical RING E3 ligases. This PHD/RING domain was shown to display E3 ligase activity towards ERK1 and 2 as well as MEKK1 itself providing efficient feedback inhibition of signaling (Lu et al., 2002). Monoubiquitination has also been shown to play a role in signaling via protein kinases. It has been shown that monoubiquitination regulates ERK1c, an alternatively spliced form of ERK1, which contains a stop codon resulting in a smaller protein that still retains kinase activity. Studies have shown that ERK1c is monoubiquitinated and targeted to the Golgi; in contrast ERK1 and 2 are not, even though the three kinases share a high degree of similarity (Aebersold et al., 2004). The method by which the ubiquitin-proteasome controls signaling in the cell is quite different from phosphorylation mediated signaling; for example, by altering the timing of signaling events. While the role of ubiquitination in the control of intracellular signaling is undisputed, more detailed studies are required to uncover which proteins are ubiquitinated and how this modification will influence signaling (Laine and Ronai, 2005).

The small ubiquitin related modifier 1 (SUMO1) also has key roles to play in cell signaling. Sumoylation of proteins is thought to regulate nuclear transport events. Recent studies have shown that the protein kinase activity of the MAP3K apoptosis signal regulating kinase 1 (ASK1) is regulated by interaction with SUMO without covalent modification (Lee et al., 2005). In *Dictyostelium*, the MAP2K MEK1 is covalently modified by SUMO and results in alteration of MEK1 activity and subcellular localization (Sobko et al., 2002).

Apart from the few post-translational modifications listed here it is easy to imagine that the slew of modifications that affect cellular proteins would also be utilized by the cell to regulate protein kinase activity. These include but are not limited to methylation, acetylation, nitrosylation, prenylation, glutathionylation, sulfonylation, glycosylation, etc. With the advent of techniques that will allow for efficient and sensitive capture of these alternative post-translational modifications, we can begin to systematically catalog their effects on the kinases and the pathways they control. It is important to realize that phosphorylation and signaling through protein kinase cascades represents one means by which signal transduction may be accomplished. The basic motif of signaling is information flow from a stimulus to an end effector via modification of a protein.

C. Protein interaction domains, scaffolds and spatiotemporal regulation of signaling

Many protein kinases phosphorylate multiple substrates and it is crucial that in response to any given signal only the subset of substrates that are required to bring about a response are activated. This additional layer of control is brought about by activating protein kinases in distinct cellular compartments, scaffolding different members of a pathway into pre-bound complexes (Figure 1-9C), and regulating interaction partners via modular domains.

The importance of a scaffolding protein that would enable components of protein kinase pathways to interact in discrete modules, so that signals can be propagated with specificity and speed was elaborated upon in the *S.cerevisiae* (Kranz et al., 1994; Marcus et al., 1994; Printen and Sprague-Jr., 1994). In the yeast pheromone-induced mating pathway,

activation of GPCR by the pheromone leads to downstream signaling via a conserved MAPK module. A MAP4K, Ste20p (identified in a screen for yeast mutants that were sterile), is recruited to $G_{\beta\gamma}$ dimers of activated heterotrimeric G protein at the membrane. Here, Ste20p activates the MAP3K Ste11p, which phosphorylates and activates the MAP2K Ste7p, which in turn phosphorylates and activates the MAPK homologs Fus3 and Kss1. The three kinases in the module are scaffolded together by interaction with the scaffold protein Ste5p (Figure 1-10) (Elion, 2000). Indeed, the importance of scaffolds is underscored by recent studies that show that specificities within pathways can be rewired by swapping out domains in scaffolds that reside in different pathways (Park et al., 2003). Subsequent to the identification of Ste5p, mammalian equivalents of these scaffolds have also been discovered. Such scaffolds include KSR (kinase suppressor of Ras), and MP1 (MEK partner1), both of which tether components of the ERK1/2 pathway and allow for a fast and selective response. KSR binds MEK constitutively and binds to ERK and Raf 1 in an inducible manner. What is interesting is that KSR itself is regulated by multiple phosphorylations and degradation (Matheny et al., 2004; Muller et al., 2001). Other scaffolds include CNK (connector enhancer of KSR), a multi-domain protein that has been proposed to scaffold proteins that may lie in four different pathways: ERK1/2 pathways, RASSF1A, Rho and certain cell polarity proteins (Kolch, 2005). All of these scaffolds provide a means by which a simple three-tier cascade like the MAPK pathway can be used pleiotropically within the cell. Additional complexity is created by regulating the scaffolds themselves, for example via phosphorylation or stabilization. Other proteins such as the A-kinase anchoring proteins (AKAPS) function similar to scaffolds (Figure 1-9D). AKAPS bind to the regulatory subunit of PKA as well as multiple

other targets in specific cellular compartments. In response to local increases in cAMP levels, the catalytic subunit of PKA is now optimally positioned so that its substrates can be quickly phosphorylated (Bregman et al., 1989; Colledge and Scott, 1999). PKA regulators such as PP2A have also been found in these AKAP complexes (Shih et al., 1999).

The use of scaffolds allows spatially restricted signaling to take place in small microdomains (e.g. in lipid rafts at the plasma membrane), but often it is necessary for multiple divergent pathways to be activated by a stimulus, e.g., changes in transcription, cell-cycle, cytoskeleton etc. The question of how limited numbers of signaling proteins are able to activate multiple signaling pathways is solved by permutation and combination of modular signaling domains. These are independently folding sequences that are capable of interacting with distinct motifs on other proteins. For example, assuming the cell has only ten discrete domains and a protein may have two such domains, the number of possible permutations of these domains in any given protein is nearly 100. If a protein may have all ten domains it can encode well over 3.5 million unique signals, assuming that the order in which these domains occur in a protein has negligible effect. New signaling domains are being discovered as more sequences are being analyzed with sophisticated sequence algorithms. At present about 46 such domains have been described (http://www.mshri.on.ca/pawson/domains.html). These include the PDZ domain which binds to peptides in the C-terminal regions of proteins; domains that recognize phospho-peptides like src-homology 2 (SH2), forkhead associated (FHA), breast cancer early onset 1 C-terminal (BRCT) and phospho-tyrosine binding (PTB), and others that bind to phosphoinositides like the pleckstrin homology (PH) domain. All these domains recognize small peptide or lipid-derived motifs in their binding partners. The

SH2 and PTB domains which bind phospho-tyrosine sequences, allow for regulated binding in the presence of signal. While phospho-tyrosine dependent interactions have been known to exist for nearly 15 years, domains that bind serines and threonines have also been identified more recently. The forkhead associated (FHA) domain and 14-3-3 proteins are such examples (Muslin et al., 1996; Sun et al., 1998). Since its identification, a number of nuclear proteins have been discovered to have FHA domains. Many of these proteins also harbor BRCT domains and take part in pathways that regulate responses to DNA damage (Durocher et al., 2000a). With an expanding repository of information and methods that can match particular domain combinations to selected functions, it is now possible to hypothesize the functions of an unknown protein merely by analyzing sequence information.

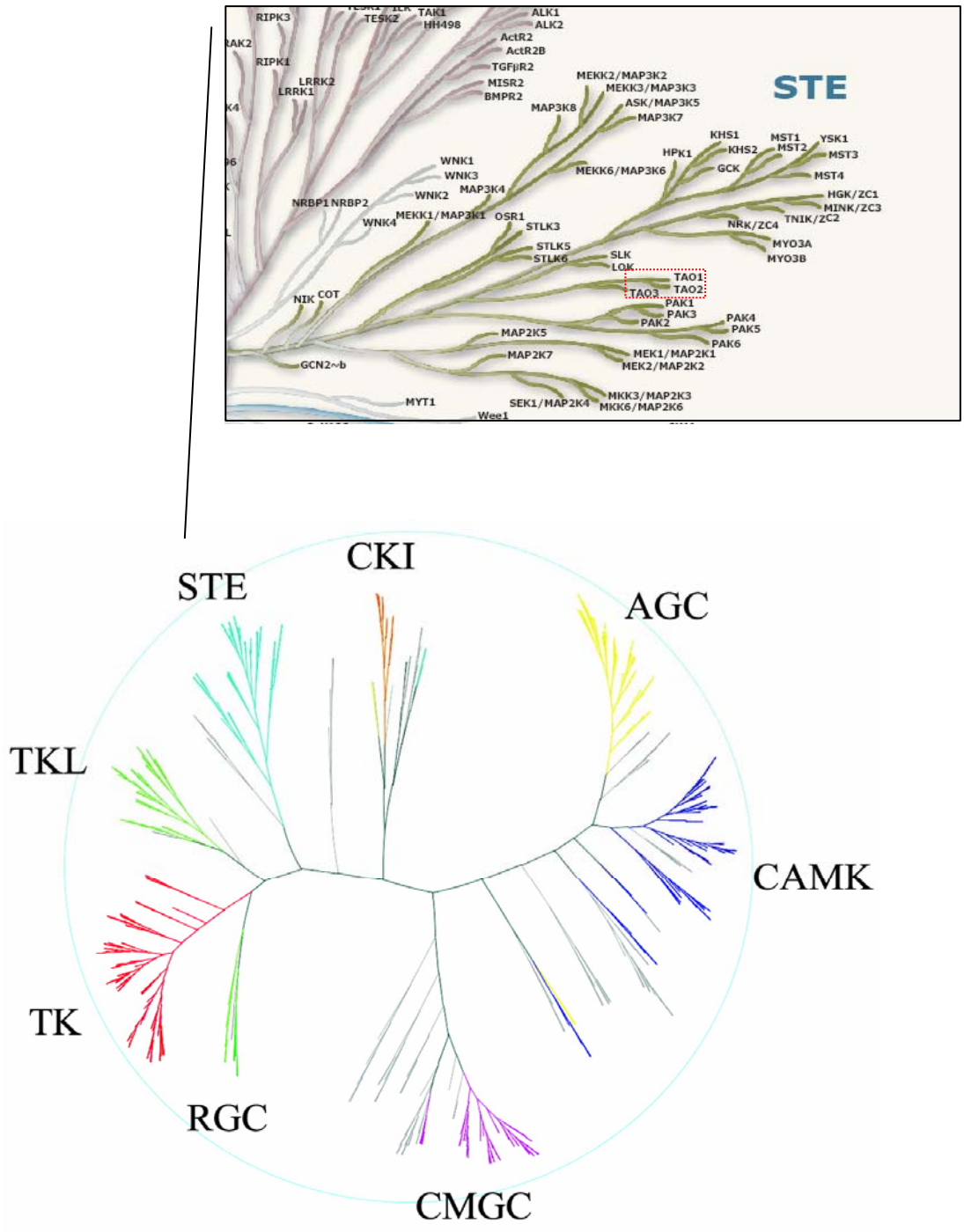

Figure 1-1. The Human Kinome. Dendrogram of 491 ePK domains from 478 genes. Inset shows STE family and position of TAO kinases (Modified from Manning et al., 2002). Reprinted from, Science, Vol 298, Manning et al., The protein kinase complement of the human genome 1912-1934, Copyright (2002), with permission from Elsevier.

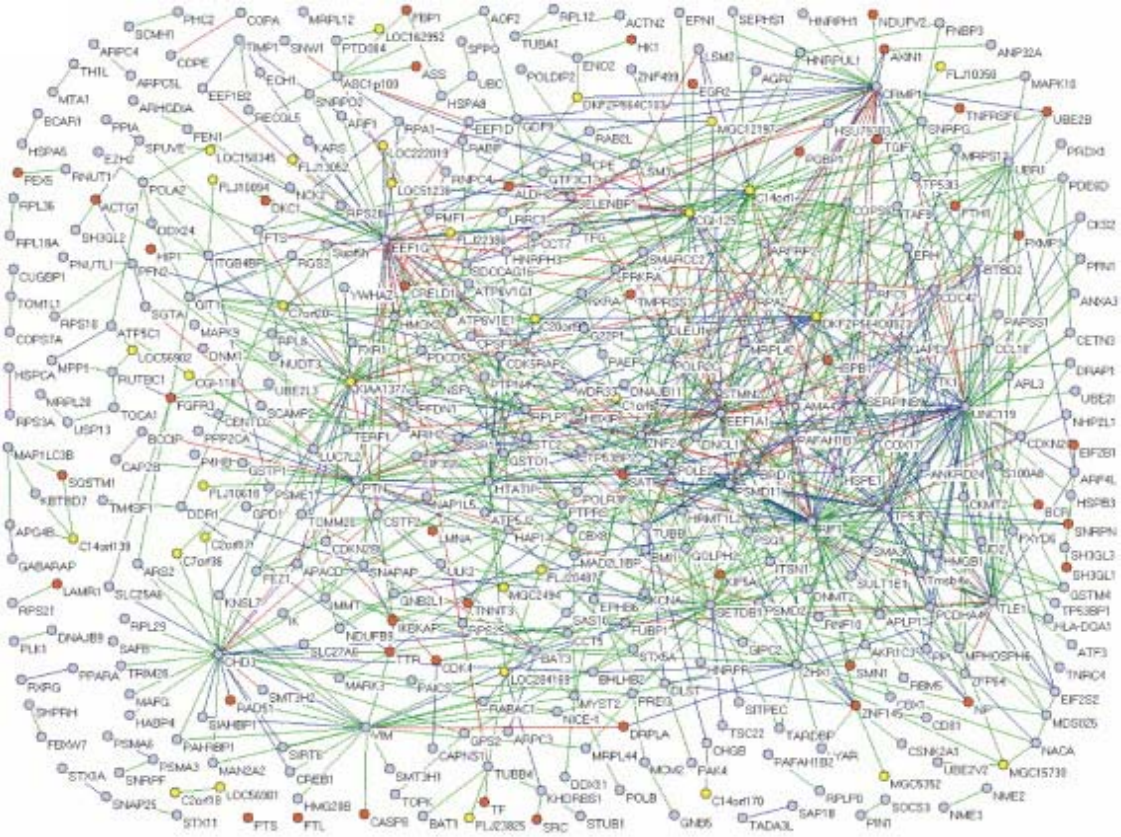

Figure1-2. Human protein-protein interaction network. A graph depicting the high confidence interaction network involving 401 proteins linked via 911 interactions. Interactions were determined by high-throughput yeast two-hybrid interactions. Note the uneven clustering of interactions on proteins in the network. Orange: disease proteins (according to OMIM morbid map, NCBI); light blue: proteins with gene ontology (GO) annotation; yellow: proteins without GO and disease annotation (From Stelzl et al., 2005). Reprinted from Cell, Vol 122, Stelzl et al., A human protein-protein interaction network: A resource for annotating the proteome, 957-968, Copyright (2005), with permission from Elsevier.

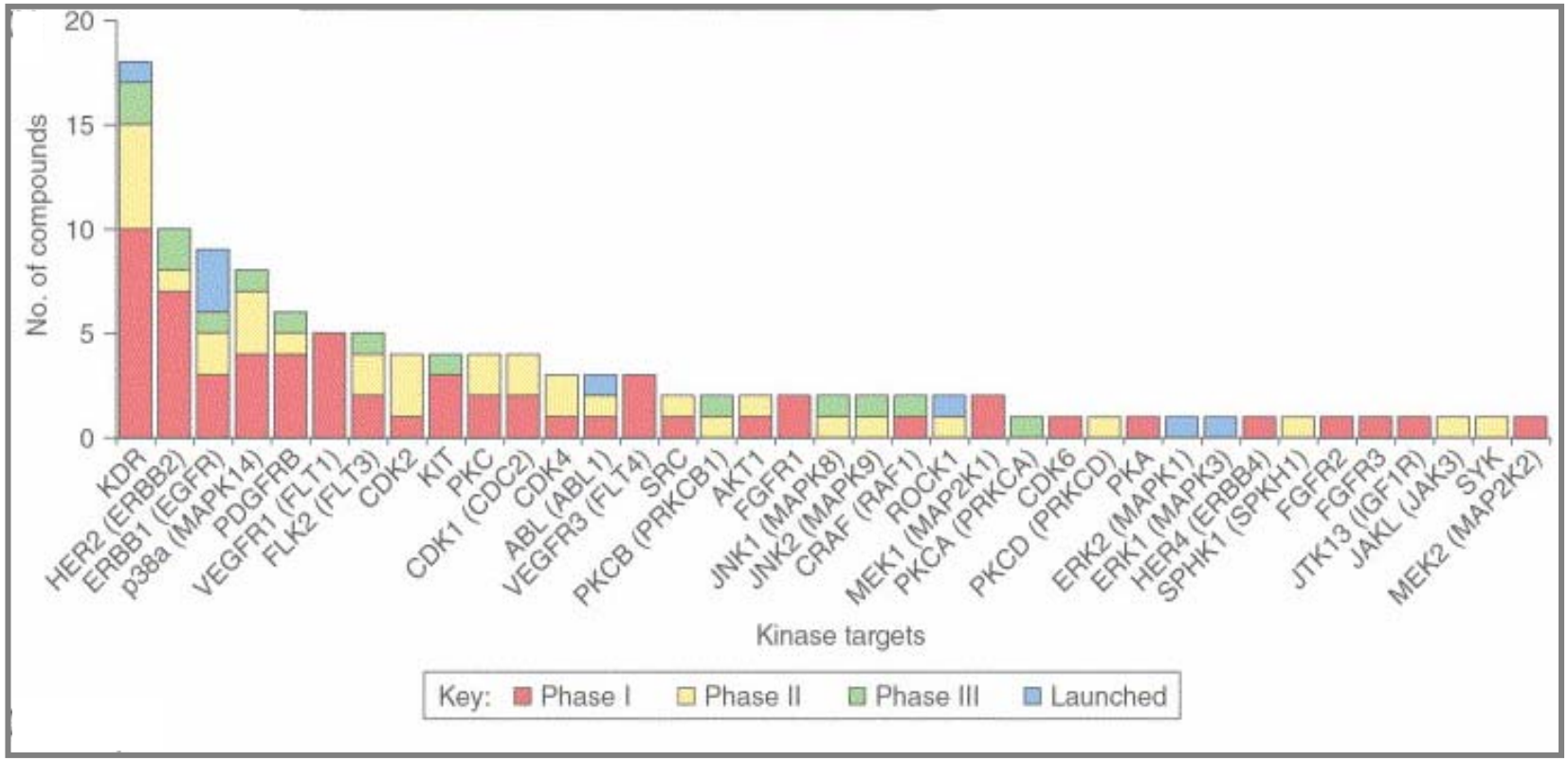

Figure 1-3. Kinase targets in clinical trials. Kinase targets pursued by 76 active clinical compoundsas of June 2005. PKC indicates typical isoforms of protein kinase C (a, ß1, ß2 and .). The number of compounds in each development stage is shown for each kinase target. KDR: kinase insert domain receptor/ vascular endothelial receptor 2 (VEGFR2) (From Veith et al., 2005). Reprinted from Drug Discovery Today, Vol 10, Vieth et al., Kinomics: characterizing the therapeutically validated kinase space, 839-846., Copyright (2005), with permission from Elsevier.

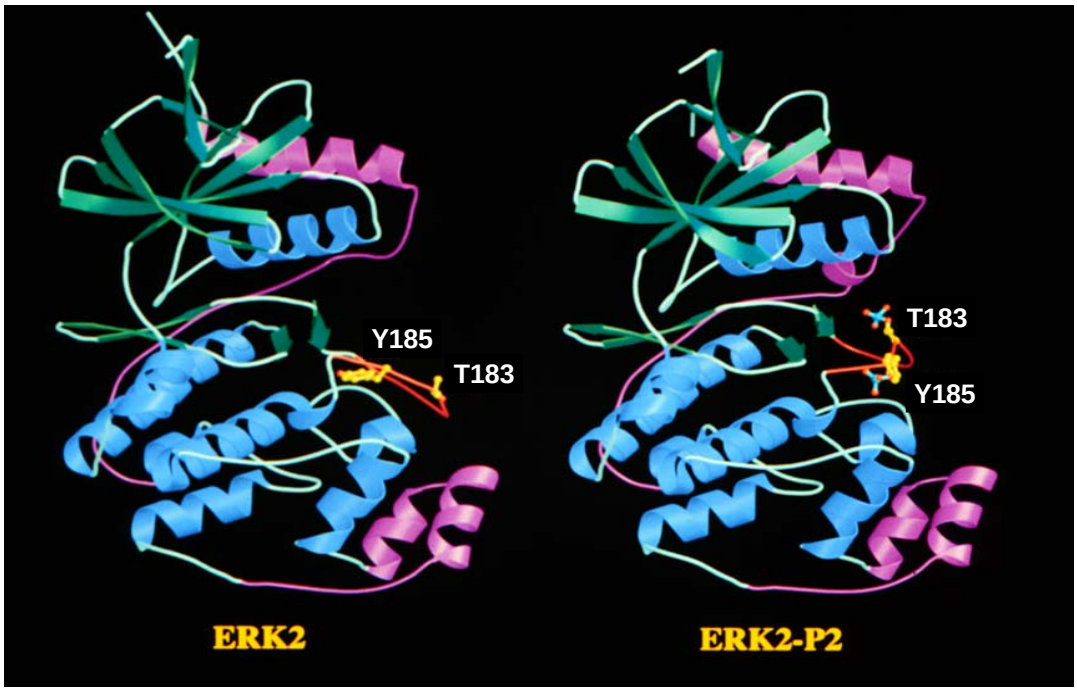

Figure 1-4. Crystal structure of ERK2. Low-activity and doubly phosphorylated ERK2 ribbon diagram of (A) Low activity, unphosphorylated ERK2 and (B) High activity, dually phosphorylated ERK2-P2 (From Canagarajah et al., 1997).

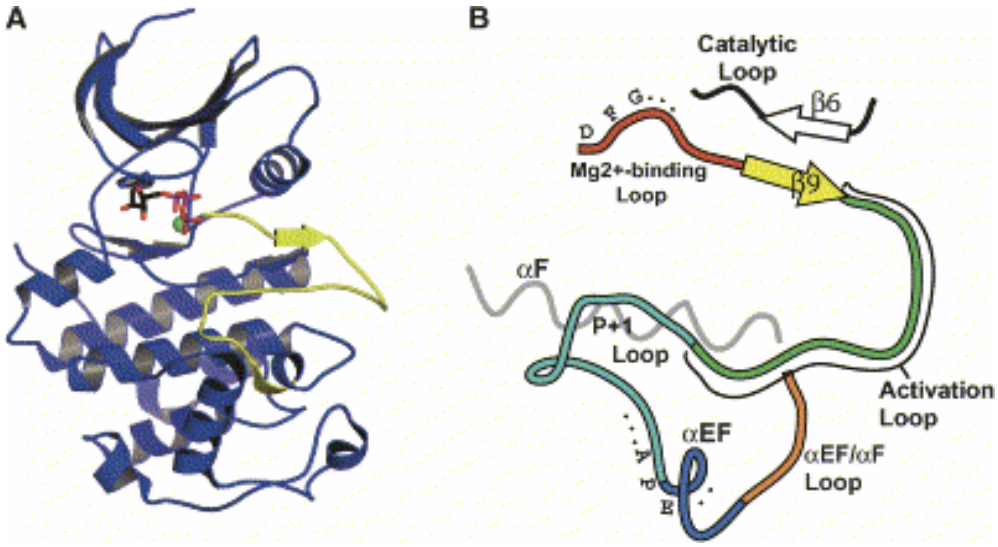

Figure 1-5. The activation segment of protein kinases (A) The structure of CDK2 showing the entire activation segment (yellow). (B) Detail of the elements that make up the segment: the activation segment starts with the conserved DFG in the magnesium binding loop and ends with the conserved APE in the P+1 loop including β9 and the activation loop (From Nolen et al., 2004). Reprinted from Molecular Cell, Vol 15, Nolen et. al, Regulation of protein kinases; controlling activity through activation segment conformation, 661-675, Copyright (2004), with permission from Elsevier.

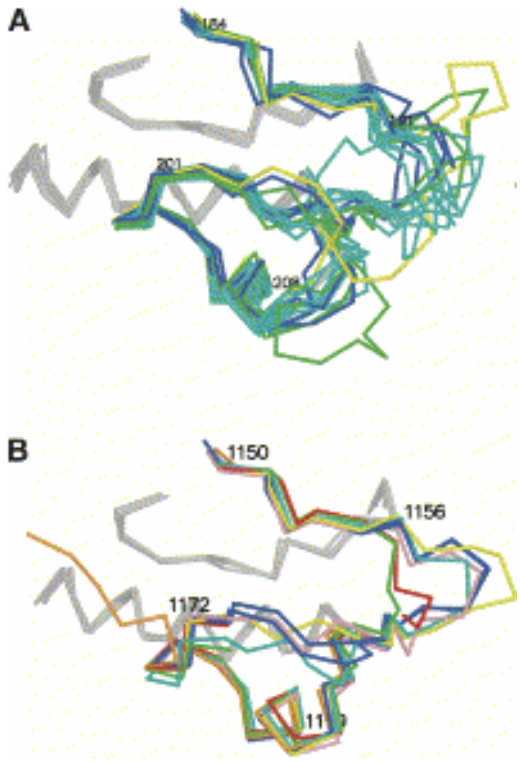

Figure 1-6. Activation segment overlays of serine/threonine and tyrosine protein kinases. (A) Superimposition of active Ser/Thr kinases showing the position of the activation segment. Note the non-overlap between activation segments from different protein kinase families. The families are colored according to the classification Manning et al., 2002. AGC, blue; CaMK, green; CMGC, cyan; CK1, yellow. (B) Similar overlays of active tyrosine kinases. Families are colored as: IRK and IGF1K, blue; LCK, cyan; EGFRK, yellow; CSK, green and red; c-KIT, pink. The catalytic loop and helix αF are gray in both Ser/Thr and tyrosine kinases (From Nolen et al., 2004). Reprinted from Molecular Cell, Vol 15, Nolen et.al, Regulation of protein kinases; controlling activity through activation segment conformation, 661-675, Copyright (2004), with permission from Elsevier.

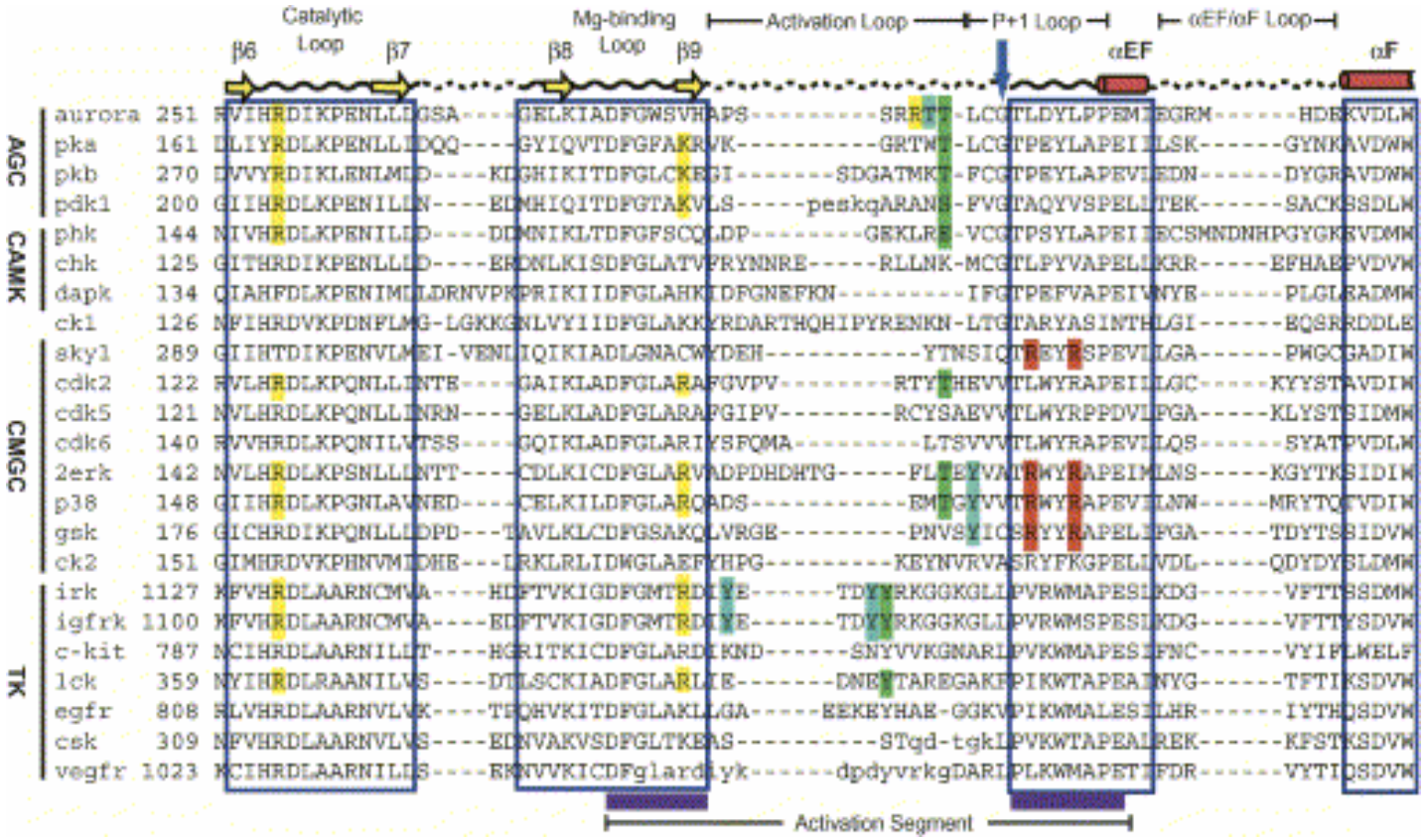

Figure 1-7. Sequence alignment of the activation segment of protein kinases. The secondary structure of the kinase core is indicated above the alignment. Dashed lined indicate sequence variance. Primary phosphorylation sites observed in the active crystal structures are boxed in green and the residues that contact the primary phosphate in yellow. Secondary phosphorylation sites are boxed in cyan. Residues that interact with primary phosphorylation sites are boxed in yellow. Residues of the basic pocket of CMGC kinases are boxed in red. The beginning of the P+1 loop is indicated by a blue arrow. The beginning and ends of the anchor points are shown below the sequence alignment (From Nolen et al., 2004). Reprinted from Molecular Cell, Vol 15, Nolen et al., Regulation of protein kinases; controlling activity through activation segment conformation, 661-675, Copyright (2004), with permission from Elsevier.

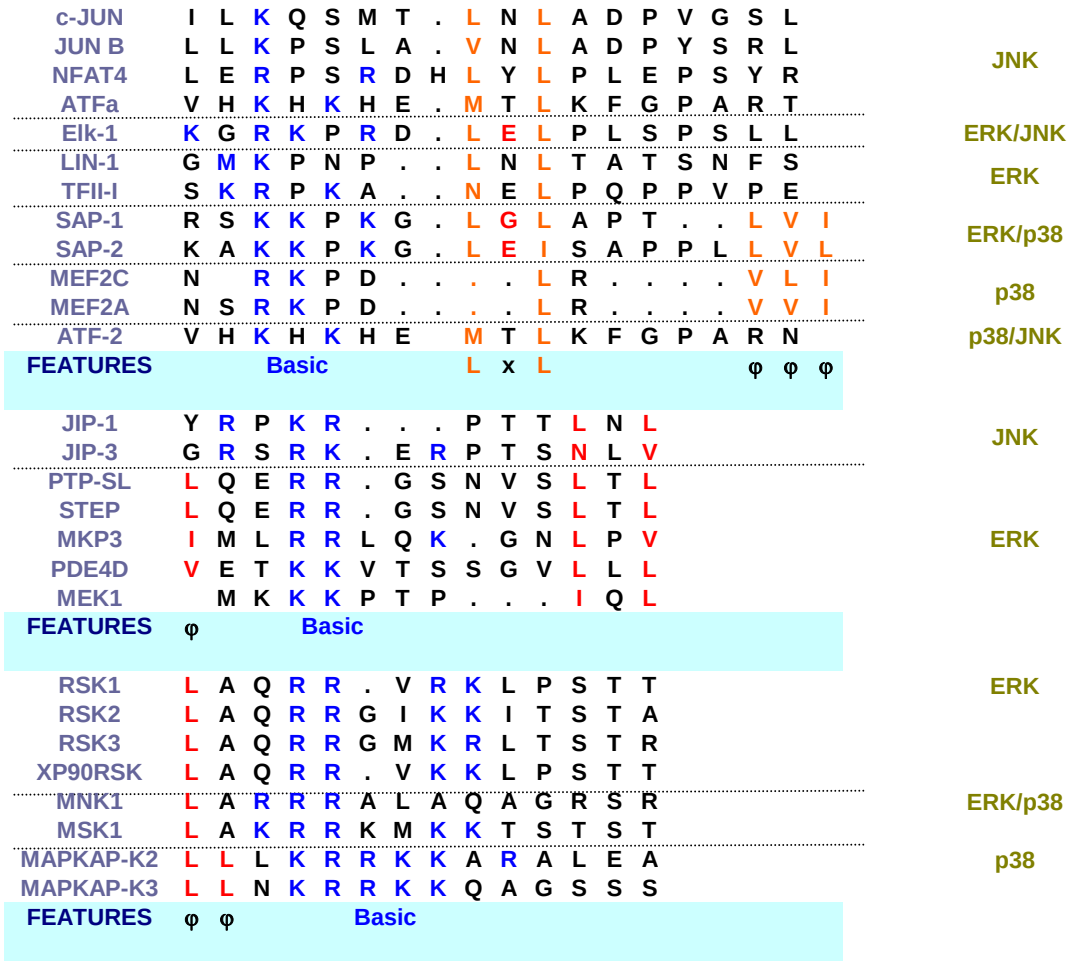

Figure 1-8. MAPK docking domains. Sequences of MAP kinase-docking domains found in transcription factors and other substrates. The kinases that interact with these domains have been shown to be targeted via the docking domain. Basic residues (blue) in the N-terminal end of the regions and conserved hydrophobic residues (red) are highlighted. φ represents a hydrophobic amino acid. Left hand column depicts kinases that interact with these domains (Modified from Sharrocks et al., 2000).

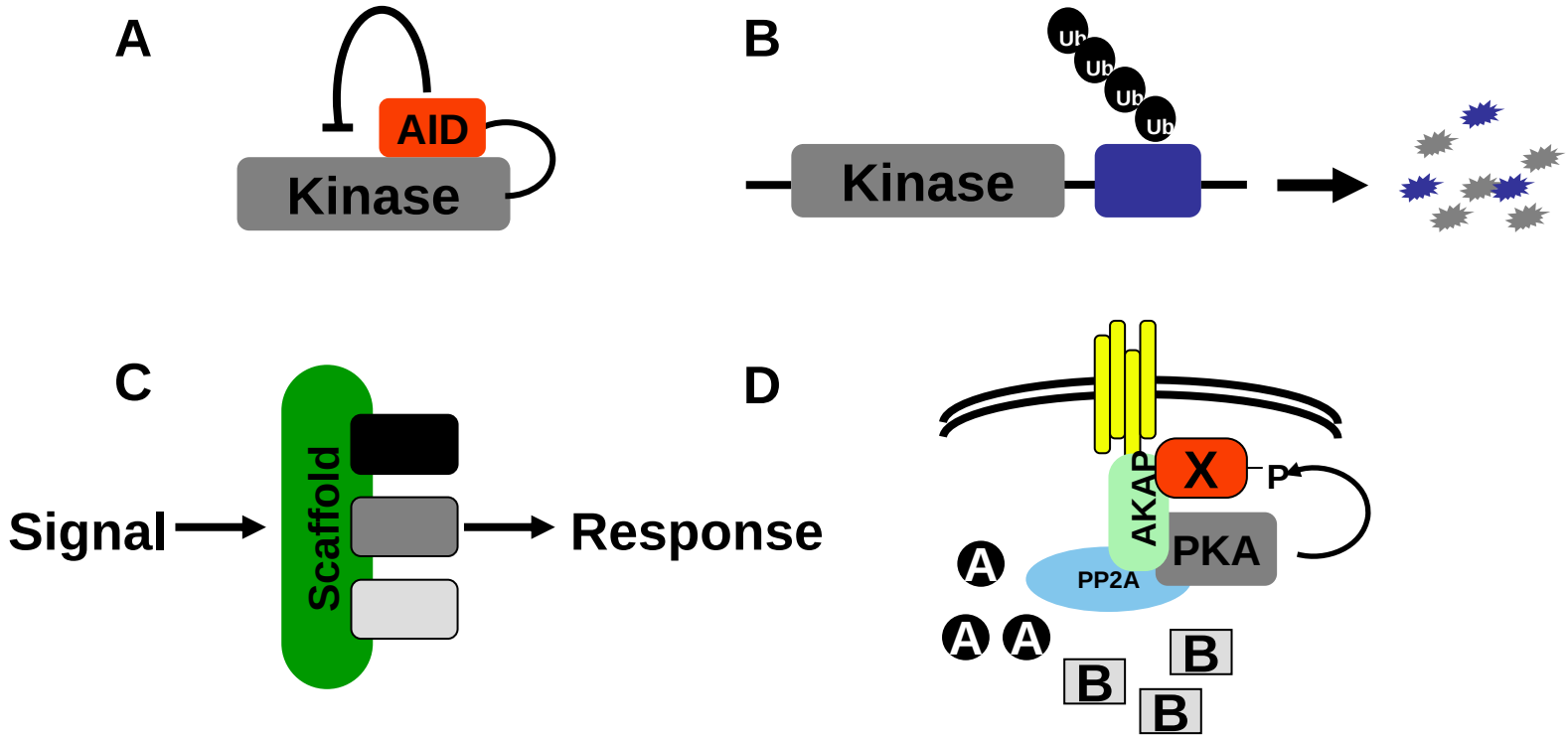

Figure 1-9. Regulation of protein kinase signaling by (A) autoinhibition or pseudo-substrate binding, (B) Ubiquitin-mediated proteosomal destruction, (C, D) spatial restriction via scaffolds e.g. Ste5p and AKAP. AID: Auto-inhibitory domain, Ub: Ubiquitin.

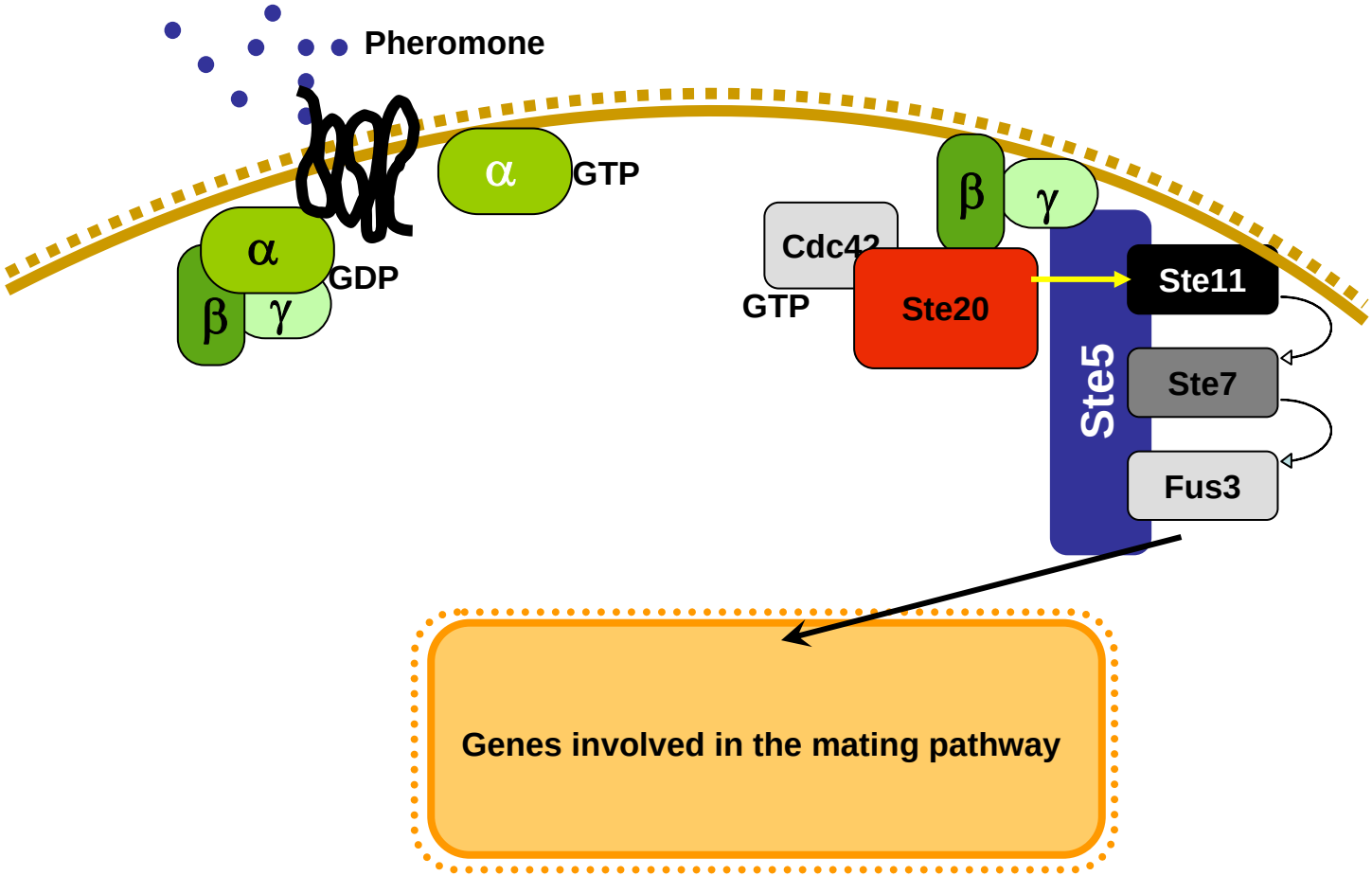

Figure 1-10. Mating MAPK cascade in *S. cerevisiae*. Pheromone binding to GPCR triggers release of $G_{\beta\gamma}$ subunit which recruits active Ste20p as well as the yeast MAPK module scaffolded by Ste5p.

CHAPTER 2. THOUSAND AND ONE AMINO ACID (TAO) KINASES

I. Biochemical properties of TAO kinases

A. Signaling via MAPK modules

MAPKs are among the best characterized signaling proteins within the cell. These enzymes propagate signals from a diverse array of stimuli and are capable of eliciting equally varied behaviors ranging from proliferation to apoptosis. The sequentially activated cascade is composed of three (sometimes four or five) protein kinases that are conserved from yeast through man. The first protein kinase in the cascade, the MAP Kinase Kinase Kinase (MAPKKK, MAP3K or MEKK), when activated phosphorylates and activates the MAP Kinase Kinase (MAPKK, MAP2K or MEK). MEKs are dual-specificity enzymes that phosphorylate the MAP kinase (MAPK) on T-X-Y motifs in the activation loop thereby activating it (Lewis et al., 1998). Dual phosphorylation of these amino acids activates the MAPK, which can either phosphorylate cytoplasmic substrates or translocate to the nucleus where it can phosphorylate and activate transcription factors. Three families of MAPKs have been identified: the extracellular signal regulated protein kinases, ERK1 and ERK2; c-Jun NH2-terminal kinases, JNK1, JNK2 and JNK3; and the p38 MAPKs, α, β, δ and γ. A handful of other MAPKs, including ERK5 and ERK3, have been discovered that are less well understood and may have divergent properties (summarized in Figure 2-1) (Chen et al., 2001). ERK1/2 were initially thought to respond to mitogenic signals to drive proliferation, but it has become apparent that these enzymes can be activated by a wide variety of stimuli

and regulate diverse cellular processes. JNK and p38 family members are also activated by a variety of agents but predominantly respond to cellular stress. Each of the MAPK families have at least two cognate MAP2Ks (except ERK5 which is activated only by MEK5) and multiple MAP3Ks. MAP2Ks display remarkable substrate specificity for their MAPKs; with several recognizing only one or two families of MAPK. In contrast, MAP3Ks have the capacity to activate multiple MAP2Ks, thereby activating multiple MAPK cascades. The multiple mammalian MAP3Ks may have arisen because mammalian cells must sense a panoply of ligands and hence have evolved multiple components sensitive to ligand subsets. The characterization of several MAP3Ks that have the capacity to activate MAPKs from more than one MAPK family has provoked a reconsideration of the cascade architecture. One possibility that would explain why there are multiple MAP3Ks for a single MAPK is that some ligands may stimulate a single MAP3K while other ligands may activate more than one MAP3K. This would provide a more complex response through both parallel activation of pathways and amplification of the signal in a pathway leading to a MAPK (Raman and Cobb, 2003).

One such validation for this hypothesis is from studies in *Drosophila* S2 cells where the relative contributions of MAP3Ks in the activation of the JNK pathway were determined (Chen et al., 2002). In these cells, loss of the transforming growth factor β (TGF β)-activated kinase (TAK1), a MAP3K, completely abrogated JNK activation by lipopolysaccharide. On the other hand, osmotic stresses used four MAP3Ks to activate JNK and loss of any one only partially reduced JNK activation. This is consistent with the observation that lipopolysaccharide acts predominantly through a single receptor, toll-like receptor 4 (TLR4),

while osmotic stresses conscript diverse mechanisms including growth factor receptor transactivation (Figure 2-2) (Cheng et al., 2002).

MEK1 and 2 display exquisite substrate specificity by only phosphorylating ERK1 and 2. These protein kinases have no other known substrates. MEK3/6 and MEK4/7 are also selective for their substrates, phosphorylating p38 and JNK, respectively (Kyriakis and Avruch, 2001). However, MKK4 can also activate p38 *in vitro*, but the physiological significance was unclear until recently. Brancho et al. (Brancho et al., 2003) re-examined the role of MKK3, MKK4 and MKK6 in p38 activation by different stimuli, using gene disruption and RNA interference (RNAi). Their studies revealed that, in spite of a differential requirement for MKK3 and MKK6, both were essential for activation of p38 by tumor necrosis factor α (TNFα). Intriguingly, they found that fibroblasts lacking both MKK3 and MKK6 showed residual UV-activation of p38 which was dependent on MKK4. This provided evidence for a physiological role of MKK4 in a p38 pathway.

Agents that engender global changes in cellular homeostasis, such as ultraviolet radiation (UV) and osmotic shock, may do so by harnessing multiple MAP2Ks and MAP3Ks in different pathways to generate a pleiotropic response. Consistent with stimulus-specific linkage of MAP2Ks to p38, the aforementioned study also showed that ligands which activate p38 use the upstream activators of p38 differentially to achieve the desired response. This feature is mirrored in the JNK pathway, where it has been shown that the JNK activators anisomycin and heat shock preferentially use MKK4 over MKK7 (Yang et al., 1997), but proinflammatory cytokines use predominantly MKK7 (Tournier et al., 2001).

With all the ligands tested, however, maximum activation required two MAP2Ks: MKK3 and MKK6 for p38, and MKK4 and MKK7 for JNK. The requirement for both MAP2Ks has been attributed to the selective recognition of individual phosphorylation sites by these MAP2Ks: *in vitro* MKK4 preferentially catalyzes phosphorylation tyrosine in the activation loop, while MKK7 phosphorylates threonine. The fact that these MAPKs are still activated in the absence of individual MAP2Ks suggests that either each MAP2K can catalyze both phosphorylations or that autophosphorylation contributes to activation. The predominant mode of MAPK activation is by dual phosphorylation by MAP2Ks on the activation loop sites. Nevertheless, MAP2K-independent activation has been reported for p38 via the TAK1 binding protein (TAB1) (Ge et al., 2002). TAB1 enhances p38 autophosphorylation in a stimulus-specific manner in the absence of MKK3 and MKK6 (Figure2-2). The activation of p38 by ischemia following myocardial injury, reportedly occurred by TAB1-induced p38 autophosphorylation (Tanno et al., 2003). Scaffolds may take a more active part in protein kinase activation than previously recognized. For example, the motor-binding protein TPX2 has been shown to promote activation of the Aurora A kinase by promoting its autophosphorylation (Eyers et al., 2003).

In conclusion, the above-cited studies provide insight into the myriad mechanisms that create specificity for the three kinase module. To summarize signals initiated by diverse extracellular ligands induce ligand-specific re-wiring of protein kinase components via scaffolding proteins and distinct binding motifs to produce signal-specific signal transduction cascades.

B. Mammalian Ste20p kinases

Ste20p is a MAP4K in the pheromone-activated mating pathway in haploid budding yeast. In response to pheromone binding to a G protein coupled receptor, the heterotrimeric G protein is activated. The disassociated $G_{\beta\gamma}$ dimer recruits two complexes to the cell surface. One contains Ste20p that has been activated by the small G protein Cdc42. The second is the MAPK module scaffolded by Ste5p. At the membrane, Ste20p phosphorylates and activates the MAP3K (Ste11p) which phosphorylates and activates the MAP2K (Ste7p). Activated Ste7p phosphorylates and activates the MAPK (Fus3). Activated Fus3 translocates to the nucleus where it modulates the transcriptional control of genes required for mating (Figure 1-10) (Elion, 2000). More than 30 mammalian homologs of Ste-20p have now been identified (in addition to homologs in *D.melanogaster* and *C.elegans*). In mammals, the Ste20p family has been divided into two main sub-families: the PAK and GCK families (Figure 2-3). Protein kinases belonging to either class can be identified by the location of the kinase domain in the protein. The PAK related protein kinases have the kinase domain in their C termini whereas the GCK related members harbor an N-terminal protein kinase domain. Apart from this feature, Ste20ps can be identified by the presence of a conserved peptide: VGTPYWMAPEV (or AGCKPYWMAPEV) located in subdomain VIII of the kinase domain (Dan et al., 2001). Despite the sequence conservation within the kinase domains, all Ste20p kinases have divergent N- or C-terminal domains. This difference may explain the ability of these enzymes to regulate diverse processes ranging from regulation of the cytoskeleton to apoptosis. Although Ste20p is a MAP4K, the mammalian homologs of Ste-20p can function either as MAP4Ks or MAP3Ks.

C. TAO kinases

Thousand and one amino acid kinase (TAO1) was originally cloned by PCR from rat brain cDNA in an attempt to identify mammalian homologs of the yeast MAP4K Ste20p (Hutchison et al., 1998). Subsequent studies identified two closely related kinases named TAO2 and TAO3 (Chen et al., 1999; Tassi et al., 1999). A single ortholog has been identified in both *C. elegans* and *D. melanogaster* (Berman et al., 2001). All three TAOs are ubiquitously expressed with highest expression in the brain. Within the cell, these enzymes are found predominantly associated either with membranes or within the nucleus (discussed in Chapter 4, Fig 4-14B). Sequence analysis of TAOs identified an N-terminal kinase domain and a long C-terminal domain. The kinase domains are 90% identical but the C-terminal tails are divergent and have only 30% identity (Figure 2-4). Unlike other Ste20p-related kinases such as PAK, TAOs do not contain a Cdc42/Rac-interactive binding motif (CRIB). The C-terminal domains of TAOs have a number of putative coiled-coil domains; TAO1 has two such regions, and both TAO2 and 3 have three coiled-coil domains each. These domains probably function as protein-protein interaction motifs. TAO2 has a stretch of 15 glutamic acid residues C terminal to the protein kinase domain that is not shared between TAO1 and TAO3. TAO2 also has hydrophobic motifs that may be putative membrane association domains. The protein kinase domain of TAO2 (residues 1-320) showed higher kinase activity *in vitro* compared to the full length protein, leading to the possibility that a region in the C terminus of the protein may function as an auto-inhibitory domain. Indeed, such a mechanism was observed for other Ste20p kinases such as PAK and is an important means of

regulation of enzyme activity. However, we have not been able to identify such a domain as C-terminal fragments failed to inhibit the activity of the kinase domain *in vitro* (Chen et al., 1999).

D. TAOs are MAP3Ks for the p38 MAPK

Our studies have indicated that TAO1 and 2 are MAP3Ks in the p38 MAPK signaling pathway. Overexpression and *in vitro* studies demonstrated that TAO1 directly phosphorylated and interacted with MEK3, and this activation led to enhanced phosphorylation of p38 (Hutchison et al., 1998). Similar results were obtained for TAO2 which phosphorylated both MEK3 and 6, the MEKs upstream of p38 (Figure 2-5 A and B). Little effect was seen on another stress-responsive MAPK - JNK (Chen et al., 1999). The MEK binding domain on TAO2 was mapped to the first coiled-coil in the C terminus (residues 314-451). A number of studies that aimed to determine pathways activated by TAO3 have led to conflicting results. Tassi et al., showed that TAO3 was a negative regulator of JNK MAPK activity in response to EGF stimulation (Tassi et al., 1999). In another study it was shown that TAO3 activated both ERK1/2 as well as JNK MAPK (Zhang et al., 2000). However these studies were done with over-expressed MAPK components which may explain the different results.

The functional requirement for TAO kinases is less clear. All TAOs are activated by high osmolarity agents that elicit p38 activation such as sodium chloride and sorbitol (Chen and Cobb, 2001). However these stimuli are global activators of intra-cellular signaling and activate many signaling pathways and certainly many MAP3Ks. Specific roles for each TAO

kinase have not been clearly demonstrated. It has been shown that TAO2 may play a role in the regulation of the cytoskeleton as it was able to co-localize with both the actin cytoskeleton and with microtubules. Micro-injection of TAO2 caused marked changes in cellular morphology and the actin cytoskeleton. Cells became rounded and there was a decrease in the amount of stress fibers. This phenotype was dependent on TAO2 kinase activity (Moore et al., 2000). In another study, over-expressed TAO2 was shown to co-localize with microtubules and bound to tubulin *in vitro*. Unlike the previous study, the association was independent of kinase activity and could be inhibited by treating cells with taxol (an agent that prevents microtubule depolymerization)(Mitsopoulos et al., 2003). We have also shown that TAO2 is an intermediate in the signaling pathway initiated from G protein coupled receptors to p38 MAPK. Treatment of cells with the $G\alpha_o$- agonist carbachol led to enhancement of TAO2 kinase activity, and dominant negative TAO2 inhibited $G\alpha_o$-mediated activation of p38 (Chen et al., 2003). Hence TAO2 maybe the upstream kinase required for signaling from GPCRs to p38 MAPK (Figure 2-6B).

TAO1 may have a similar role as TAO2 in regulation of microtubule stability. TAO1 was identified as the kinase that phosphorylated microtubule affinity regulating kinase (MARK) in brain extracts. MARK phosphorylates microtubule-associated protein (MAP) and tau (a neuronal microtubule-associated protein that when aggregated causes Alzheimer's disease). Phosphorylation of tau or MAPs on the serine residue within the KXGS motif caused these proteins to dissociate from the microtubules and led to the destabilization of the microtubule network. TAO1 phosphorylated MARK in the activation loop and enhanced its kinase activity (Figure 2-6A). This study also showed that cells over-expressing TAO1 had a

disrupted microtubule network and this phenotype was dependent on TAO1 kinase activity. TAO1 knock-down by siRNA in nerve growth factor (NGF) treated PC12 cells led to decreased neurite elaboration, underscoring the importance of TAO1 regulation of microtubule organization in neuronal cells (Timm et al., 2003). TAO1 mRNA levels were increased significantly in analysis of genes up-regulated in Schwann cells over-expressing the transcription factor Egr2. Mutations in Egr2 have been identified in patients with neuropathies (Nagarajan et al., 2001). Complementing these results in an organismal context, TAO1 was identified as an enhancer of tau neuropathy in a *Drosophila* screen.

In contrast to TAO1 and 2, TAO3 appears to have a critical role in the regulation of cell viability. Two separate siRNA screens identified TAO3 as a major survival kinase (Aza-Blanc et al., 2003; MacKeigan et al., 2005). TAO3 was identified as a negative regulator of apoptosis in a screen for modulators of TNF-related apoptosis inducing ligand (TRAIL)-induced apoptosis. Knock-down of TAO3 sensitized cells to TRAIL-induced apoptosis as well as enhancing cell death in untreated cells (Aza-Blanc et al., 2003). In a similar study, TAO3 was identified again as a protein kinase required for cell survival, and siRNA of TAO3 sensitized cells to cell death caused by chemo-therapeutic agents via the activation of caspases (Figure 2-6C) (MacKeigan et al., 2005). While these studies did not provide the mechanism by which TAO3 mediates cell survival, other studies indicate that it may be through the ability of TAO3 to interact with the protein TRAF2. Yoneda et al. demonstrated that TAO3 enhanced the interaction between TNFα-Receptor Associated Factor 2 (TRAF2) and inositol requiring enzyme (IREα) to activate JNK signaling in response to ER stress. The TAO3-TRAF2 interaction also resulted in the activation of caspase 12 (Yoneda et al., 2001).

Although detailed characterization of the mechanism by which TAO protein kinases bring about the above phenotypes is absent, it is clear that TAOs are critical for many important cellular processes through their ability to activate either p38 or other signaling pathways that are still unknown.

II. Maintaining Genomic Integrity

A. The DNA damage response

Cellular DNA is constantly challenged to maintain its integrity against insults arising during normal cell metabolism and specific DNA damaging agents. It is estimated that for a mammalian cell, the base loss due to spontaneous hydrolysis of DNA glycosyl bonds is on the order of 10^4 events per day (Lindahl and Nyberg, 1972). Eukaryotic cells have evolved multiple mechanisms to detect and repair damaged DNA. This is a critical process without which potentially deleterious mutations will be passed on to daughter cells. The discovery that cells have mechanisms to survey chromosome stability, came from observations that cells treated with ionizing radiation ceased to progress through the cell cycle. These results were followed by screens in yeast to identify the molecular components that resulted in cell cycle arrest. From these studies it was determined that the cell cycle arrest was merely one aspect of what is now termed the DNA damage response (DDR). DDR is a series of events that starts with detection of the DNA lesion, followed by the initiation of numerous signaling cascades that result in cell cycle arrest, activation of DNA repair, maintenance of genomic stability, and in cases where the damage cannot be repaired, the cells will either permanently block cell cycle progression (cellular senescence) or initiate apoptosis (Figure 2-7) (Zhou and

Bartek, 2004). Central to the DNA damage response are the phosphatidyl inositol 3-kinase-related kinases (PIKK) - ataxia telangiectasia mutated (ATM) and ataxia telangiectasia and Rad3-related (ATR). These two kinases regulate all aspects of the damage response from sensing the initial damage to inducing apoptosis if necessary. Ataxia telangiectasia (AT) is a rare childhood disease in which patients lack the ATM protein. Individuals with AT are extremely sensitive to ionizing radiation (IR), have chromosomal breakages, and show checkpoint defects. They are characterized by progressive cerebellar ataxia, oculo-cutaneous telangiectasias (spider-like veining), immune deficiencies, gonadal atrophy, premature aging, radiation sensitivity, and an increased predisposition to cancers (Bakkenist and Kastan, 2004). Prognosis is poor and most individuals die in their early twenties. There is currently no cure for AT. In contrast to ATM, ATR knockout mice are embryonic lethal indicating that this kinase, unlike ATM, may have a more general role as a sensor for cellular integrity (Brown and Baltimore, 2000; O'Driscoll et al., 2003). Mutations in ATR that reduce ATR protein levels have been identified in Seckel syndrome (O'Driscoll et al., 2003). These patients are characterized by intrauterine growth retardation, dwarfism, and mental retardation. Current studies support the notion that ATM is the protein kinase that detects and responds to double strand DNA breaks (DSBs) that result from exposure to IR. In contrast, ATR is primarily activated by replication stressors such as UV radiation (that causes pyrimidine dimers and bulky base products) and antimetabolites like hydroxyurea (HU) that inhibit ribonucleotide reductase and hence deplete the nucleotide pool (Table 2-1) (Sancar et al., 2004). Given the many types of DNA lesions that occur in the cell, it remains unclear

whether there are distinct sensors for each type of lesion or if the damage is converted to a common intermediate that is detected by a single molecule.

B. Molecular mechanism of DDR

Cells respond to even small doses of IR (as low as 0.5Gy) by rapid activation of ATM within a few minutes of treatment. Inactive ATM resides as a dimer or as a higher order multimer bound to DNA. In response to double strand breaks (DSBs) that generate free DNA ends, ATM undergoes inter-molecular phosphorylation on serine 1981. This phosphorylation relieves the inhibition and renders ATM active and causes it to dissociate into monomers. Once activated, ATM translocates to the DSB sites marked by phosphorylated Histone H2AX (γH2AX), and rapidly phosphorylates a host of substrates (Andegeko et al., 2001). Full activation of ATM requires the Miotic Recombination11 (Mre11)-Rad50-Nijmegen breakage syndrome 1 (Nbs1) (MRN) complex. This complex is required for sensing DSBs (Lee and Paull, 2004). The MRN complex is implicated in the repair of DSBs by non-homologous end joining (NHEJ) and homologous recombination (HR). Mutations in Mre11 and Nbs1 cause an AT-like disorder (ATLD) and Nijemegen Breakage syndrome (NBS) respectively. ATLD is characterized by cerebellar degeneration, immune deficiency, mental deficiency, sensitivity to IR, and cancer predisposition. NBS patients suffer from microcephaly rather than ataxia (Bakkenist and Kastan, 2004). Interestingly, Nbs1 is also phosphorylated by ATM in response to IR, which leads to further activation of ATM in a positive feedback manner (Lee and Paull, 2005). Activated ATM and ATR phosphorylate multiple proteins in the nucleus. These proteins serve as effectors for inducing cell cycle

arrest, initiating repair and causing cell death. Key among these is p53 which is phosphorylated directly on serine 15 by ATM and ATR, and indirectly on serine 20 (Banin et al., 1998; Lakin et al., 1999). Phosporylation of p53 inhibits its nuclear export and degradation, thereby stabilizing its protein levels. Target genes of p53 such as $p21^{WAF1/CIP1}$, are activated leading to inhibition of S-phase promoting Cdk2-CyclinE complex. As a result, S-phase arrest is maintained (Sancar et al., 2004). In this manner ATM and ATR phosphorylate and activate many proteins that regulate all aspects of the DNA damage response. While many of the substrates of ATM and ATR are distinct, a number are also shared. All ATM and ATR substrates have a consensus phosphorylation site of a serine or threonine residue followed by a glutamine residue (pS/pTQ). Screening of oriented peptide libraries have allowed for the elaboration of this motif to include residues on either side of the phosphorylated serine or threonine (O'Neill et al., 2000). The cell cycle arrest that is a hallmark of DDR is brought about by the phosphorylation and activation of ATM and ATR substrates, Chk2 and Chk1 respectively. These kinases in turn, phosphorylate and inactivate a group of phosphatases named Cdc25 A, B and C. These phosphatases regulate cell cycle transitions at G1/S and G2/M, as well as regulating other proteins such as p53. Once Cdc25A is phosphorylated, it is degraded by the ubiquitin proteasome system. Phosphorylated Cdc25C binds to 14-3-3 proteins and is exported from the nucleus (Lee et al., 1992). Cdc25C dephosphorylates Cdc2 on tyrosine15 (Y15), thereby activating it. In response to DNA damage, Cdc2 cannot be activated by dephosphorylation due to the inhibition of Cdc25C; this failure causes G2/M arrest (Figure 2-8). Additional substrates and regulators of ATM and ATR that are required for various aspects of the DDR are still being identified.

Characterizations of the functional roles of these elements are necessary to enhance our understanding of the network. Current drugs used in the treatment of cancer such as anti-metabolites topoisomerase inhibitors and radiomimetics (e.g. bleomycin) have a narrow therapeutic window, cause severe side-effects, and patients frequently develop resistance to them. These complications have created an interest in developing drugs that target cancer-specific molecules, e.g., Gleevec which targets BCR-Abl. DDR inhibitors are currently under scrutiny as a means to sensitize cancers to therapeutic radiation. These studies are based on the idea that inhibition of the checkpoint and subsequent DNA repair in tumor cells will sensitize them to the deleterious effects of radiation (Zhou and Bartek, 2004). However, two recent studies show that in pre-neoplastic lesions the DDR is activated as a means to inhibit oncogene-driven proliferation. As these cells progressed to malignant tumors the DDR was overcome and resulted in genetic instability and accelerated cancer progression (Bartkova et al., 2005; Gorgoulis et al., 2005). DDR inhibitors may inhibit the protective response in pre-cancer cells and in the long-term may prove to be detrimental.

C. Regulation of the G2/M checkpoint by p38

Additional components that bring about cell cycle arrest in an ATM/ATR independent manner were discovered in early studies in *Xenopus* egg extracts. In this system it was shown that replication arrest induced by treatment with methyl methanesulfonate (MMS) was intact even when the extract was treated with the ATM/ATR inhibitor caffeine (Stokes and Michael, 2003). It has also been shown that Cdc25-dependent activation of CyclinA/Cdk2 was blocked in G2 in response to genotoxic stress independently of

ATM/ATR (Goldstone et al., 2001). Subsequently, many MAPK family members were shown to be activated by UV radiation and phosphorylate p53 (She et al., 2000; She et al., 2002). Only the role of p38 in regulating the checkpoint has been studied in detail. Wang et al., have shown that p38 (specifically the γ isoform) is activated by IR in a MEK6-dependent manner. Interestingly, they show that this activation is dependent on ATM as it is diminished in cells from AT patients. Constitutively active MEK6 is sufficient to cause G2/M arrest even in the absence of DNA damage. Dominant negative p38 was shown to block phosphorylation of Chk2. In a two-stage protein kinase assay where p38 is activated by MEK6, active p38 was not able to enhance Chk2 kinase activity towards its substrate Cdc25C (Wang et al., 2000). These results indicate that p38 MAPK may be downstream of ATM/ATR, although the pathway leading to p38 activation is not known. DNA methylating agents that induce DDR have also been shown to activate p38 (Hirose et al., 2003). Therapeutic agents such as temozolamide that are used in the treatment of melanomas and brain tumors cause activation of the G2 checkpoint in a p38-dependent manner. In the same study, p38 siRNA caused a decrease in the phosphorylation of Cdc25C at serine 216, the same site phosphorylated by Chk1 and 2 (Hirose et al., 2003). Other chemotherapeutic drugs such as topoisomerase inhibitors and histone deacetylase inhibitors also inhibit the G2/M transition in a p38-dependent manner (Mikhailov et al., 2004). Treatment of cells with UV leads to a significant and prolonged activation of p38. Activation is rapid, occurring within a few minutes of treatment and lasting for several hours. Bulavin and co-workers showed that p38 α and β isoforms were primarily responsible for the UV induced G2/M checkpoint, as siRNA of these two isoforms abrogated the checkpoint. *In vitro*, p38 bound to and phosphorylated Cdc25B

and C family members and regulated their binding to 14-3-3 proteins (Bulavin et al., 2001). This finding was further refined when it was discovered that p38 did not directly phosphorylate Cdc25C, rather phosphorylation occurred via p38's ability to phosphorylate and activate its substrate MAPKAP kinase 2 (MK2). MK2 phosphorylated both Cdc25 B and C and was responsible for maintaining the G1, S and G2/M checkpoints in response to UV radiation. However in this study, MK2 siRNA did not cause any changes to the activation of Chk1 and 2 as was earlier reported by Wang and co-workers implying that p38 may regulate other substrates when activated by IR (Figure 2-9) (Manke et al., 2005; Wang et al., 2000). These studies yield a model in which p38 functions as a mediator of DDR by activating its substrate MK2, which in a manner analogous to Chk1 and Chk2 inhibits cell cycle progression by inactivating Cdc25 phosphatases. Some of these findings also hint at a role for ATM/ATR in the regulation of p38-MK2 depending on the nature of the damage (Figure 2-8). This manner of control would be an efficient way of rapidly initiating checkpoints minutes after the damage is perceived.

My research was aimed at identifying pathways unique to TAOs. In order to address this, I used a two-pronged approach: a ligand screen to identify agents that stimulated endogenous TAO2 kinase activity, and a yeast two-hybrid screen to determine regulators and effectors for this protein kinase. These experiments allowed us to elaborate a role for TAO2 in the regulation of G protein signaling, supporting pre-existing findings from this lab (Chen et al., 2003). Our studies also demonstrated that TAO2 is an important regulator of the DNA damage checkpoint via activation of p38 MAPK. A surprising outcome of our studies is that the other TAO family members also collaborate in this pathway by association with one

another as well as with p38. The yeast two-hybrid screen also uncovered interactors such as kinesin 3A (Kif3A) that hint at roles for TAO2 in motor transport. These studies point to a role for TAOs in regulating important and diverse cellular events both at the membrane as well as the nucleus.

DNA Damaging Agent	Type of Damage
Ionizing Radiation (IR)	Double strand DNA breaks Base damages: O6-methylguanine, thymine glycols and fragmented bases
Ultraviolet radiation (UV)	Reactive oxygen species produce base damages Cyclobutane dimers and base damages
Hydroxyurea (HU)	Inhibits ribonucleotide reductase and stalls replication
Cisplatin and other alkylating agents	Interstrand crosslinks
5-Fluorouracil and Gemcitabine	Inhibits DNA synthesis
Etoposide and other topoisomerase inhibitors	Stabilizes Topo II-DNA cleavable complex
Bleomycin	Double strand DNA breaks

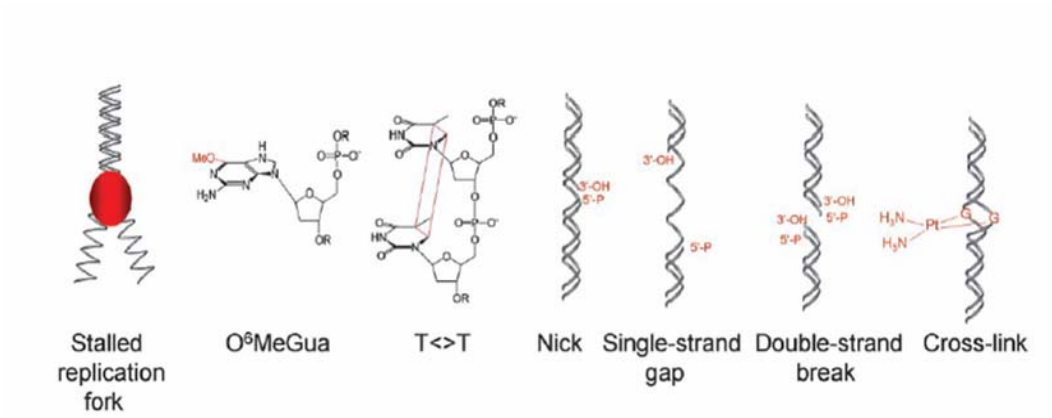

Table 2-1. DNA damaging agents and the types of DNA damage caused. (Modified from Sancar et al., 2004).

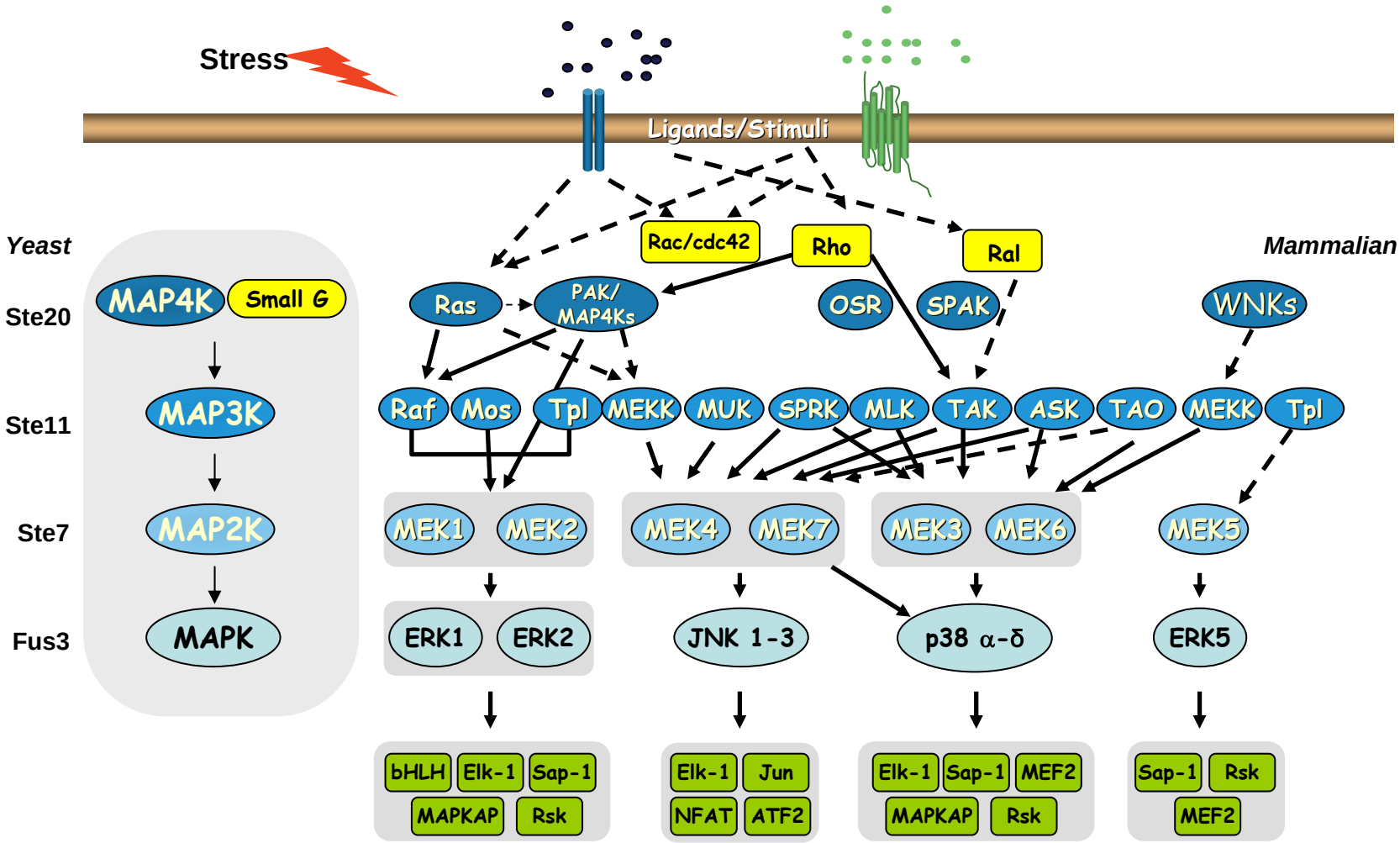

Figure 2-1. A MAP kinase network

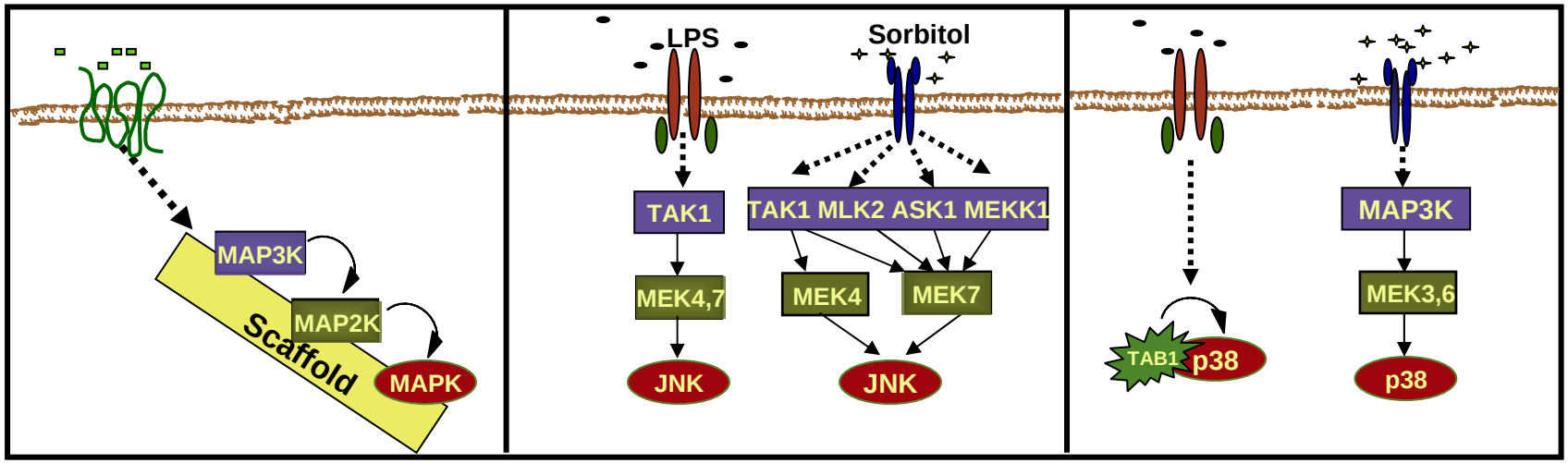

Figure 2-2. Building specificity into MAPK cascades. MAPK cascades use multiple methods to achieve specific responses to diverse stimuli. These include using scaffolds, the differential use of MAP2Ks and MAP3Ks, and the use of proteins such as TAB1 which activates MAPKs independently of MAP2Ks.

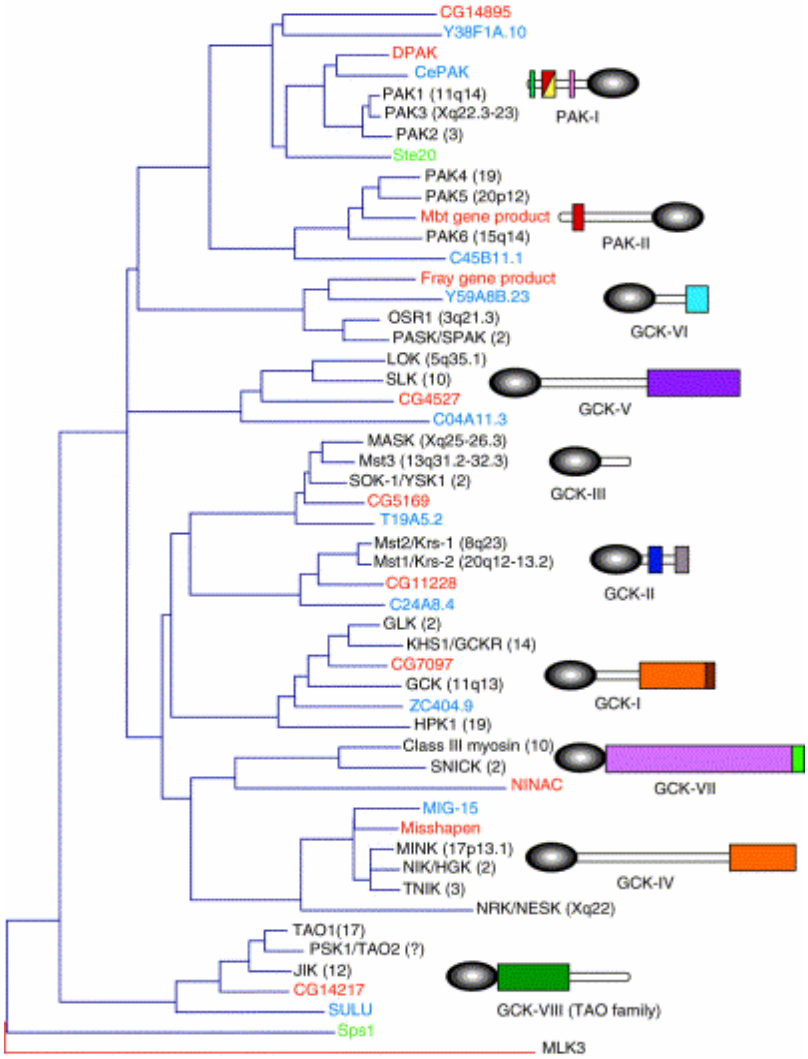

Figure 2-3. Phylogenetic relations among mammalian Ste20p group kinases and their positions within each subfamily. Kinases from human (black letters), *Drosophila* (red letters) and *C. elegans* (blue letters) were used for the construction of this tree. General topology of kinases in each subfamily are shown on the right. Legend: kinase domains (black ovals), conserved domains (colored rectangles) and the variable regions (white bars) (From Dan et al., 2001). Reprinted from Trends in Cell Biology, Vol 11, Dan et al., The Ste 20 group of kinases as regulators of MAP kinase cascades, 220-230, Copyright (2001), with permission from Elsevier.

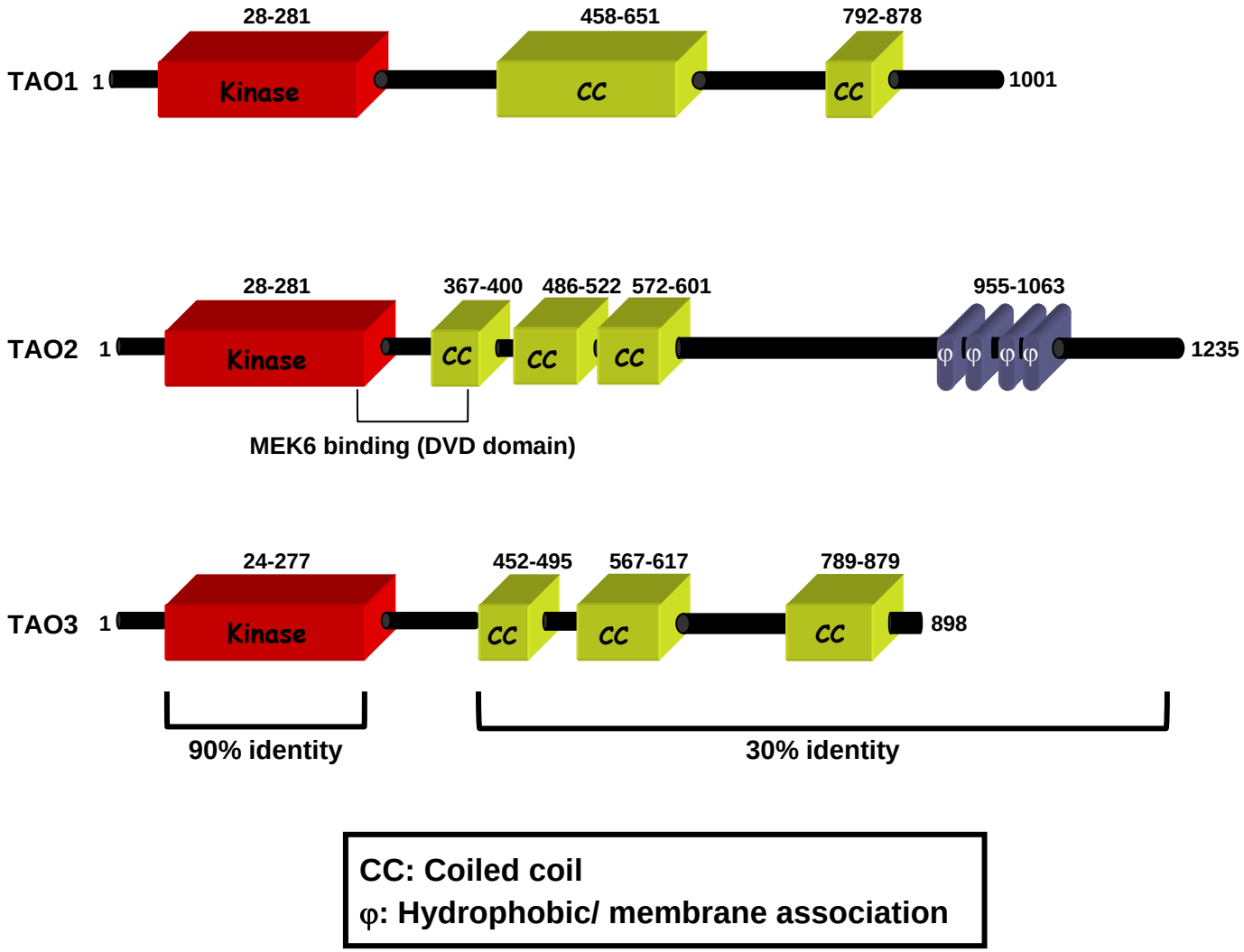

Figure 2-4. Domain architecture of TAO kinases. Sequence analysis and domain characterization carried out using the SMART algorithm. http://smart.embl-heidelberg.de/.

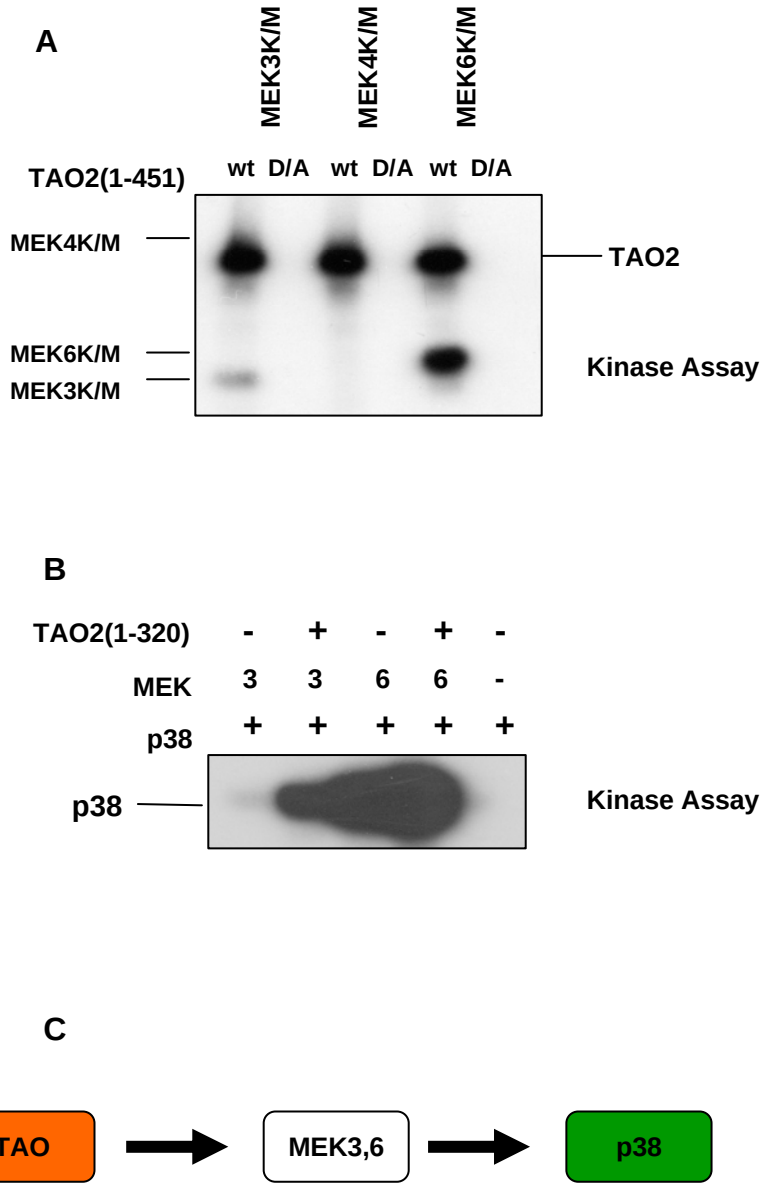

Figure 2-5: TAO kinases are MAP3Ks in the p38 cascade. (A) TAO2 phosphorylates MEK3 and 6 *in vitro*. (B) TAO2 activates MEK3 and 6 towards p38 in coupled kinase assays. (C) Schematic showing TAO mediated activation of p38 (Modified from Chen et al., 1999). Reprinted from Journal of Biological Chemistry, Vol 274, Chen et al., Isolation of TAO2 and identification of its MEK binding domain, 28803-28807, Copyright (1999), with permission from ASBMB.

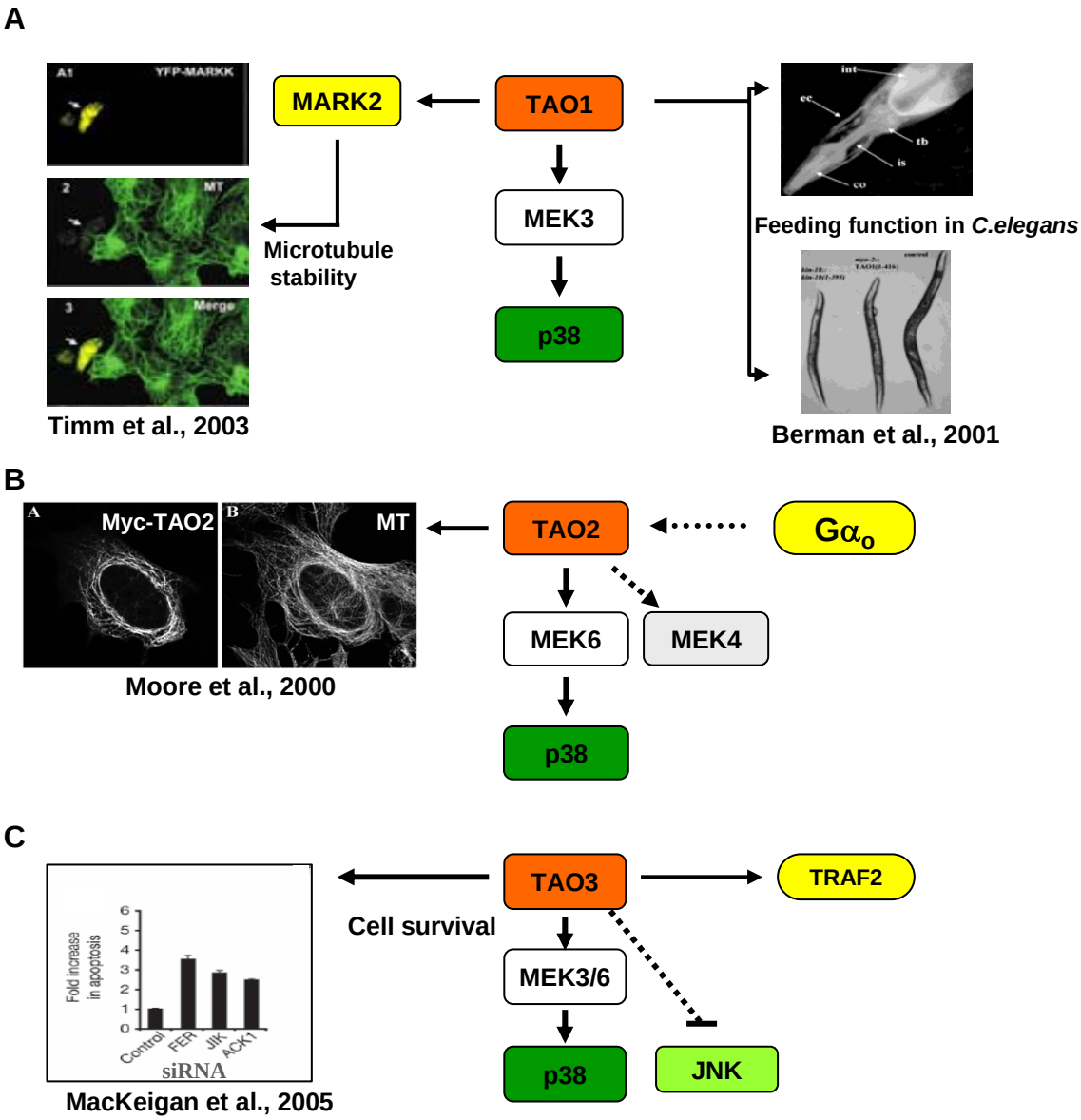

Figure 2-6. Pathways regulated by TAO kinases. (A) TAO1 regulates p38 activation, phosphorylates MARK2 to regulate microtubule stability, and is involved in feeding in *C.elegans.* (B) TAO2 regulates p38, co-localizes with microtubules, and is regulated indirectly by $G\alpha_o$ subunits. (C) TAO3 activates p38 and inhibits JNK activation by EGF, is a cell survival kinase (JIK) , and interacts with TRAF2.

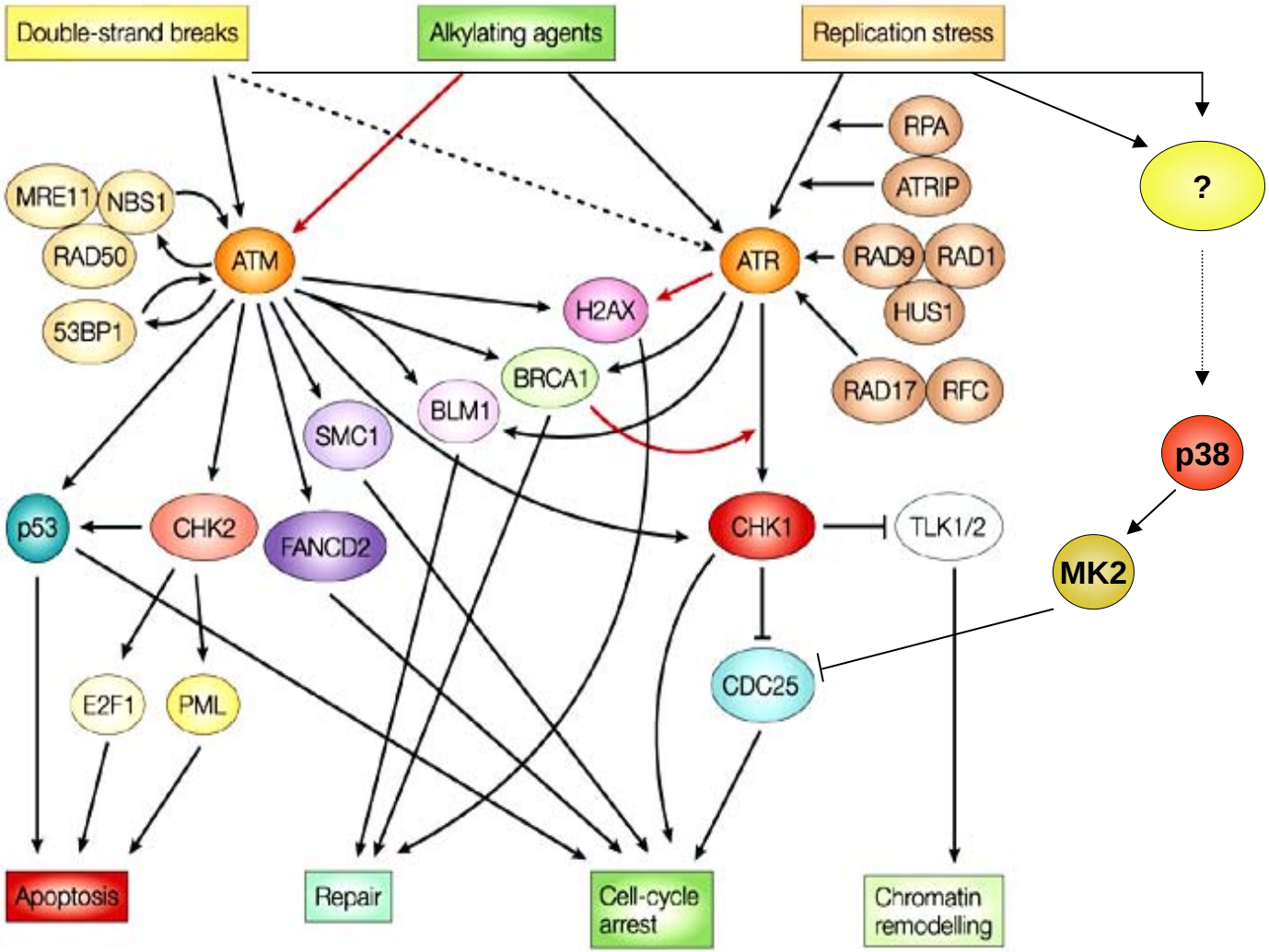

Figure 2-7. The DNA damage response network (Modified from Zhou and Bartek 2004). Reprinted from Nature Review Cancer, Vol 4, Zhou and Bartek, Targeting checkpoint kinases: chemosensitization versus chemoprotection, 216-225, Copyright (2004), with permission from Nature publishing group.

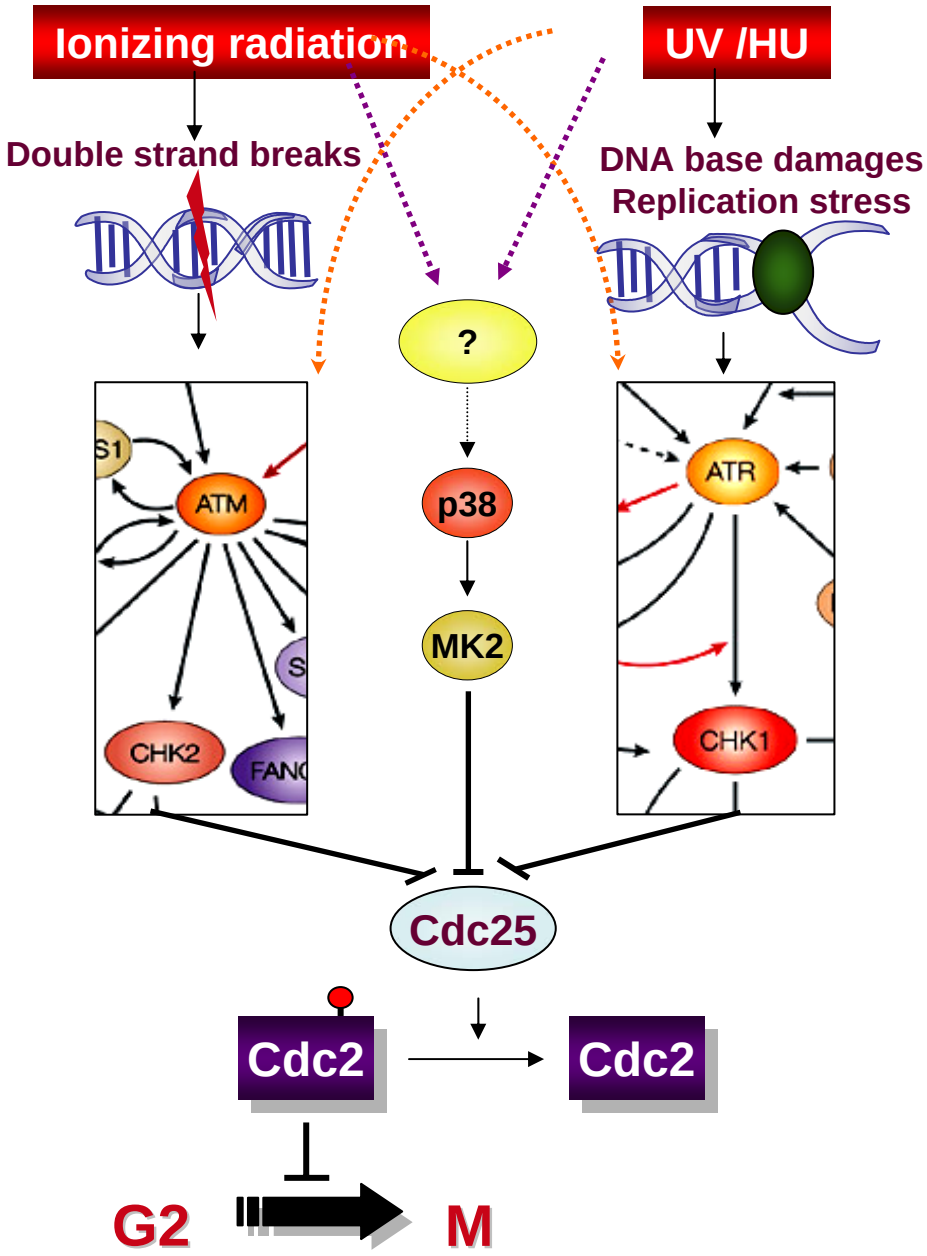

Figure 2-8. Regulation of the G2/M DNA damage checkpoint by ATM/ATR-Chk1/2 kinases and by p38 MAPK (Modified from Zhou and Bartek 2004).

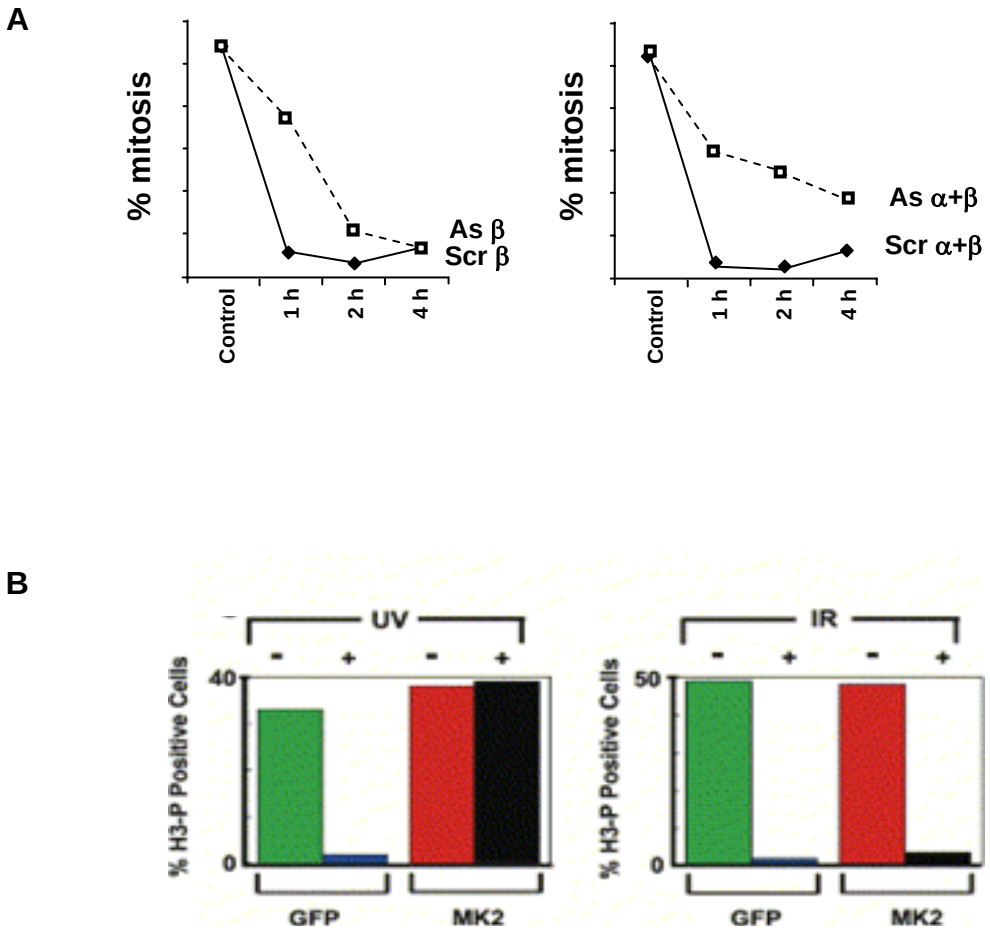

Figure 2-9. Regulation of the G2/M checkpoint by p38-MK2. (A) siRNA of p38 α and β isoforms inhibits the UV-mediated G2/M checkpoint (Bulavin et al., 2001). (B) MAPKAP kinase 2 (MK2) siRNA abrogates the UV-mediated G2/M checkpoint but not the IR-mediated checkpoint (From Manke et al., 2005). Reprinted from Nature, Vol 411, Bulavin et al.,Initiation of the G2/M checkpoint after UV radiation requires p38 kinase, 102-107, Copyright (2001), with permission from Nature publishing group. Reprinted from Molecular Cell, Vol 17, Manke et al., MK2 is a cell cycle checkpoint kinase that regulates the G2/M transition and S phase progression in response to UV radiation, 37-48, Copyright (2005) with permission from Elsevier.□□

CHAPTER 3. TAO2 INTERACTS WITH AND PHOSPHORYLATES $G\alpha_S$ SUBUNITS

I. Abstract

To identify TAO2 interactors, a yeast two-hybrid screen was performed with fragments of TAO2 and a mouse neo-natal mouse brain cDNA library. A number of interactors were identified, including TAO3, $G\alpha_s$, a forkhead-associated (FHA) domain containing protein microspherule 1 (MSP1), a B subunit family member of protein phosphatase 2A (PP2A), and others (Table 3-1). The $G\alpha_s$ interaction was pursued due to existing findings that TAO2 might be regulated by G protein-coupled receptors (GPCRs) (Chen et al., 2003). The TAO2-$G\alpha_s$ interaction was specific in that TAO2 only weakly interacted with other $G\alpha$ isoforms. TAO2 phosphorylated $G\alpha_s$ on Thr9 in the N-terminal α helix as determined by phosphoamino-acid analysis and limited tryptic proteolysis of $G\alpha_s$. TAO2 appeared to phosphorylate the inactive GDP-bound form of the subunit as $G\alpha_s$-GTPγS was not a substrate. The phosphorylation was not inhibited by G_β subunits even in millimolar amounts, indicating that TAO2 may phosphorylate $G\alpha_s$ in the inactive heterotrimer. I was not able to identify any changes in activation of $G\alpha_s$ when it was phosphorylated. TAO2 also interacted with G_β family members 1-4, which are most similar to one another, but not with $G_{\beta 5,}$ which is distinct in sequence from other family members. The G_β interaction was confirmed *in vivo* from detergent-soluble membrane extracts. These results indicate that TAO2 may be a regulator of GPCR signaling by phosphorylating $G\alpha_s$ and interacting with $G_{\beta\gamma}$ family members but the mechanism is unknown.

II. Introduction

A. Overview of G protein signaling

Heterotrimeric G protein-coupled receptors (GPCRs) are the largest family of cell surface receptors. These are seven-transmembrane spanning proteins that regulate associated heterotrimerc G proteins. These receptors are activated by a wide variety of ligands including hormones, peptides, phospholipids, photons, chemoattractants, neurotransmitters, odorants and growth factors to regulate diverse and critical cell programs. To date, an estimated 60% of pharmaceutical therapeutics currently available target these receptors. When GPCRs bind to their cognate ligands they undergo conformational changes that regulate activation of their cognate G protein. Heterotrimeric G proteins are composed of α, β and γ subunits but essentially signal as dimers (α and βγ). G proteins regulate multiple effector molecules including enzymes, channels and transporters. There are about 18 Gα, 6 Gβ and 13 Gγ subunits. Gα subunits are broadly classified into four families (s, i, q and 12) based on sequence similarity and effector coupling. Effector regulation is controlled by cycles of GTP binding and hydrolysis. In unstimulated cells, Gα subunits are inactive and bound to $G_{\beta\gamma}$ and GDP. The GDP/GTP exchange rate is low for the heterotrimer. Ligand-bound receptors activate G proteins by opening a nucleotide binding site on the G protein thereby accelerating the dissociation of GDP and association of GTP. This acceleration of the exchange rate of GDP for GTP will increase the relative amounts of GTP-bound active Gα subunit. The Gα subunits have an intrinsic GTPase activity that causes the hydrolysis of GTP to GDP and resets the cycle (Figure 3-1). In addition GTPase activating proteins (GAPs) can accelerate the GTP to GDP conversion. Since the GTPase activity of Gα subunits is low, GAPs are

required for rapid termination of the signal. There are two forms of GAP proteins: the regulators of G protein signaling (RGS) or proteins that contain RGS domains and phospholipase C-β (PLC β). PLC-β enzymes are unique in that they are effectors of $G\alpha_q$ signaling as well as GAPs for $G\alpha_q$. Another example of GTPase activating molecule is p115 Rho guanine nucleotide exchange factor (p115 RhoGEF) (Kozasa et al., 1998) which causes GTP hydrolysis on $G\alpha_{12/13}$. Activation of Gα also allows $G_{\beta\gamma}$ to initiate signaling events. $G_{\beta\gamma}$ dimers form immediately after translation of G_β and G_γ subunits and the dimer reversibly associates with Gα subunits. G_β subunits are ~ 35 kDa proteins that are composed of seven β strand repeats that form a characteristic cylindrical β propeller structure. Of the 5 G_β subunits, 1-4 are similar in sequence but $G_{\beta5}$ is less similar to other G_β subunits and interacts with G_γ-like (GGL) domains in other proteins rather that G_γ itself (Snow et al., 1998). G_γ subunits are small polypeptides of about 7 kDa that exhibit great sequence diversity. The C-terminal tails of G_γ are proteolyzed to expose a conserved cysteine residue that is irreversibly prenylated allowing the $G_{\beta\gamma}$ dimer to associate with the membrane (Clapham and Neer, 1997). Most G_β and G_γ isoforms are capable of associating with one another and cells usually express a number of $G_{\beta\gamma}$ combinations. As a result it has been difficult to rigorously assign roles for specific $G_{\beta\gamma}$ dimers.

B. Activation of MAPK cascades by G protein-coupled receptors

MAPKs have been shown to be activated by a number of ligands that activate GPCRs including peptides such as endothelin and somatostatin, lipid mediators like lysophosphatidic

acid (LPA) and prostaglandin, and bioactive amines such as serotonin. The mechanism by which this connectivity is established is being intensely investigated. Originally it was envisioned that MAPK activation by GPCRs was mediated by Gα subunits, for example, $G\alpha_q$ directly stimulates Bruton's tyrosine kinase (Btk) (Bence et al., 1997). However, in certain contexts, studies using other constitutively activated Gα subunits failed to elicit MAPK activation (Crespo et al., 1994; Faure et al., 1994; Qian et al., 1993). It was found that overexpression of $G_{\beta\gamma}$ was sufficient to activate ERK1/2 in a Ras-dependent manner (Crespo et al., 1994). Additional studies determined that $G_{\beta\gamma}$ overexpression resulted in the phosphorylation and activation of a non-receptor tyrosine kinase Shc in a PI3-kinase dependent manner (Touhara et al., 1995). Hence βγ dimers are also capable of linking GPCR activation to MAPK by activating intermediates normally utilized by receptor tyrosine kinases (Figure 3-2).

ERK1/2 MAPK activation by G proteins has been well studied. ERK1/2 activation by β-adrenergic receptor agonists has been shown to be via the activation of Src. Ligand-bound receptor is phosphorylated by G protein-coupled receptor kinase (GRK) which recruits β-arrestin. β-arrestin functions as an adaptor to recruit Src to the membrane where it is activated (Luttrell et al., 1999). Many other non-receptor tyrosine kinases have been implicated in MAPK activation in restricted cell types. In lymphoid cells, a Src-related kinase Lyn and the COOH-terminal Src kinase (Csk) have been shown to be required for ERK activation by $G\alpha_q$-coupled receptors. In cells lacking Bruton's tyrosine kinase (Btk) $G\alpha_i$ mediated ERK1/2 activation is inhibited. Proline-rich tyrosine kinase (Pyk2) and the

related focal adhesion kinase (FAK) are activated by elevated Ca^{2+} concentrations and are required for the activation of ERK1/2 by many $G\alpha_{i,\ q}$–coupled receptors. These pathways are especially important in neuronal and cardiomyocyte signaling pathways (Bence et al., 1997; Della Rocca et al., 1999; Della Rocca et al., 1997)

A particularly interesting form of GPCR-mediated activation of MAPK is by trans-activation of receptor tyrosine kinases (Fischer et al., 2003). Studies have shown that stimulation of cells with GPCR agonists induces phosphorylation of cytoplasmic tails of platelet-derived growth factor (PDGF) and epidermal growth factor (EGF) receptors and subsequent MAPK activation. It is believed that one manner in which EGFR and PDGFR transactivation is caused is via the GPCR- activated Src kinase. Another mechanism that is gaining acceptance is that activation of the G protein-coupled receptor induces the cleavage of a membrane bound ligand of a tyrosine kinase receptor. Prenzel and co-workers demonstrated that GPCR stimulation led to the cleavage of heparin-binding EGF (HB-EGF) possibly via a disintegrin and metalloprotease domain-containing metalloprotease (ADAM). Cleaved HB-EGF bound to the EGFR and activated MAPK signaling cascades (Prenzel et al., 1999). The activation mechanism that stimulates ADAM when G proteins are activated is still a mystery (Figure 3-2). GPCR mediated transactivation of receptor tyrosine kinases has been observed in about 60 human carcinoma cell lines, underscoring the importance of this means of MAPK regulation in cancer (Fischer et al., 2003)

Ras-independent activation of ERK1/2 by GPCR agonists has also been characterized. ERK1/2 has been shown to be activated by PKC in a Ras-independent manner in certain cell types when stimulated with agents such as carbachol. PKC activated by PLCβ

or Ca^{2+} directly phosphorylates Raf and causes MAPK activation (Kolch et al., 1993). B-Raf, another Raf isoform is not activated by PKC. Rather, studies have shown that a small G protein Rap1 activates B-Raf via agents that stimulate $G\alpha_{s,}$ or $G\alpha_{i}$ Rap1 can be activated by either cAMP-PKA or via the Rap GTP exchange factor (GEF), Epac (Schmitt and Stork, 2000; Schmitt and Stork, 2002; Stork and Schmitt, 2002). Despite the large number of studies, a consensus for MAPK activation by different GPCRs is difficult to draw because many of the studies have been limited to specific cell types where the receptors are expressed endogenously and pathway components are regulated in a cell type-specific manner.

Activation of JNK, p38 and ERK5 by GPCRs is even less well understood because of the large number of MAP3Ks that are capable of activating these pathways. JNK activation by $\beta\gamma$ subunits and $G\alpha_{12/13}$ is thought to occur via the small G proteins Cdc42 and Rac (Voyno-Yasenetskaya et al., 1996) and other tyrosine kinases such as Pyk2 and FAK (Dikic et al., 1996; Tokiwa et al., 1996). Activation of p38 by a number of GPCR ligands has also been reported. Again, it is difficult to determine the connections within pathways, because mechanisms are apparently different in different cell types. In HEK 293 cells, endogenous β-adrenergic and M_1 receptors activate p38 via $\beta\gamma$ dimers and $G\alpha_{q\,,\,11}$ (Yamauchi et al., 1997). However, in adult rat ventricular myocytes, $G\alpha_{i}$ activates p38 when treated with β-adrenergic receptor agonists and prevents cell death (Communal et al., 2000). In Chinese hamster ovary cells (CHO), adenosine (2B) receptor stimulation causes a $G\alpha_{s}$ coupled activation of p38 (Schulte and Fredholm, 2003). The MAP3Ks that are activated by these receptors are also largely unknown. A handful of studies have implicated ASK and TAO2 in p38 activation by

specific GPCRs. In aggregate, MAPK family members are activated by all the $G\alpha_{s, i, 12/13, o, q/11}$ subunits and $G_{\beta\gamma}$ in multiple cell types by diverse mechanisms.

C. Post-translational modification of G protein signaling by phosphorylation

Regulation of G protein signaling occurs by a variety of mechanisms including post-translational modification of the G protein subunits. Gα subunits are irreversibly N-terminally myristoylated or reversibly palmitoylated which allows them to reside at the membrane. Mutants that lack the ability to acquire these N-terminal modifications have been shown to lose their transforming phenotype in model systems (Gallego et al., 1992). $G_{\beta\gamma}$ dimers are also membrane-bound by the prenylation of the G_γ subunit. While α and βγ dimers are generally found in association at the plasma membrane, some groups reported that these subunits may reside in distinct sub-cellular compartments such as the Golgi and nucleus (Crouch and Simson, 1997; Jamora et al., 1997). The α and βγ subunits do not necessarily exist as heterotrimers – they have also been found independent of one another in certain contexts.

A number of instances have been reported in which Gα subunits are phosphorylated by protein kinases to enhance the strength and duration of signaling. $G\alpha_z$ has been shown to be phosphorylated both *in vitro* and *in vivo* by PKC and PAK. The major site of phosphorylation is Ser27, with Ser16 used as a secondary site (Lounsbury et al., 1991). The studies have disagreed about the activation state of the $G\alpha_z$ subunit that is phosphorylated. $G\alpha_z$ produced in *E.coli* was preferentially phosphorylated in the inactive GDP bound form

and GTPγS inhibited phosphorylation by up to 70% (Lounsbury et al., 1991). In contrast, $G\alpha_z$ produced in Sf9 cells was phosphorylated by PKC or PAK regardless of the activation state (Kozasa and Gilman, 1996; Wang et al., 1999). This may have occurred due to the difference in the systems used for purifying recombinant $G\alpha_z$. *E.coli* lack the ability to myristoylate Gα subunits, while Sf9 cells are capable of carrying out this process. Post-translational lipid modification and membrane localization may be an important pre-requisite for phosphorylation to occur. $G\alpha_{12}$ is also phosphorylated at the N-terminus by PKC both *in vivo* and *in vitro* while $G\alpha_{13}$ has been shown to be phosphorylated in a PKC-dependent manner in cells (Kozasa and Gilman, 1996). Additionally, $G\alpha_{13}$ is phosphorylated by PKA in cells; possibly on Thr203. Phosphorylation stabilized coupling of $G\alpha_{13}$ to the thromboxane (A2) receptor but inhibited βγ binding. PKA phosphorylation of $G\alpha_{13}$ inhibited Rho activation in CHO cells (Manganello et al., 2003). Phosphorylation of the α subunit in all reported cases blocked $G_{\beta\gamma}$ binding because the site phosphorylated was in a region that bound the βγ dimer. Phosphorylation also inhibits the action of RGS proteins to hydrolyze GTP and turn off signaling. In general, phosphorylation provides a means of enhancing the duration of signaling in a two-pronged manner; first, by inhibiting association of the phosphorylated subunit with the βγ dimer and second, by inhibiting the GAP activity of RGS proteins (Figure 3-3). Whether phosphorylation of α subunits is a general means of regulating G protein activity is unknown at present. Phosphorylation of other Gα subunits (by protein kinases) has not been reported. Since GPCRs are expressed in a cell-type specific manner, identification of ligands that induce G protein phosphorylation is limited to these

often specialized cell types. Hence extrapolation of underlying signaling mechanisms may prove to be difficult.

III. Materials and Methods

Yeast two-hybrid screen.

Yeast two-hybrid screens were performed against a neonatal mouse brain library (gift from Mark Henkemeyer) in yeast strain L40. Bait plasmids were cloned as LexA-DNA-binding domain fusions into pVJL11. Three bait plasmids were constructed; TAO2 kinase domain (1-320), both wild type and kinase dead (D169A), and a fragment of the C-terminus encompassing all three putative coiled-coil domains (320-620) (Figure 2-4). Bait plasmid expression was tested from transformed yeast lysates by probing with either the TAO2 antibody (U2253) or anti-lexA (Clontech). Yeast were plated on complete synthetic medium (CSM) or dropout medium (DO) lacking the amino acids leucine (Leu), tryptophan (Trp) and histidine (His) either with [baits (1-320) and (320-620)] or without [bait (1-320) D169A] 3-aminotriazole (3-AT) (Sigma). From 3 x 10^7 transformants screened, thirty nine (positive) interacting colonies were recovered. The inserts were obtained by sequencing the plasmid DNA isolated from the prey vector. Pair-wise interactions were reconfirmed by re-cloning the insert into pGADGH vectors and co-transforming bait and prey plasmid into L40 strains using Frozen EZ-Yeast transformation II (Zymo Research). LexA-lamin, WNK1 or OSR1 (gifts from Byung Hoon Lee and Wei Chen) was used in these experiments as a negative control. Transformations were plated on CSM lacking Leu and Trp as well as CSM lacking Leu, Trp and His. Interactions were confirmed with β-galactosidase assays. Briefly, yeast

streaked on triple drop-out plates were lifted with Hybond-C nitrocellulose filters (Amersham) and rapidly immersed in liquid nitrogen for 30 seconds to lyse the yeast. Filters were wet with a solution of LacZ buffer (60 mM $Na_2H\ PO_4$,, 40 mM NaH_2PO_4, 10 mM KCl, 1 mM $MgSO_4$) containing X-gal (Sigma) at a final concentration of 10 mg/ml .

Subcloning and mutagenesis

Two-hybrid vectors were generated by PCR from either pCMV-Myc-(full length) TAO2 wild type or pCMV-Myc-(full length) TAO D169A as template and introduced into pVJL11. pGADGH-$G\alpha_s$ and $G\alpha_i$ were gifts from Greg Tall (this department). Prey plasmids encoding pGADGH-$G_{\beta 1\text{-}5}$ were created by PCR amplification using pQE60-$G_{\beta 1\text{-}5}$ as templates (gift from Andrejs Krumins, this department). pGEX-GST-$G\alpha_s$ and pQE60-His_6-$G\alpha_s$ were gifts from Elliott Ross and Ron Taussig respectively. Site-directed mutagenesis was carried out with the Quikchange mutagenesis kit (Stratagene) and all constructs were confirmed by sequencing.

Expression of recombinant proteins

Purification of His_6-$G\alpha_s$ was carried out as described (Lee et al., 1994). Briefly, pQE60-His_6-Gαs was transformed into the BL21 strain of *E.coli* carrying the pREP4 plasmid encoding the *laqI* gene. Transformants were cultured in T7 medium and induced with 30 μM isopropylthioglycolate (IPTG) and expressed overnight at room temperature. Cell pellets were lysed in 100 mM NaCl, 20 mM β-mercaptoethanol (β-ME), 10 μM GDP, 50 mM Tris-Cl [pH 8.0] and protease inhibitor cocktail PTT (3 μg/ml tosylphenylalanylchloromethane

(TPCK), 3 μg/ml N-tosyl-L-lysine chloromethylketone (TLCK) and 3.5 mg/ml phenylmethylsulphonylfluoride (PMSF). Lysates were pelleted by centrifugation at 35,000 rpm for 35 min and supernatants were applied to a Ni-NTA column (Qiagen). The column was washed with 10 column volumes of 400 mM NaCl, 10 mM $MgCl_2$, 2 mM β-mercaptoethanol (β-ME), 30 μM $AlCl_3$, 10 mM NaF, 10 mM imidazole, 25 μM GDP, 50 mM Tris-Cl [pH 8.0], and PTT and 5 column volumes of 10 mM $MgCl_2$, 2 mM β-ME, 10 mM imidazole, 25 μM GDP, 50 mM Tris-Cl [pH 8.0] and PTT. Bound proteins were eluted with elution buffer (2 mM β-ME, 150 mM imidazole, 10 μM GDP, 50 mM Tris-Cl [pH 8.0] and PTT. The eluted proteins were further purified on a Hi-Trap Mono Q^{TM} column (Pharmacia). Protein concentrations were determined by amido black assay.

Purification of $G_{\beta\gamma}$ subunits was achieved as follows. His_6-$G_i\alpha$ and $G_{\beta\gamma}$ were co-expressed in Sf9 cells from recombinant baculoviruses. Cells were lysed 48 hrs post-infection and Sf9 membranes were prepared. The cell pellet was lysed in 1 mM $MgCl_2$, 20 mM Tris-Cl [pH 8.0], 0.1 mM PMSF, 10 μg/ml leupeptin and 1 μg/ml aprotinin. The lysate was dounced and pelleted by centrifugation at 14,000 rpm for 15 min. The supernatant was discarded and the pellet was resuspended in lysis buffer containing 3 mM $MgCl_2$ and 10 μg/ml DNase I. The lysate was re-homogenized and pelleted as above and the pellet was resuspended in $MgCl_2$/Dnase I-containing lysis buffer. The lysate was stirred at 4° C for 30 min and snap-frozen in liquid nitrogen. Membranes were thawed on ice and solubilized in extraction buffer (1% cholate, 100 mM NaCl, 5 mM β-me, 10 μM GDP, 20 mM Tris-Cl [pH 8.0], 0.1 mM PMSF, 10 μg/ml leupeptin and 1 μg/ml aprotinin) for 1 hr at 4°C with stirring. The lysate was pelleted by centrifugation at 35,000 rpm for 1 hr and the supernatant was

diluted 5 fold with Lubrol buffer (100 mM NaCl, 1 mM $MgCl_2$, 0.5% Lubrol, 5 mM β-ME, 10 μM GDP, 20 mM HEPES [pH 7.5], 0.1 mM PMSF, 10 μg/ml leupeptin, and 1 μg/ml aprotinin). The mixture was batch-bound to Ni/NTA resin for 1 hr at 4°C and then packed into a column by gravity flow. The resin was washed with 500 mM NaCl, 10 mM imidazole in Lubrol buffer. The column was brought to room temperature and the $G\alpha_i$ was eluted by washing the column with AMF buffer (100 mM NaCl, 5 mM β-ME, 30 μM $AlCl_3$, 50 mM $MgCl_2$, 10 mM NaF, 20 mM HEPES [pH 7.5] and 0.1 mM PMSF, 10 μg/ml leupeptin and 1 μg/ml aprotinin). $G_{\beta\gamma}$ subunit was eluted from the column with 100 mM NaCl, 5 mM β-ME, 50 mM EDTA, 20 mM HEPES [pH 8.0], 0.1 mM PMSF, 10 μg/ml leupeptin and 1 μg/ml aprotinin. Protein was concentrated and the concentration was estimated by silver staining and comparing to bovine serum albumin (BSA) standards. His_6-tagged TAO2 (1-320) was purified from Sf9 cells as described elsewhere (Zhou et al., 2004).

Protein kinase assays and limited tryptic proteolysis

In vitro kinase assays were carried out to phosphorylate $G\alpha_s$ with TAO2 (1-320). Assays were performed in 30 μl reaction volumes containing 10 mM $MgCl_2$, 5 μM ATP, 15 cpm/fmol [γ-^{32}P] ATP, approximately 6 pmol of either His_6-$G\alpha_s$ or GST-$G\alpha_s$, 8 pmol TAO2 (1-320) and 50 mM HEPES [pH 8.0]. Reactions were performed at 30°C for 30 min and terminated with 5X SDS-sample buffer. Samples were boiled for 5 min at 90°C and then resolved by SDS-PAGE gels for autoradiography. ^{32}P incorporation was quantified by excising bands from the gel and liquid scintillation counting in a scintillation counter (Beckman). Approximately 20 pmol of $G\alpha_{q,\ i,\ s,\ o\ and\ z}$ were used in control experiments. In

other experiments $G_{\beta\gamma}$ was included in the assay at concentration ranging from 10 nM to 2 μM. To determine if TAO2 phosphorylated activated $G\alpha_s$, kinase assays were performed as above but including either AMF (10 μM GDP, 30 μM $AlCl_3$, 10 mM $MgCl_2$, 10 mM NaF, 0.1% Lubrol and 25 mM HEPES [pH 8.0]) or GTPγS buffer (10 μM GTPγS, 1 mM EDTA, 1 mM $MgCl_2$, 1 mM DTT, 0.1% Lubrol and 25 mM HEPES [pH 8.0]). Limited tryptic protection assays were carried out as described elsewhere (Kozasa and Gilman, 1995). Briefly, GST-$G\alpha_s$ was treated with TEV protease (gift from X.Min) to cleave the GST tag. The cleaved protein was used as substrate in a kinase assay as described above with the assay volume reduced to 10 μl. The assay mix was then treated with either 20 μl of AMF buffer or GDP buffer (10 μM GDP and 25 mM HEPES [pH 8.0]) for 20 min at 30°C. The samples were treated with 5 ng of TPCK-treated trypsin for 5 min at 20°C. Reactions were terminated with 5X SDS sample buffer, boiled briefly, and resolved by SDS-PAGE. The gels were stained with Coomassie Brilliant Blue or silver and dried for autoradiography.

GTPγS binding assays

$G\alpha_s$ (final concentration per assay 2 pmol) was phosphorylated *in vitro* with TAO2 (1-320) as described above for 30 min at 30°C. After adjusting the free Mg^{2+} concentration to 1 μM with EDTA, the samples were pre-incubated for 10 min at 0°C with or with out $G_{\beta\gamma}$. Binding of [^{35}S] GTPγS was measured as described (Wang et al., 1997). Binding assays were initiated by adding the protein to 50 μl of reaction buffer (0.1% Lubrol, 50 μg/ml BSA, 1 mM dithiothretol (DTT), 0.5 mM EDTA, 100 mM NaCl, 1 mM $MgCl_2$, 100 μM ATP, 5 μM

GTPγS, 25 mM HEPES [pH 7.5]) containing 1000 cpm/pmol [^{35}S] GTPγS. Reactions were carried out for 45 min or the indicated times at 30°C and terminated with 100 µl of 100 mM NaCl, 20 mM $MgCl_2$ and 20 mM Tris-Cl [pH 8.0]. The bound [^{35}S] GTPγS was determined by filtration through BA85 membranes (Schleicher and Schuell) and quantitated using a scintillation counter.

Phosphoamino acid analysis

In vitro kinase assays were performed to phosphorylate $G\alpha_s$. Fractions were resolved by SDS-PAGE gels and transferred onto polyvinylidene fluoride (PVDF) membranes. The $G\alpha_s$ band was excised from the membrane and the protein was digested with 6N HCl by heating to 100°C for 2 hrs. The samples were dried under vacuum and resuspended in 20 µl of 2.5% formic acid, 7.8% glacial acetic acid. Thin layer chromatography (TLC) was performed on silica gel plates (Kodak). Samples were resolved by electrophoresis in one dimension against phospho-serine, threonine and tyrosine standards in electrode buffer (0.5% pyridine, 5% glacial acetic acid). Plates were dried and exposed to film.

Cell culture, immunoprecipitation and detergent-soluble membrane preparation

HEK-293 and HeLa cells were obtained from ATCC. Cells were cultured in Dulbecco's modified eagle's medium (DMEM) supplemented with 10% fetal bovine serum (FBS), 2 mM glutamine and antibiotics. Cells grown to 90% confluency in 10 cm dishes were washed once in 1X PBS, and then lysed with hypotonic buffer (10 mM HEPES pH 8.0, 1.5 mM $MgCl_2$, 10 mM KCl, 0.5 mM DTT, 10 mM sodium fluoride, 10 µg/ml aprotonin,

2μg/ml leupeptin, 10 μg/ml pepstatin A, 2 mM Na_2VO_3, and 1 mM PMSF). Cells were allowed to swell on ice for 5 min and dounced with 10 strokes of a dounce homogenizer. The lysed cells were pelleted at 1000g for 5 min at 4°C to pellet nuclei. The supernatant was pelleted by centrifugation at 100,000g for 1 hr to pellet membranes. The pellet was solubilized in Buffer A (50 mM HEPES [pH 8.0], 150 mM NaCl, 0.5% cholic acid, 10 mM sodium fluoride, 10 μg/ml aprotonin, 2 μg/ml leupeptin, 10 μg/ml pepstatin, 2 mM Na_2VO_3 and 1 mM phenylmethysulfonyl fluoride), lysates were pelleted again by centrifugation to obtain a detergent soluble membrane fraction. Supernatants were immediately processed for immunoprecipitations (IP). For co-IPs membrane fractions were probed with either pre-immune serum or anti-G_β antibody (Santa Cruz) and a 1:1 slurry of protein A-sepharose CL-4B (Amersham) in PBS for 2 hrs at 4°C. The beads were washed 3 times with 200 mM NaCl, 0.5% Triton X-100, 50 mM HEPES [pH 8.0], resuspended in 30 μL of 1X SDS-sample buffer and resolved by SDS-PAGE for immunoblotting. In transient transfection experiments, HEK-293 cells were transfected by calcium phosphate with either vector alone or pCMV-Myc-TAO2 (1-451) with or without pcDNA-$G_{\beta 1}$ and pcDNA-$G_{\gamma 2}$. Cells were harvested in Buffer A 48 hrs post-transfection.

IV. Results

A. TAO2 interactors identified from yeast two-hybrid screens

Three yeast two-hybrid baits were generated for TAO2, a fragment spanning the kinase domain (residues 1-320) both wild type and dead (D169→A mutation) as well as a region spanning residues (320-620) after the kinase domain (Figure 3-4). The kinase

deficient mutant was used so that it might trap weaker or transient interactions that would be stabilized due to catalytic deficiency. These baits were designed to identify both substrates and regulators of TAO2. The C-terminal bait harbored all three coiled-coil motifs that were putative protein-protein interaction domains. All three baits were transformed into yeast and tested for expression by immunoblotting with an anti-lexA antibody as well as a TAO2 antibody. The three fragments were expressed in yeast, although the (320-620) bait appeared to express better that the others (Figure 3-5A and data not shown). The baits were also tested for autoactivation using growth selection and β-galactosidase activity. The kinase dead bait (1-320 D169A) did not show autoactivation but both the wild type kinase domain bait and the fragment (320-620) were auto-activators (Figure 3-5B). The autoactivation was suppressed by using 3-aminotrazole (3-AT) at a final concentration of 2 mM in the screens with these baits. Two-hybrid screens were then carried out with the above baits (including 2 mM 3-AT for the indicated baits) with a neo-natal mouse brain cDNA library. Up to 10^7 transformants were obtained for each screen indicating that the screen had been completed to saturation. A number of interesting interactors were identified including TAO3 (further explored in chapter 4), $G\alpha_s$, an FHA-domain containing protein microspherule 1 (MSP1), ERK3 and a B subunit family member of protein phosphatase 2A (PP2A). We also identified MEK6, a known TAO2 interactor and a bonafide substrate with the kinase-dead bait. A summary of the interactors obtained with the three baits is described in Table 3-1.

B. TAO2 interacts with $G\alpha_s$

The $G\alpha_s$ subunit of the heterotrimeric G protein was obtained as an interactor in two-hybrid screens using TAO2 (1-320) D169A as bait. The plasmid encoding $G\alpha_s$ was rescued and recloned into a GADGH-DNA binding domain vector and retested for interaction against all the three baits used in the screen. Interestingly, the interaction with TAO2 (1-320) was much stronger than (1-320) D169A, indicating that the kinase-dead bait allowed for the detection of a weak interaction that was more pronounced than with the wild type construct. The C-terminal fragment of TAO2 (320-620) also interacted with $G\alpha_s$ implying that TAO2 may employ multiple surfaces for the interaction. Constitutively active $G\alpha_s$ subunits can be engineered by mutating the conserved Q227 to a leucine in the G3 region which abolishes intrinsic GTPase activity. We assessed whether the interaction between TAO2 and $G\alpha_s$ was altered when the Q227L mutation was introduced into $G\alpha_s$. TAO2 (1-320) and (320-620) interacted with $G\alpha_s$ Q227L as well as with wild type suggesting that the GTPase activity of $G\alpha_s$ does not influence the interaction in yeast (Figure 3-6A). The $G\alpha_s$ subunits (both wild-type and Q227L) did not interact with lamin or other kinases such as OSR1 and WNK1 as assayed by either growth on dropout medium or β-galactosidase assay (Figure 3-6B).

To determine if this interaction was specific to the $G\alpha_s$ subunit, TAO2 (1-320) was tested in directed two-hybrid tests with Gαi. A weak interaction between these proteins was also observed (data not shown). TAO2 has been shown previously to be regulated by $G\alpha_o$ subunits downstream of the muscarinic M2 receptor (Chen et al., 2003). In these studies it was shown that TAO2 kinase activity was a required component of signaling from M2

receptors to p38 MAPK. Dominant negative TAO2 and MEK3/6 constructs blocked p38 activation by the M2 muscarinic receptor and carbachol (Figure 3-7). It was not known whether the regulation of TAO2 by the G protein was direct or required intermediates at the time of the study. The two-hybrid results indicated that the regulation may be direct, and that TAO2 may be an intermediate in p38 activation by different GPCRs. To determine if the TAO2-Gα_s interaction occurred *in vivo*, co-immunoprecipitation experiments were carried out in HEK 293 cells. We used both over-expressed constructs and endogenous proteins. In these experiments, we were not able to discern an interaction between these proteins even though a significant fraction of TAO2 resides in membrane fractions of cells (discussed in Chapter 4). Since the interaction between TAOs and Gα_s is weak, it is possible that these proteins interact transiently under specific cell conditions, e.g. upon GPCR stimulation. Also, the cellular pool of Gα_s is very small, making the detection of endogenous protein difficult. Additionally, even though a direct interaction between these proteins was found by the two-hybrid screen, additional proteins or post-translational modifications on Gα_s maybe required for this association. Further experiments are required to characterize conditions in which TAO2 interacts with Gα_s.

C. TAO2 interacts with G$_{\beta\gamma}$ subunits

In *S.cerevisiae*, Ste20p interacts with free G$_{\beta\gamma}$ subunits at the membrane to regulate MAPK cascade activation. It has been shown that PAK1, another mammalian Ste20p homolog, is also capable of interacting with G$_{\beta\gamma}$ subunits at the same sites as Ste20p (Leeuw et al., 1998). This conserved mode of binding prompted us to test if TAO2 was also capable

of interacting with $G_{\beta\gamma}$ subunits. To this end, we utilized the two-hybrid system to test if a direct interaction between the various TAO2 fragments and G_{β} was detectable. It was not necessary to transform Gγ in these experiments as it has been reported that G_{β} can utilize the endogenous G_{γ} (Dell et al., 2002; Yan and Gautam, 1996). Five $G_{\beta\gamma}$ isoforms have been identified, with G_{β} subunits 1-4 showing the greatest degree of similarity. $G_{\beta 5}$ shows significant sequence diversity from the other isoforms. Binding was obtained between TAO2 (320-620) and $G_{\beta 2\text{-}4}$ but not $G_{\beta 5}$ (Figure 3-8A and data not shown). The interaction between $G_{\beta 1}$ and TAO2 was not conclusively demonstrated, perhaps due to poor expression of $G_{\beta 1}$ in yeast. We further established an interaction between TAO2 and $G_{\beta\gamma}$ using transient transfection experiments in HEK293 cells. Myc-TAO2 fragments (residues 1-451) were expressed in cells with or without $G_{\beta\gamma}$ subunits and lysates were immunoprecipitated with an antibody against G_{β}. As shown in the Figure 3-8B, TAO2 co-precipitated with over-expressed G_{β}. To obtain a native complex with these two proteins in cells, detergent soluble membrane fractions were prepared from HEK293 cells. Cholic acid, a non-ionic and non-denaturing detergent frequently used for the solubilization of membrane proteins was used in these studies to isolate G_{β} complexes. A significant proportion of endogenous TAO2 was present in G_{β}-immunoprecipitates when membrane extracts were prepared with cholic acid (Figure 3-8C). Similar interactions were seen when cells were lysed in Lubrol, another non-ionic detergent that solubilizes membrane proteins. In control experiments, no interaction was seen between OSR1, another Ste20p, and $G_{\beta\gamma}$ subunits. Binding to G_{β} did not alter the ability of TAO2 to phosphorylate MEK6 (data not shown). G_{β} interacts with a number of

effectors that have a small domain with conserved residues **Q**-x-x-**E**-**R** (where x is any amino acid). Adenylyl cyclase (AC 2, 4, 7), β-adrenergic receptor kinase 1 (βARK1) and G protein-gated inward rectifying K+ channel subunits 1(GIRK1) have been shown to interact with G_{β} via these residues (Chen et al., 1995) (Figure 3-9A). TAO2 also contains these consensus sites within the fragment (320-620) that interacts with G_{β}. We created two fragments of TAO2, one encompassing residues 320-500 (ΔQxxER) which does not include the conserved motif and a fragment containing residues 500-620 (QxxER) which harbors the conserved motif. These fragments were used in directed two-hybrid tests with $G_{\beta 2}$. TAO2 (ΔQxxER) failed to bind $G_{\beta 2}$ indicating that this region may be critical for interaction (Figure 3-9B). However, TAO2 (500-620) also failed to bind to $G_{\beta 2}$. It is possible that TAO2 binds to $G_{\beta 2}$ via the QxxER motif as well as other regions not contained within the 500-620 fragment used in these studies. To address the requirement of this motif in greater detail, the conserved residues were mutated individually to alanine, and the triple mutant was also created. All these fragments were auto-activators in yeast and conclusive results could not be drawn (data not shown). Future experiments will be conducted using *in vitro* binding assays between TAO2 and $G_{\beta 2}$. Peptide fragments containing QxxER or the triple mutant will be used to compete for binding with TAO2. We will also determine if a TAO2 mutant with the QxxER residues mutated to alanine will behave as a dominant negative in signaling to p38 by activated GPCRs.

D. TAO2 phosphorylates $G\alpha_s$ on Thr9

Based on previous studies that demonstrated that TAO2 was regulated by G proteins, we wished to explore if reciprocal signaling existed between TAO2 and $G\alpha_s$. Indeed, $G\alpha_s$ was phosphorylated by both endogenous immunoprecipitated TAO2, as well as a Sf9-expressed kinase domain fragment (Figure 3-10 A and B). To determine if this was specific for $G\alpha_s$, we included other Gα subunits in the assay. Surprisingly we found that endogenous TAO2 phosphorylated multiple Gα subunits to varying extents (Figure 3-10A). $G\alpha_s$ was most efficiently phosphorylated, reaching a stoichiometry approximately equal to 0.7mol phosphate/mol of $G\alpha_s$. TAO2 also phosphorylated $G_{i,o \text{ and } z}$ but not G_q. The implication of this is not immediately clear. There are 6 G_β subunits and 5 G_γ subunits in the cell and different combinations of βγ interact with various Gα subunits. Perhaps the interaction between TAO2 and a number of G_β subunits allows it to regulate and be regulated by multiple Gα isoforms. More detailed studies will be required to understand the contributions of different Gα subunits in the regulation of TAO2 kinase activity and vice versa. A number of Gα subunits have been identified to be phosphorylated by kinases which alter the kinetics of signaling. For example $G\alpha_z$, a sparsely expressed member of the $G\alpha_i$ family, is phosphorylated by both PKC and PAK (Wang et al., 1999). Phosphorylation decreases the affinity between $G\alpha_z$ and $G_{\beta\gamma}$ and desensitizes $G\alpha_z$ to GAP activity of RGS proteins. In the few reported cases, it was thought that kinases potentiate signaling from Gα subunits by inhibiting the mechanisms that down-regulate Gα signaling. Phosphorylation in certain instances occurs in the N-terminal α-helix in Gα, a region that is unstructured. This helix forms a surface through which Gα

subunits interact with G_β. Phosphorylation in the N-terminal domain prevents binding because the large phosphate group interrupts association between Gα and Gβ (Figure 3-11). To determine if this region in $G\alpha_s$ was phosphorylated by TAO2, we phosphorylated $G\alpha_s$ using a fragment of TAO2 (1-451) immunoprecipitated from HEK293 cells (Figure 3-12A). The phosphorylated $G\alpha_s$ was activated using AlF_4^-. AlF_4^- binds next to GDP and mimics the γ-phosphate on GTP. Activated phospho-$G\alpha_s$ was treated with trypsin which cleaves after Arg26 (Figure 3-12B). Hence, the N-terminal α helix will be proteolyzed and any phosphorylation in this domain will be lost. Indeed, limited tryptic proteolysis after activation resulted in loss of phosphate in $G\alpha_s$ indicating that TAO2 phosphorylated $G\alpha_s$ in the N-terminal helix (Figure 3-12A, lane 2). The sequence within this region contained one serine (Ser7) and one threonine (Thr9) residue. Each site was mutated individually or in combination to alanine, and *in vitro* kinase assays comparing the wild type and mutant $G\alpha_s$ were performed. Mutation of either site resulted in loss of phosphorylation (Figure 3-12C). To determine if TAO2 phosphorylated serine or threonine on $G\alpha_s$, phosphorylated $G\alpha_s$ was subjected to phosphoamino acid analysis. By this method, we only detected phospho-threonine on $G\alpha_s$; hence it appears that TAO2 phosphorylates Thr9 on $G\alpha_s$ (Figure 3-12D). Because both Ser7 and Thr9 are close to each other in the sequence it is possible that mutation of Ser7 disordered the helix and prevented Thr9 from being phosphorylated, resulting in lack of phosphorylation in the Ser7A mutant.

E. TAO2 phosphorylates inactive GDP-bound $G\alpha_s$

The activation state of Gα could alter the ability of protein kinases to phosphorylate them. In the case of PAK phosphorylation of $G\alpha_z$ however, the activation state of Gα did not affect phosphorylation. We determined if activation of $G\alpha_s$ using AlF_4^- or GTPγS had any effect on its ability to be phosphorylated by TAO2 and/or altered TAO2 protein kinase activity in any way. Activated $G\alpha_s$ was not phosphorylated relative to $G\alpha_s$-GDP, implying that TAO2 preferentially phosphorylates inactive GDP bound $G\alpha_s$ (Figure 3-13). In control experiments, neither GTPγS nor AlF_4^- had any effect on MEK6K82M phosphorylation by TAO2. Activated $G\alpha_s$ did not alter TAO2 autophosphorylation under these conditions. However, given that differences have been observed in $G\alpha_z$ phosphorylation depending upon the expression system used to purify the α subunit; these experiments may have to be repeated with substrate produced in a system such as Sf9 that is capable of myristoylating the protein.

In other examples, phosphorylation in the N-terminal helix of Gα impairs $G_{\beta\gamma}$ binding. *In vitro* kinase assays were performed to phosphorylate $G\alpha_s$ and increasing concentrations of $G_{\beta\gamma}$ were titrated into the samples to determine if phosphorylation was inhibited in the heterotrimeric state. However, even with a 100-fold excess of $G_{\beta\gamma}$ (up to 2 mM) there was no change in the phosphorylation of $G\alpha_s$ (Figure 3-14A). It appears that TAO2 phosphorylates inactive $G\alpha_s$ bound to $G_{\beta\gamma}$. Although this mode of action does not conform to the hypothesis that phosphorylation hinders $G_{\beta\gamma}$ binding, it is possible that the

threonine in the N-terminus is oriented away from the surface used for $G_{\beta\gamma}$ binding and hence a phosphate on this site might not affect binding in any way.

F. TAO2 phosphorylation of $G\alpha_s$ does not alter $G_{\beta\gamma}$ binding

To confirm that the TAO2 catalyzed phosphorylation of $G\alpha_s$ did not impair $G_{\beta\gamma}$ binding, we monitored the effect of phosphorylation on the time dependence with which $G_{\beta\gamma}$ inhibits GDP/GTPγS exchange. In these experiments, phosphorylated $G\alpha_s$ was incubated with an excess of $G_{\beta\gamma}$ and the samples were evaluated for the ability to exchange GDP for GTPγS. Incubation of non-phosphorylated $G\alpha_s$ with $G_{\beta\gamma}$ markedly inhibited the nucleotide exchange rate as expected. Phosphorylation of $G\alpha_s$ did not have an effect on the intrinsic nucleotide exchange rate. Similar to the results described in the previous section, phosphorylation of $G\alpha_s$ by TAO2 did not attenuate the ability of $G_{\beta\gamma}$ to inhibit nucleotide exchange on $G\alpha_s$. Indeed it appeared that phosphorylated $G\alpha_s$ incubated with $G_{\beta\gamma}$ exchanged GTPγS for GDP less efficiently than the non-phosphorylated form (Figure 3-14B). These data agree with our previous finding that $G\alpha_s$ can be phosphorylated by TAO2 in the GDP bound form in a complex with $G_{\beta\gamma}$.

In the case of $G\alpha_i$ phosphorylation by PKC, it was shown that cAMP production was attenuated when $G\alpha_i$ was phosphorylated. To determine if phosphorylation of $G\alpha_s$ activated TAO2 via a feedback loop, we investigated if elements downstream of $G\alpha_s$ signaling enhanced TAO2 protein kinase activity. Stimulation of $G\alpha_s$ enhances cAMP production and activates PKA. TAO2 protein kinase activity was also activated by elevated cAMP levels.

HEK293 cells were treated with forskolin, an agent that directly activates adenylyl cyclase, and endogenous TAO2 was immunoprecipitated and assayed for kinase activity. Compared to control samples, forskolin-treated cells demonstrated a 2-fold activation of the protein kinase (Figure 3-15A). Forskolin also activates p38 and both p38 activation and TAO2 activation can be inhibited by pre-treating cells with H89, a pharmacological inhibitor of PKA (Figure 3-15B and C). These experiments indicate that TAO2 is capable of regulating $G\alpha_s$ directly by phosphorylation, and that enhanced $G\alpha_s$ signaling resulting in elevated cAMP levels may cause activation of TAO2, possibly by PKA. This is also consistent with our finding that PKA can phosphorylate TAO2 *in vitro* (data not shown).

IV. Discussion

Activation of GPCRs eventually leads to downstream signaling by protein kinases, but the methods by which the protein kinase pathways are activated by GPCRs are varied. Some of these pathways utilize intermediates such as PKA, PKC, non-receptor tyrosine kinases, and in some instances, second messengers generated by G protein-regulated effectors. GPCRs can transactivate receptor tyrosine kinases and indirectly enhance signaling through MAPK cascades. Evidence is accumulating that signaling through protein kinases allows for feedback control of pathway activity by directly modulating the activity of G proteins themselves or their effectors.

We have shown that $G\alpha_s$ is a TAO2 interactor from a two-hybrid screen. However, we were not able to confirm the interaction *in vivo* or *in vitro* using pull-down experiments. $G\alpha_s$ was isolated using (1-320) D169A; a fragment of TAO2 that is catalytically deficient so

that weaker interactions with substrates may be trapped. This suggests that the interaction of $G\alpha_s$ with TAO2 is weak or transient in nature an potentially explains why it could not be reliably detected under the conditions in which *in vitro* pull down experiments are conducted. *In vivo*, the interaction may occur in membrane micro-domains or indirectly via other as yet unidentified proteins or modifications. The cell lysis conditions used for our co-precipitation assays may have disrupted critical interactions with bridging proteins or removed modifications that strengthen the interaction. TAO2 has a large C-terminal domain that contains a number of coiled-coil motifs as well a region that is hydrophobic in nature and may bind membranes. All i*n vitro* binding experiments were carried out with the kinase domain fragment of TAO2 that lacks these distal regions. TAOs are large proteins, full length TAO2 is poorly expressed in both mammalian cells and bacterial expression systems limiting our studies to the use of small fragments. C-terminal fragments of TAO2 should be tested in directed two-hybrid tests and *in vitro* binding assays to locate additional regions in the C-terminus that may be required for the interaction. Given our data that TAO2 may phosphorylate the α subunit in the heterotrimeric state, it is envisioned that TAO2 may make multiple contacts or use a large surface area to interact with the trimeric complex. Detailed analysis of conditions required for optimal extraction of both proteins in the presence or absence of stimuli will have to be carried out to isolate this complex. A surprising outcome of our experiments is that TAO2 also interacts with $G_{\beta\gamma.}$ We were able to confirm this interaction by transient transfection experiments as well as immunoprecipitation of endogenous proteins. TAO2 contains a motif conserved in other $G_{\beta\gamma}$ effectors. The QxxER motif is present in the fragment (320-620) in TAO2 that interacts with $G_{\beta\gamma}$. A construct of

TAO2 that is truncated just before the QxxER motif fails to bind $G_{\beta\gamma}$. Further experiments will define the requirement of this motif in binding to $G_{\beta\gamma}$ using peptide competition assays. Hence, unlike the $G\alpha_s$ interaction, it appears that TAO2 and $G_{\beta\gamma}$ interact in a more direct manner. Perhaps it is via $G_{\beta\gamma}$ that TAO2 interacts with $G\alpha_s$ and identifying conditions to isolate the inactive heterotrimer will allow us to observe the TAO2-$G\alpha_s$ interaction.

TAO2 phosphorylated $G\alpha_s$ *in vitro* with a stoichiometry approaching 1 mol phosphate/mol $G\alpha_s$. Phosphorylation of $G\alpha_s$ subunits by protein kinases they ultimately regulate constitutes a feedback loop that is a powerful means of manipulating the strength and duration of signaling from G proteins. Phosphorylation of $G\alpha$ subunits is thought to enhance signaling in two ways: by inhibiting $G_{\beta\gamma}$ binding that sequesters the $G\alpha$ in the inactive heterotrimeric state, and by inhibiting binding of RGS proteins that reset the activation by enhancing hydrolysis of bound GTP to GDP. Frequently, the site of phosphorylation is at the N-terminus of $G\alpha$ subunits on the α-helix that is used for interaction with both $G_{\beta\gamma}$ as well as RGS proteins. We demonstrated *in vitro* that TAO2 phosphorylated $G\alpha_s$ on Thr9 on the N-terminal helix using AlF_4^- protection and limited tryptic proteolysis assays. We will determine if this site is phosphorylated in cells by labeling cells with ^{32}P-orthophosphate and monitoring phosphorylation on this site by knocking down TAO2 using siRNA. This experiment is important for determining the *in vivo* relevance of this site and whether it is a critical determinant of $G\alpha_s$ signaling. *In vitro* TAO2 preferentially phosphorylates the inactive GDP bound form of $G\alpha_s$. We also found that including $G_{\beta\gamma}$ in these assays had no effect on phosphorylation. In other experiments phosphorylated $G\alpha_s$

showed no intrinsic difference in GDP-GTPγS exchange. The significance of TAO2 phosphorylating the heterotrimer is unclear but perhaps phosphorylation is not an activating mechanism but rather a means of limiting signaling from the Gα subunit by stabilizing its inactive state.

The extreme N-terminal helix of Gα subunits is also crucial for interacting with GTPase activating proteins (GAPs) such as those of the RGS family. Only one RGS protein has been identified for $G\alpha_s$ compared to the numerous GAPs that regulate other Gα members (Zheng et al., 2001). How the association and regulation of $G\alpha_s$ by RGS-PX1 is manipulated by post-translational modification is unknown at present. We attempted to evaluate phospho-$G\alpha_s$ regulation of cAMP production using a reconstituted cyclase assay (Rodbell, 1971) as well as in GAP assays with fragments of RGS-PX1 (Zheng et al., 2001). Preliminary experiments to deduce how phosphorylation may affect $G\alpha_s$ signaling have not yielded conclusive results. One reason for this may be that the fraction of $G\alpha_s$ that is phosphorylated in our assays is not sufficient to produce significant differences in phenotype. Kinase assay conditions that increase the fraction of phosphorylated $G\alpha_s$ or phospho-mimetic mutants will be utilized in the future. Reagents for knock-down of TAOs as well as G protein subunits are available. We can now use loss-of-function experiments to assign roles for TAO2 and G proteins *in vivo* using siRNA. Activation of endogenous p38 by various GPCR agonists will be tested in relevant cell types in the background of TAO2 and Gα/βγ knockdowns. The activation of TAO2 by overexpression of $G\alpha_s$ and βγ subunits will also be attempted to determine relative contributions of these subunits in signaling to TAO2. Tests of all possible

functions have not been completed. Thus no clear hypothesis that accounts for potential regulatory interactions of TAO2 and G proteins can be formulated. Further experiments such as those described above will help identify the biological relevance behind the binding and phosphorylation events we have observed *in vitro*.

BAIT	INTERACTOR	NUMBER OF INSERTS	FUNCTION
TAO2 (1-320)	Bup1a	1	Metabolism
	Ldb1a	5	Lim domain binding protein
	HNFα dimerization cofactor	1	Transcription
	CAPS	2	Calcium activated protein for vesicular sorting
	TAO3	1	Kinase
TAO2(1-320)D169A	Neuroendocrine Differentiation factor (NDF)	1	Unknown function
	Zinedin	5	Putative B subunit (PP2A)
	Bup1a	1	Metabolism
	ERK3	1	Kinase
	MEK6	1	Kinase
	Gαs	1	G protein
TAO2 (320-620)	Microspherule 1a	<20	Unknown function. FHA domain
	B56ε (PP2A)	1	B subunit (PP2A)
	Kif3A	3	Kinesin

Table 3-1. TAO2 interactors rescued from two-hybrid screens with a neonatal mouse brain cDNA library. TAO2 D169A is kinase dead mutant.

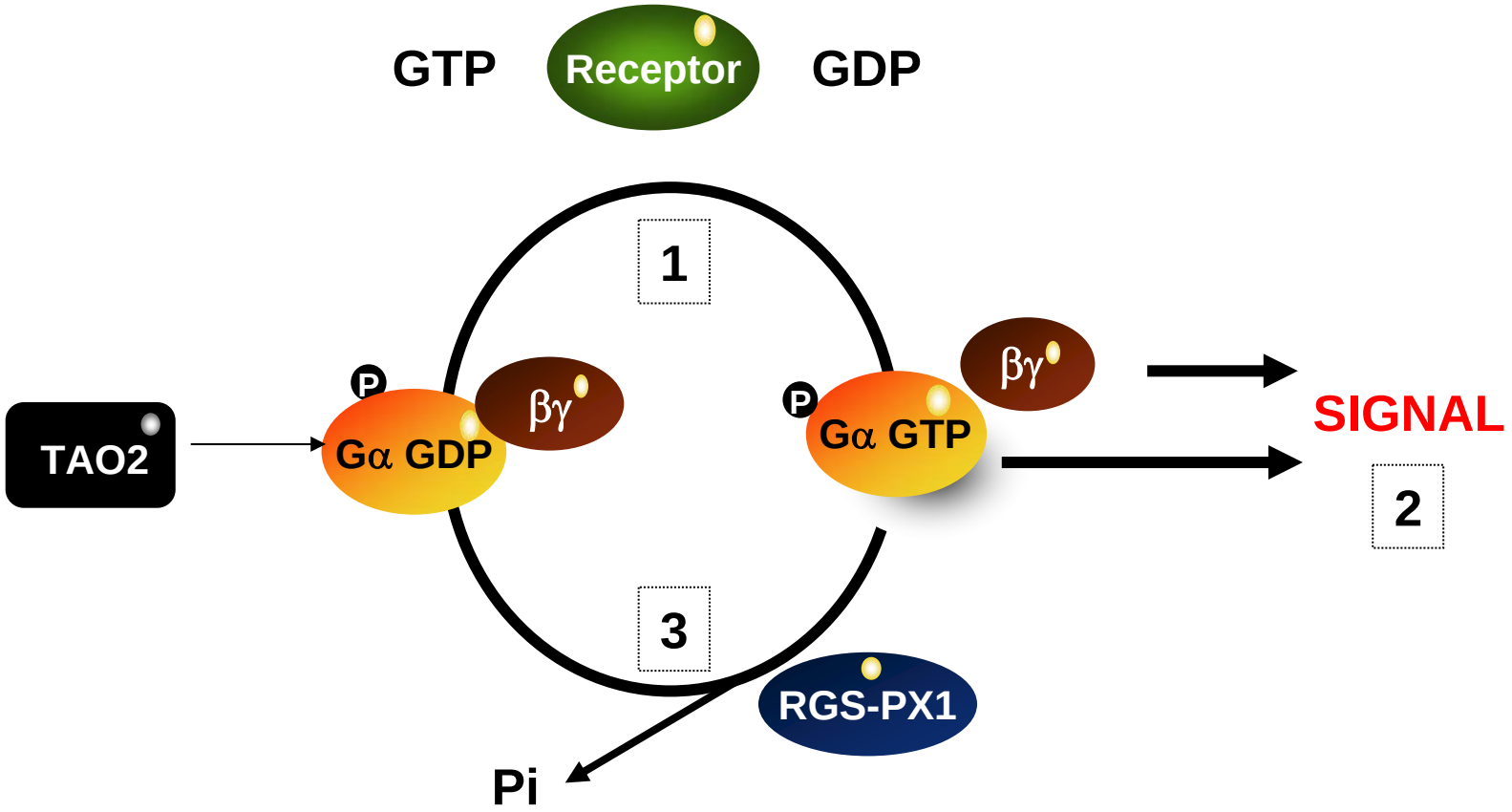

Figure 3-1. G protein GTPase cycle. See text for details

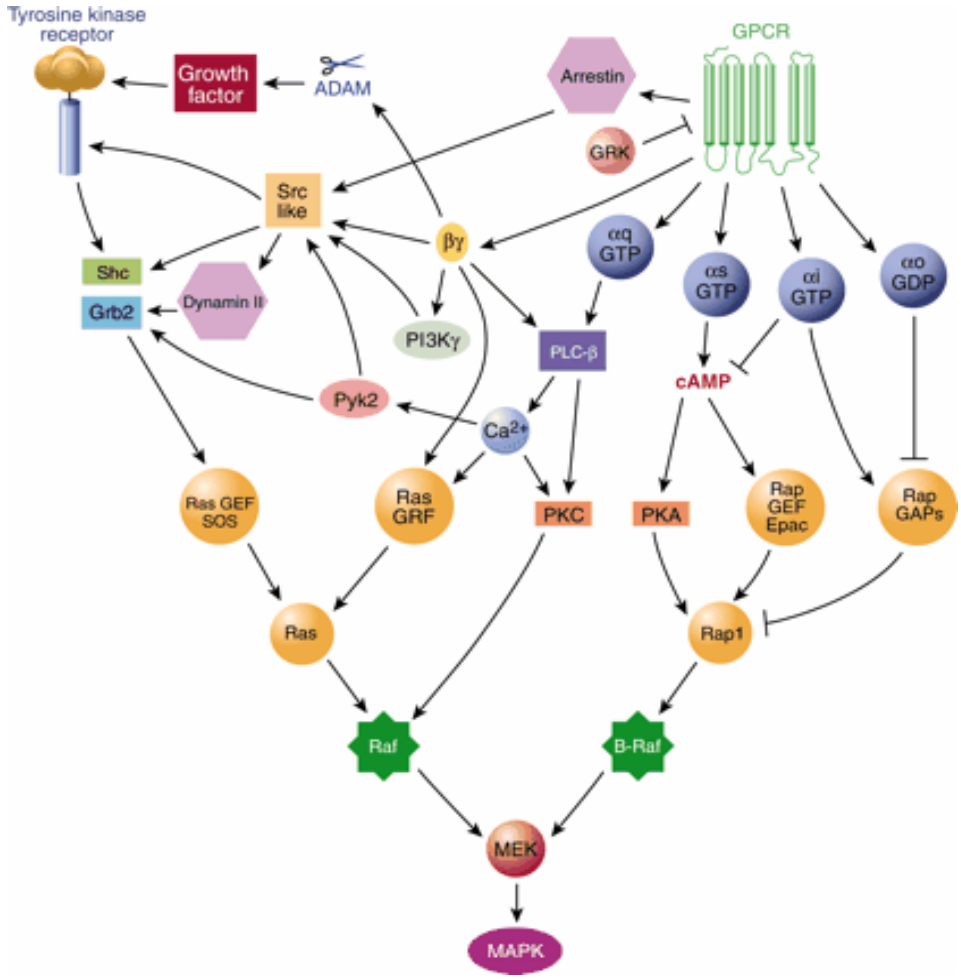

Figure 3-2. GPCRs activate MAPK signaling by different mechanisms (From Gutkind, 2001). Reprinted from Gutkind,J. S. (2000) Regulation of Mitogen-Activated Protein Kinase Signaling Networks by G Protein-Coupled Receptors. Science's STKE: http://www.stke.org/cgi/content/full/OC_sigtrans;2000/40/re1□□

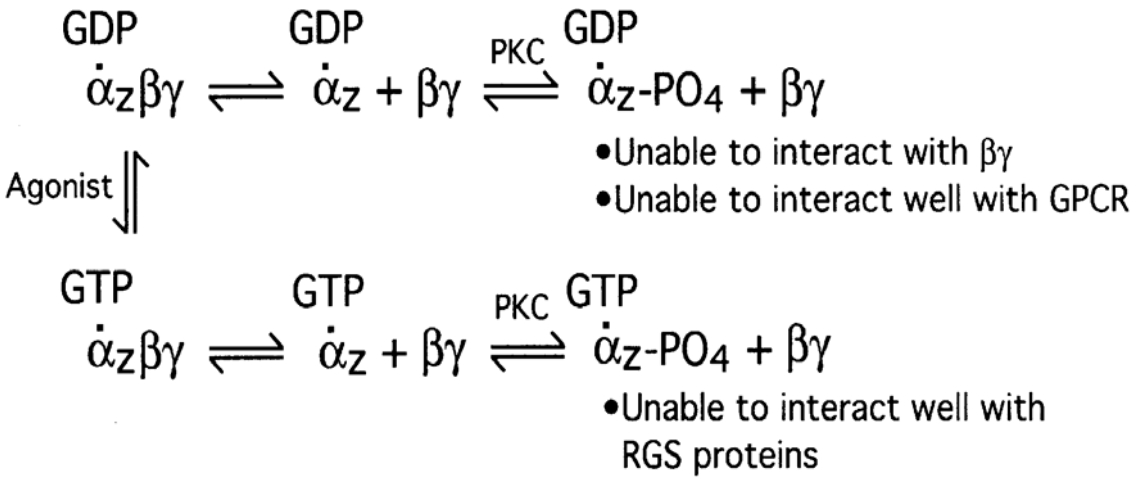

Figure 3-3. Phosphorylation of Gα subunits (for example $G\alpha_z$) inhibits Gβγ binding and GAP activity of RGS proteins (From Chen and Manning, 2001). Reprinted from Oncogene, Vol 26, Chen and Manning, Regulation of G proteins by covalent modification, 1643-1652, Copyright (2001), with permission from Nature publishing group.

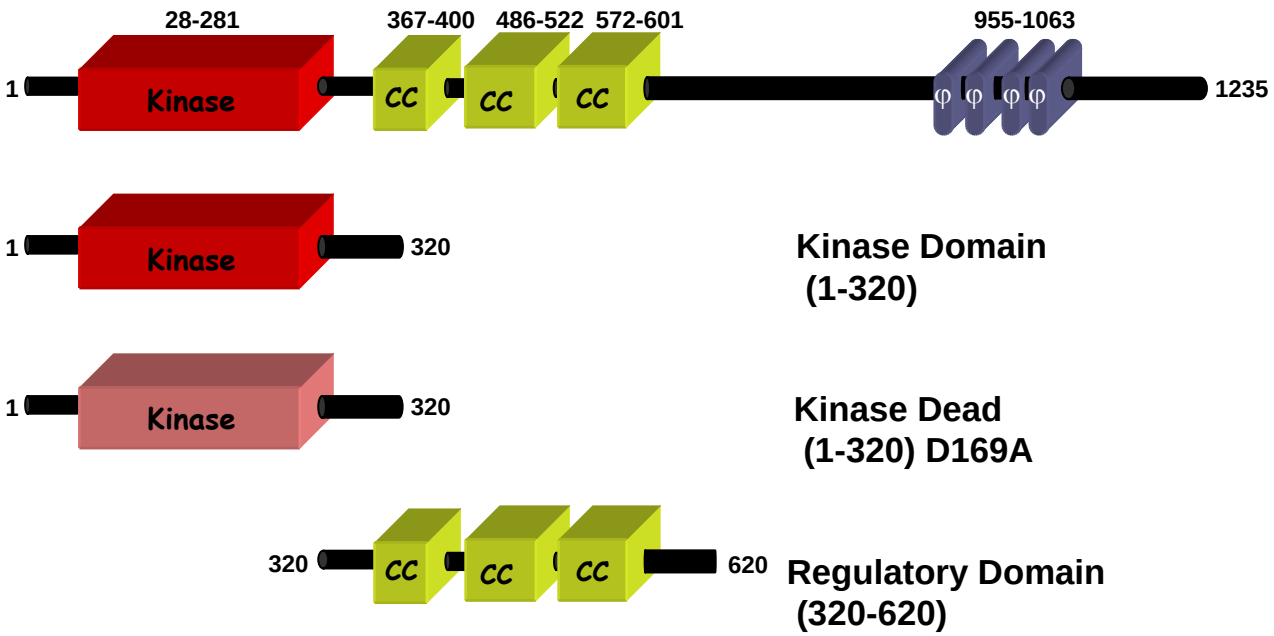

Figure 3-4. TAO2 baits constructed for two-hybrid screens.

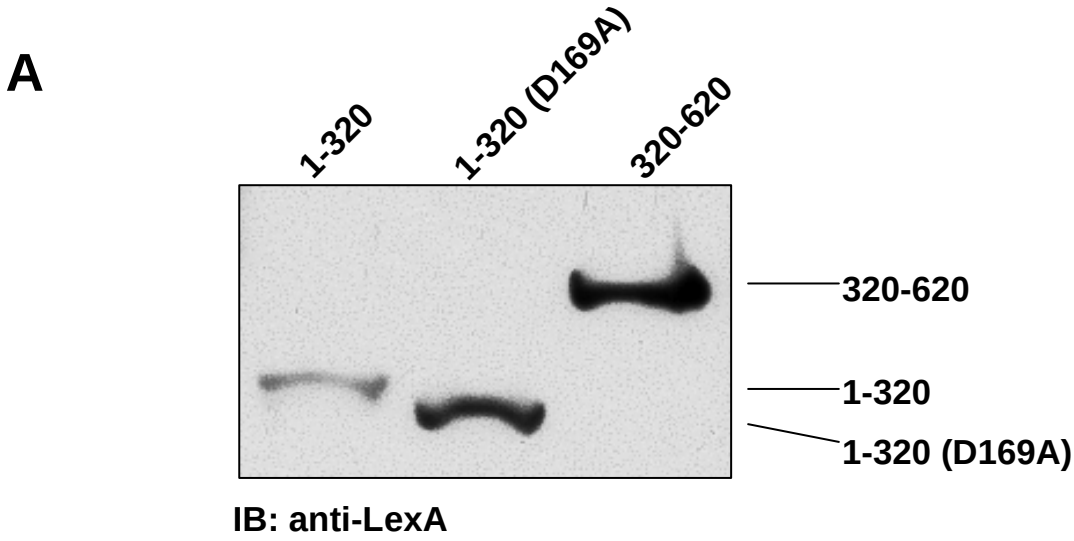

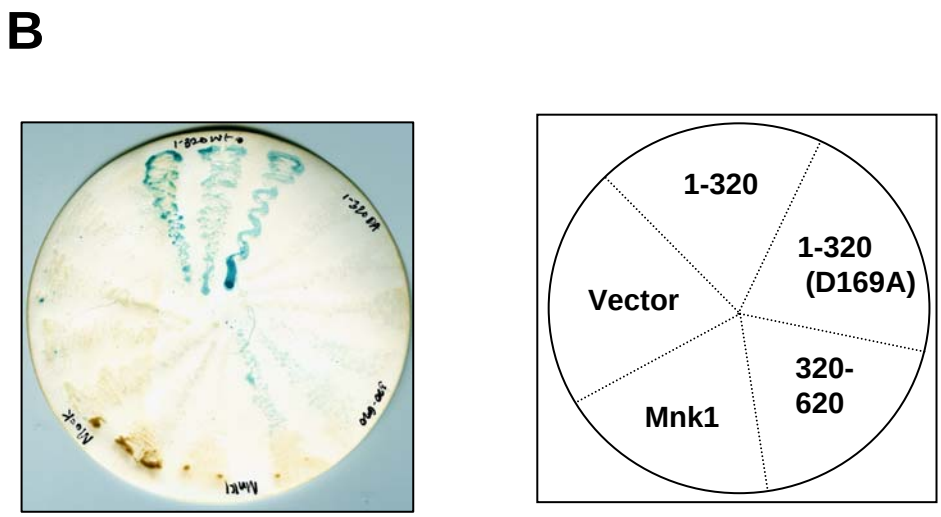

Figure 3-5. Expression of yeast two-hybrid baits. (A) Expression of TAO2 baits in L40. Yeast lysates were probed with anti-LexA antibody. (B) Autoactivation of baits: baits were transformed into L40 and streaked out onto dropout medium, autoactivation was determined by growth and blue color in β-galactosidase assays.

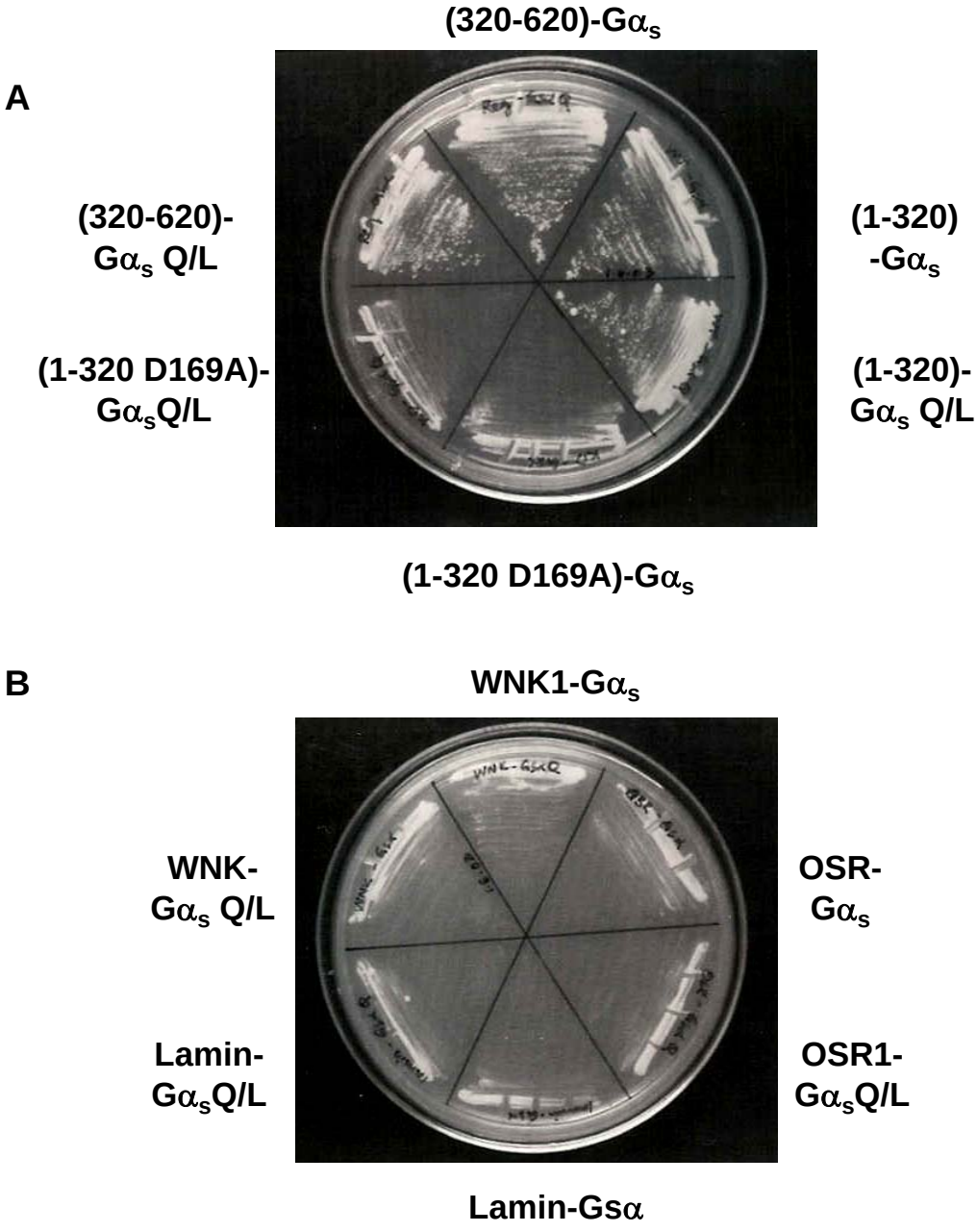

Figure 3-6. Pair-wise two-hybrid tests of interaction between TAO2 baits and $G\alpha_s$. (A) TAO2 baits (1-320, and 320-620) interacted with both wild-type and constitutively active $G\alpha_s$ subunits. Kinase dead TAO2 interacted weakly. (B) Negative controls. $G\alpha_s$ did not interact with WNK1, OSR1 or lamin.

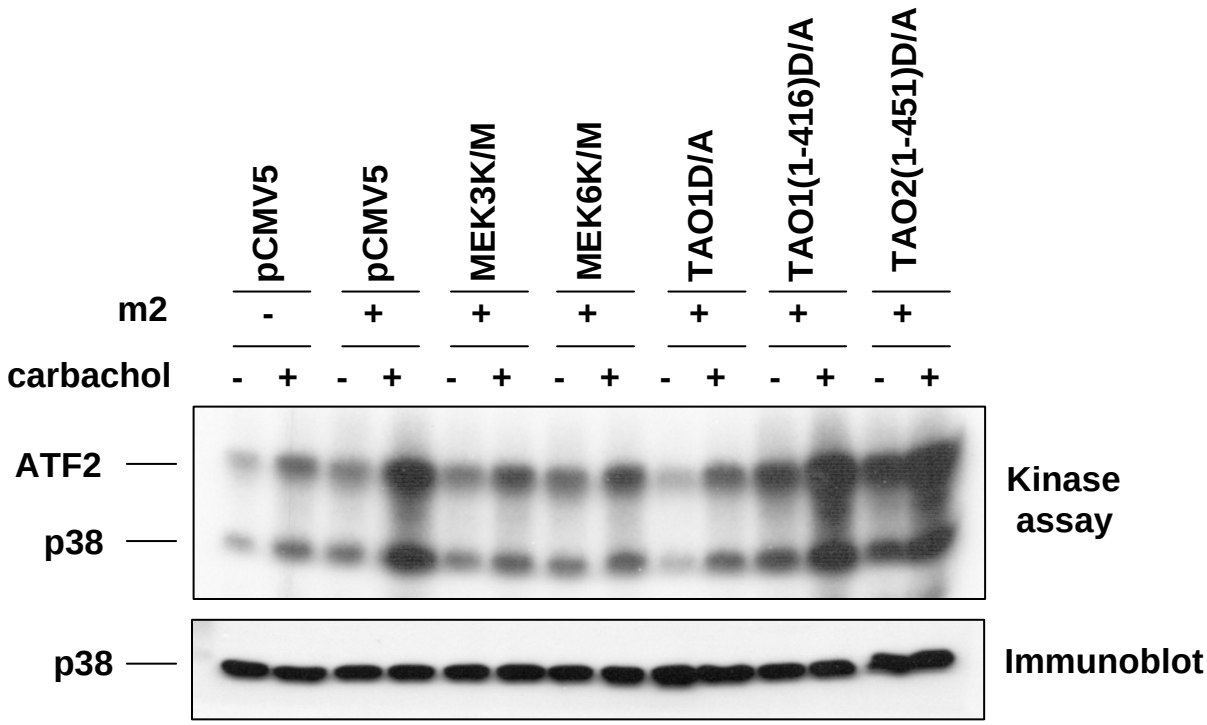

Figure 3-7. TAO2 is required for activation of p38 by muscarinic receptors. HEK293 cells were transfected with the indicated TAO and MEK dominant negative constructs with or with out co-expression of the m2 receptor. Cells were stimulated with 10 μM carbachol and the activity of p38 was determined in an immune-complex kinase assay with ATF2 as substrate (From Chen et al., 2003).

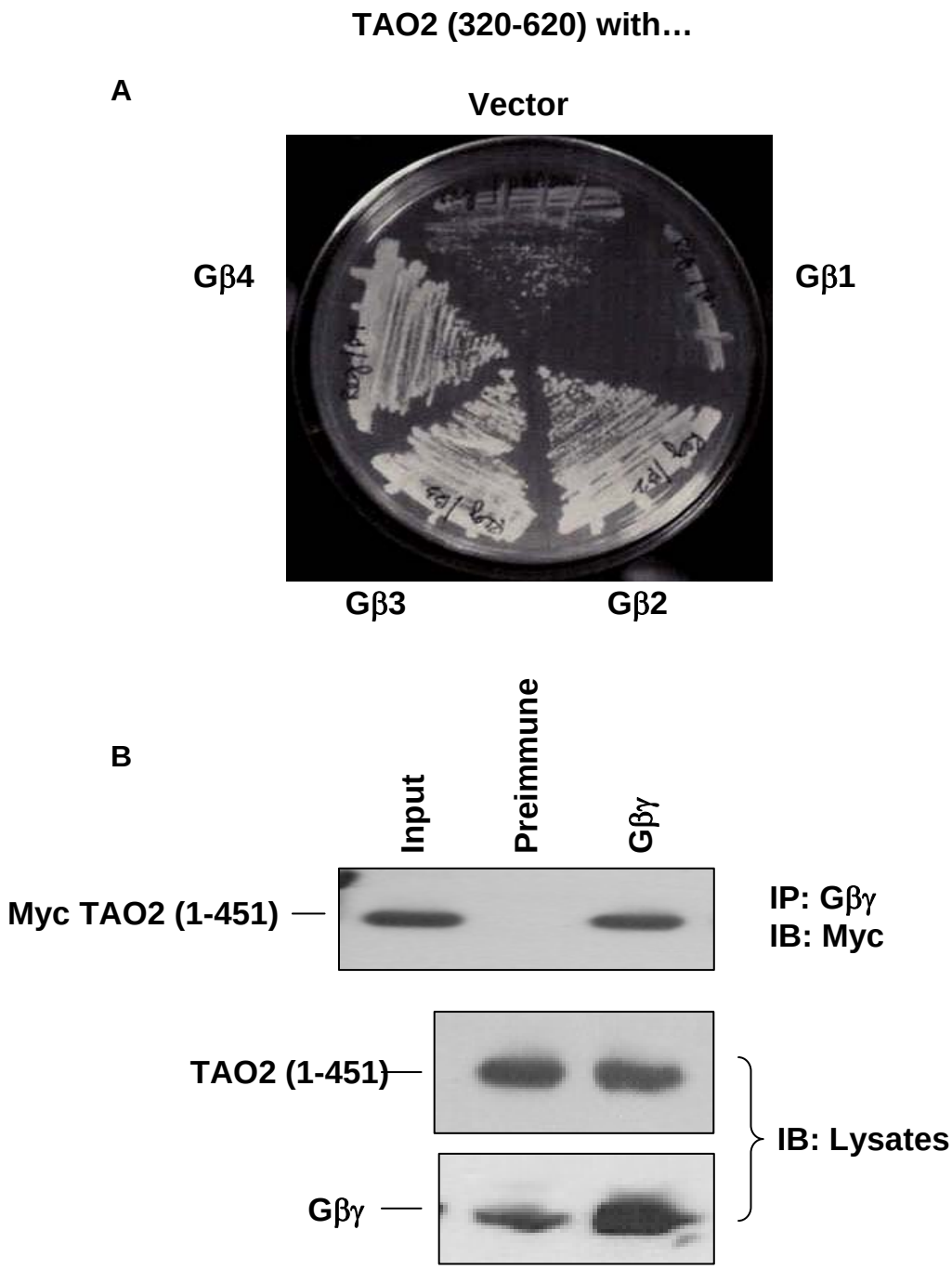

Figure 3-8. TAO2 interacts with Gβγ subunits. (A) Pair-wise yeast two hybrid of interaction between TAO2 (320-620) and Gβ1-4. (B) Myc- TAO2(1-451) was transfected into HEK293 cells. Endogenous Gβγ subunits were immunoprecipitated and interaction with Myc-TAO2 detected. IP: Immunoprecipitation, IB: Immunoblotting (Continued on next page).

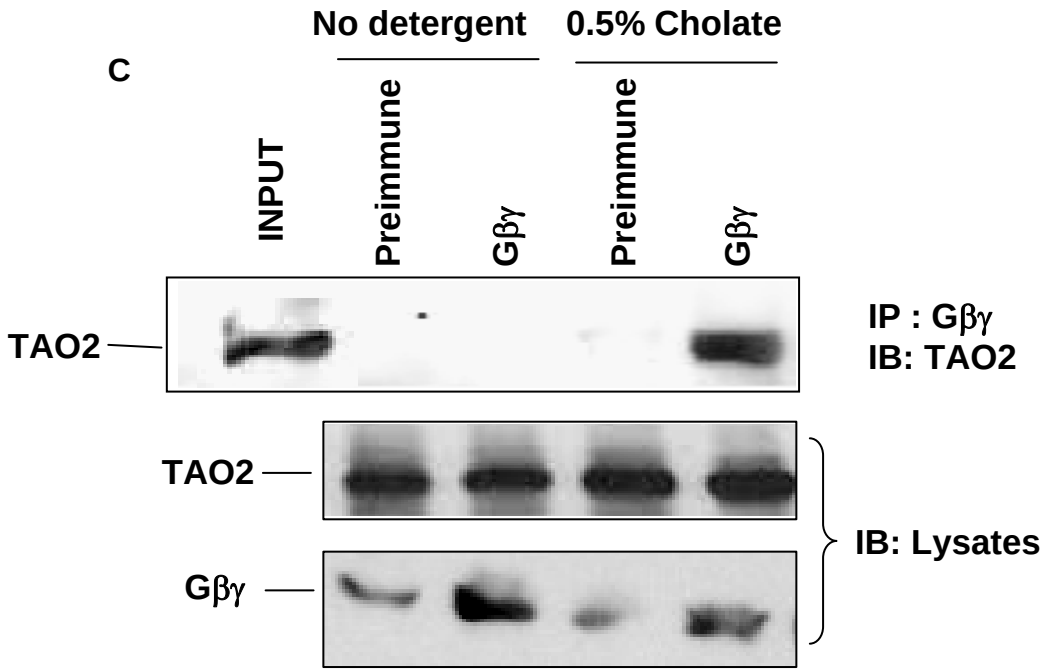

Figure 3-8. (C) Membrane extracts were prepared from HEK293 cells either in the presence or absence of 0.5% cholic acid. Endogenous Gβγ subunits were immunoprecipitated and associated TAO2 was detected. TAO2 did not bind to preimmune immunoprecipitates.

A

```
b-ARK1   VEETQIKERKC
b-ARK2   VEETQIKDKKC
    AC4  QDTQQDAERSC
    AC2  QEHAQEPERQY
   TAO2  ARAAQAEERKF
    AC7  GHENQDLERKH
  GIRK-1 AITNNSKERHN
Consensus  .... Q .. ER. .
```

B

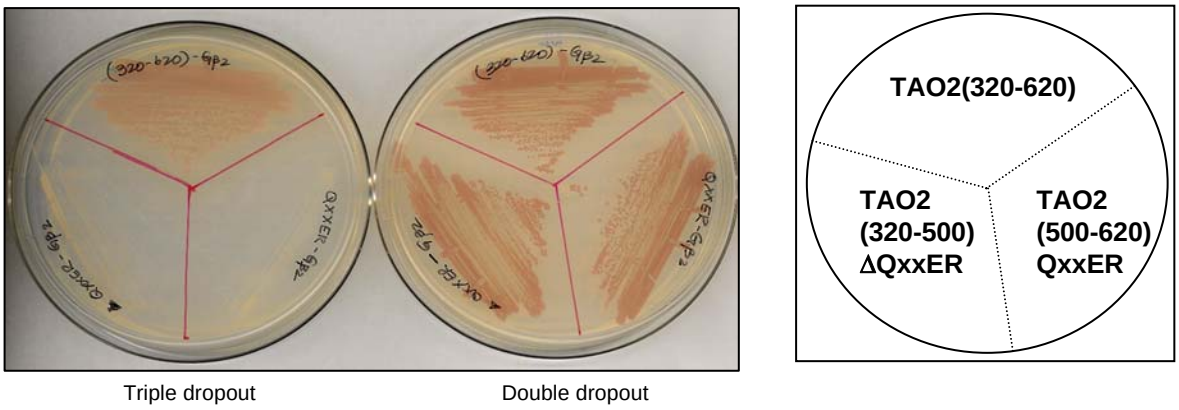

Figure 3-9. TAO2 contains a Gβγ interaction motif (A) Comparison of amino acid sequences from Gβγ interactors containing the Q-x-x-E-R motif. (B) Pair-wise two hybrid interactions between TAO2 (320-620), TAO2 (500-620) QxxER or TAO2 (320-500) ΔQxxER with Gβ2. Left plate: triple drop-out medium (-WHL), right plate: double drop-out medium (-LH).

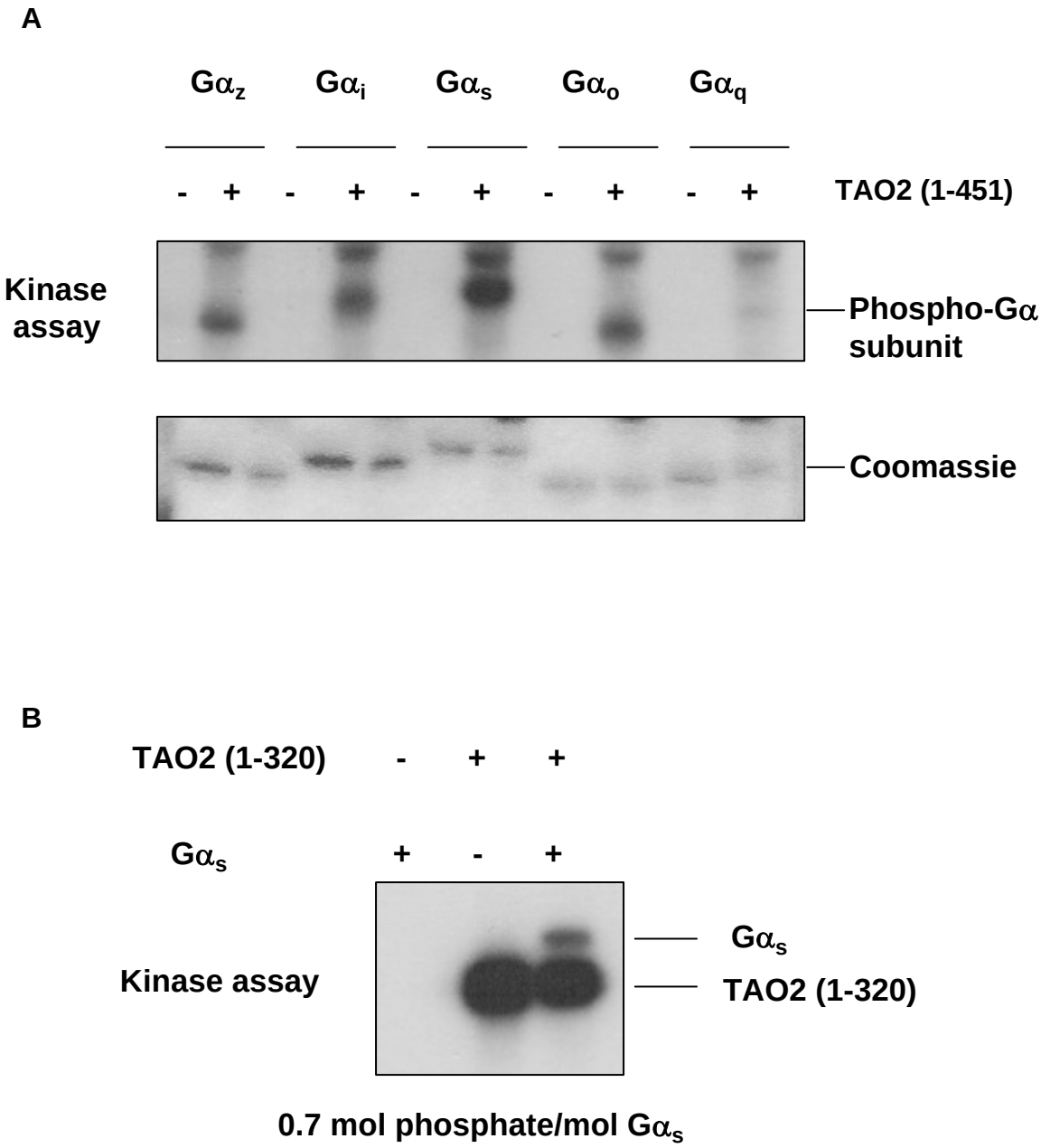

Figure 3-10. TAO2 phosphorylates $G\alpha_s$. (A) Endogenous TAO2 immunoprecipitated from HEK293 cells phosphorylated a number Gα subunits. (B) TAO2 (1-320) purified from Sf9 cells phosphorylated $G\alpha_s$ with a stoichiometry of 0.7 mol phosphate/mole $G\alpha_s$ [n = 2(A) or 4(B)].

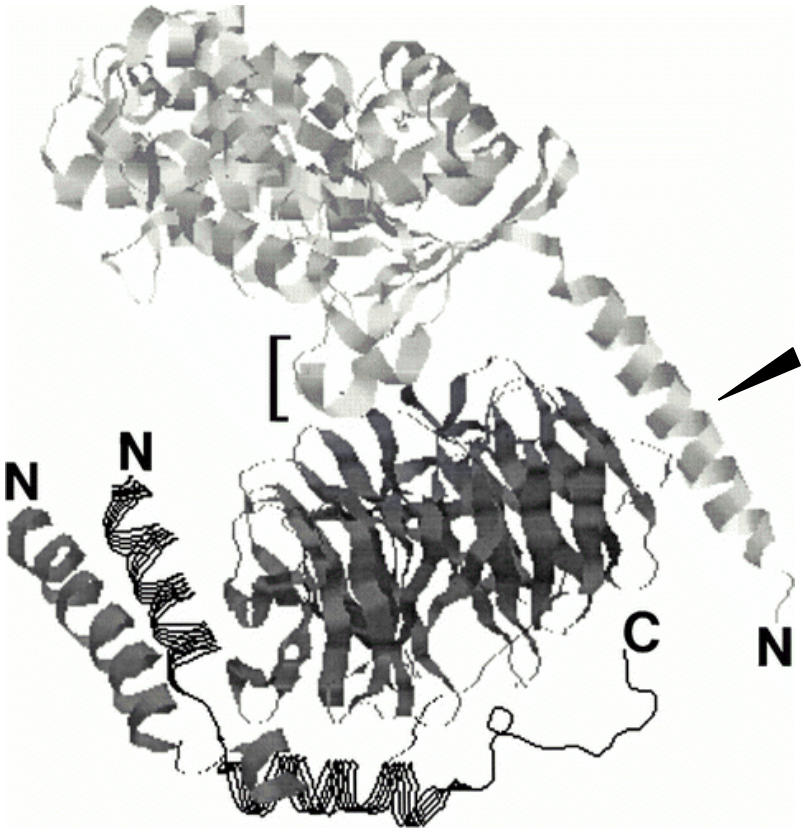

Figure 3-11. Structure of G protein heterotrimer.$G\alpha_s$ (light grey) shown in complex with Gβ (dark grey) and Gγ (black lines). Note the N-terminal helix (arrow-head) from Gα making contact with Gβ. (From Clapham, 1997).

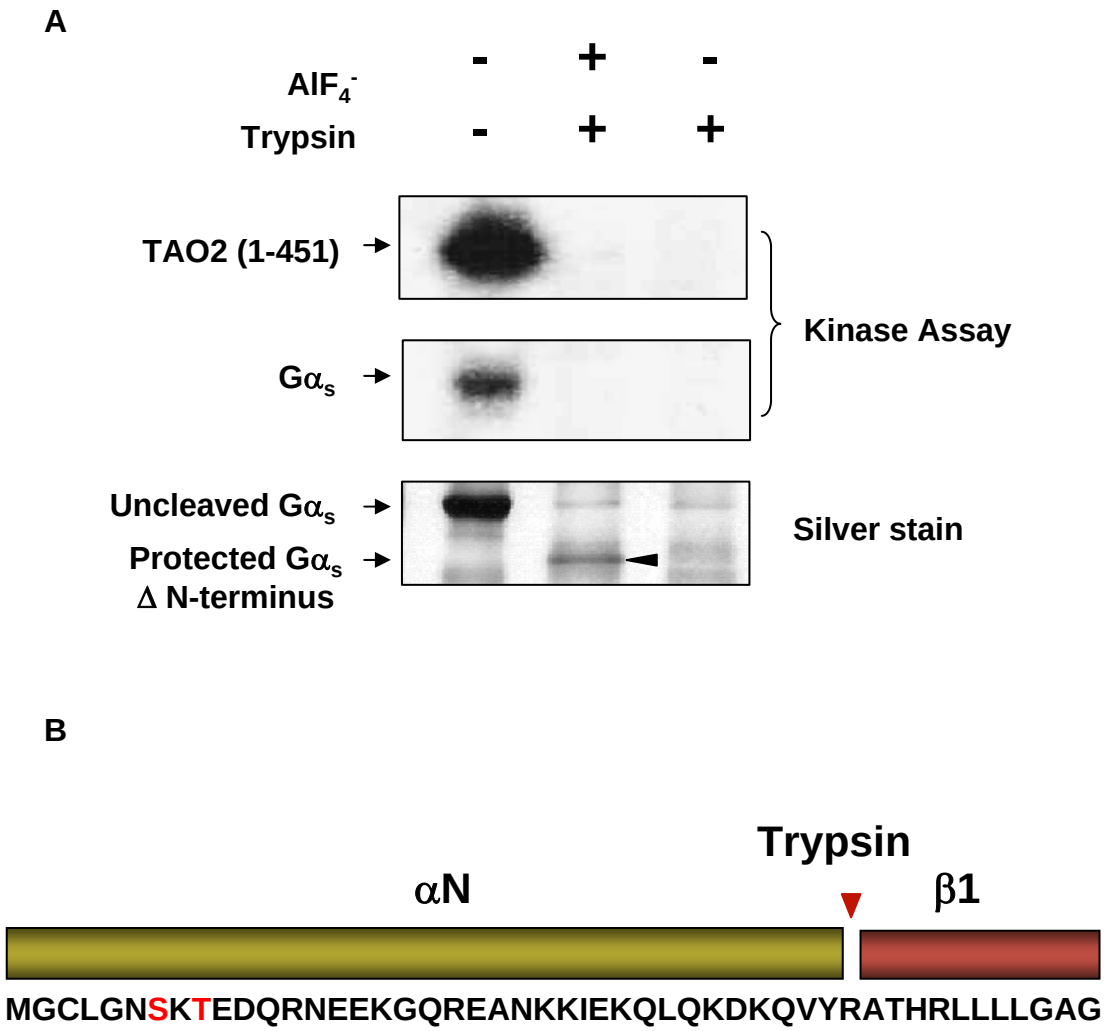

Figure 3-12. Limited tryptic proteolysis of $G\alpha_s$. (A) $G\alpha_s$ is phosphorylated on the N-terminal helix as determined by tryptic digestion after AlF_4^- protection. Phosphate incorporation is lost when N-terminal helix is proteolyzed (lane 2). (B) Schematic representation of trypsin cleavage site on $G\alpha_s$ (Arg29) and the position of the Ser7 and Thr9 (n = 4) (Continued on next page).

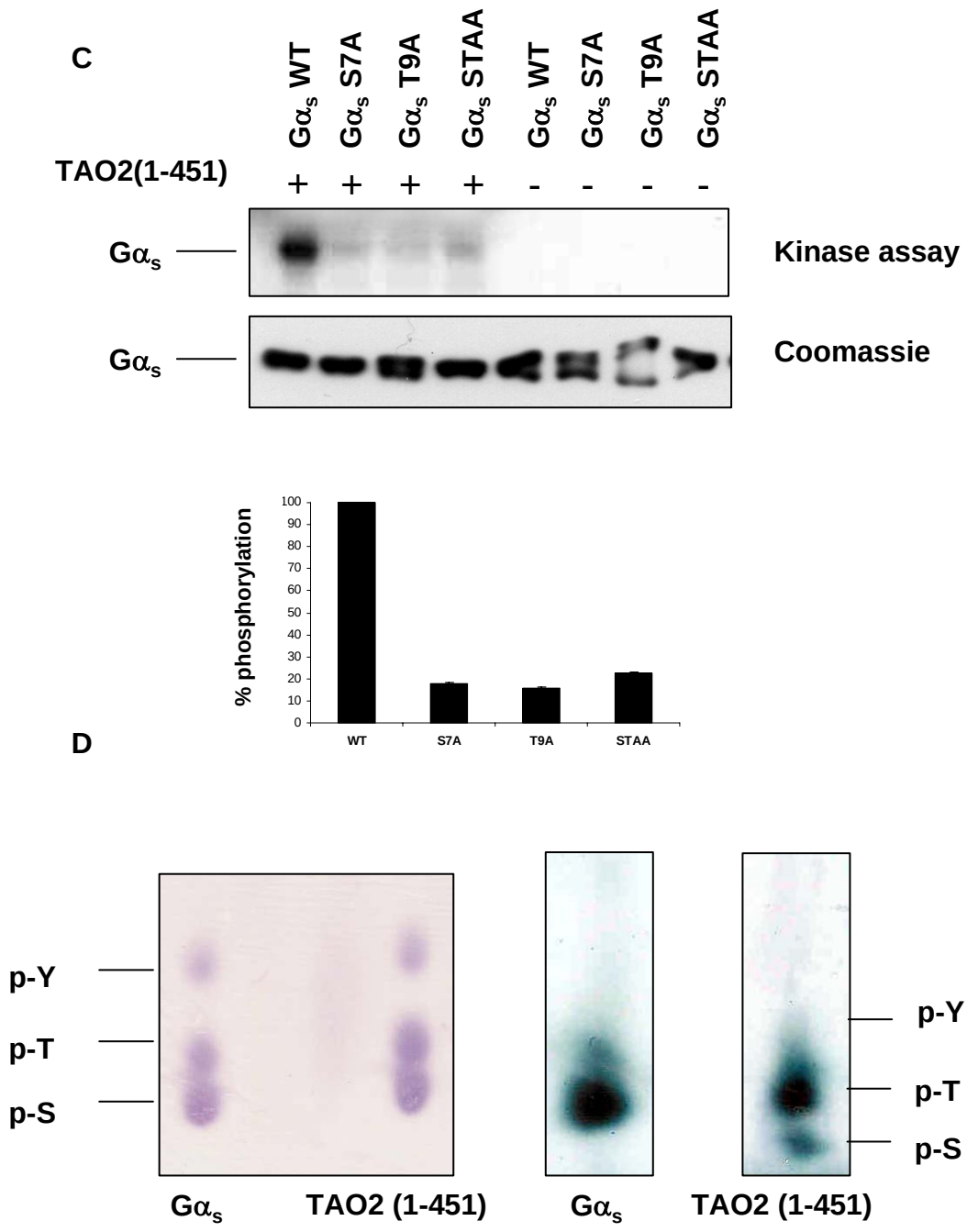

Figure 3-12. (Continued) TAO2 phosphorylates $G\alpha_s$ on Thr9. (A) Kinase assay of TAO2 (1-451) with wild-type or S7A/T9A $G\alpha_s$. (B) Phosphoamino acid analysis of TAO2 (1-451) and $G\alpha_s$. $G\alpha_s$ is phosphorylated on threonine (n = 2).

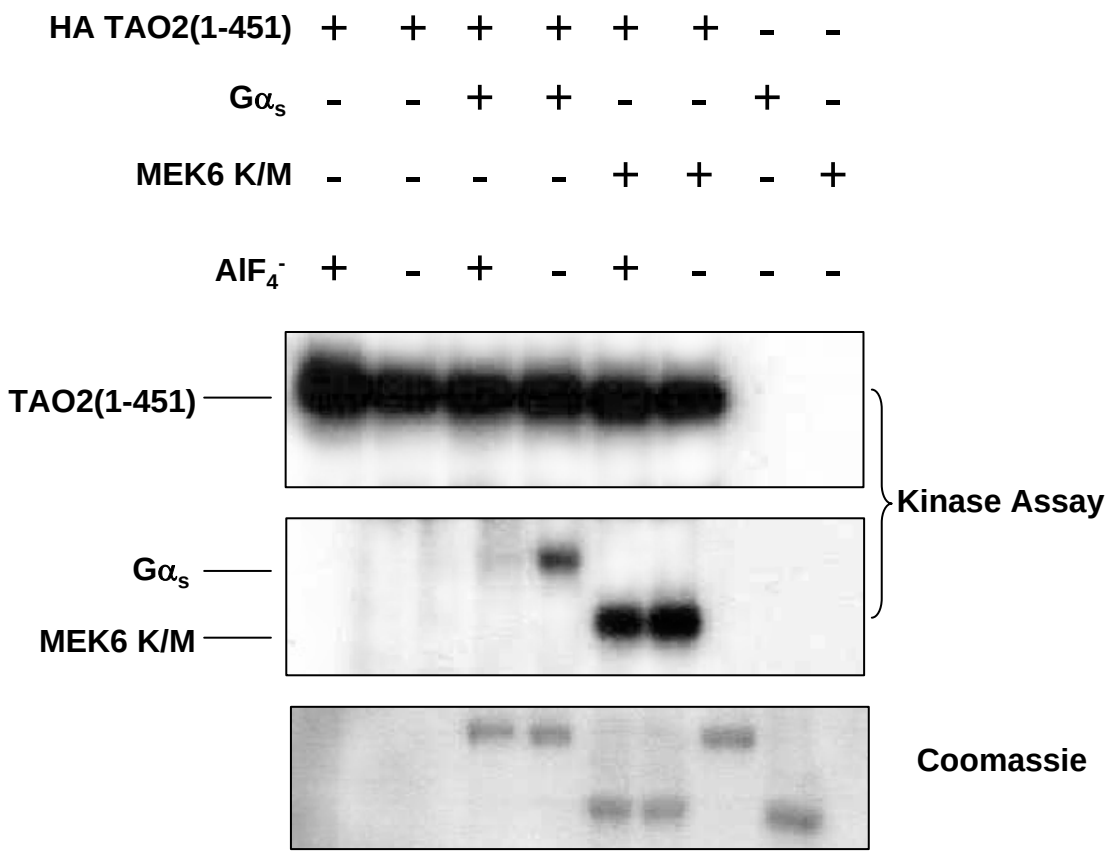

Figure 3-13. TAO2 phosphorylates GDP-bound $G\alpha_s$. TAO2(1-451) was immunoprecipitated from HEK293 cells and used to phosphorylate $G\alpha_s$. $G\alpha_s$ was either inactive/GDP bound or activated with AlF_4^- or GTPγS. MEK6K/M was used as a control and was not affected by AlF_4^- treatment (n = 3).

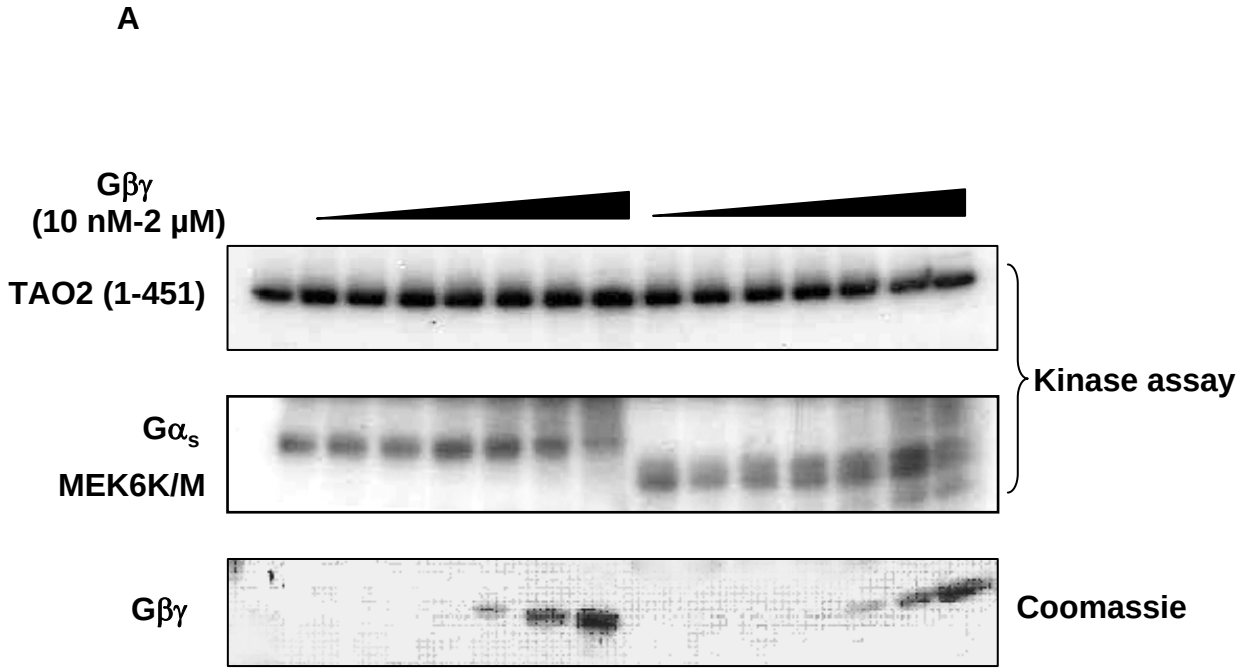

Figure 3-14. Gβγ does not inhibit phosphorylation of $G\alpha_s$ by TAO2. TAO2 (1-451) transfected and immunoprecipitated from HEK293 cells. Kinase assays were performed with either $G\alpha_s$ or MEK6K/M in the presence of increasing Gβγ concentrations (10 nM to 2 μM) (n = 3).

B

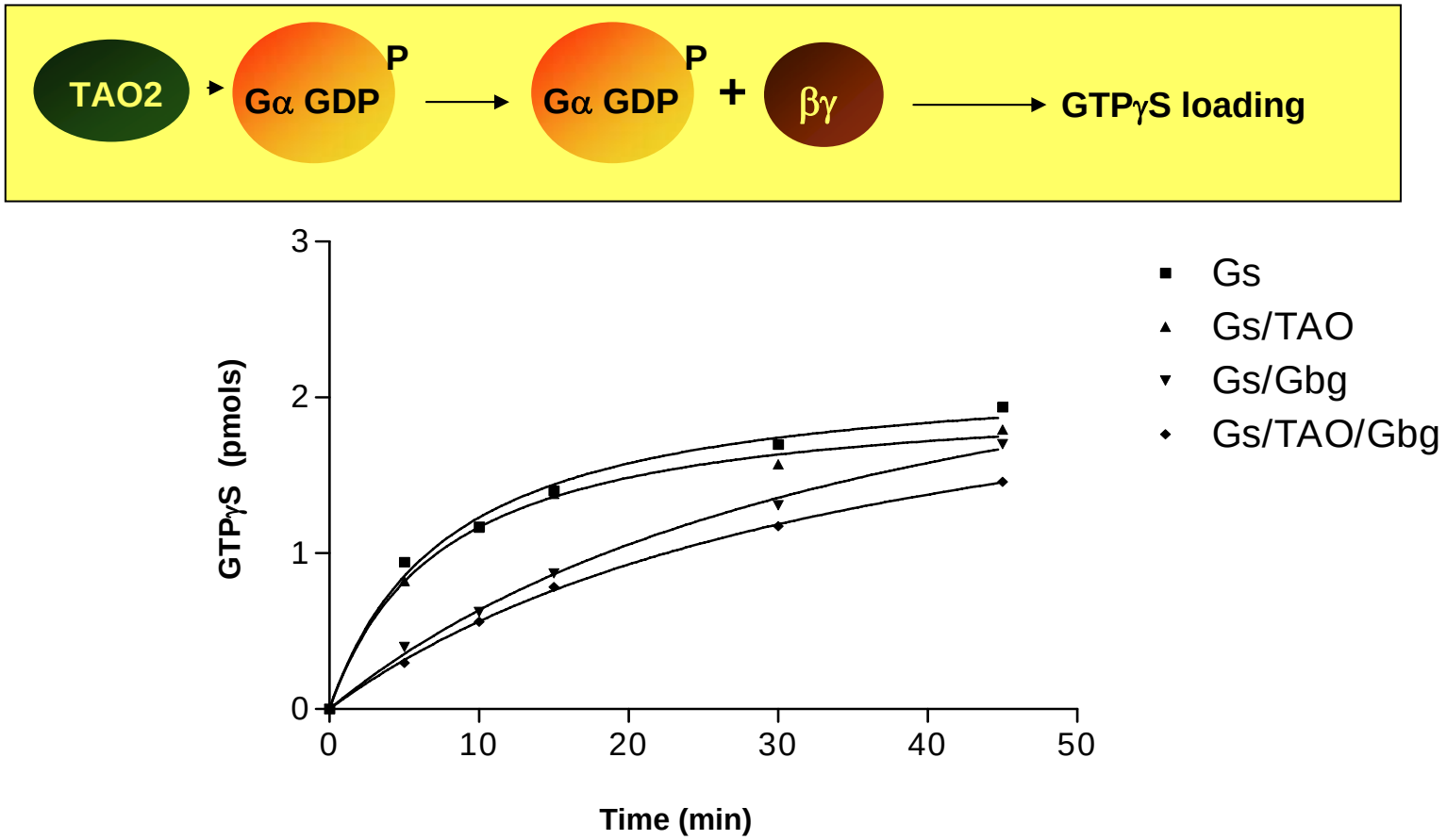

Figure 3-14. Phosphorylation of $G\alpha_s$ does not inhibit $G\beta\gamma$ binding. $G\alpha_s$ was phosphorylated with TAO2 (1-320) and then incubated with $G\beta\gamma$. The ability of phospho-$G\alpha_s$ to exchange GDP for GTPγS was determined.

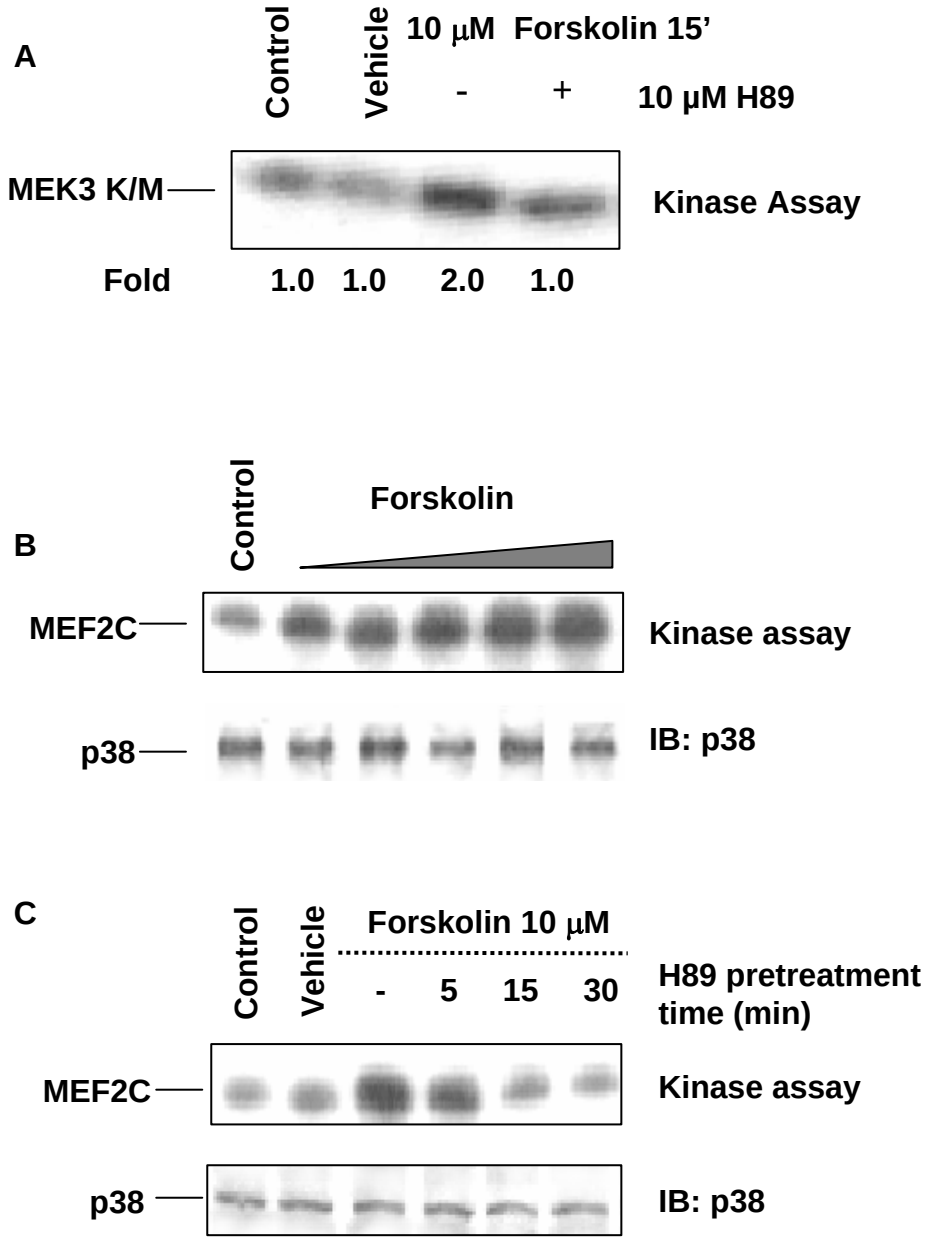

Figure 3-15. TAO2 and p38 are activated by cAMP. (A) HEK293 cells were treated with 10 μM forskolin in the presence or absence of 10 μM of the PKA inhibitor H89. Endogenous TAO2 was immunoprecipitated from cell lysates and assayed for activity with MEK6KM as substrate. (B) p38 was activated in a time-dependent manner by forskolin. (C) Activation of p38 by forskolin was inhibited by pretreatment of cells with H89 (n = 4).

CHAPTER 4. TAO KINASES REGULATE THE DNA DAMAGE CHECKPOINT VIA p38 MAPK

I. Abstract

In an effort to identify physiological stimuli that utilize TAO2 to activate intracellular signaling pathways, I screened for agents that activated the endogenous protein kinase in a variety of cell types. Several stimuli tested were capable of consistent activation of TAO2, but two that stand out are agents that cause DNA damage such as ultraviolet radiation (UV) and ionizing radiation (IR). Activation was not restricted to TAO2 alone, as both TAO1 and TAO3 also displayed similar modes of activation. The DNA damage response (DDR) is controlled by both the ataxia telangiectasia mutated (ATM), and ATM and Rad50-related (ATR) PI-3 kinase-related kinases (PIKK), as well as p38 MAPK. ATM and ATR control checkpoints by phosphorylating and activating the Chk2 and Chk1 protein kinases respectively, while p38 plays a similar role by activating its substrate MAPKAP kinase 2 (MK2). While both the p38 and the ATM and ATR checkpoint pathways collaborate in the initiation and execution of the checkpoint, it is unknown if cross talk exists between these pathways. Although MEK3/6 are known to be required for the activation of p38 in response to DNA damage, components further upstream have not been conclusively identified. Here we showed that the TAO kinases can activate p38 in response to various genotoxic stimuli. Full-length and truncated fragments of dominant negative TAOs inhibit p38 activation by UV and Hydroxyurea (HU). Knockdown of TAOs using siRNA either singly or in combination, also recapitulated this result. Further, TAOs bind one another as well as p38,

indicating that there may be a preformed signaling complex of these protein kinases within cells. Cells in which TAO1 and 3 have been knocked-down are less capable of engaging the UV-induced G2/M checkpoint, and mitotic cyclin/Cdc2 remained activated. ATM/ATR phosphorylated TAO3 in cells treated with hydroxyurea; and TAO and p38 activation was compromised in cells from a patient with ataxia telangiectasia (AT) (lacking the ATM protein kinase). These findings indicate that TAO kinases are regulators of p38-mediated G2/M checkpoint activation in response to DNA damage. All three TAOs may be substrates of ATM/ATR and this may explain the rapid activation of p38 by DNA damage.

II. Introduction

Evolutionarily conserved mechanisms exist in cells to sense and respond to aberrances in genomic content. Without such mechanisms, deleterious mutations would be passed on to subsequent generations and diminish organismal viability. This process, known as the DNA damage response (DDR), is executed by a network of proteins that include sensors that detect the damage, halt the cell cycle, repair the sites of damage, and activate apoptosis if repair is insufficient to alleviate the insult. It is remarkable that only a handful of evolutionarily conserved proteins take part in this process, given that DNA damage can be caused by many different agents that cause different types of damage. ATM and ATR Ser/Thr kinases are key players in this pathway. These proteins orchestrate all aspects of the DDR from short term events such as regulation by phosphorylation to long term programs such as transcription (Bakkenist and Kastan, 2004). While the two protein kinases share

some overlapping functions, ATM responds primarily to ionizing radiation-induced double strand breaks (DSBs), while ATR detects damage induced by UV and replication inhibitors.

The roles of ATM and ATR are not restricted to the classical DDR, as they act to prevent genomic instability. For example, ATM has been shown to localize with telomere ends during the G2 phase of the cell cycle. Telomeres are the ends of chromosomes and resemble double-strand DNA breaks. If the DDR were to recognize the natural chromosome ends as damaged DNA, repair would be initiated and would result in chromosome fusion. Mitosis in the presence of fused chromosomes would lead to breakage and fusion cycles and eventual genomic instability (Sherr, 2004). The possibility that every chromosome end would be recognized as damaged DNA has been circumvented in a number of ways. The telomeres loop back onto themselves and invade the telomeric repeats to form a structure known as the t-loop. Thus, the free ends of the telomeres are masked and bypass surveillance. Another mechanism employed is the recruitment of telomere interacting proteins such as telomere repeat binding factor 1/2 (TRF1/2) and protection of telomeres 1 (Pot1) that also aid in masking the ends by catalyzing t-loop formation and suppressing ATM protein kinase activity (Karlseder et al., 2004). However, recent studies have shown that ATM localizes to telomere ends during G2 phase of the cell cycle when Pot1 is displaced. More interestingly, this interaction is not a classical DDR because the checkpoint kinase Chk2 is not activated and γH2A.X foci are not formed (Verdun et al., 2005). Hence, it is hypothesized that ATM interaction with telomeres results in the recruitment of end-processing machinery that is required for the formation of the chromosome end-protection complex.

ATM also has functions in V(D)J recombination, although the exact mechanism is not entirely clear. V(D)J recombination is the mechanism by which a diverse repertoire of immunoglobulins and T cell receptors are generated from a small set of genes. DSBs are generated at the ends of the recombination targeting sequences by the RAG1 and 2 proteins. Although $ATM^{-/-}$ mice, as well as patients with AT show normal repertoires of antigen-bearing lymphocytes, and efficiently carry out V(D)J recombination with exogenous substrate, AT patients as well as ATM null mice have lymphoid malignancies associated with translocations in antigen receptor genes. Perkins et al., have shown that ATM, upon phosphorylation on Ser1981, was recruited to sites of V(D)J recombination without activation of DDR substrates. These findings imply that ATM function can be modulated by associating with proteins from different pathways. In fact, ATM/ATR substrates are still being identified, and the consequence of phosphorylation is not always immediately apparent. For example, ATM has been shown to phosphorylate LKB1 *in vitro* and *in vivo* on a SQ site in an IR-dependent manner, but whether this is required for the DNA damage response is unknown (Sapkota et al., 2002). A combination of bioinformatics approaches to search for ATM/ATR consensus phosphorylation sites, and biochemical experiments will aid in the identification of ATM/ATR substrates and pathways governed by these protein kinases.

While the response to damaged DNA is quite complex and involves multiple proteins, it can minimally be viewed as the activation of cell cycle checkpoints. Chk1 and Chk2 are the effectors phosphorylated by ATR and ATM, respectively. Chk1 and Chk2 engage cell

cycle checkpoints after DNA damage (Zhou and Bartek, 2004). These kinases halt the cell cycle by indirectly controlling the activation of cyclin/CDK complexes.

It has long been known that many cellular stressors like heat shock, osmotic stress and microtubule depolymerization induce cell cycle arrest via robust activation of p38. Furthermore, studies suggest that p38 MAPK may also regulate the cell cycle checkpoints in response to DNA damage (Bulavin et al., 2001; Wang et al., 2000). It has been shown that the p38 MAPK plays an important role in regulating the G1/S and the early G2/M checkpoints in response to UV radiation by its ability to phosphorylate MAPKAP Kinase-2 (MK2) at Thr344 thereby activating MK2. Active MK2 phosphorylates Ser323 in Cdc25B as well as Ser216 in Cdc25C. These two phosphorylation sites lie within the 14-3-3 binding site (Manke et al., 2005). It is controversial whether ionizing radiation also causes a similar activation of p38/MK2, although one study has shown that the IR-induced G2/M checkpoint is mediated by an activation of MEK6 and p38γ (Wang et al., 2000). Interestingly, this study also proposed that the activation of p38 by IR was ATM dependent, because p38 activation in response to IR was diminished in $ATM^{-/-}$ fibroblasts. How does DNA damage induce p38 activation? No evidence exists for the direct phosphorylation of p38 by ATM or ATR, nor are there reports of direct interactions between p38 and damaged DNA. Given the compromised p38 activation in AT cells, ATM/ATR-mediated regulation of p38 is indirect. If so, the MAP3Ks in this pathway remain to be identified and perhaps one or a number of these enzymes may mediate the signal from ATM/ATR to p38.

In an effort to identify physiological ligands that activate TAO kinases, we identified UV, IR, and HU as agents that activated TAOs to a similar if not greater extent than sorbitol,

which was previously considered a significant activator of TAOs. Dominant negative TAOs inhibited UV- and HU- induced activation of p38 MAPK. siRNA of TAO protein kinases also inhibits p38 activation. RNAi of TAO family members inhibits checkpoint activation in response to UV. TAOs interact among themselves as well as with p38. In AT cells, activation of TAO2 and p38 by IR is diminished. These findings suggest that TAOs may be phosphorylated by ATM/ATR and are upstream components of p38 signaling cascades that are activated by DNA damage.

III. Material and Methods

Cell Culture and Treatments

HEK 293, and Hela cell lines were obtained from ATCC. Hela S3 cells and U2-OS osteosarcoma cells were gifts from Hongtao Yu (Department of Phamacology). Human skin fibroblasts from a normal individual (1BR3) and a patient with AT (AT-V) were gifts from Benjamin Chen (Department of Radiation Oncology). HEK-293, HeLa, HeLa-S3 and U2-OS cell lines were maintained in Dulbecco's modified Eagle's medium (DMEM) supplemented with 10 % fetal bovine serum (FBS) and 2 mM glutamine. 1BR3 and AT-V cells were grown in α-minimal essential medium (MEM) with 10% FBS. For γ-radiation treatments, medium was removed from cells and they were treated from a ^{137}Cs source at 3 Gy, 10 Gy or 20 Gy, depending on experiment. Medium was added back for the duration of treatment. UV activation experiments were performed with 254 nm (UV-C) using a Stratalinker 2400 (Stratagene) at 20-80 J/m^2 in the same manner as above for various times. Cells were treated with 2 mM HU (Sigma) overnight for 20 hrs.

Cloning and siRNA oligonucleotides

Full length TAO3 was amplified by PCR from HEK 293 cDNA and ligated into pCMV5 and p3XFLAG-CMV7.1 (Sigma), and the sequence was verified by automated sequencing. Phosphorylation site mutants on TAO3 (S324A, S359A, S782A and the triple mutant), and TAO1 (T502A, T643A, T785, and S990A) were produced by Quikchange mutagenesis according to the manufacturer's instructions (Stratagene). Dominant negative TAO 1 and 2 mutants were described elsewhere (Chen and Cobb, 2001; Hutchison et al., 1998). TAO3 (1-442) wild type and D165A were amplified by PCR from full length constructs and ligated into p3XFLAG-CMV7.1. Full length Chk2 and Cdc25C in p3XFLAG-CMV7.1 were gifts from Helen Piwnica-Worms (Washington University in St.Louis). Fragments of Chk2 [SQ/TQ cluster domain (SCD) (1-97), FHA (97-220), SCD/FHA (1-220) and kinase domain (215-543)] were PCR amplified and ligated into pGEX-KG. Cdc25C (200-259) was amplified by PCR and ligated into pGEX-KG. The pcDNA3-FLAG ATM and pBJ5.1-FLAG ATR (wild type and kinase dead) were kind gifts from Michael Kastan (St. Jude's Children's Hospital, Tennessee) and Stuart Schreiber and Karlene Cimprich (Harvard University, Stanford University respectively) respectively. All constructs were verified by sequencing. Due to the large size of full length ATM and ATR, they frequently undergo recombination events in *E.coli.* Plasmid DNA was transformed into DH10α using standard protocols and cultured for 1 hr at 30°C. Cells were plated on Luria-Bertani (LB) plates supplemented with 100 μg/ml ampicillin and colonies were allowed to form for 48 hrs at 30°C. Colonies that form within 24 hrs represent the rearranged clones and those that form

after 48 hrs are wild-type (Shiloh et al., 1998). Colonies were amplified by growth in LB-ampicillin broth for 48 hrs at 30°C and plasmid DNA was isolated by standard alkaline lysis. Plasmids were verified by sequencing as well as with restriction enzyme digestion with NcoI which produces fragments corresponding to 0.4Kb, 0.8Kb, 1.8Kb and 3.5Kb.

Small interfering oligonucleotides corresponding to the TAO1 sense strand 5'-CCAGGCCAGGUGAAACUUGdTdT-3' and the antisense strand 5'-CAAGUUUCACCUGGUCUGGdTdT-3' and the TAO3 sense strand 5'-GGACAGUAUGAUGGGAAAGdTdT-3' and the antisense strand 5'-CUUUCCCAUCAUACUGUCCdTdT -3' were from purchased from Ambion. TAO2 siRNA oligonucleotides were purchased from Ambion and all oligonucleotides used at a final concentration of 100 nM. The siRNAs were used according to the manufacturer's recommendations and were transfected into trypsinized cells with oligofectamine (Invitrogen) using the suggested protocol. A second round of siRNA transfections was performed at 48 hrs and cells were harvested after indicated treatments after another 24 hrs (total time 72 hrs).

Transfection and Co-immunoprecipitation

HEK 293 or Hela cells were trypsinized and transfected simultaneously with Fugene (Roche) as per the manufacturer's instructions into 60 mm dishes. For dominant negative experiments, 3 μg of pCMV-HA-TAO1 D169A, pCMV-Myc-TAO2 (1-451) D169A and pCMV-3XFLAG-TAO3 (1-442) D165A were used. Cells were allowed to recover for either 48 hrs and then treated with UV, or for 24 hrs and then treated with HU for a further 20 hrs

as described above. For co-immunoprecipitation experiments, 3 μg of the indicated plasmids were co-transfected into HEK293 cells and harvested after 48 hrs. Cells were washed once in 1X phosphate buffered saline (PBS) and then lysed with Buffer A (50 mM HEPES [pH 8.0], 150 mM NaCl, 0.5% Triton X-100, 10 mM sodium fluoride, 10 μg/ml aprotonin, 2 μg/ml leupeptin, 10 μg/ml pepstatin, 2 mM Na_2VO_3 and 1 mM PMSF) for dominant negative and siRNA experiments. For co-immunoprecipitations, cells were harvested in Buffer A without detergent and supplemented with 10% glycerol, 15 mM $MgCl_2$ and 20 mM EGTA. Lysates were rocked at 4°C for 10 min and then clarified by centrifugation at 14,000 rpm for 15 min. Protein concentrations were determined by Bradford assay (Biorad) and quantified with an Emax microplate reader (Molecular Devices). Immunoprecipitation was carried out using ~0.6 mg total lysate with indicated antibodies.

Antibodies and immuno-blotting

Antibodies to Chk1/2, phospho-ATM/ATR substrate, phospho (Tyr15)-Cdc2 and MAPKAP kinase-2 were obtained from Cell Signaling Technologies. Goat-TAO3 antibody was purchased from Serotec and mouse TAO1 antibody was obtained from BD Biosciences. TAO2 and p38 antibodies have been described elsewhere (Chen et al., 1999).

Proteins in sample buffer were fractionated by SDS-PAGE-gels and transferred onto nitrocellulose membranes (Schleicher and Schuell). Membranes were blocked in 5% non-fat milk in TBS-T (20 mM Tris-Cl, 0.5 M NaCl, 0.1% Tween-20) and incubated with the indicated antibodies as per the manufacturer's instructions. Signal was detected with horse

radish peroxidase (HRP)-conjugated secondary antibodies and using enhanced chemiluminescence (ECL).

Immunofluorescence

All experiments were performed in duplicate using cells grown on two coverslips per condition. HeLa cells were fixed and permeabilized for 10 min in methanol at −20°C. Cells were then blocked for 60 min in PBTA (1× phosphate-buffered saline, 5% bovine serum albumin, 0.1% Tween-20). TAO2 antibodies were used at a 1:5000 dilution in PBTA for 1 hr at room temperature followed by washing and secondary antibody staining with Alexa 488 (Molecular Probes) for 30 min at 37°C. Cells were washed and mounted with Polymount. Images of HeLa cells were acquired at magnifications of ×63 using a Zeiss Axiocam microscope equipped with an Orca II Hamamatsu black and white charge-coupled device camera.

Expression of recombinant proteins and kinase assays

Expression of GST-MEF2C (204-321) was induced with 1 mM IPTG in BL21 (DE3) *E.coli* as previously described (Chen et al., 2003). Expression of GST-Cdc25C (200-259), full length GST-Chk2, and the fragments SCD, FHA, SCD/FHA, and kinase domain were induced at 1 mM IPTG at 37°C for 4 hrs. Cells were lysed in Buffer B (1 mM EDTA, 10 mM Tris-Cl [pH 7.4], 1 mM DTT, 1 mM PMSF 1 μg/ml leupeptin, 1 μg/ml pepstatin A, 1 mM benzamidine) and sonicated. The lysate was then pelleted by centrifugation at 35,000 rpm for 45 min at 4°C. The supernatant was incubated with 1:1 (vol/vol) slurry of glutathione agarose

beads (Sigma) in Buffer C (100 mM KCl, 1 mM EDTA, 20% glycerol, 20 mM HEPES [pH 7.6], 1 mM DTT, 1 μg/ml leupeptin, 1 μg/ml pepstatin A, and 1mM benzamidine) for 3 hrs at 4°C. The beads were washed in Buffer C and bound proteins were eluted with 10 mM glutathione in Buffer C. Proteins were dialyzed in 150 mM NaCl, 5% glycerol, 20 mM HEPES [pH 7.6], and protease inhibitors. Samples were spin-concentrated (Amicon) and protein concentrations were determined as before.

Kinase assays were performed in 30 μl reactions containing 10 mM $MgCl_2$, 10 μM ATP, 15 cpm/fmol [γ-^{32}P] ATP, 1 mM DTT and 10 mM HEPES [pH 7.5]. Approximately 10 pmol of GST-MEF2C, GST-Cdc25C (200-259) or His_6-MEK6K82M was used as substrate in these assays. Myelin basic protein (MBP) was used at a final concentration of 0.3 mg/ml. Reactions were performed at 30°C for 30 min and terminated with the addition of 5X SDS sample buffer. Samples were boiled briefly and resolved by SDS-PAGE gels, dried and processed for autoradiography.

Fluorescence activated cell sorting (FACS) analysis

G2/M checkpoint activation was determined by FACS. HeLa S3 cells were synchronized with double thymidine block (Bostock et al., 1971). Cells in log phase were treated with 2 mM thymidine for 18 hrs and then released into thymidine-free serum containing medium for a further 8 hrs. Cells were again blocked with 2 mM thymidine for 15 hrs and then released. Cells in the G1/S boundary were allowed to progress through S phase for 4-6 hrs and then left untreated or irradiated with 10 Gy or 80 J/m^2 UV for 2-6 hrs. Cells were trypsinized and fixed in 70% ethanol overnight at 4°C and permeabilized with 0.25%

Triton X-100/ PBS for 10 min on ice. Cells were stained with 10 μg/ml of the mitotic marker phospho-serine 10-Histone H3 (Upstate) for 3 hrs at room temperature. Following washing, cells were incubated for 30 min at room temperature in the dark with FITC-conjugated goat-anti rabbit secondary (Molecular Probes). Samples were washed and incubated with 0.25 μg/ml propidium iodide, 0.1 mg/ml RNaseA in PBS for 30 min at 37°C and processed immediately for FACS analysis. Data was collected with a Becton Dickinson FACS machine and analyzed using Cell Quest software.

IV. Results

A. TAO kinases are activated by DNA damaging agents

We were interested in identifying agents that stimulated TAO2 kinase activity in cells to identify signaling pathways that may utilize TAO kinases as proximal sensors. HeLa cells were treated with a variety of ligands and cells were harvested at different times. Endogenous TAO2 was immunoprecipitated and activation was measured by its ability to autophosphorylate or phosphorylate the substrate MEK6K82M. This was a kinase dead MEK6, used to remove background autophosphorylation that would interfere with the signal. Receptor tyrosine kinase ligands did not cause significant activation of endogenous TAO2 (data not shown). A number of GPCR agonists such as carbachol, as well as agents that elevate intracellular cAMP levels activated TAO2 2 fold over basal levels(discussed in chapter 3) (Figure 4-1) (Chen et al., 2003). This is commensurate with the activation seen with a known activator of TAO2, sorbitol. Among a number of ligands tested, we found that agents that induced DNA damage activated TAO2. HeLa cells were treated for the indicated

times with either ionizing radiation or the known TAO activator sorbitol. Cells were harvested and the activity of immunoprecipitated TAO2 was determined using kinase dead MEK6. TAO2 was significantly activated by ionizing radiation within 10 min of treatment; activation declined after one hour of treatment. Activation ranged from 5 to 10 fold over basal levels (Figure 4-2A). In contrast, activation of TAO2 by UV and hydroxyurea was a modest 2 fold over basal (Figure 4-2 B and C). We wished to determine if DNA damaging agents activated TAO2 specifically or stimulated all three TAO kinases. To determine this, similar experiments were carried out and the kinase activities of TAO1 and TAO3 were assayed. HU did not significantly alter activation of TAO1 and TAO3. However, both TAO1 and TAO3 were activated several fold over basal by UV and IR (Figure 4-3). TAO1 activation by IR was maximal at 2 hours and decreased at later times. The time-course of activation was similar to that of the known checkpoint kinase Chk2 as determined by phosphorylation of Cdc25C (Figure 4-2A). Consistent with previous studies, p38 was activated robustly (40 fold) by UV within 15 mins of treatment in these experiments. Activation was sustained many hours after the treatment (Figure 4-4). Both IR and HU also activated p38 about 5 fold, with IR-mediated activation observed at later times (2 hours) in agreement with published findings (She et al., 2002). In summary, we have shown that all members of the TAO family show sensitivity to DNA damage. This alludes to a common function for these protein kinases in regulating p38 activation by DNA damaging agents.

B. Dominant negative TAOs block p38 activation by genotoxic stress

To determine if the activation of p38 by DNA damage was mediated by TAOs, the effects of expression of kinase dead TAO mutants was investigated in HEK293 cells. Dominant negative TAO constructs were transfected into 293 cells, and these cells were subsequently treated with either UV or HU to induce DNA damage. Endogenous p38 was immunoprecipitated, and its activity was determined in an *in vitro* kinase assay with MEF2C as substrate. While transfection of these constructs did not alter the basal activity of p38 (data not shown), we found that full-length TAO1 and truncated TAO2 (1-451) inhibited HU-induced activation of p38 by up to 60% (Figure 4-5A). Identical effects were seen with these dominant negative constructs when cells were treated with UV (Figure 4-5B). We did not see blockade by full length TAO2 due to the poor expression of the full length protein (data not shown). Kinase dead TAO3 (a fragment encompassing residues 1-442) also blocked HU activation of p38 and modestly blocked p38 activation by UV (Figure 4-5C). These findings clearly indicate that all three TAOs are required for the activation of p38 by DNA damaging agents.

MEK3 and 6 are TAO substrates and in turn activate p38. The relative contributions of MEK3 and 6 in the activation of p38 by DNA damage are unknown. One study suggested that MEK6 was capable of activating the IR-mediated G2/M checkpoint but the requirement for MEK3 was not examined (Wang et al., 2000). We show that both MEK3 and 6 are required to varying extents for p38 activation. UV-mediated activation of p38 appeared to be primarily through MEK6, as dominant negative MEK6 inhibited p38 kinase activity by 70% relative to control. HU activation of p38 also appeared to be dependent on MEK6 with 90%

inhibition of p38 activity. Kinase dead MEK3 blocked UV and HU activation by approximately 50% (Figure 4-6 A and B). In control experiments, dominant negative MEK1 and MEK5, MEKs specific for the ERK1/2 and ERK5 pathways, respectively, had no effect on p38 activity. Over-expression of wild type TAO kinases was sufficient to activate basal p38 activity (Figure 4-6) and enhanced stimulation of p38 by UV and HU (data not shown). These experiments suggest that TAO1, 2 and 3 are required for the activation of p38 by genotoxic stress, and that this activation is predominantly mediated by MEK6 and secondarily by MEK3. This is the first report that shows that TAOs are the MAP3Ks in the activation of p38 by DNA damaging agents.

C. TAOs interact with one another and with p38

We noticed a phosphorylated co-precipitating protein in the p38 kinase assays that migrated at the same molecular weight as over-expressed TAO3 in our dominant negative experiments. Indeed, Myc-TAO3 was detected by immunoblotting the p38 immunoprecipitates (data not shown). This unexpected result led us to question if the other TAOs were also capable of binding to p38. To address this, fragments of TAO1, 2 and 3 were transfected into HEK 293s, endogenous p38 was immunoprecipitated and associated proteins were detected by immunoblotting. Similar to TAO3, both TAO1 and 2 co-precipitated with p38 but not with preimmune serum (Figure 4-7A, B and C). As a negative control, we did not see association between a related kinase WNK1 (1-1000) and p38 (Figure 4-7D). C-terminal fragments of TAO2 containing the three putative coiled-coils also interacted with p38 (Figure 4-7E). Some non-specific binding was seen in these experiments

with pre-immune serum. However, the co-precipitating bands in the p38 immune serum lanes were more intense than pre-immune controls. Conditions need to be optimized to demonstrate specific binding to the C-terminal fragments. In summary, all three TAOs are capable of forming binary complexes with p38, and it is possible that higher order complexes may be formed.

We had previously found TAO3 as an interactor in an unbiased two-hybrid screen with TAO2 as bait. TAO2 (320-620) encompasses three putative coiled-coil domains in its C-terminal regulatory sequence. This region was fused to the LexA DNA binding domain. A cDNA library from mouse neonatal brain was screened with this bait and a fragment corresponding to the complete C-terminal domain of TAO3 was identified as an interactor (Figure 4-8A). To test if this interaction occurs *in vivo*, we asked if TAOs could form complexes among themselves. HA- full length TAO1, Myc-TAO2 (1-451) and 3XFLAG-TAO3 (1-442) were co-expressed in a pair-wise manner in HEK293 cells, and the ability of these proteins to interact was tested by co-immunoprecipitation and western blot analysis. Full length TAO1 interacted with fragments of TAO2 and TAO3 (residues 1-451 and 1-442 respectively) and TAO2 (1-451) and TAO3 (1-442) also interact with each other (Figure 4-8 B-D). The minimal interaction domain for interaction between TAOs is unknown but the C-terminal fragments of TAO2 failed to interact with TAO1 (data not shown). The interactions identified by the yeast two-hybrid screens were confirmed with endogenous proteins. TAO2 and 3 were capable of interacting with immunoprecipitated TAO1 but not with the preimmune serum (Figure 4-8E). We did not see any stimulus-dependent increase or decrease in the interaction between any of these proteins (data not shown). Taken together,

the data suggest that TAOs are able to interact with one another as well as with p38. Other MAP3Ks such as MEKK1 have been shown to scaffold the pathways they activate; this is an efficient way to localize pathway components and ensure fidelity in signaling (Karandikar et al., 2000).

D. Knockdown of TAO kinases inhibits activation of p38 by DNA damage

To obtain additional evidence that TAOs are required for the DNA damage response mediated by p38, we used small interfering RNAs (siRNA) against each of the TAO kinases and studied the activation of p38 by UV. We achieved a modest (~50%) knockdown of TAO1 and 2 and up to 75% knockdown of TAO3 with the oligonucleotides in HeLa cells (Figure 4-9 A and B). Also, knockdown of one TAO kinase did not seem to affect protein levels of the other family members in our assay (Figure 4-9 A and B). Interestingly, knockdown of TAO3 resulted in extensive cell death, in agreement with previous studies that identified TAO3 as a cell survival kinase (Figure 4-10). Knockdown of TAO1 and 2 had no effect on cell viability. Compared to control oligonucleotides, the activation of p38 by UV was diminished by up to 50% in TAO knockdown cells (Figure 4-9).

Since knocking down TAO1, 2 and 3 individually in HeLa cells had modest effect on p38 activation; we hypothesized that all three kinases cooperated in the activation of p38 by UV treatment. This idea complements our previous findings that TAOs interact with each other and with p38, and all three kinases are stimulated by DNA damage. However, we were unable to ablate expression of all three TAO kinases satisfactorily. We had modest success in double-knockdowns of TAO1 and 3; but we saw no further inhibition of p38 activation by

UV when both TAO1 and 3 amounts were diminished (Figure 4-11). It is possible that we did not achieve sufficient decrease in TAO protein expression; residual TAO1 and 3 may have been sufficient for signaling to p38. Alternatively, endogenous TAO2 in these cells was capable of p38 activation even in the background of TAO1 and 3 knockdowns. Finally, there may be additional MAP3Ks that contribute to the activation of p38.

E. Inhibition of TAO1 and 3 leads to activation of Cdc2

The p38 MAPK has been implicated previously in G2/M cell cycle arrest in response to DNA damage and other cellular stresses (Bulavin et al., 2001). Manke and co-workers demonstrated that p38 exerts its checkpoint control by activating MAPKAP kinase-2 (MK2) (Manke et al., 2005). MK2 negatively regulates Cdc25C, a phosphatase that is required for the activation of mitotic cyclin Cdc2. Cyclin/Cdc2 activation is tightly regulated by multiple phosphorylations. Cdc2 is inhibited by Myt1- and Wee1-mediated phosphorylation on Tyr15 (Lundgren et al., 1991; Mueller et al., 1995). The key step in the activation of Cdc2 is the dephosphorylation of Tyr15 by Cdc25C. G2/M arrest by DNA damage causes the accumulation of inactive phospho-Tyr15 Cdc2 (Figure 4-12). To explore events further downstream of p38, we tested whether siRNA of TAO kinases affected the activation of Cdc2 in response to DNA damage. HeLa cells were transfected with TAO1 and 3 oligonucleotides and treated with UV or HU. In cells transfected with a control oligonucleotide, HU or UV treatment caused accumulation of Cdc2 phosphorylated at Tyr15 (pY15-Cdc2) as seen with a phospho-specific antibody (Figure 4-12). Knockdown of either TAO1 or TAO3 decreased the amount of pY15-Cdc2 substantially relative to control

oligonucleotide, indicating that less Cdc2 was inactivated despite the presence of DNA damage. These data further support the idea that TAO-mediated activation of p38 in response to DNA damage is critical for preventing entry into mitosis. In summary, decreasing the expression of TAO1 and 3 was sufficient to bypass inhibition of mitotic cyclin/Cdc2 in response to damaged DNA.

F. SiRNA of TAO1/3 inhibits the UV-induced G2/M checkpoint

Given the evidence that TAO kinases appeared to be important mediators of p38 in the DNA damage response, we reasoned that siRNA of TAOs might result in the abrogation of the UV-induced G2/M checkpoint. To investigate this, we used a well-established FACS-based assay to quantitate the percentage of cells in mitosis. HeLa S3 cells were synchronized by a double-thymidine block which arrests cells at the G1/S boundary. Cells were released and allowed to progress through S-phase until they reached the G2/M boundary. At this point the cells were treated with UV for 2-4 hours and the number of cells in mitosis was determined by dual staining of the cells with propidium iodide (DNA content) and phospho-serine 10 Histone H3 (pSer10-H3), a marker for mitotic cells. In control cells, UV treatment arrested cells in G2, and negligible staining was seen with pSer10-H3 indicating that the G2/M checkpoint was efficiently engaged (Figure 4-13 A and B). Knockdown of TAO1 and 3 or the combination had no effect on cell cycle in the absence of DNA damage (Figure 4-16 and data not shown). However, in contrast to control cells which were arrested in G2, a significantly higher proportion of TAO1 and 3-depleted cells entered mitosis, indicating the importance of these kinases in damage-induced arrest. Further experiments will be conducted

to explore if TAOs are required for the G2/M checkpoint induced by ionizing radiation. Prior studies have presented conflicting results regarding the requirement of p38 activation for the IR-mediated checkpoint (Manke et al., 2005; Wang et al., 2000). In summary, these data establish the importance of TAO kinases in regulating the p38-arm of the G2/M DNA damage checkpoint.

G. ATM/ATR are upstream of TAOs in the DNA damage response

To determine how damaged DNA stimulates TAO kinases, we next asked if we could observe TAO kinases in the nucleus. Indeed, endogenous TAO2 was observed in discrete foci within the nucleus of resting HeLa cells (Figure 4-14A). In addition, TAO2 was also observed in nuclear pools of fractionated HeLa cells (Figure 4-14B). Interestingly, very little TAO2 is observed in the cytosol by fractionation, instead it appears to be tightly localized to membrane and nuclear fractions. Because ATM may play a role in the activation of p38 by IR (Wang et al., 2000), we explored the possibility that TAO kinases may be downstream of ATM/ATR in signaling cascades initiated by DNA damage. Canonical ATM and ATR substrates are phosphorylated on a serine or threonine residue followed by a glutamine residue (pSQ/pTQ). Analysis of the TAO3 protein sequence by the SCANSITE program (http://www.scansite.mit.edu) and by manual sequence analysis led to the identification of three potential phosphorylation sites, S324, S359 and S782. Of these three sites, Ser359 is conserved in all three TAO kinases (Ser363 in both TAO1 and TAO2) (Figure 4-15A). HeLa cells were treated with the replication stressor HU overnight, and whole cell lysates were probed with anti phospho-Ser1981 ATM, an autophosphorylation site on ATM that conforms

to the pSQ consensus motif. This antibody also recognizes pSQ sites on other ATM/ATR substrates. Cross-reacting bands were excised and the identity of the phospho-peptides was determined by mass spectroscopy. Phospho-specific antibodies were synthesized against the newly identified sites and used to probe for further cross-reacting bands. This iterative-manner of screening helped in the identification of TAO3 as a putative substrate of ATM/ATR by our collaborator Jun Qin at Baylor Health Science Center (Texas). To determine the significance of these phosphorylation sites, we mutated the serines (either singly or in combination) to alanine and asked whether over-expression of these TAO3 mutants affected p38 activation by damaged DNA. None of these mutants behaved in a dominant negative manner (data not shown). This may be because these mutants still retain kinase activity (phosphorylation of TAOs by ATM/ATR is but one manner in which activation is controlled). Alternatively, a number of these sites may need to be phosphorylated for activation to occur and mutation of any one site is insufficient to block activation. All three TAO kinases have a number of SQ/TQ sites in their C-terminal domains (TAO1: 6, TAO2: 6 and TAO3: 7), whereas a related protein kinase PAK only has one site. We decided to mutate the SQ/TQ sites on TAO1 as it is the only member that behaves as a dominant negative when the full length protein is transfected. Overexpression of TAO1 T643A and T785A resulted in 50% inhibition of p38 activation in response to UV treatment (Figure 4-15B). Further experiments will be required to test if ATM/ATR directly phosphorylate these sites *in vitro* and *in vivo*, and if similar sites exist on TAO2 and 3.

As an alternate means to assess the requirement of ATM in the activation of TAO kinases and p38 by DNA damage, we tested if TAOs or p38 could be activated in cells

lacking ATM. Protein kinase activity for p38 and TAO2 was assayed from wild type human skin fibroblasts (1BR3) and skin fibroblasts from a patient with AT that do not express detectable ATM. Activation of p38 and TAO2 was intact in wild type fibroblasts treated with IR (Figure 4-16). However, in AT cells the activation of these protein kinases was diminished implying that ATM is required for their activation. Taken together, these studies implicate the ATM/ATR protein kinases in the activation of TAOs and p38 by genotoxic stress.

G. TAO2 phosphorylates and binds to Chk2

The ATM protein kinase is primarily responsible for Thr68 phosphorylation on Chk2; however in cells from AT patients who lack functional ATM there is residual activation of Chk2 in response to UV and IR (Matsuoka et al., 2000). Indeed, there have been recent reports that polo-like kinase 1 (Plk1) and a MAP3K - MRK (a member of the MLK family) are both capable of phosphorylating Chk2 on Thr68 in response to DNA damage, indicating that other kinases in addition to ATM may play a role in regulating Chk2 in response to DNA damage (Tosti et al., 2004; Tsvetkov et al., 2003). To explore the activation of TAO2 by DNA damage further, we studied whether TAO2 was also capable of phosphorylating Chk2. To address this question, full-length GST-Chk2 was produced in bacteria and used as a substrate in an *in vitro* kinase assay with the recombinant kinase domain of TAO2 (1-320). In this assay, we found that TAO2 was able to phosphorylate Chk2 efficiently, while a related Ste20p like kinase WNK1 did not (Figure 4-17A). We determined the stoichiometry of phosphorylation to be greater than 1 mol phosphate/mol Chk2, indicating that TAO2 may phosphorylate multiple sites on Chk2. Using a panel of phospho-specific antibodies to Chk2

we found that TAO2 phosphorylates Chk2 on Thr68, but this phosphorylation was weak compared to the autophosphorylation on wild type Chk2 that was used as a positive control (Figure 4-17B). This led us to believe that TAO2 phosphorylated other sites on Chk2 in addition to Thr68. In an attempt to identify phosphorylation sites we made fragments of Chk2 purified from *E.coli*. We found that maximal phosphorylation of Chk2 occurred in the forkhead associated (FHA) domain of Chk2 that is essential for complete activation of Chk2 (data not shown). While the FHA domain binds phospho-serine/threonine containing peptides, there have been no reports to date of phosphorylation sites within the FHA domain itself. Mass spectroscopy analysis of phosphorylated GST-Chk2 K249A identified three phospho-peptides (Table 4-1). These were situated in the N-terminal SQ/TQ cluster domain (SCD), the FHA domain and at the extreme C-terminus of Chk2. Serine 566 in the C-terminal tail of Chk2 has been identified as a site of autophosphorylation (Schwarz et al., 2003), but it is possible that other protein kinases phosphorylate this site also. TAO2 and Chk2 are capable of associating in cells when both proteins are over-expressed. HEK293 cells were transfected with a fragment of Myc-tagged TAO2 (residues 1-451) and 3XFLAG-Chk2. FLAG-Chk2 was present in TAO2 immunoprecipitates and vice-versa (Figure 4-17C and data not shown). While more detailed experiments are warranted here, the preliminary data provide evidence that TAO2 may be capable of regulating the DDR by modulating both p38 and Chk2 kinase activity.

IV. Discussion

DNA damage occurs at a rapid rate in every cell both as a result of normal metabolism as well as by exogenous agents such as UV and IR. To counterbalance the deleterious effects of damage occurring in essential genes, mechanisms are in place to rapidly detect damaged DNA and respond in an appropriate manner to redress the damage. One of the hallmarks of DDR is the ability to halt the cell cycle to allow for damaged DNA to be repaired. These cell cycle checkpoints occur at the G1/S boundary, within S phase, and at the G2/M boundary. The G2/M checkpoint is thought to be the final "net" that catches cells that may have escaped the G1/S and intra-S phase checkpoints. In this manner, it is ensured that cells do not undergo mitosis until the damage is corrected. Failure to engage these checkpoints will result in the propagation of potentially lethal mutations to daughter cells and eventual decline of viability of the organism. The Chk1 and Chk2 protein kinases are critical regulators of cell cycle checkpoints and can engage checkpoints at every stage of the cell cycle, depending on the type of genotoxic stress. The p38 MAPK is another important player in the DNA damage response. Here I have shown that the TAO family of MAP3Ks is an important mediator of the DNA damage response. TAO 1 and 2 have been shown by our group to activate p38 by cellular stressors such as sorbitol (Chen and Cobb, 2001; Hutchison et al., 1998). TAO3 has been shown to activate ERK1/2 and JNK pathways by one group (Zhang et al., 2000) and negatively regulate JNK signaling in response to EGF in another study (Tassi et al., 1999). We show that overexpression of TAO3 enhances endogenous p38 activity (Figure 4-5C). Certainly more detailed studies of this protein kinase are necessary to appropriately assign it to the MAPK pathway(s) it regulates. All three TAO kinases are

activated by a variety of stimuli that stress or damage DNA. Ionizing radiation which causes double strand DNA breaks (DSB) activated the protein kinase activity of TAO1 and 2 the best (up to 10 fold over basal). Of all stimuli tested so far, IR is by far the best activator of these kinases. UV radiation which causes DNA damage in a number of ways, including the formation of DSBs, activates all three kinases moderately (2-5 fold over basal). Interestingly, maximal activation of p38 MAPK is observed when cells are treated with UV (40 fold relative to control), and IR activates p38 approximately 5 fold over basal. It is highly likely that p38 is activated robustly by UV because of the multiple ways in which this agent stresses the cell. UV indirectly damages DNA by the production of reactive oxygen species (ROS), which is a potent activator of p38 (Benhar et al., 2001). Indeed many MAP3Ks (such as ASK) are activated by ROS, which may facilitate the rapid (within minutes) activation of p38 (Tobiume et al., 2001). It is possible that one or all the TAOs are activated by the ROS produced as a by-product of UV treatment; future studies will determine if this is the case. In contrast, IR specifically activates the DDR by causing double strand DNA breaks, an event that activates ATM and DNA-PK (Chen et al., 2005; Stiff et al., 2004). Hence, the moderate activation of p38 by IR may be due to the limited number of upstream kinases activated by this agent. Since TAO kinases are activated by IR, they may well be the kinases that mediate p38 activation by this agent. Han's group has shown that MEK6/p38γ is required for the IR-induced checkpoint (Wang et al., 2000). However MK2, the p38 substrate that phosphorylates Cdc25C in response to UV, was shown to be dispensable for the IR-mediated G2/M checkpoint (Manke et al., 2005). This discrepancy may be explained by the fact that p38 may regulate other as yet unidentified proteins that are important in the IR-mediated

checkpoint. For example, Bhoumik and colleagues have shown that ATM phosphorylates the p38 substrate activating transcription factor 2 (ATF2) and localizes it to DNA damage-induced foci (Bhoumik et al., 2005). However, inhibiting p38 activation with the p38α and β isoform-specific drug SB203580 had no effect on the localization of ATF2. The group concluded that p38 was not required for ATF2 action in response to DNA damage, but since Wang's study has implicated p38γ as the isoform most sensitive to IR, these studies will need to be re-evaluated with drugs such as BIRB796 which inhibits all p38 isoforms (Kuma et al., 2005; Wang et al., 2000). TAO kinase activation by IR may also have consequences independent of p38. We have shown that TAO2 can phosphorylate and interact with the checkpoint kinase Chk2 (Figure 4-17). While more detailed *in vivo* analysis of this finding is presently lacking, it implies that these kinases may also regulate other aspects of the DDR. In support of this idea, TAO2 was found to interact with microspherule 1 (MSP1) in our yeast two-hybrid screen (Table 3-1). Very little is currently known about the function of MSP1 in the cell. It is a nucleolar protein that interacts with other nucleolar proteins such as p120 and Ret-finger protein to regulate ribosomal gene transcription (Lin and Shih, 2002; Ren et al., 1998; Shimono et al., 2005). MSP1 has an N-terminal FHA domain that interacts with phospho-threonine residues. These domains have been found (with few exceptions) in nuclear proteins that take part in the DNA damage response e.g, Chk2, breast cancer 1 early onset (BRCA1), mediator of DNA damage checkpoint 1 (MDC1) among others. MSP1 interactors that bind to the FHA domain have not been discovered. We have shown that TAO2 interacts with MSP1 in overexpression studies (discussed in Chapter 5), but have not conclusively determined if this interaction is dependent on the FHA domain. TAO2

interacted with the isolated FHA domain of Chk2 and Msp1 in pair-wise two-hybrid tests. TAO2 is predominantly phosphorylated on threonine residues (Figure 3-12D), the preferred phospho-residue that binds FHA domains. Additionally, the amino-acid residues surrounding putative threonine phosphorylation sites on TAO2 conform to consensus sites for FHA domain binding identified by peptide library screens (Durocher et al., 2000a; Durocher et al., 2000b).

The protein kinase activities of TAOs are required for the activation of p38 by UV and HU. Dominant negative constructs of TAO1, 2 and 3 blocked the activation of p38 by these agents. This agrees well with the activation of all three kinases by UV and may explain why we did not observe 100% inhibition of p38 kinase activity with any one dominant negative construct. Transfection efficiency in these experiments ranged from 70-80% Knockdown of TAO kinases by siRNA recapitulated the dominant negative results in that p38 activity was diminished by 50% by individually knocking down these kinases. Our attempts to determine if TAO kinases cooperate in the activation of p38 have not yielded conclusive results. We were not successful in knocking down all three protein kinases by siRNA and double knockdown of TAO1 and 3 did not inhibit p38 activation more than the individual knock-downs. Given that we achieve about 75% knock-down of protein expression in our experiments at best, it is highly likely that residual protein kinase activity is sufficient for the activation of p38 under our assay conditions. DNA damage checkpoints are crucial for the viability of the cell; hence many safe-guards may be in place to make the signaling system robust to perturbations. If this is the case, p38 may be redundantly activated by other MAP3Ks when TAO kinases are knocked-down. It would be useful therefore to

determine the relative contribution of MAP3Ks in the activation of p38 by UV. Mammalian MAP3Ks are numerous, and efficiently knocking these kinases down is a difficult task. Therefore, these studies are probably best carried out in a simpler system and the results extrapolated. Drosophila S2 cells provide an ideal testing bed for such studies. They have an intact DDR, far fewer MAP3Ks, and are amenable to efficient RNAi experiments. In fact the system has been used successfully to map the inputs from various MAP3Ks in the activation of he JNK cascade by various stimuli (Chen et al., 2002).

Our results that TAO1, 2 and 3 interact with one another as well as with p38 indicate that association of these kinases is an important means of regulating activity. TAO kinases interacted with one another in overexpression studies and endogenous TAO1 was found in TAO2 and TAO3 immunoprecipitates. TAO3 was also identified as a TAO2 interactor in our two-hybrid screen. While our studies do not address whether the three proteins exist in the same complex, we speculate that the large C-terminal domains of TAOs mediate both inter- and intra-molecular associations with one another. This may well be a general method by which MAP3K activity is regulated. For example, a related protein kinase WNK1, undergoes homo-tetramerization and also phosphorylates WNK4, another family member (Lenertz et al., 2005). Additionally WNK1 also interacts with another Ste20p kinase OSR1 to regulate its activity (Anselmo and Cobb in revision; (Moriguchi et al., 2005; Vitari et al., 2005). TAO protein kinases also interact with p38 MAPK and we isolated MEK6 as a TAO2 interactor in our two-hybrid screen. Hence we believe that TAO 1, 2 and 3 exist in a pre-formed complex with p38 (and possibly MEKs 3 and 6) in resting cells poised to respond rapidly to stimulation. Further experiments are required to map the domains involved in these

interactions and to determine whether these proteins do indeed exist in a high molecular weight complex in cells. We will also determine if TAOs regulate one another by direct phosphorylation.

Our studies show that the ability of TAOs to regulate p38 by UV is not merely a general stress response, but rather an important means of activating the G2/M checkpoint. Lowering TAO1 and 3 protein levels by siRNA led to significant inhibition of the UV-induced G2/M checkpoint. Additionally, TAO1/3 siRNA resulted in loss of Cdc2 inhibition despite UV treatment, another indication that cells aberrantly entered mitosis in the absence of these protein kinases. How does damaged DNA serve to activate TAO protein kinases and subsequently p38? We believe that TAOs may be immediately downstream of ATM/ATR in these signaling cascades. Mass spectroscopic analysis of cell lysates treated with the replication inhibitor hydroxyurea identified TAO3 as an ATM/ATR substrate when probed with an antibody that recognizes pSQ/TQ sites. While we did not see significant activation of these protein kinases with HU, dominant negative constructs blocked HU activation of p38. Perhaps the pool of protein kinase that is activated by these agents is small or specifically localized (e.g. in the nucleus) such that our current experimental conditions are not conducive for their isolation. In support of the idea that TAOs may be downstream of ATM/ATR, specific TQ$\rightarrow$AQ mutants in TAO1 inhibited p38 activation by UV. It remains to be seen if these are *bona fide* sites of ATM/ATR phosphorylation, and if TAO2 and TAO3 are also phosphorylated by these kinases. Our preliminary results show that the activation of p38 by IR is impeded in cells from a patient with AT. This confirms previous studies that showed impaired p38 activation in the absence of ATM (Wang et al., 2000). In these cells we

also observed impairment in the activation of TAO2 by IR. In total, these findings strongly suggests that one or all the TAOs are direct substrates of ATM (and possibly ATR) protein kinases in the DNA damage activated pathway (Figure 4-18).

The contribution of p38 in the engagement of cell cycle checkpoints after DNA damage is well-established. However, why is p38 required for the activation when protein kinases such as Chk1 and Chk2 engage these checkpoints in response to DNA damage? Cellular DNA is damaged not only by radiation but also as a consequence of cell stress by other agents. For example, high osmolarity agents such as sodium chloride also induce double strand DNA breaks (Dmitrieva et al., 2003; Kultz and Chakravarty, 2001). These studies have shown that Chk1 is not phosphorylated by high salt treatment. Interestingly, pre-treating cells with high salt prior to UV or IR treatment prevented DNA repair from occurring, presumably because meiotic recombination 11(Mre11) exits the nucleus in the presence of high salt and cells can no longer repair damaged DNA. Hence, alternative pathways to Chk1/2 must exist that are able to sense damaged DNA either directly or indirectly. The p38 MAPK family is ideal for this purpose because it is sensitive to a host of cellular stresses. ATM/ATR mediated control of p38 via TAO kinases allows ATM and ATR to activate checkpoints rapidly in response to damage caused by many different agents.

In summary, we have identified the TAO family of protein kinases to be important regulators of the G2/M DNA damage checkpoint via their ability to activate p38 MAPK. We have also shown that TAOs may be activated in this regard because they are substrates of the master regulators of the DNA damage response-ATM and ATR.

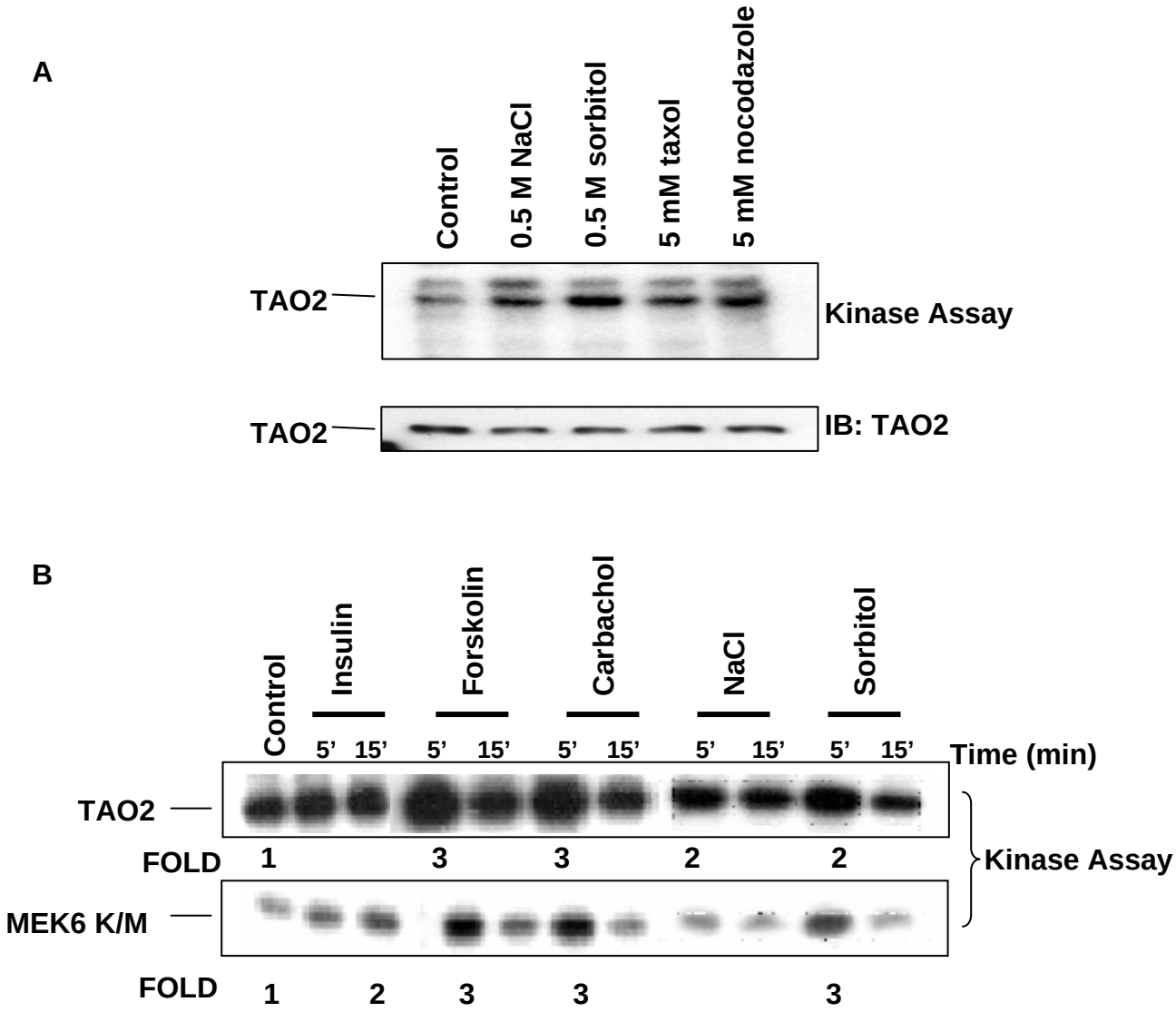

Figure 4-1. Effects of ligands on the activation of endogenous TAO2. (A) HEK293 cells were untreated or treated with 0.5 M NaCl, 0.5 M sorbitol, 5 mM taxol or 5 mM nocodazole for 15 min. Cells were lysed and TAO2 was immunoprecipitated and assayed for autophosphorylation as an indicator of activation. (B) HeLa cells were untreated or treated with 60 ng/ml insulin, 10 μM forskolin, 10 μM carbachol, 0.5 M NaCl or 0.5 M sorbitol for 5 min or 15 min. Cells were lysed and endogenous TAO2 was immunoprecipitated and assayed for activation with MEK6K/M as substrate (n = 4).

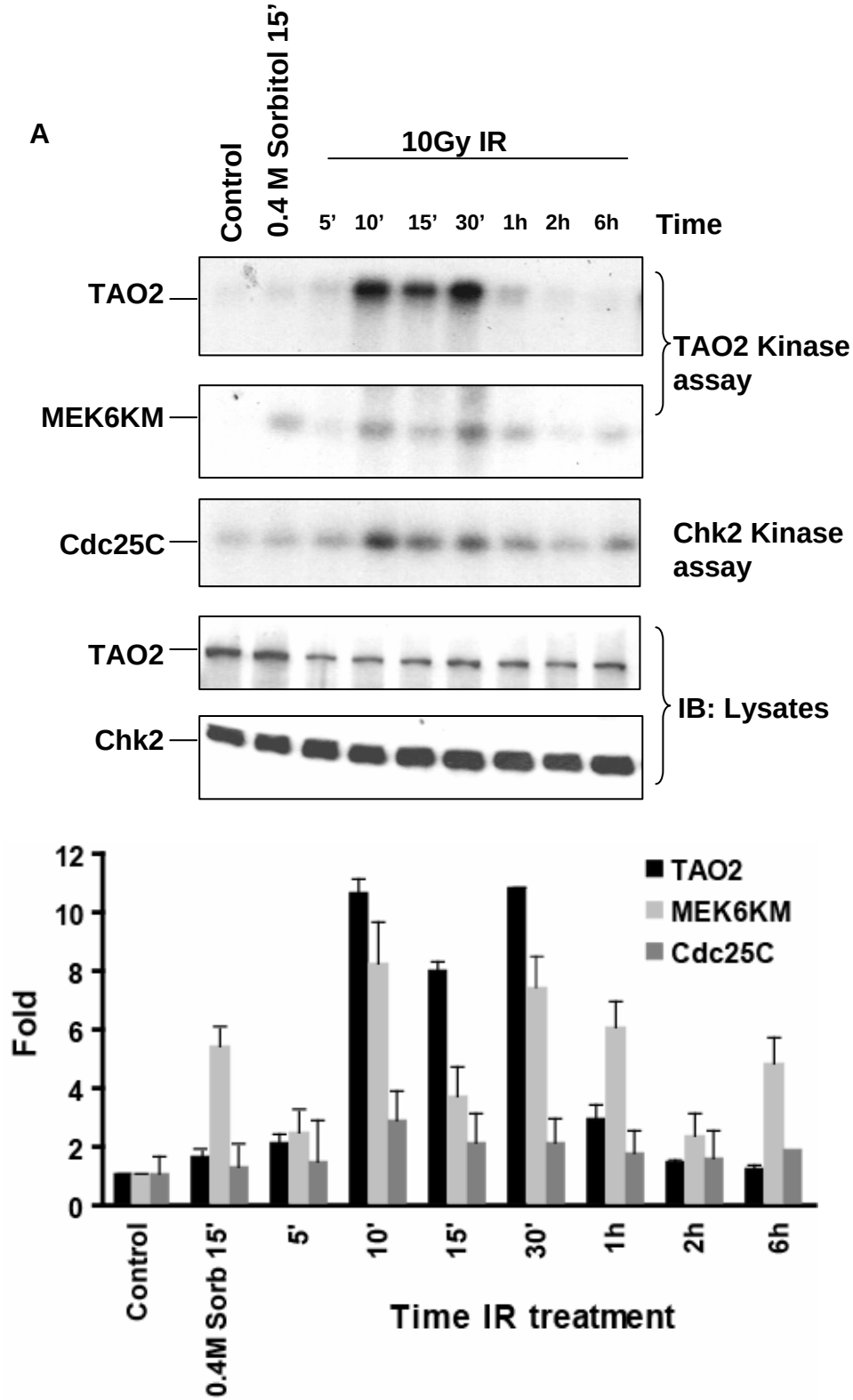

Figure 4-2. TAO2 is activated by DNA damage. (A) HeLa cells were untreated or treated with 0.5 M sorbitol for 15 min or with 10 Gy IR for the indicated times. Cells were harvested and TAO2 or Chk2 were immunoprecipitated and assayed for activation with kinase dead MEK6 and Cdc25C (200-259) as substrates respectively. Graph shows fold activation, values are mean ± s.e.m (n = 5) (Continued on next page).

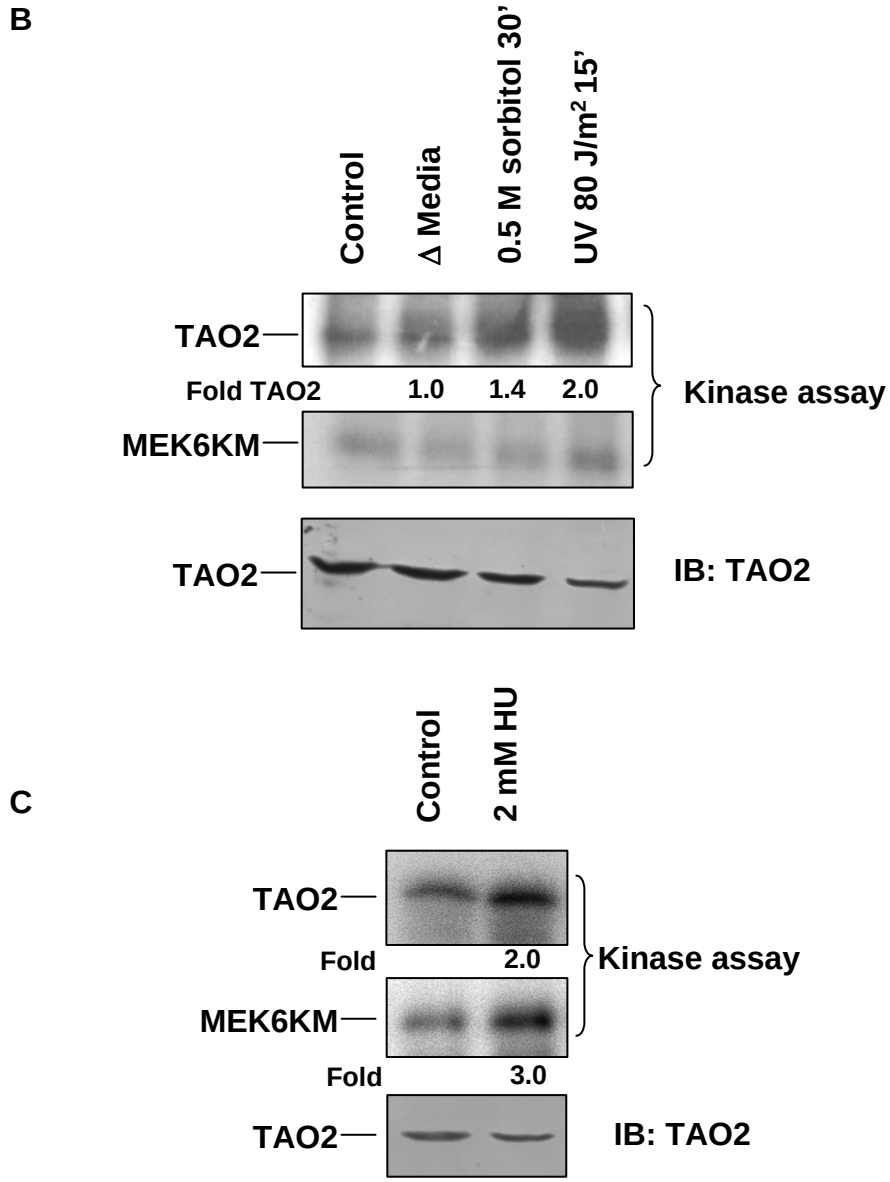

Figure 4-2. (Continued) TAO2 is activated by DNA damage. (B) HeLa cells were untreated or treated with 0.5 M sorbitol for 15 min or with 80 J/m2 UV for 15 min. Cells were harvested and immunoprecipitated for TAO2 and assayed for activation with kinase dead MEK6. (C) HeLa cells were untreated or treated with 2 mM HU overnight for 20 hrs. Cells were harvested, immunoprecipitated for TAO2 and assayed for activation (n = 4).

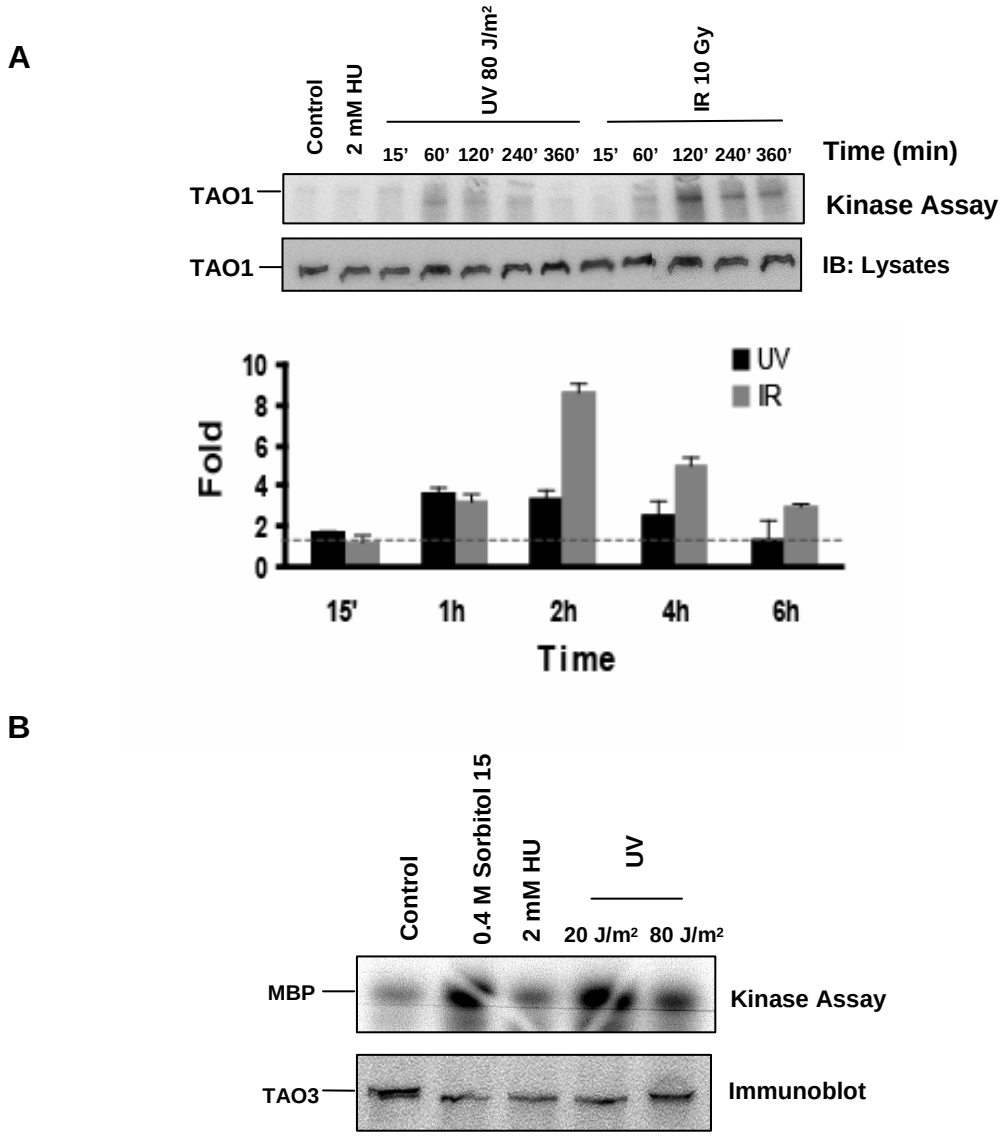

Figure 4-3. TAO1 and 3 are activated by DNA damage. (A) HeLa cells were untreated or treated with 2 mM HU overnight, 80 J/m^2 UV or 10 Gy IR for the indicated times. Cells were harvested and TAO1 activity was assayed in an *in vitro* kinase assay to measure autophosphorylation. Graph shows fold activation, values are mean ± s.e.m. (B) HeLa cells were treated with 0.4 M sorbitol for 15 min, 2 mM HU overnight or either 20 J/m^2 or 80 J/m^2 UV for 15 or 30 min. Cells were harvested and TAO3 activity was measured in an *in vitro* kinase assay with MBP as substrate (n = 3).

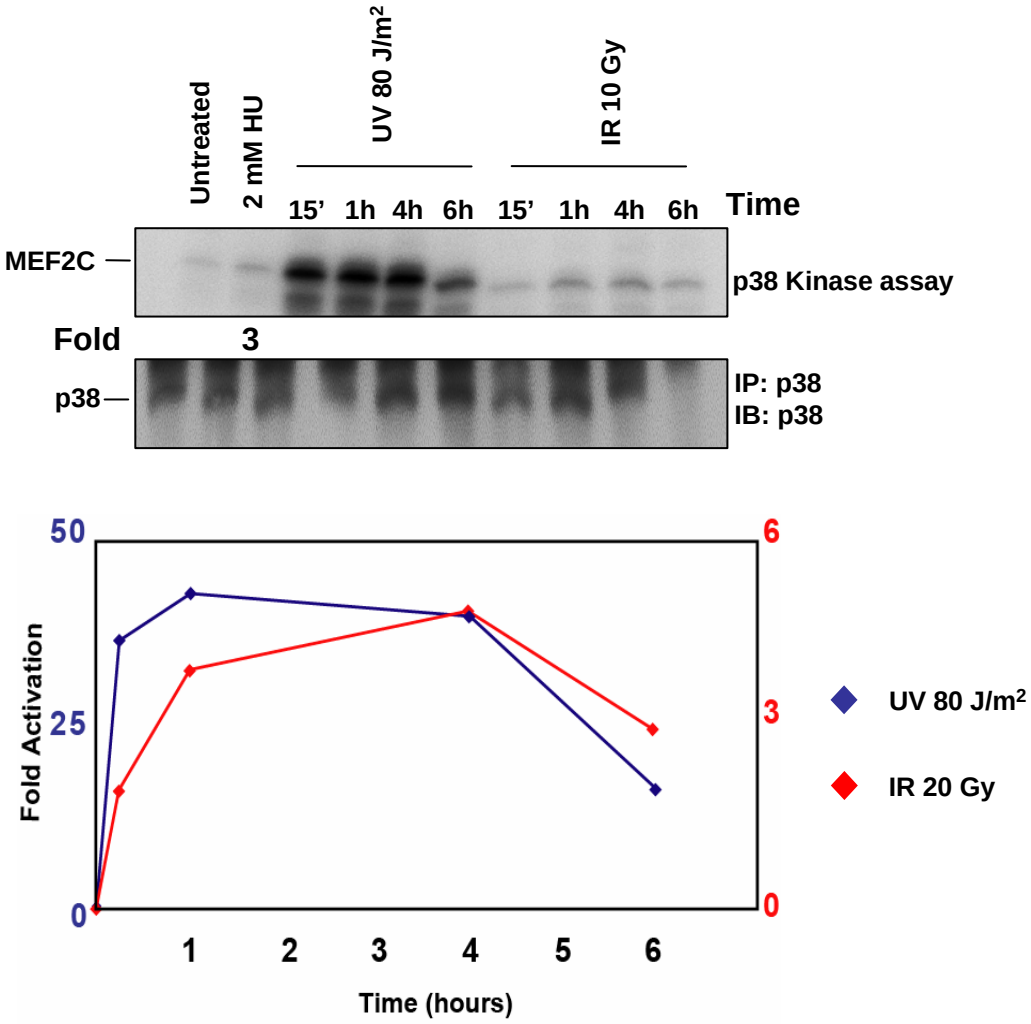

Figure 4-4. p38 is activated by DNA damage. HeLa cells were untreated or treated with 2 mM HU overnight, 80 J/m^2 UV or 10 Gy IR for the indicated times. Cells were harvested and p38 activity was assayed in an *in vitro* kinase assay with MEF2C as substrate (n = 3).

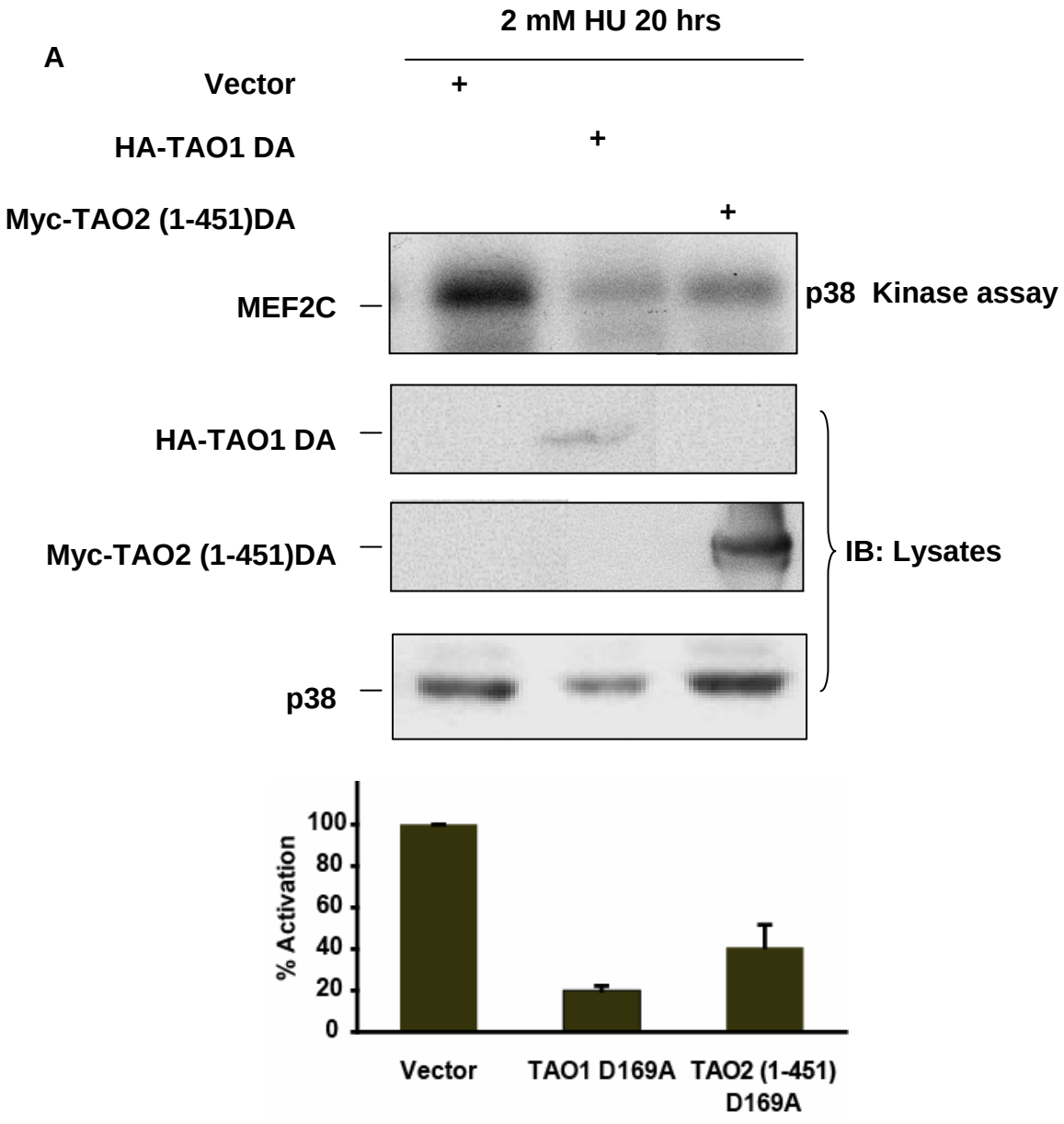

Figure 4-5. p38 activation by HU/UV is inhibited by dominant negative TAOs (A) HEK293 cells were transfected with vector alone and HA-TAO1D169A or Myc-TAO2 (1-451) D169A. Cells were untreated or treated with 2 mM HU overnight. Cells were harvested and p38 activity was assayed in an *in vitro* kinase assay with MEF2C as substrate. Graph shows % activation, values are mean ± s.e.m (n = 5).

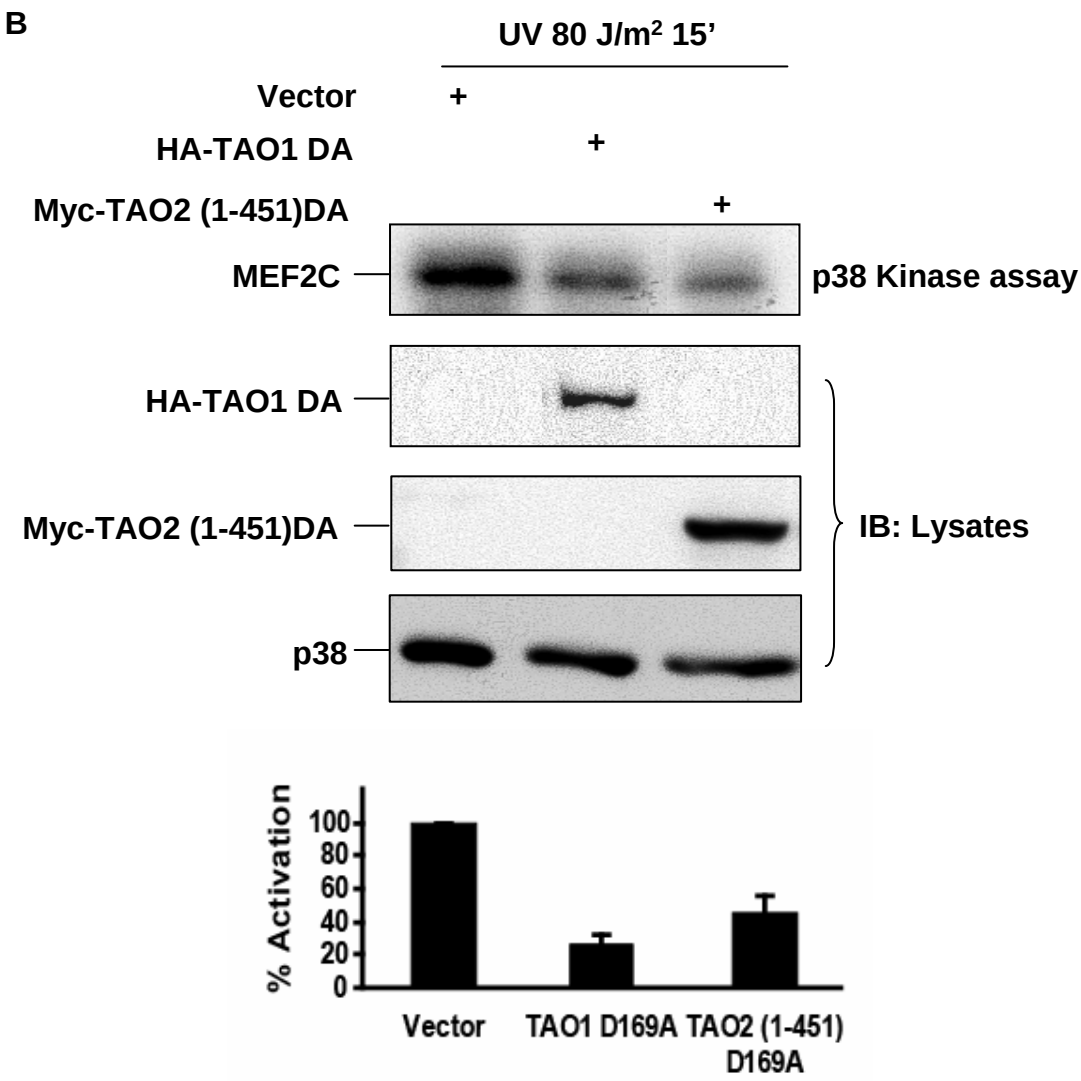

Figure 4-5. (Continued) p38 activation by HU/UV is inhibited by dominant negative TAOs (B) HEK293 cells were transfected with vector alone and HA-TAO1 D169A or Myc-TAO2 (1-451) D169A. Cells were untreated or treated with 80 J/m^2 UV for 15 minutes. Cells were harvested and p38 activity was assayed in an *in vitro* kinase assay with MEF2C as substrate. Graph shows % activation, values are mean ± s.e.m (n = 5).

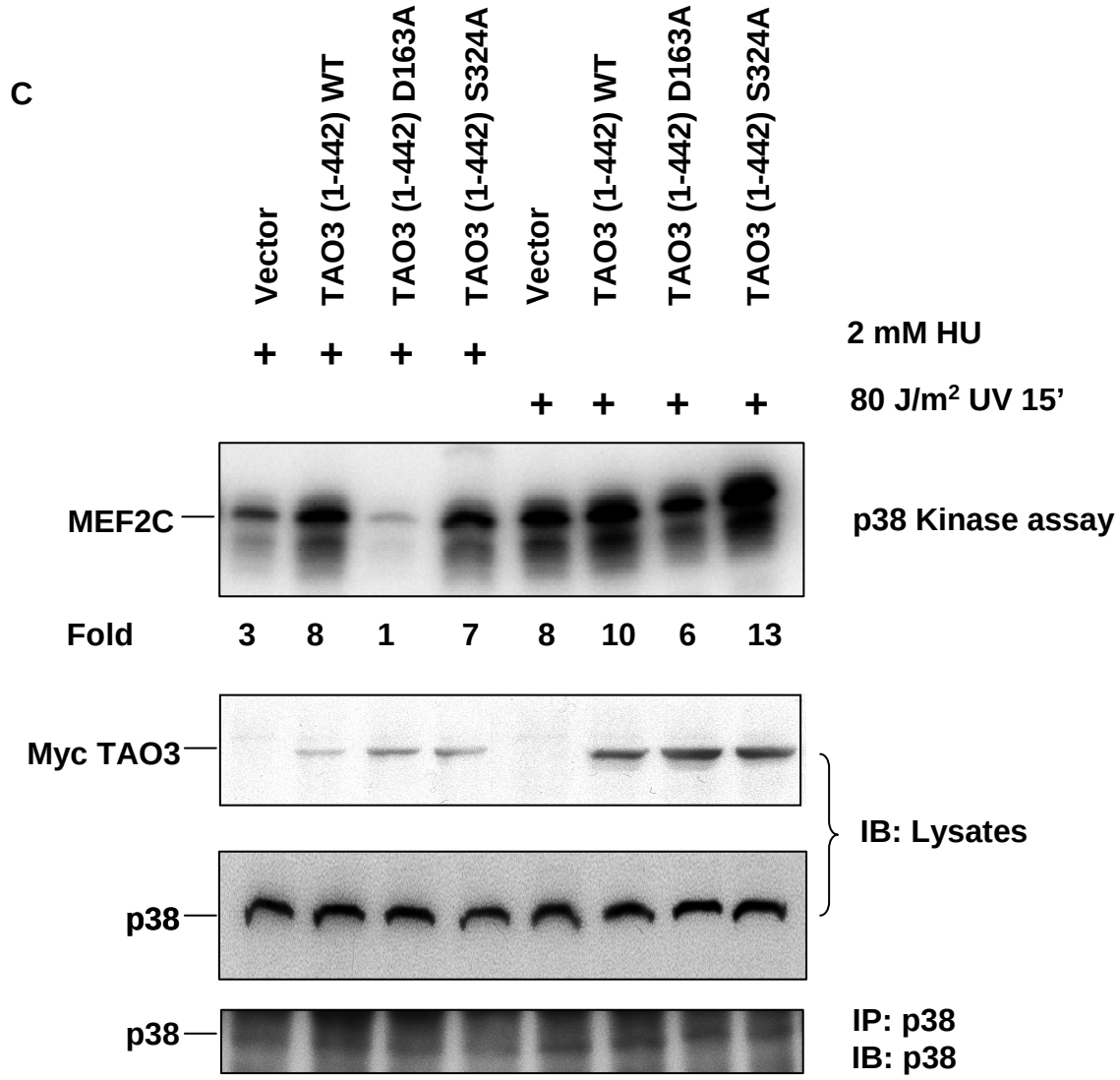

Figure 4-5. (Continued) p38 activation by HU/UV is inhibited by dominant negative TAOs (C) HEK293 cells were transfected with vector alone, or Myc-TAO3 (1-442) wild type, kinase dead D165A or the ATM/ATR phosphorylation site mutant TAO3 S324A. Cells were untreated or treated with 2 mM HU for 20 hrs or 80 J/m^2 UV for 15 min. Cells were harvested and p38 activity was assayed in an *in vitro* kinase assay with MEF2C as substrate. Wild type TAO3 activated p38 while kinase dead TAO3 inhibited activation. Fold activation shown relative to untreated vector control (not shown in panel)(n = 3).

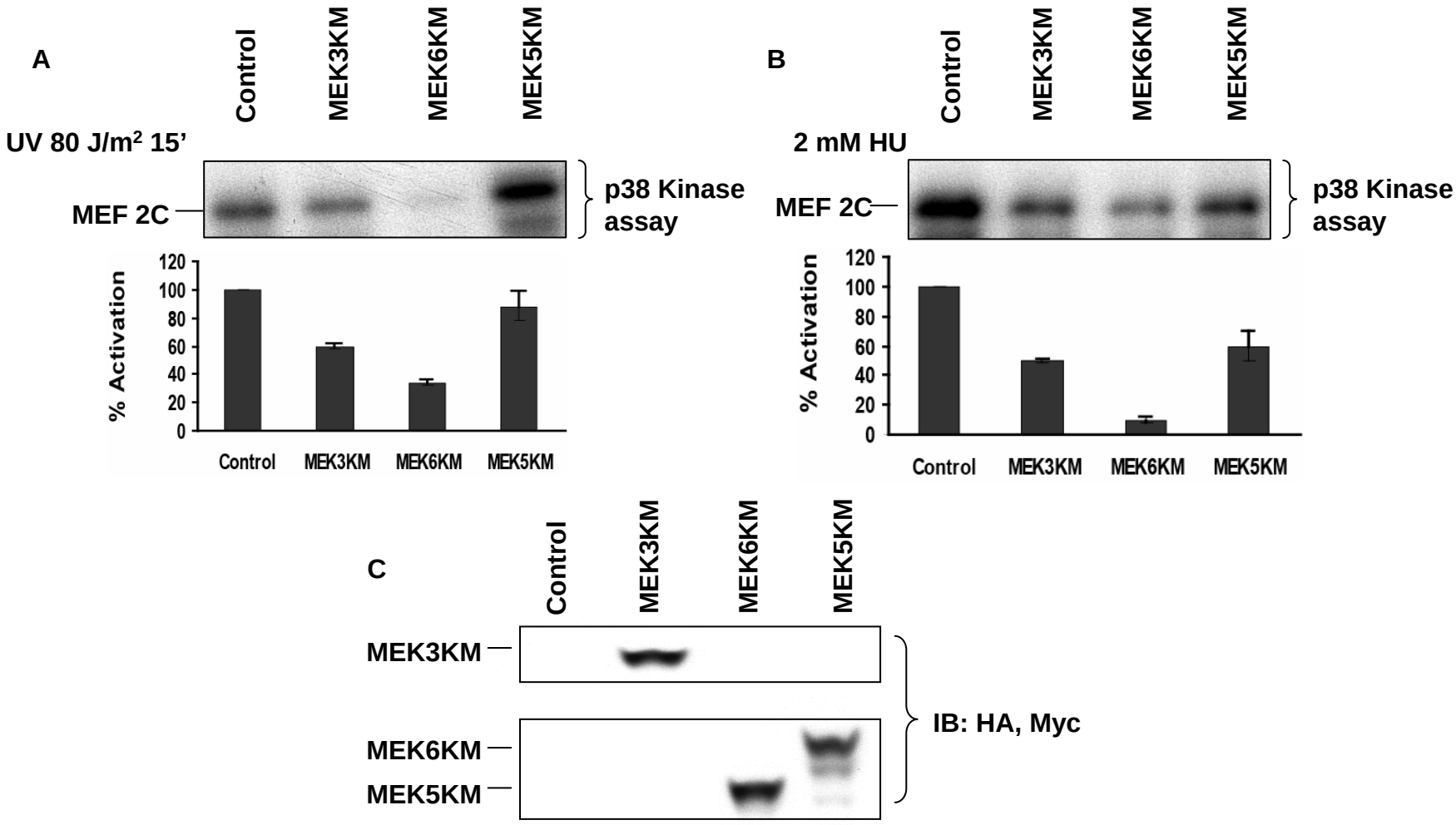

Figure 4-6. p38 activation by HU and UV is blocked by dominant negative MEK3/6. HEK293 cells were transfected with vector alone, or HA-MEK3KM, Myc-MEK6KM and HA-MEK5KM. Cells were untreated or treated with (A) 80 J/m^2 UV for 15 min or (B) 2 mM HU for 20 hrrs Cells were harvested and p38 activity was assayed in an in vitro kinase assay with MEF2C as substrate. (C) Bottom panel shows MEK expression in experiments. Graphs show % activation, values are mean ± s.e.m. (n = 3).

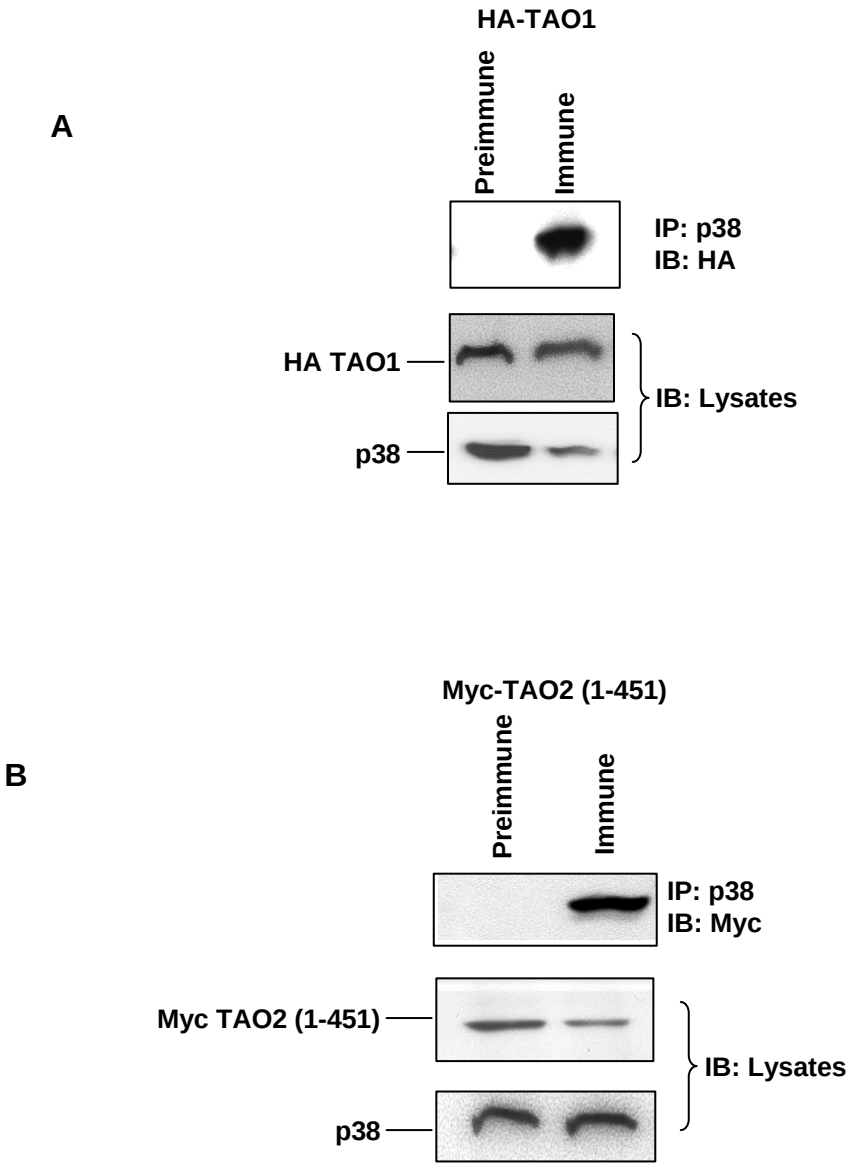

Figure 4-7. p38 binds to TAO1, 2 and 3. (A) HEK293 cells were transfected with HA-TAO1. Cell lysates were immunoprecipitated with preimmune serum or anti-p38 and probed for interaction with HA-TAO1. (B) HEK293 cells were transfected with Myc-TAO2 (1-451). Cell lysates were immunoprecipitated with preimmune serum or anti-p38 and probed for interaction with Myc-TAO2 (1-451).

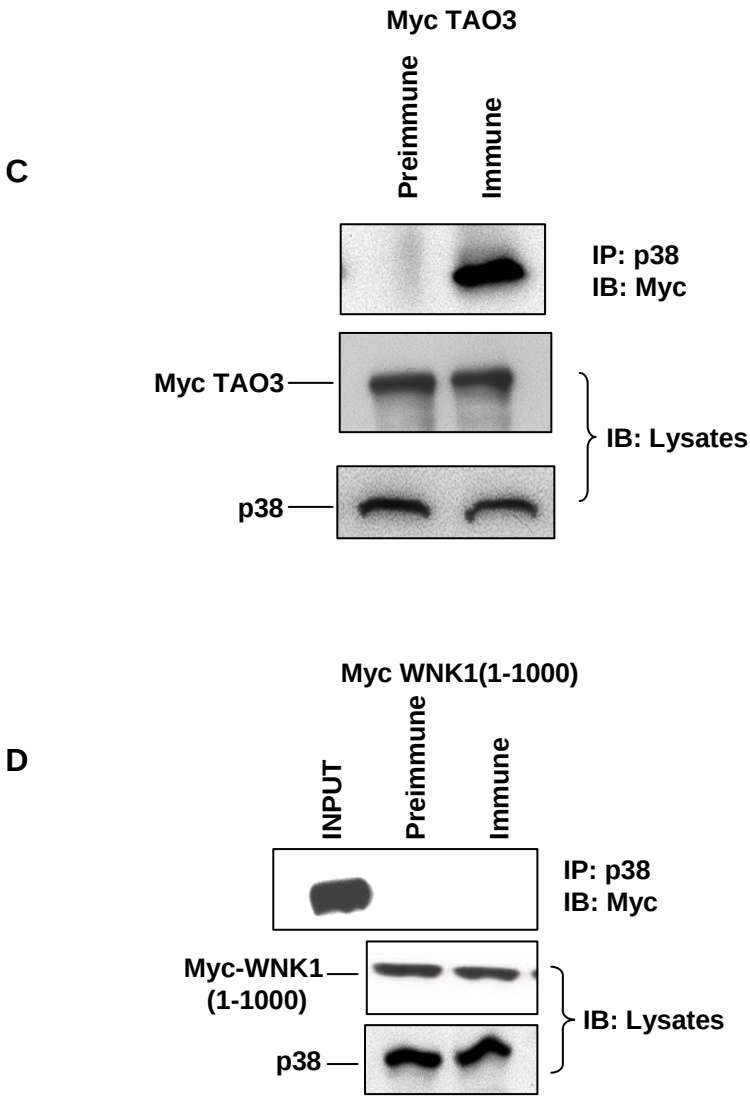

Figure 4-7. (Continued) p38 binds to TAO1, 2 and 3 (C) HEK293 cells were transfected with Myc-TAO3. Cell lysates were immunoprecipitated with preimmune serum or anti-p38 and probed for interaction with Myc-TAO3. (D) HEK293 cells were transfected with Myc-WNK1 (1-1000) as a negative control. Cell lysates were immunoprecipitated with preimmune serum or anti-p38 and probed for interaction with Myc-WNK1 (1-1000). No interaction was seen with Myc-WNK1 (1-1000).

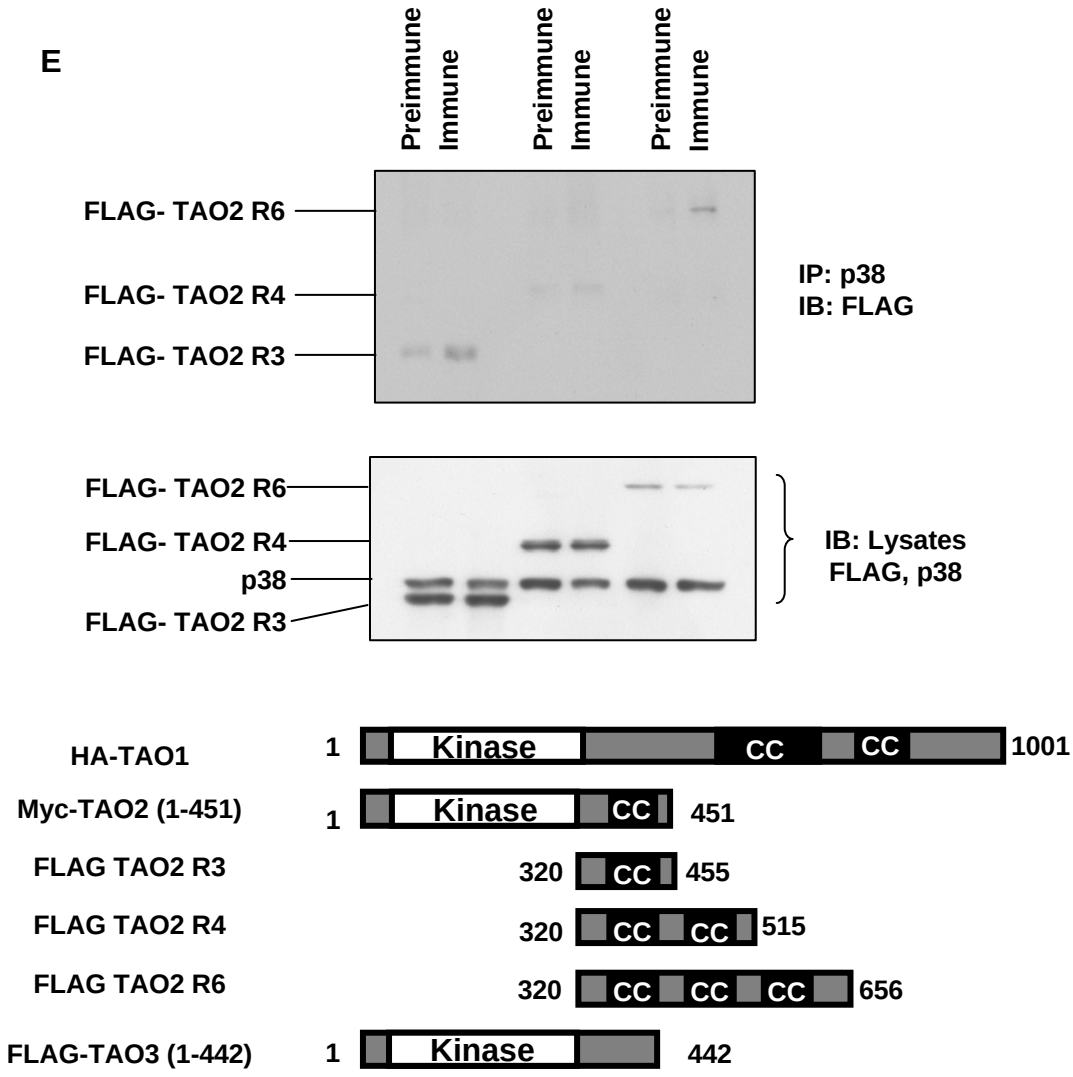

Figure 4-7. (Continued) p38 binds to TAO1, 2 and 3 (E) HEK293 cells were transfected with FLAG-TAO2 C-terminal fragments encompassing the putative coiled-coil motifs. Cell lysates were immunoprecipitated with preimmune serum or anti-p38 and probed for interaction with FLAG-TAO2. Bottom panel shows TAO1, 2, and 3 constructs transfected in these studies.

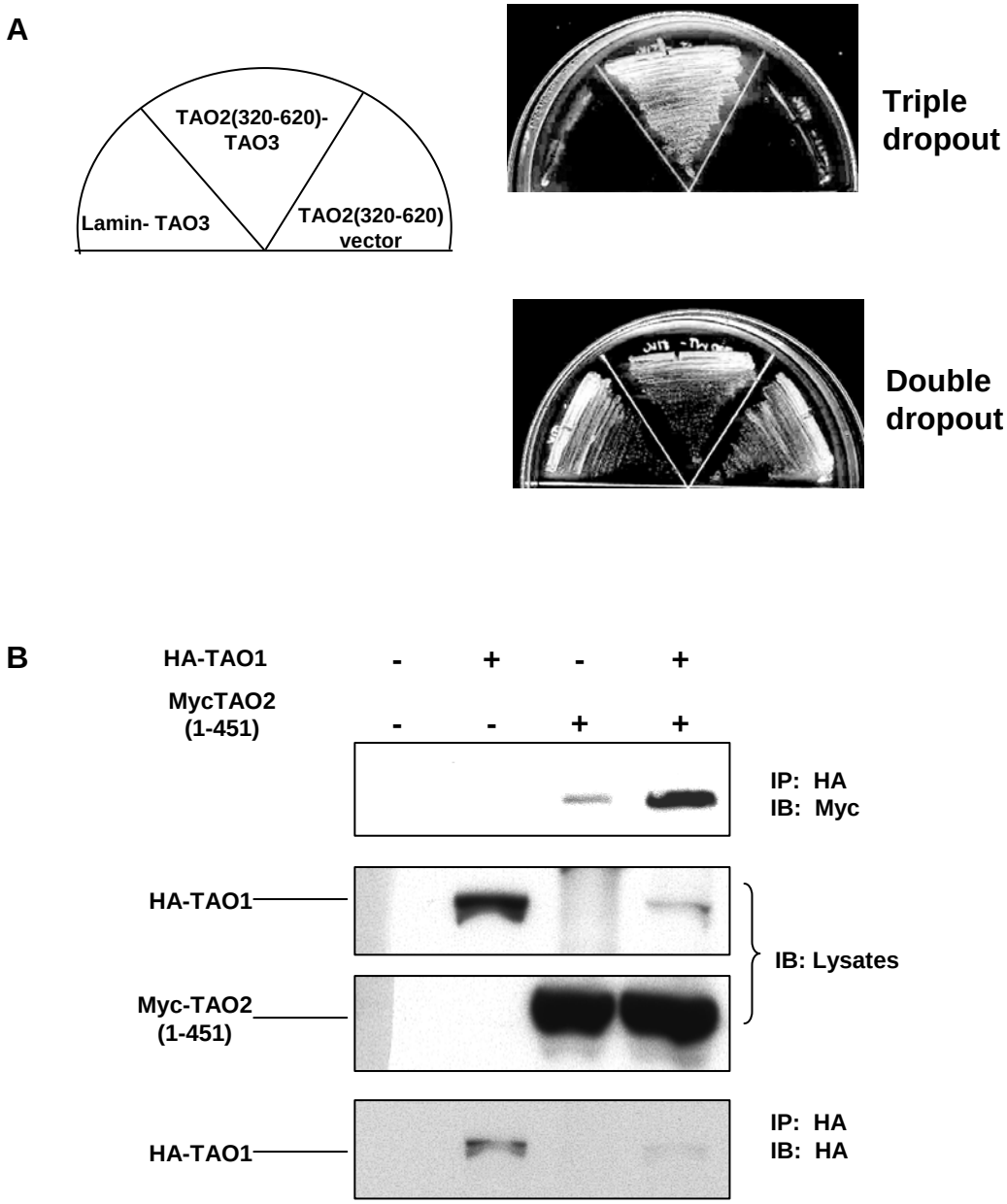

Figure 4-8. TAO kinases interact with one another. (A) Pair-wise yeast two-hybrid of the interaction between TAO2 (320-620) and TAO3. (B) HEK293 cells were transfected with HA-TAO1 and Myc-TAO2 (1-451). HA-TAO1 was immunoprecipitated from lysates and probed for TAO2.

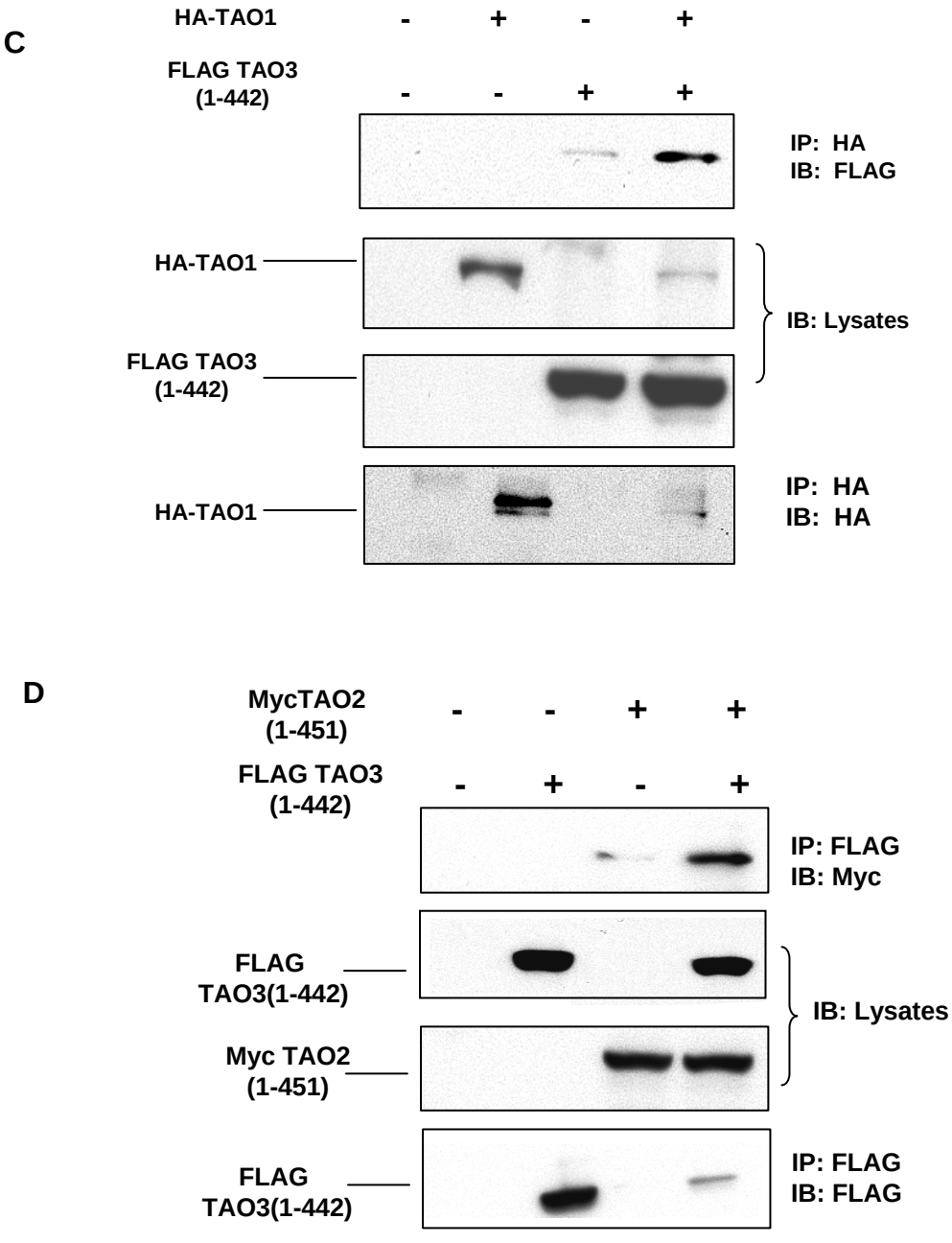

Figure 4-8. (Continued) TAO kinases interact with one another. (C) HEK293 cells were transfected with HA-TAO1 and FLAG-TAO3 (1-442). HA-TAO1 was immunoprecipitated from lysates and probed for TAO3. (D) HEK293 cells were transfected with Myc-TAO2 (1-451) and FLAG-TAO3 (1-442). FLAG-TAO3 was immunoprecipitated from lysates and probed for TAO2.

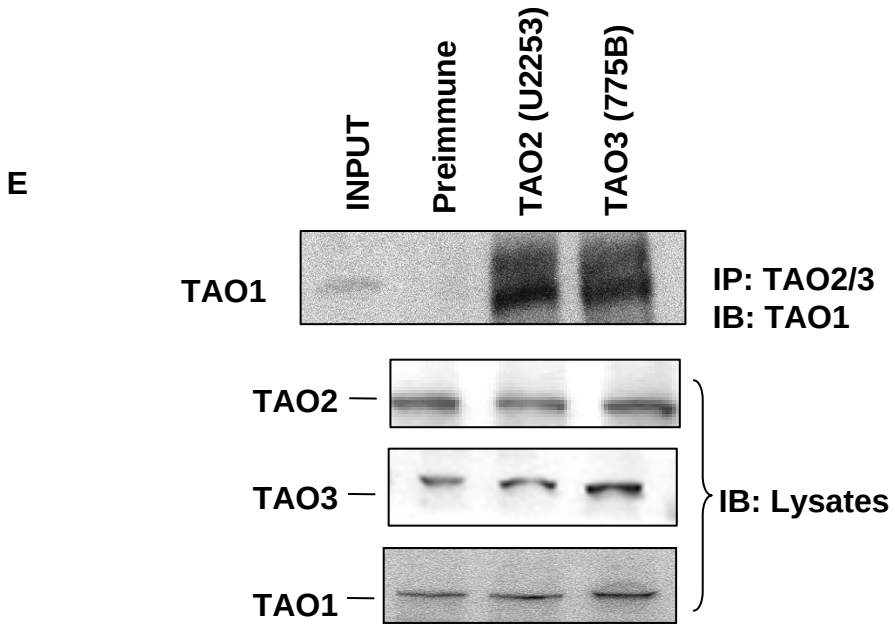

Figure 4-8. (Continued) TAO kinases interact with one another. (E) HEK293 cells immunoprecipitated with preimmune serum or anti-TAO2 and TAO3. Immunoprecipitates were probed with anti-TAO1.

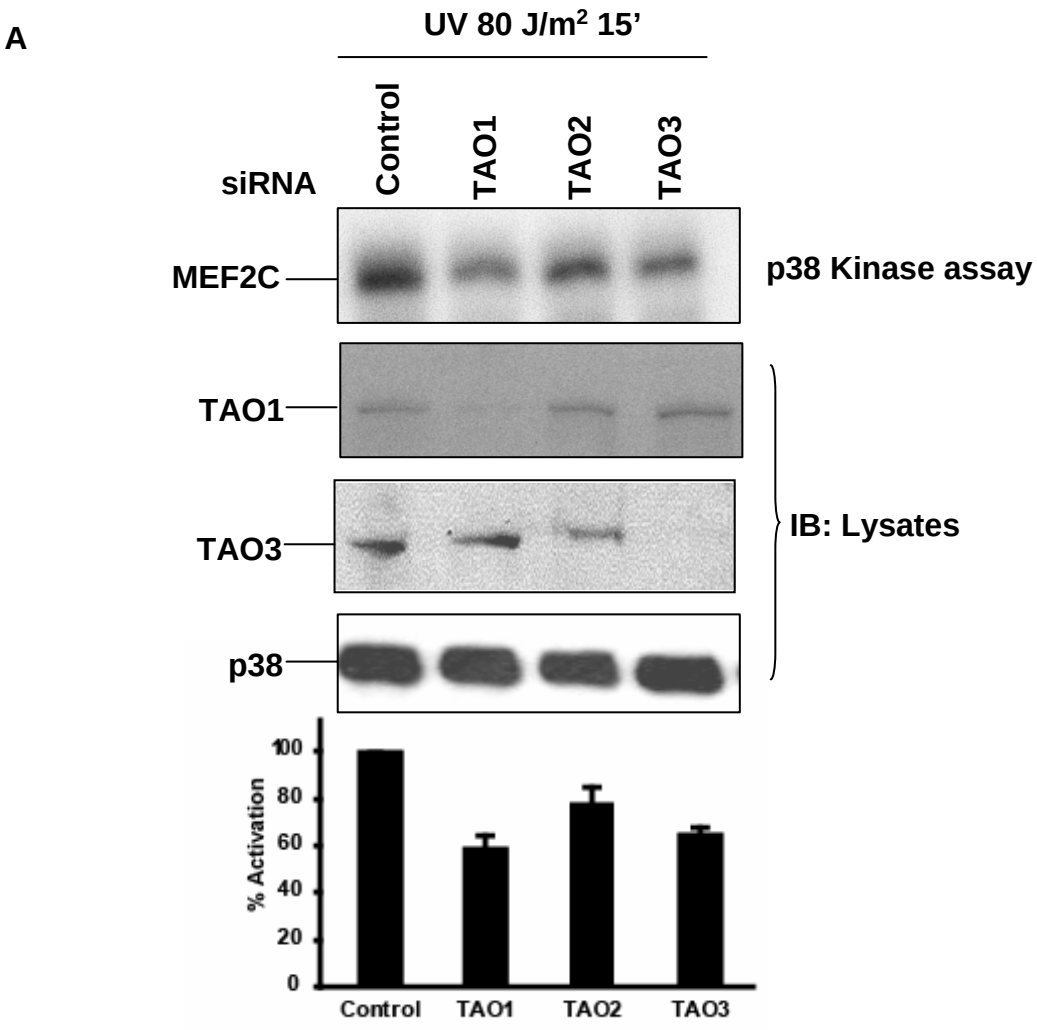

Figure 4-9. TAO kinases are required for UV-induced p38 activation. (A) HeLa cells were transfected with siRNA oligonucleotides to rat TAO2 (Control) or TAO1 and TAO3 (final concentration 100 nM). After 72 hrs cells were treated with 80 J/m^2 UV for 15 min and the activation of endogenous p38 was determined by immune complex kinase assay with MEF2C as substrate. Graph shows % activation, values are mean ± s.e.m. (n = 3).

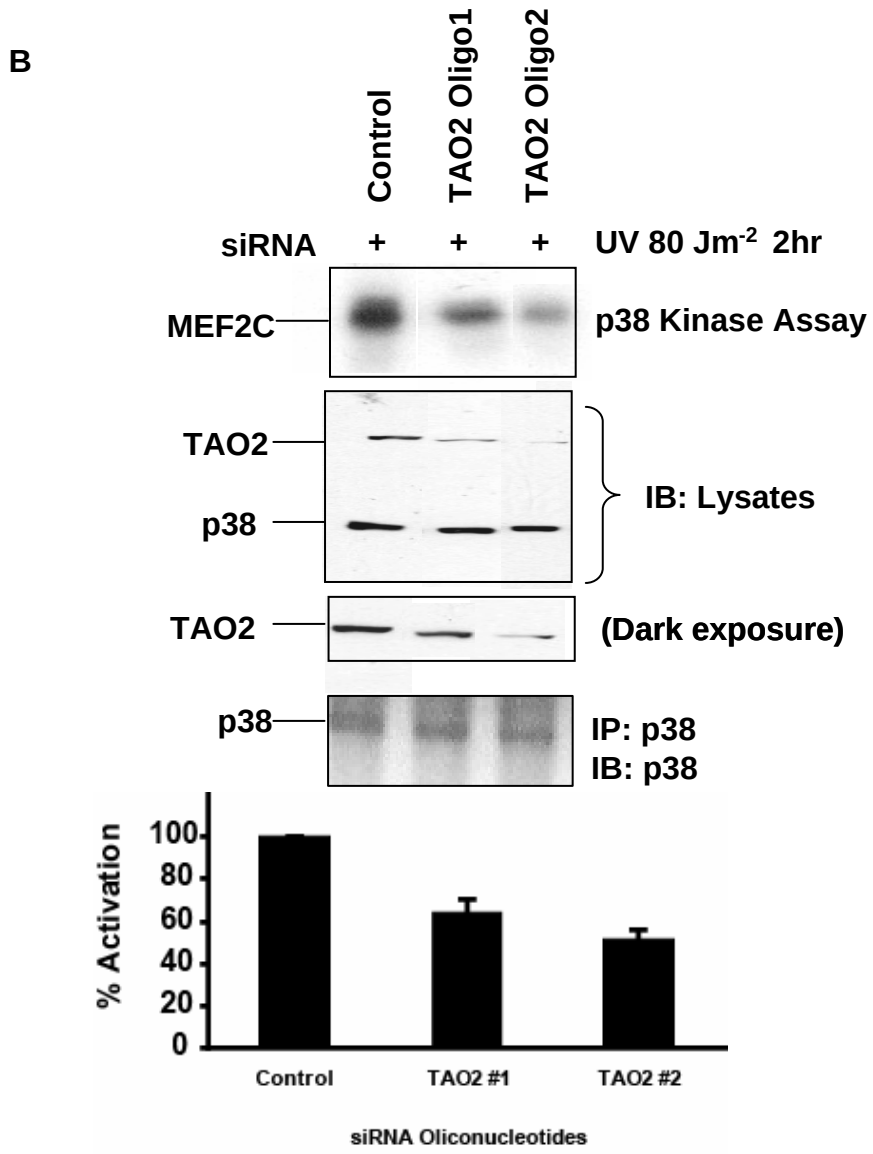

Figure 4-9. (Continued) TAO kinases are required for UV-induced p38 activation. (B) HeLa cells were transfected with siRNA oligonucleotides to rat TAO2 (control) or TAO2 (final concentration 100 nM). After 72 hrs cells were treated with 80 J/m^2 UV for 15 min and the activation of endogenous p38 was determined by immune complex kinase assay with MEF2C as substrate. Graph shows % activation, values are mean ± s.e.m. (n = 3).

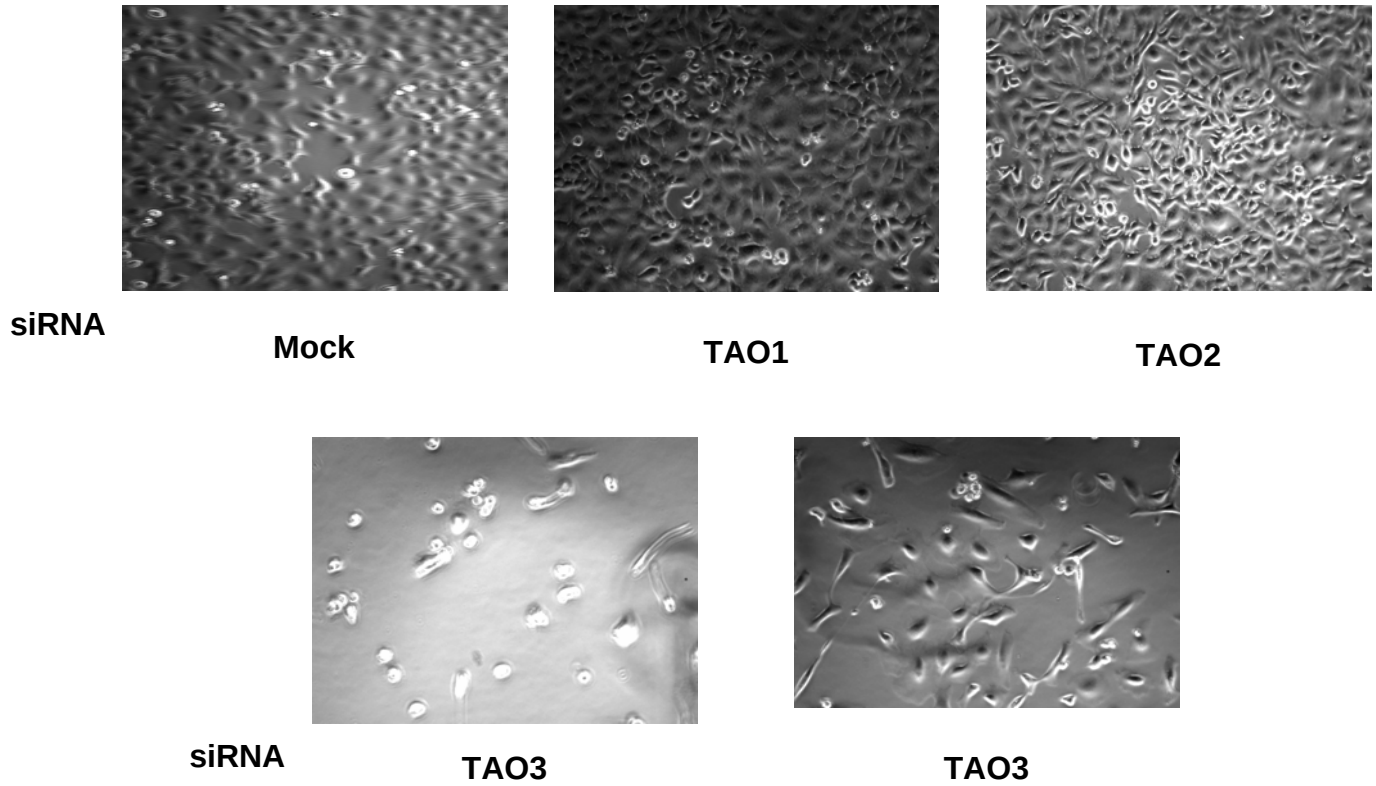

Figure 4-10. Knockdown of TAO3 reduces cell viability. HeLa cells were transfected with TAO1, 2 and 3 oligonucleotides (final concentration 100 nM). DIC images of cells were taken 72 hrs after transfection.

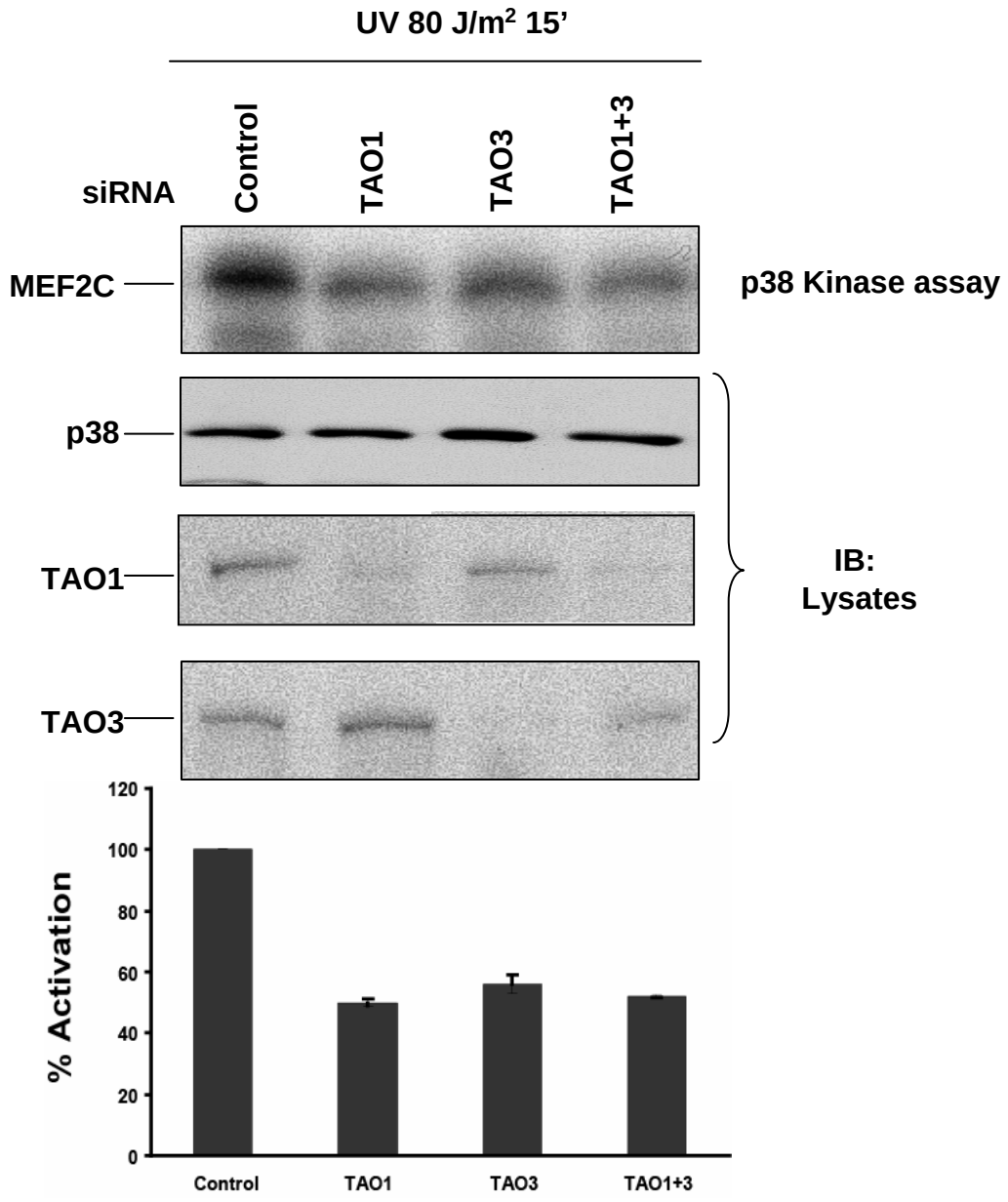

Figure 4-11. Double knockdown of TAO1, 3 is not significantly different from single knockdown. (A) HeLa cells were transfected with siRNA oligonucleotides to rat TAO2 (Control) or TAO1 and TAO3 either singly or in combination (final concentration 100 nM). After 72 hrs cells were treated with 80 J/m^2 UV for 15 min and the activation of endogenous p38 was determined by immune complex kinase assay with MEF2C as substrate. Graph shows % activation, values are mean ± s.e.m. (n = 3).

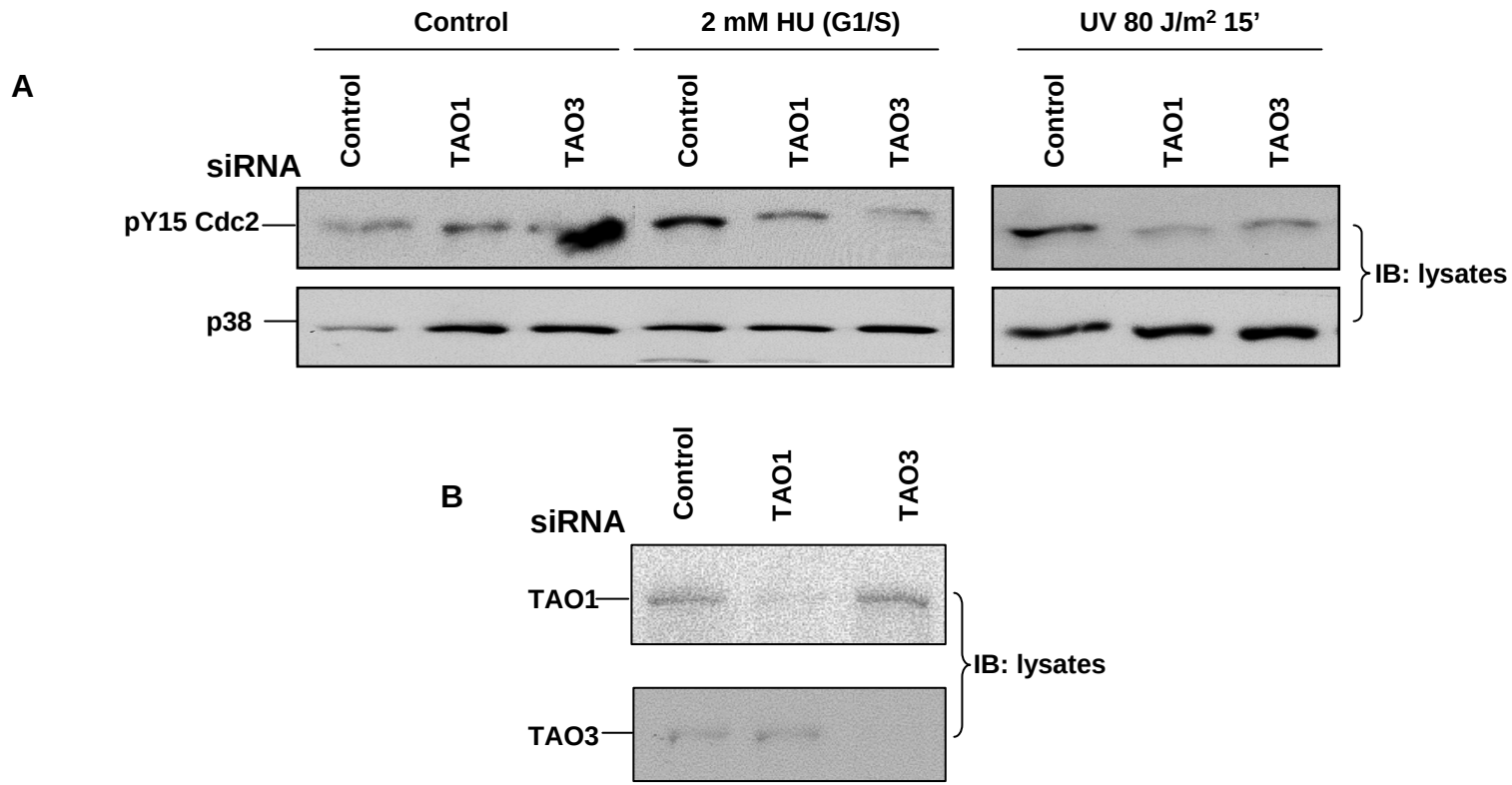

Figure 4-12. Knockdown of TAO1 and 3 prevents inhibition of the cyclin/Cdc2 activation by DNA damage. (A) HeLa cells were transfected with rat TAO2 (control) or human TAO1 and 3 oligonucleotides (final concentration 100 nM). After 72 hrs cells were untreated or treated with 2 mM HU for 20 hrs or 80 J/m^2 UV for 15 min Lysates were probed with anti-phospho Y15 Cdc2 or p38 as a loading control. (B) Western blot of TAO1 and 3 to shown knockdown levels.

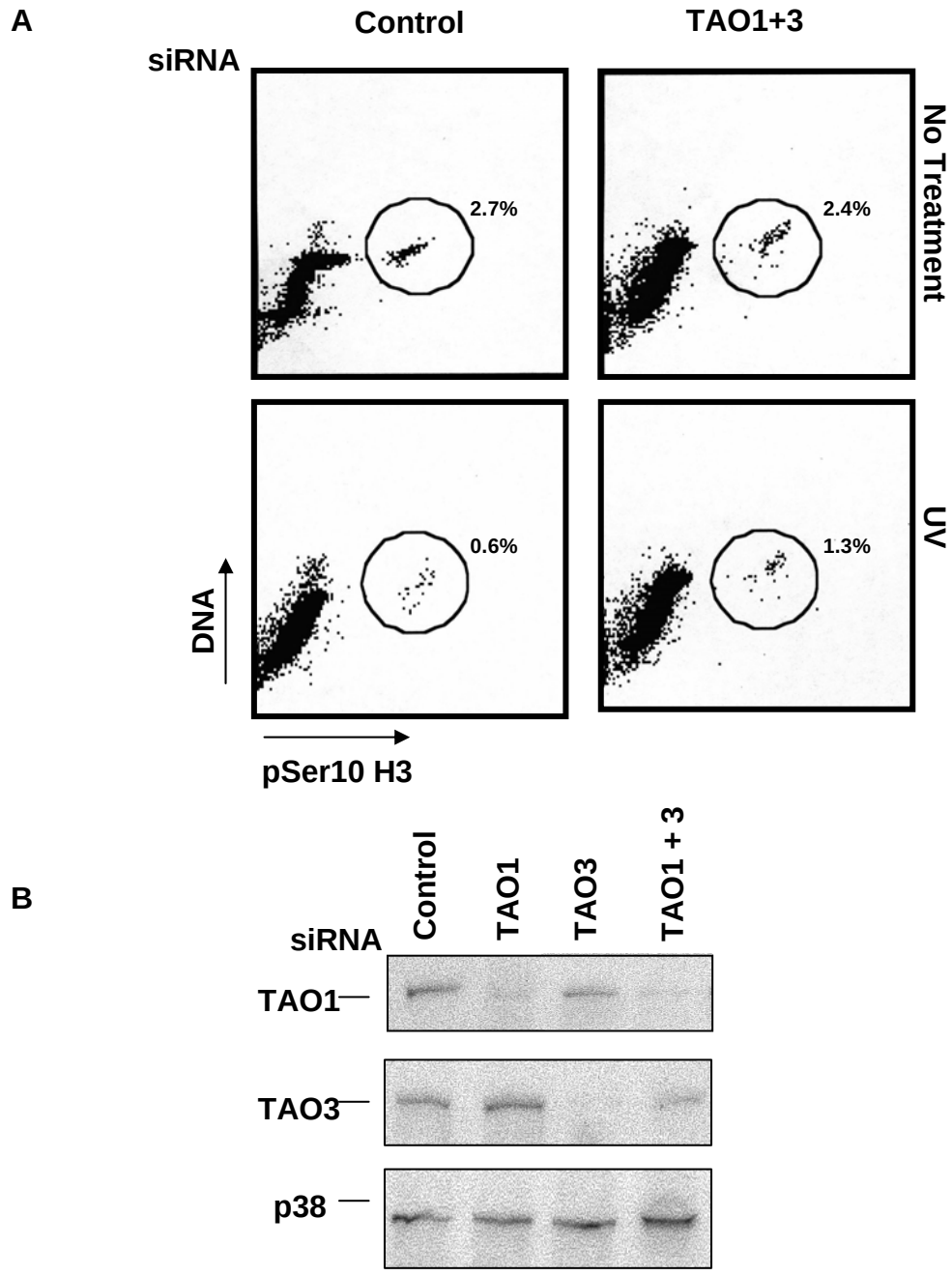

Figure 4-13. Knockdown of TAO1 and 3 inhibits UV-mediated G2/M cell cycle arrest. (A) HeLa S3 cells were transfected with siRNA oligonucleotides to rat TAO2 (Control) or TAO1 and TAO3 either singly or in combination (final concentration 100 nM). Cells were synchronized at G1/S with double thymidine block and then released for 4 hrs. Cells were treated with 80 J/m^2 UV for 2 hrs and the percentage of mitotic cells was determined by dual staining with propidium iodide (DNA) and phospho-Ser10 Histone H3. Representative FACS of TAO3 shown. (B) Immunoblot of TAO1 and TAO3 (n = 3).

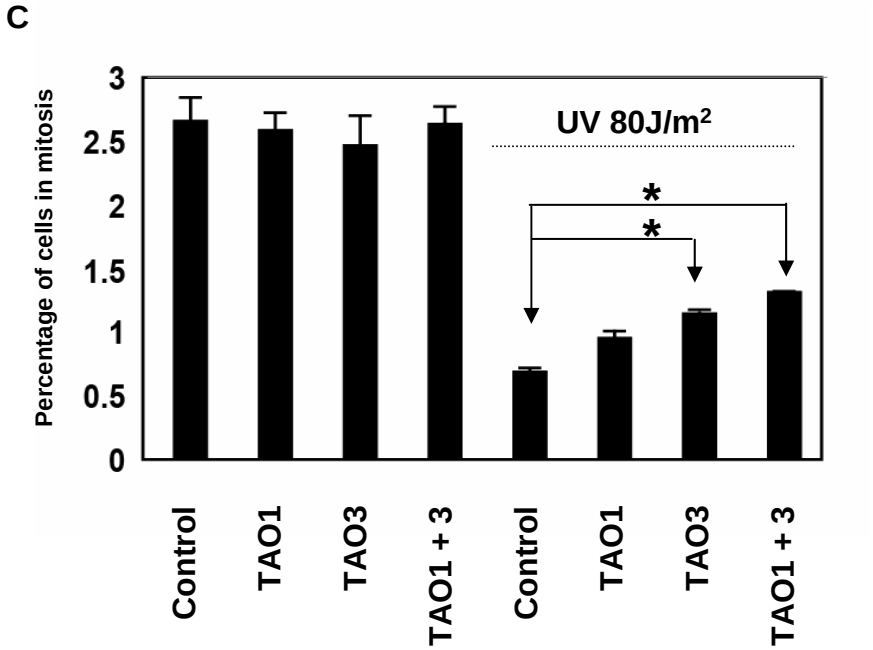

Figure 4-13. (Continued) TAO kinases are required for the UV-induced G2/M checkpoint. (C) Quantitation of mitotic cells in TAO1 and TAO3 knockdown cells. Values shown are means ± s.e.m. of three experiments $p \leq 0.05$ (*).

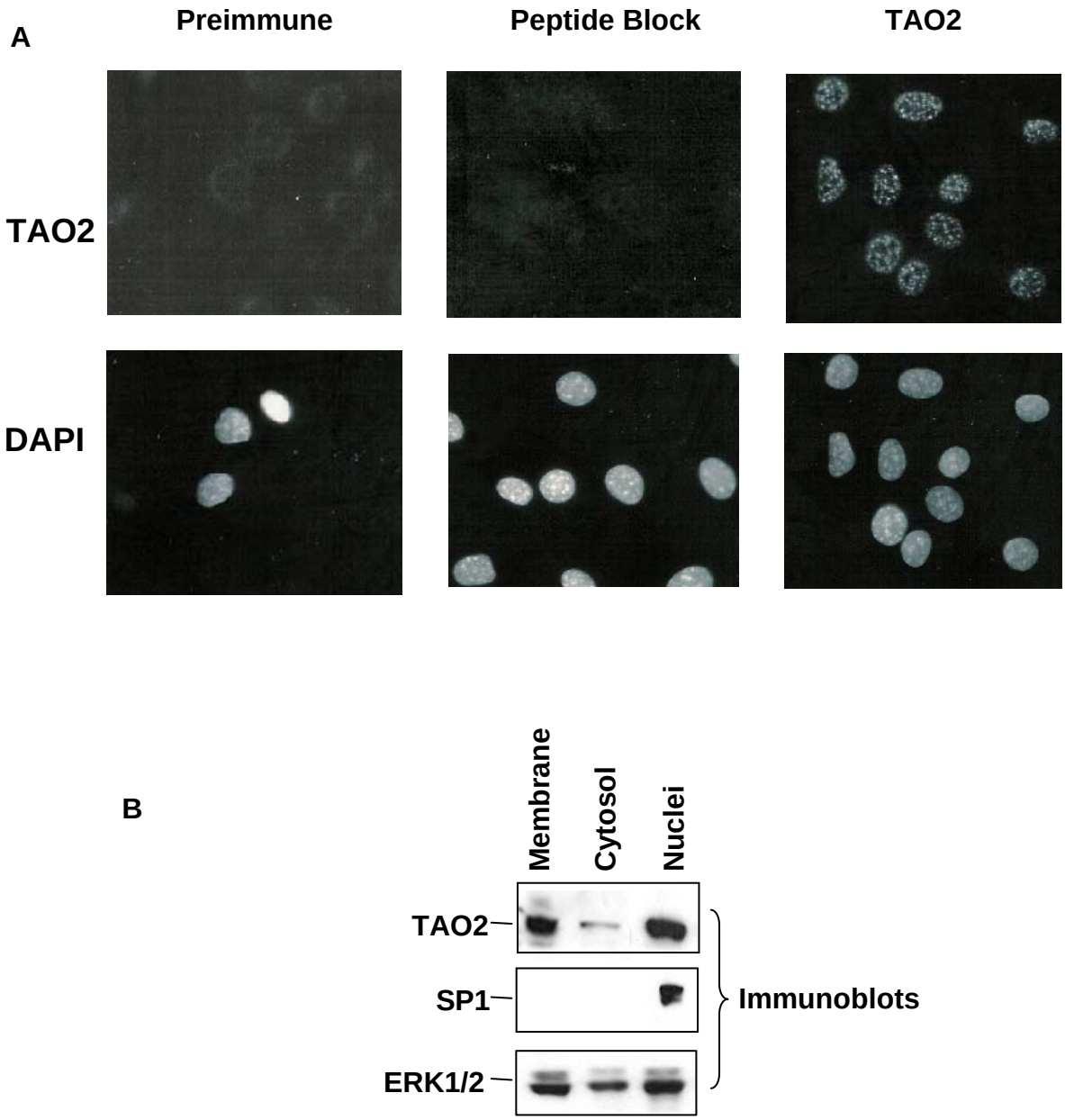

Figure 4-14. TAO2 is localized at the membrane and in the nucleus. (A) HeLa cells were fixed and stained with preimmune serum or anti-TAO2 and localization was visualized. (B) HeLa cells were fractionated into membrane, cytosol and nuclear fractions. Equal protein was loaded on SDS-PAGE gels and probed for TAO2, SP1 and ERK1/2. SP1 is a nuclear transcription factor.

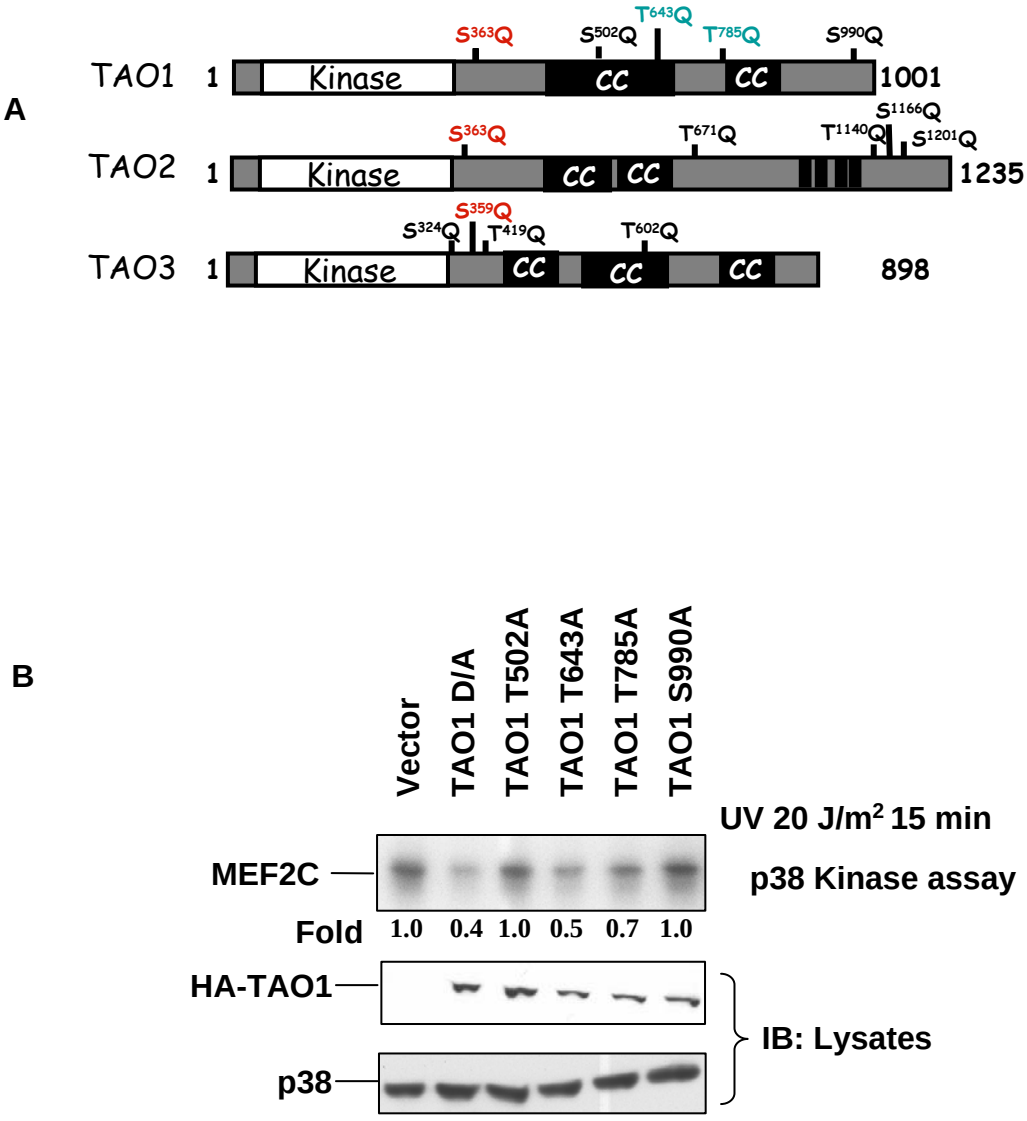

Figure 4-15. TAO kinases may be phosphorylated by ATM/ATR. (A) Organization of SQ/TQ sites on TAO1, 2 and 3. Red sites are conserved among the kinases. Cyan sites behave as dominant negatives in p38 activation by UV. (B) HEK293 cells were transfected with HA-TAO1 D/A or the SQ/AQ mutants: T502A, T643A, T785A and S990A. Cells were treated with 20 J/m^2 UV for 15 min and the activation of endogenous p38 was determined in kinase assays with MEF2C as substrate (n = 2).

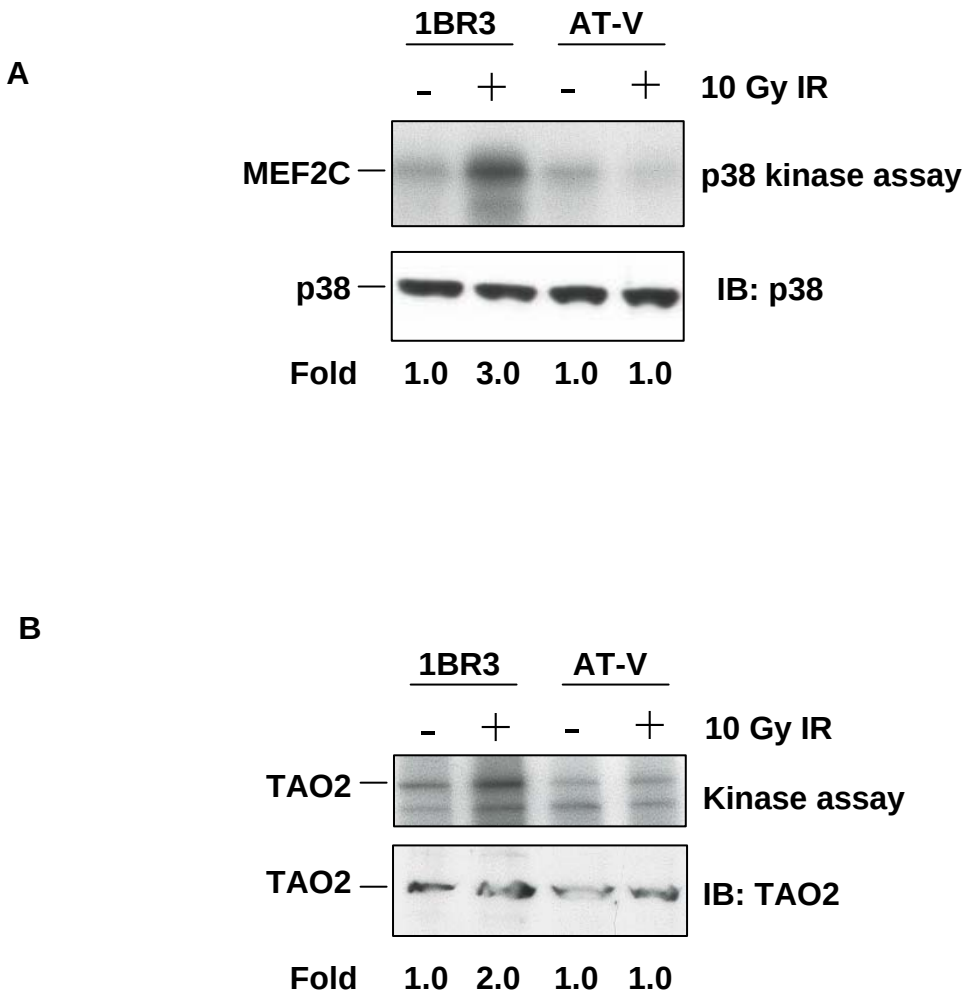

Figure 4-16. AT cells display poor activation of p38 and TAO2 by IR. (A) Wild type and ATM-deficient human skin fibroblasts (1BR3 and AT-V respectively) were untreated or treated with 10 Gy IR for the 2 hrs. p38 was immunoprecipitated from lysates and activity was assayed with MEF2C as substrate (B) Wild type and ATM-deficient human skin fibroblasts (1BR3 and AT-V respectively) were untreated or treated with 10 Gy IR for 30 min. TAO2 was immunoprecipitated from cell lysates and activation was assayed (n = 2).

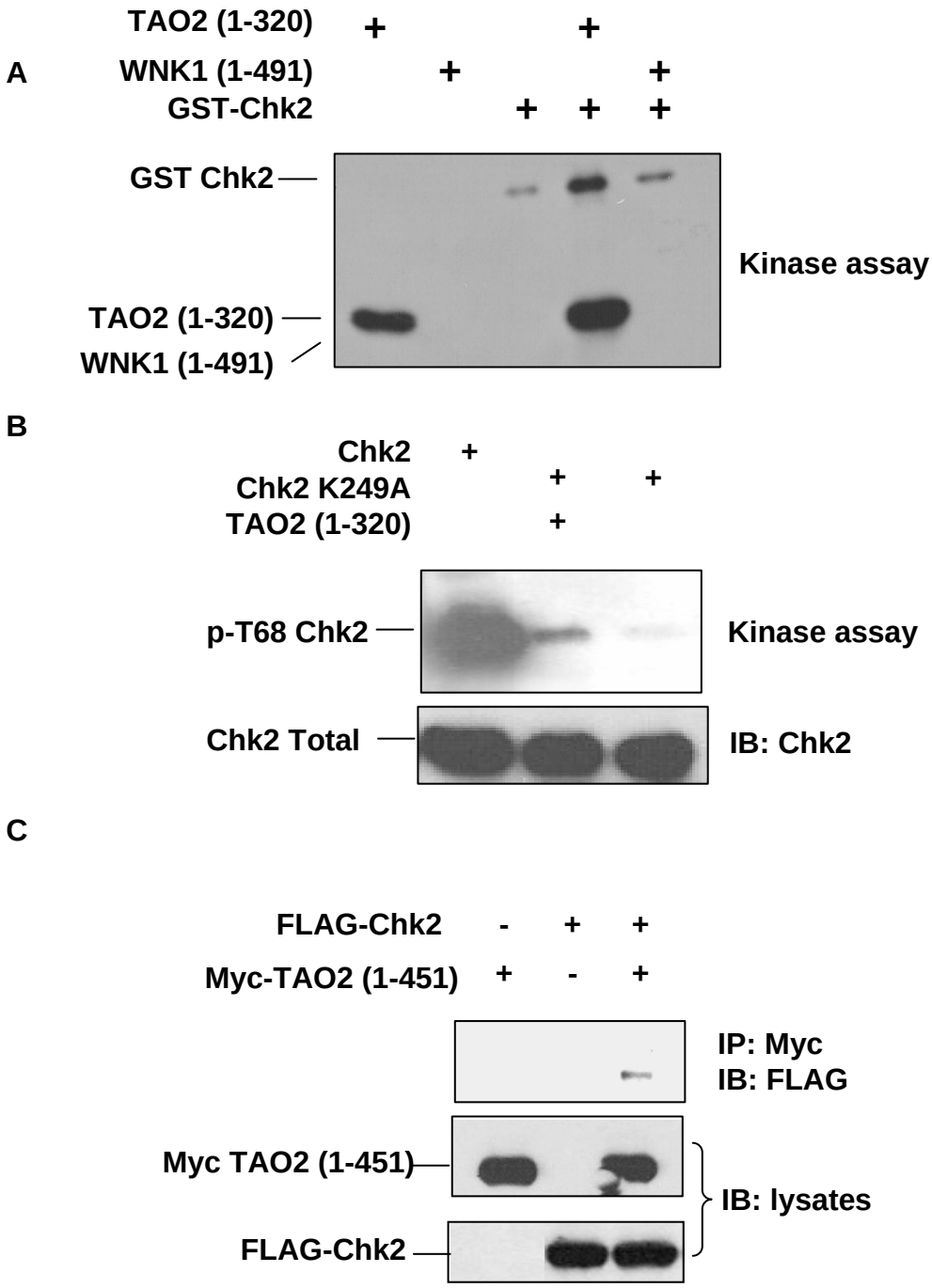

Figure 4-17. TAO2 phosphorylates and interacts with Chk2. (A) *In vitro* kinase assay demonstrating that TAO2 phosphorylates GST-Chk2 while WNK1 (1-491) does not. (B) *In vitro* kinase assay to phosphorylate kinase dead Chk2 with TAO2 (1-320). Samples were probed with an antibody to phospho-Thr68 and total Chk2. Wild type Chk2 was used as a control. (C) HEK293 cells were transfected with Myc-TAO2 (1-451) and FLAG-Chk2. Myc immunoprecipitates were probed with FLAG antibody to detect associated Chk2.

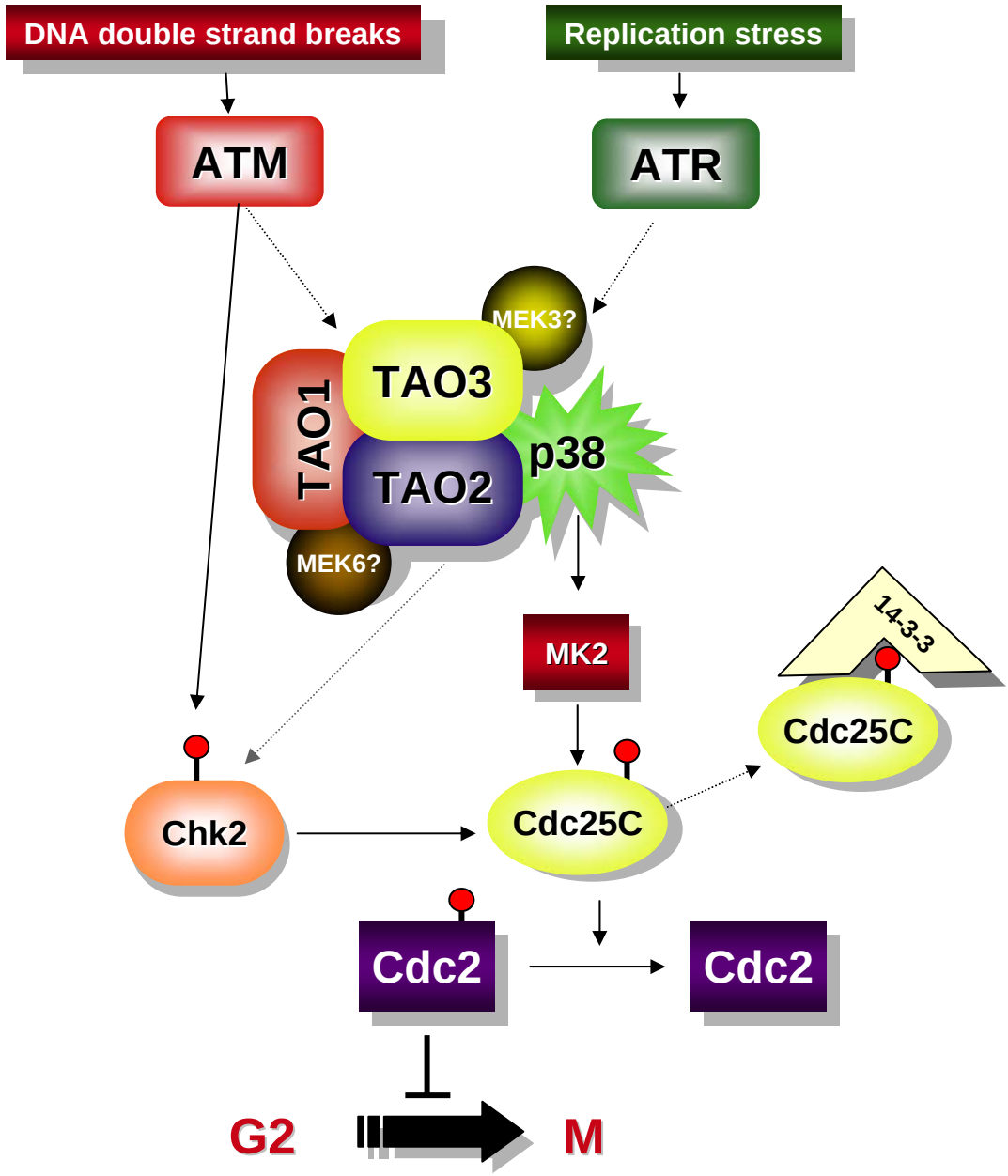

Figure 4-18. TAO kinases are required for the G2/M DNA damage checkpoint. TAO kinases are required for the DNA damage induced activation of p38 MAPK and subsequent cell-cycle checkpoints. See text for details.

RESIDUES	Phospho-peptides
154-177	NSYIAYIEDHSGNGTSVNTELVGK
181-195	RPLNNNSEIALSLSR
495-520	FQDLLSEENESTALPQVLAQPSTSRK

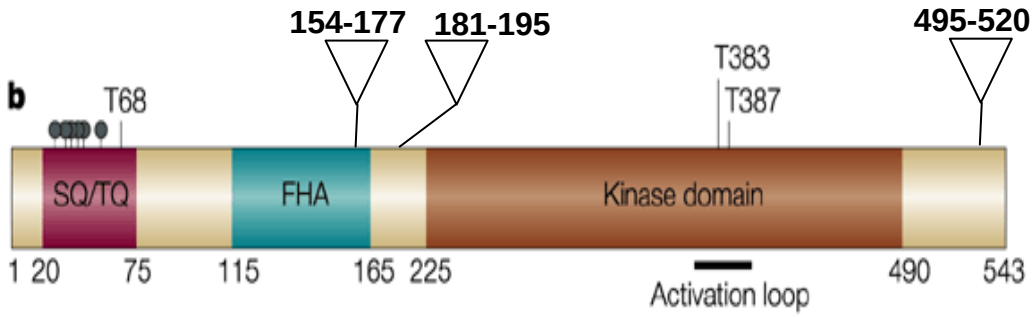

Table 4-1. Phospho-Chk2 phospho-peptides identified by mass-spectroscopy of GST-Chk2 K249A phosphorylated in vitro by TAO2 (1-320). Lower panel shows location of the peptides in the protein kinase.

CHAPTER 5. STRUCTURE-FUNCTION STUDIES OF TAO2 AND OTHER OBSERVATIONS

I. Abstract

The crystal structure of the TAO2 kinase domain in its active form was solved in collaboration with the Goldsmith lab. This was the first structure of a Ste20p kinase in its active conformation. Based on predictions from structural studies, we mutated residues in a substrate binding groove in TAO2 that resulted in impaired phosphorylation of the TAO2 substrate MEK6. The structure also showed that TAO2 had interactions with ATP that were different from other protein kinase structures, presenting the opportunity to exploit this characteristic in developing TAO protein kinase specific inhibitors.

A yeast two-hybrid screen for TAO2 interactors identified microspherule 1 multiple times. MSP1 is a nucleolar protein with an FHA domain. TAO2 interacted with MSP1 in transient transfection experiments. TAO2 associated with the FHA domain of MSP1 in directed-two-hybrid experiments, but this finding was not adequately repeated in other systems.

II. Materials and Methods

Cell culture and treatments

HEK293 and HeLa cells were obtained from ATCC. Cells were cultured in DMEM supplemented with 10% FBS, 2 mM glutamine and antibiotics. Cell lysis, immunoprecipitation, immunoblotting and associated techniques are described in detail in Chapters 3 and 4.

Yeast-two-hybrid techniques

Two-hybrid screening, pair-wise two-hybrid interactions and related techniques are detailed in Chapter 3.

Protein purification, crystallization and structure determination

All techniques related to purification of TAO2 (1-320), crystallization and structure determination are available elsewhere (Zhou et al., 2004).

Mutagenesis experiments

TAO2 mutants from crystallographic studies were created in pCMV-Myc TAO2 (1-320) using the Quikchange kit (Stratagene). All sequences were verified by sequencing. HEK 293 cells were transfected at 40% confluency by the standard calcium phosphate technique. Cells were transfected with 1μg of vector alone of the TAO2 mutant constructs (K120A, R221A, K222A, R221A K222A, K120A R221A R222A) for 24 hrs and starved overnight in DMEM containing 1% FBS. Cells were harvested in 500 μl of lysis buffer (150 mM NaCl, 1.5 mM $MgCl_2$, 1 mM EGTA, 10% glycerol, 0.2 mM $NaVO_4$, 100 mM NaF, 50 mM β-glycerophosphate and 0.1% Nonidet P-40 and 50 mM HEPES [pH 7.7]) and protease inhibitors. Transfected proteins were detected by immunoblotting with an anti-Myc antibody (9E10). Immunoprecipitations were carried out from 0.8 mg of cell lysate and the anti-Myc antibody and 30 μl of 1:1 slurry of protein A sepharose Cl-4B (Amersham). The beads were washed four times with kinase assay wash buffer (1 M NaCl, 0.25 M Tris-Cl [pH 7.4], 0.1% Triton X-100 and 0.1% deoxycholic acid) and two times with 10 mM HEPES [pH 7.4].

In vitro kinase assays were performed in 10 mM HEPES [pH 7.4], 10 mM MgCl2, 10 μM ATP, 15 cpm/fmol [γ-^{32}P] ATP, and either 0.5 mg/ml MBP or 100 ng MEK6 K82M as substrates. Reactions were incubated at 30°C for the indicated time points and then terminated with 5X SDS-sample buffer. Samples were briefly boiled and then resolved by SDS-PAGE gels. Gels were either processed for auto-radiography or subjected to immunoblotting with anti-MEK3/6[pSpT$^{189/193}$]/pSpT$^{207/211}$] (Biosource International).

Subcloning and mutagenesis

Cloning of Myc-TAO2 (1-451) was described in Chapter 3. Myc-TAO2 (317-667) was amplified by PCR from Myc-TAO2 full length and ligated into pCMV5 vector. The MSP1 clone rescued from two-hybrid consisted of the entire coding sequence lacking the first 25 amino acids. MSP1Δ25 and the MSP FHA domain were amplified from this clone by PCR and ligated into p-3XFLAG-CMV7.1 as well as pGADGH. Point mutations in the FHA domain of MSP1 G366A, R367A, S388A, N429A and the G366AR367A were created by Quikchange mutagenesis according to the manufacturer's instructions (Stratagene). All samples were verified by sequencing.

III. Results

A. TAO2 is constitutively phosphorylated on Serine 181.

To gain greater insight into the function of TAO2, the crystal structure of the kinase domain of TAO2 was solved from protein purified from a *Baculovirus*/Sf9 system in the Goldsmith laboratory (Department of Biochemistry). Both the apo-form as well as the kinase

domain in complex with Mg^{2+}/ATP were determined (Figure 5-1). The crystal consisted of two monomers of the kinase domain indicating that protein is capable of self association. This agrees well with our data that TAO kinases are capable of interacting with one another (Chapter 4, Figure 4-8). Interestingly, the kinase was constitutively phosphorylated on Ser181, active, and adopted a closed conformation. The structure of TAO2 adopted the classic protein kinase fold composed of the small, upper N-terminal β- sheet and the lower helical C-terminal domain. The structure lacked helix B found in the N-terminal domain of AGC kinases. TAO2 has two extra N-terminal helices named αA and αB (Figure 5-1) which are shared in the related Ste20p kinase PAK (Lei et al., 2000). In the C-terminal half of the kinase, additional helices J and K were observed. Helix K spans the distance between the upper and lower domains and is lacking in PAK. Helix J, which is present in PAK, is generally in the area on p38 MAPK that binds to substrates (Chang et al., 2002).

The structure of the kinase in complex with Mg^{2+}-ATP revealed an altered position of the γ-phosphate of ATP. The orientation was reminiscent of the interactions observed between MgAMP-PNP in complex with the insulin receptor kinase. Interestingly, Lys314 in helix K (unique to TAO2) bonds with the ribose of ATP. Additionally, Lys153 in the catalytic loop is not in close proximity to the γ-phosphate of ATP as it is in other active kinases. Lys314 in helix K is not conserved in other Ste20p kinases. This feature offers the tantalizing possibility of designing inhibitors unique to TAO2 that will not affect other Ste20ps.

Next we wished to determine the significance of Ser181 phosphorylation and its impact on TAO2 kinase activity. Ser181 is positioned in the activation loop of TAO2 and is a

site of phosphorylation in other kinases. We mutated the residue to alanine and transfected the construct into HEK293 cells. We assayed the activity of wild type TAO2 (1-320) as well as the S181A mutant by immunoprecipitating the kinase and assaying it with MEK6K82M as a substrate. While wild type TAO2 phosphorylated MEK6K/M efficiently, the S181A mutant was catalytically deficient as it failed to phosphorylate the substrate, similar to kinase dead TAO2 (1-451) D169A. Auto-phosphorylation was also completely inhibited (Figure 5-2). This indicates that Ser181 is a critical determinant of TAO2 kinase activity.

The MEK6 substrate peptide was modeled into the substrate binding groove of TAO2 (interface between upper and lower domains). TAO2 phosphorylates MEK6 in the activation loop sequence D**S**^{207}VAK**T**^{211}I (Figure 5-3). In the model, D206 appeared to make contact with a positively charged groove in TAO2 comprising of residues Lys120, Arg211 and Lys222. To determine if these residues were indeed required for orienting and binding the MEK6 activation loop, we mutated these three residues either singly or in combination to alanine and assayed the mutants for activity in our assay. TAO2 K120A was only marginally deficient in activity (approximately 20% decrease compared to wild type). The R221 and K222 mutants were comparable to wild type in activity also (Figure 5-4A). However, mutation of both R221 and K222 (RKAA in Figure 5-4A) resulted in a 40% decrease in kinase activity. Mutation of all three residues to alanine resulted in further decrease in MEK6 phosphorylation (60% relative to wild-type) (Figure 5-4B). These results strongly suggest that the positively charged residues lining this pocket are partly required for the recognition of specific substrate. In control experiments, these mutants phosphorylated the general substrate MBP as efficiently as wild type kinase (Figure-5-4A). These results were also

confirmed with an antibody that recognizes the dually phosphorylated form of MEK6. As shown in Figure 5-4B, the KRKAAA TAO2 triple mutant phosphorylated MEK6KM poorly compared to wild type TAO2.

In many cases of substrates that are phosphorylated onto two residues, there is an obligate order in the phosphorylation events. For example, in the dual phosphorylation of ERK2 by MEK2, the tyrosine in the TEY motif must be phosphorylated before the threonine is phosphorylated (Burack and Sturgill, 1997; Robbins and Cobb, 1992; Robbins et al., 1993; Zhang et al., 1995). Mutation of the tyrosine prevents threonine phosphorylation and is a required step in activation. We mutated serine 207 and threonine 211 in the activation loop of MEK6 (D**S**^{207}VAK**T**^{211}I) to alanine in the background of the K82M mutation. The MEK6 S207A mutant was phosphorylated in a manner similar to wild type. However, the T211A mutant was a poor substrate and was only phosphorylated to 40% of control MEK6 KM levels (Figure 5-5). These results indicate that activation loop sites are phosphorylated in an ordered manner by TAO2. Based on the structure of the modeled MEK6 peptide in the TAO2 structure, the aspartic acid at position 206 appeared to be in close proximity to the positively charged pocket in TAO2. To determine if this site was required for phosphorylation, the D206A mutation was engineered in the background of the S207A, K82M mutations in MEK6 and assayed for phosphorylation. Compared to S207A mutant, the D206A, S207A mutant was not efficiently phosphorylated by TAO2 (only 20% of control levels), indicating D206 was probably required for interaction with TAO2. The D**S**^{207}VAK**T**^{211}I peptide is quite well-conserved among MEKs, the isoleucine at position 212 (P+1 residue) especially so. This residue was mutated to glycines also in the background of the S207A, K82M mutant

and used in our assays. This mutant was a very poor substrate and showed only negligible phosphorylation compared to control (Figure 5-5).

These studies provided important insight into the mode in which TAO2 substrates are recognized and phosphorylated. The Ser181 site in the activation loop is likely an important means of regulating activity of TAO2 and may act as the switch that releases auto-inhibition

B. TAO2 interacts with microspherule 1 (MSP1)

Microspherule 1 (MSP1) was identified multiple times as a TAO2 interactor using the (320-620) fragment as bait (Table 3-1). The clone was rescued and sequenced and determined to contain the entire coding region except the first 25 amino acids. MSP1 harbors a C-terminal forkhead associated (FHA) domain which in other proteins has been shown to bind phosphorylated threonine (Durocher et al., 1999; Hofmann and Bucher, 1995). This clone was isolated multiple times (>20 inserts), and phospho-amino acid analysis of TAO2 demonstrated preferential phosphorylation on threonine residues. Hence, we reasoned that TAO2 might bind to MSP1 in a FHA domain-dependent manner. To test this, we constructed fragments of MSP1 that were truncated before the FHA domain and tested them in pair-wise two-hybrid analysis with TAO2 baits in yeast. TAO2 (320-620) interacted with both full length MSP1 as well as the ΔFHA MSP1 (Figure 5-6A).These constructs were also cloned into mammalian expression vectors and co-transfected with a fragment of TAO2 containing the coiled-coil domains (314-667) into HEK293 cells. TAO2 was detected in immunoprecipitates of MSP1. The ΔMSP1 protein also interacted with TAO2 but appeared to be weaker than the interaction seen with full length MSP1 (Figure5-6B). In order to show

that the FHA domain was necessary for interaction, point mutations were made on critical residues within the FHA domain. These residues have been shown in a number of studies to be required for the interaction with the phospho-threonine (see Materials and Methods)(Durocher et al., 1999). We were not able to determine conclusively whether these sites were required for interaction as these mutants expressed very poorly both in HEK293 cells and in bacteria (data not shown).

We also conducted experiments to determine if TAO2 was capable of phosphorylating MSP1, but under our standard assay conditions we did not see any significant phosphorylation.

IV. Discussion

Here, I have discussed studies we carried based on the crystal structure of the kinase domain of TAO2. A number of interesting observations were made based on these studies. Firstly, it appears that serine 181 in the activation loop is constitutively phosphorylated in the structure and is an important means of regulating kinase activity. Mutation of this site to an alanine residue or a glutamate residue to mimic phosphorylation dramatically diminished kinase activity. This may either be a site of auto-phosphorylation or be phosphorylated by other kinases to regulate activity. Additionally, the crystals contained two molecules of TAO2 and indicated that the kinase is capable of associating to form dimers or higher order multimers. Based on our data that TAO family members are capable of binary interactions with one another, we predict that the three kinases occur as part of a high molecular weight

complex within cells. Further analysis by gel filtration or immunoprecipitation of endogenous proteins will help us identify interactors.

The orientation of the γ-phosphate of ATP in the crystal structure was also altered in position and contacts with other residues. Lysine 314 in the K helix unique to TAO2 made contacts with the ATP and could possibly be exploited in the future to make selective inhibitors with this family of kinases. The order of dual phosphorylation also appears to be non-random. We noted that TAO2 catalyzes phosphorylation on T211 first before phosphorylating S206. Importantly, the structure aided in the identification of residues in both TAO2 and its substrate MEK6 that are important determinants of phosphorylation. A positively charged groove is present in TAO2 composed of K120, R221 and K222. This region may be utilized to bind to D206 in MEK6 and serve to orient and stabilize the MEK6 activation loop. Isoleucine 212 (P+1 residue) was likewise important in the orientation of the MEK6 peptide. Mutation of the positively charged residues in TAO2 decreased catalytic activity and MEK6 D206A and I212A mutants were poor substrates. Recently another group identified the presence of a novel docking site in MEKs called the domain for versatile docking (DVD) (Takekawa et al., 2005). This domain was identified in MEK1, MEK4/7 and MEK3/6. It was determined to be required for the interaction of these MEKs with their cognate MAP3Ks, MEKK1/4, ASK1, TAK1, Raf-1 and notably TAO2. While we observed that residues surrounding the phosphorylation sites in the activation loop of MEK6 made contacts with TAO2, this study identified a DVD domain at the extreme C-termini of MEKs. In previous studies, we showed that the N-terminus of MEK6 is required for binding to TAO2 and interacted with a region in TAO2 between residues 314-451(Chen et al., 1999).

Based on our and others' studies, it appears that MEK6 and TAO2 interact with one another via a number of surfaces and perhaps this is a means of creating added specificity to prevent inappropriate activation of parallel cascades. This is reminiscent of p38 substrates using multiple surfaces on the protein kinase in binding.

The two-hybrid screen undertaken with fragments of TAO2 helped identify MSP1 as a TAO2 interactor. MSP1 is a nucleolar protein whose function is largely unknown. Two recent studies have alluded to a possible role for MSP1 as a tumor suppressor (Okumura et al., 2005). Proteins that interact with the FHA domain of MSP1 have not been identified. We were also unable to show conclusively that TAO2 interacted with MSP1 via its FHA domain. TAO2 localizes to nuclear foci by immunofluorescence. These domains bear a striking resemblance to the subcellular localization of MSP1. Perhaps TAO2 has an important role within the nucleolus in processes such as ribosomal biosynthesis. FHA domains have been identified in multiple nuclear proteins that take part in the DNA damage response. No role for MSP1 in the DDR has been identified. It would be interesting to knockdown this protein in conjunction with DNA damage and observe if there are any defects in the engagement of cell cycle checkpoints.

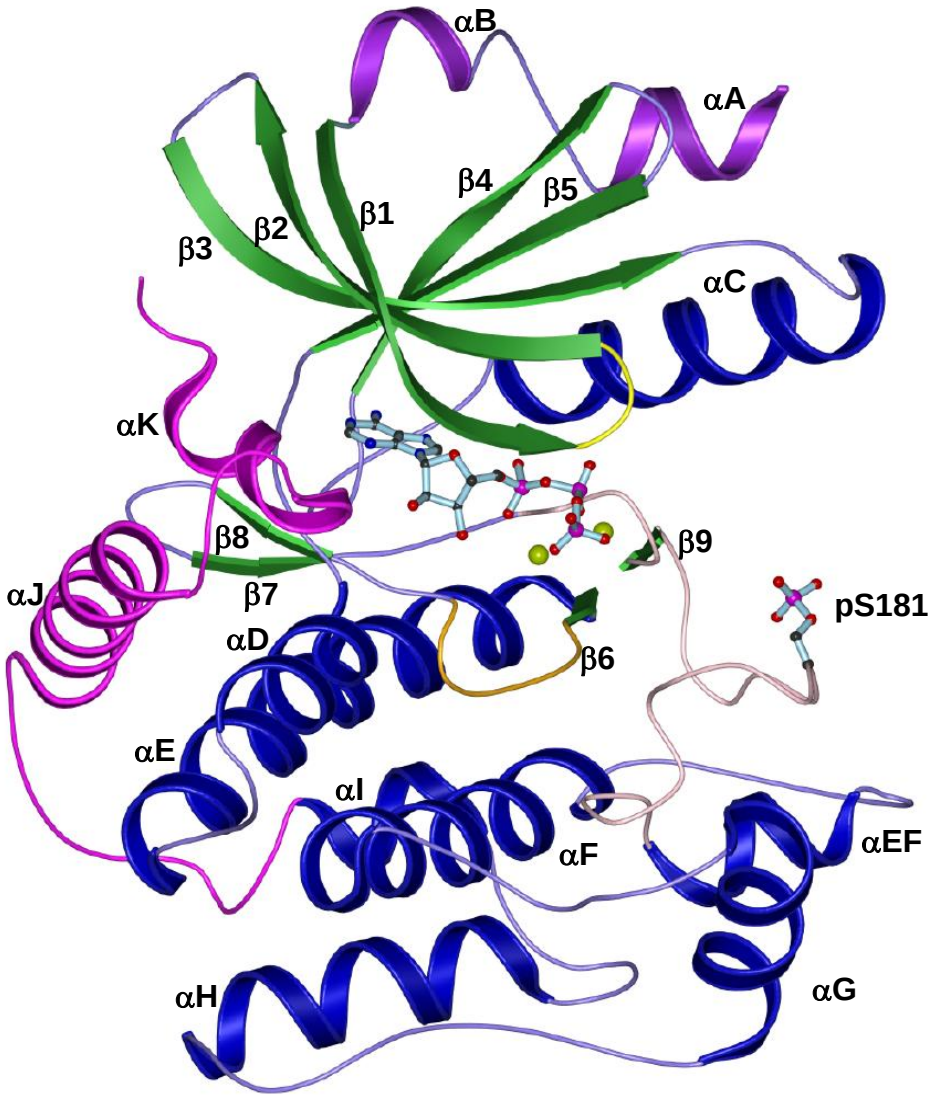

Figure 5-1. Structure of TAO2 kinase domain. Ribbon diagram of TAO2 (1-320) in complex with Mg-ATP. Phosphate binding ribbon is yellow, catalytic loop is orange and the activation loop is pink. The N-terminal β strands are colored green and the conserved α helices are blue. The additional helices A and B in the N-terminal domain are purple and helices J and K are magenta. Phospho-serine 181 and the Mg-ATP complex are shown using a ball and stick representation. (From Zhou et al., 2004).

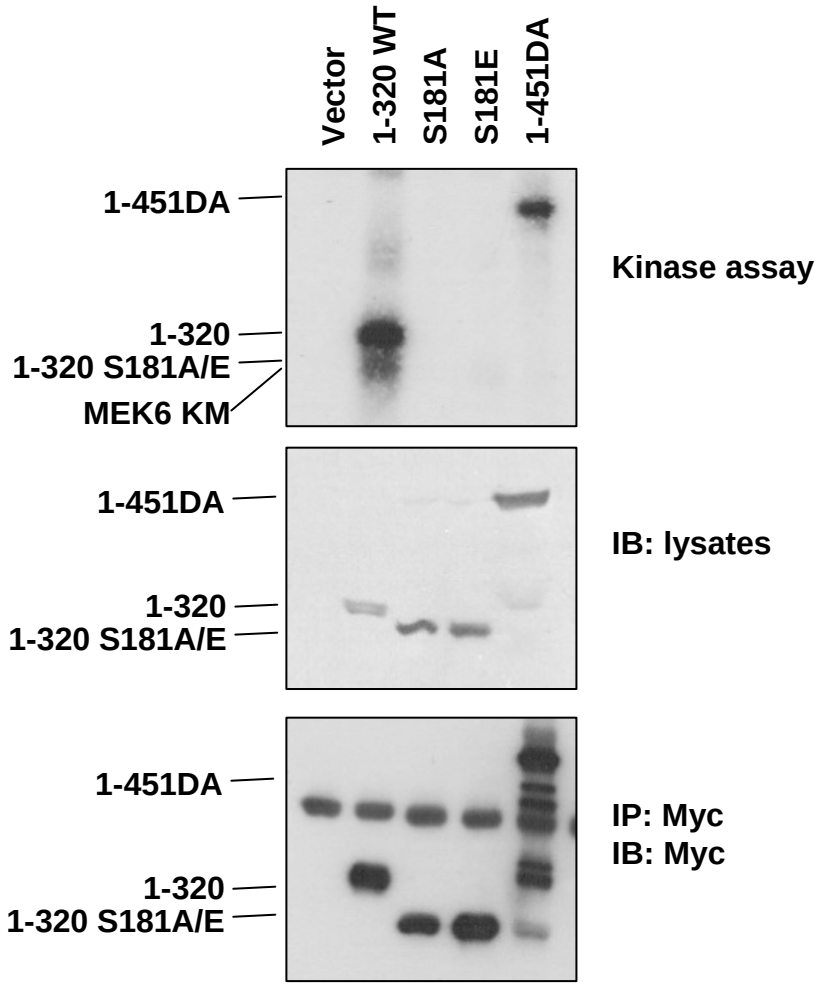

Figure 5-2. TAO2 is constitutively phosphorylated on serine 181. HEK293 cells were transfected with empty vector or Myc-TAO2 (1-320) wild type, S181A or E mutants or Myc-TAO2 (1-451) D169A. Cell lysates were immunoprecipitated with anti-Myc and kinase assays were performed with MEK6KM as substrate. TAO2 (1-451) DA is phosphorylated in cells by an unknown associated kinase.

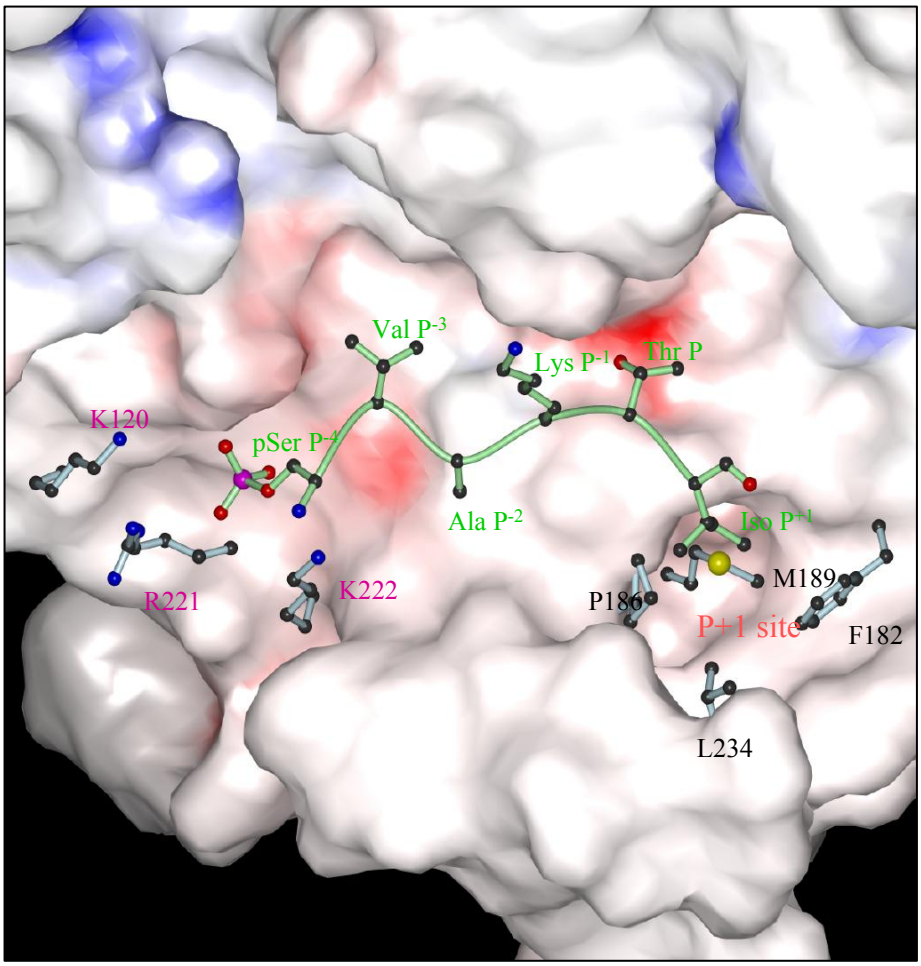

Figure 5-3. Surface representation of MEK6 binding pocket. Residues from the positively charged pocket (blue), P+1 pocket (blue) and the MEK6 peptide (green) are in stick representation (Courtesy T. Zhou).

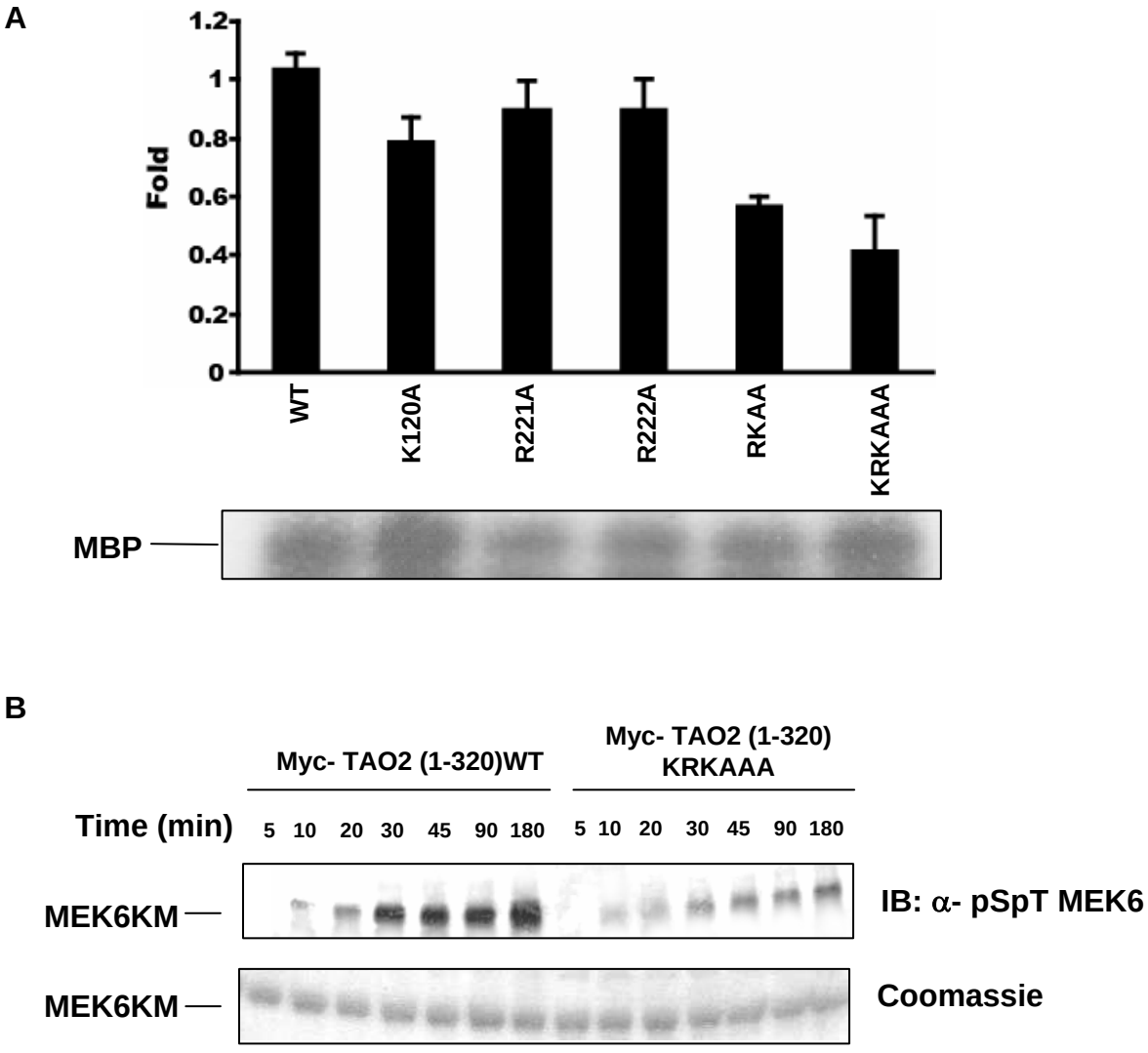

Figure 5-4. Influence of mutation on the positively charged pocket of TAO2 on MEK6 phosphorylation. (A) Kinase activities of TAO2 (1-320) and mutants K120A, R221A, K222A, RKAA and KRKAAA in the positively charged pocket towards MEK6KM (upper panel) and MBP (lower panel). Graph shows fold phosphorylation mean ± s.e.m. (B) Time course of phosphorylation of MEK6KM by wild type TAO2 and the KRKAAA triple mutant. MEK6 phosphorylation was detected with an antibody against dually phosphorylated MEK6 (Modified from Zhou et al., 2004).

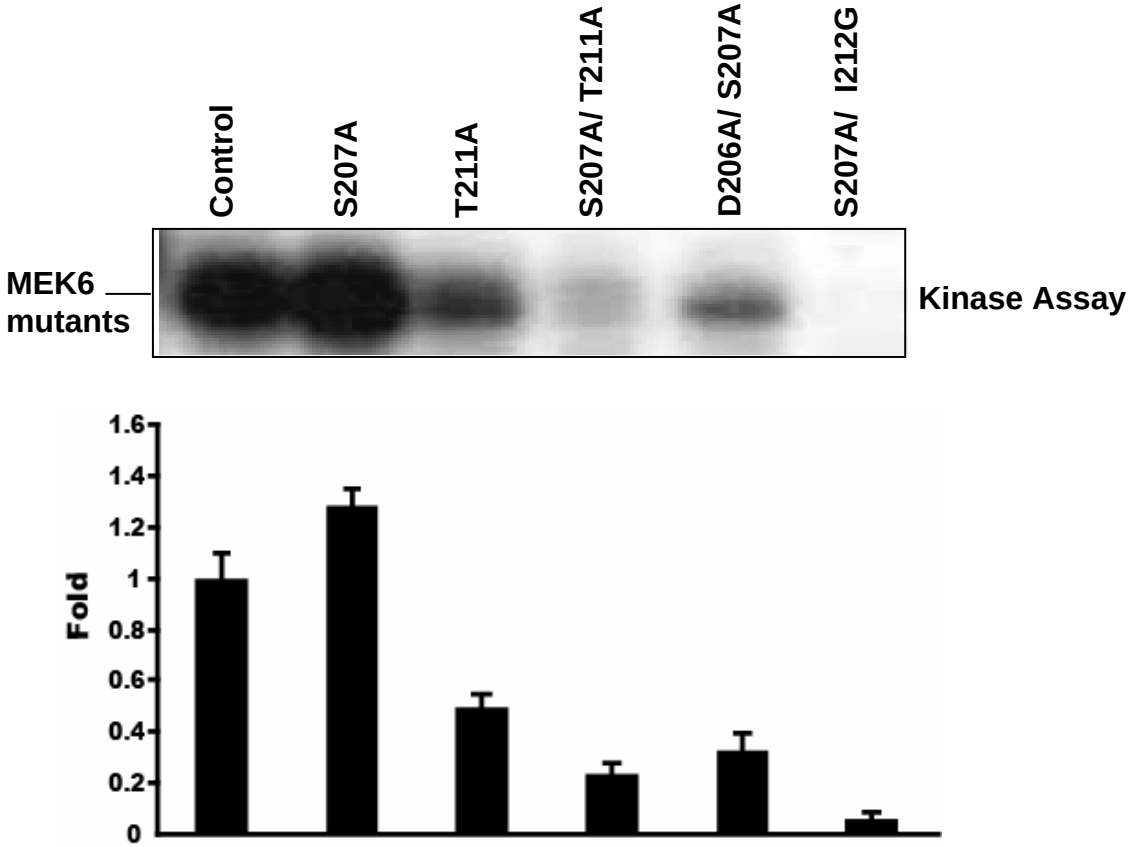

Figure 5-5. Phosphorylation of various MEK6 mutants by TAO2 (1-451). All MEK6 mutants were in the background of the kinase inactivating K82M mutation. Lower panel shows fold phosphorylation (mean ± s.e.m.) (From Zhou at al, 2004).

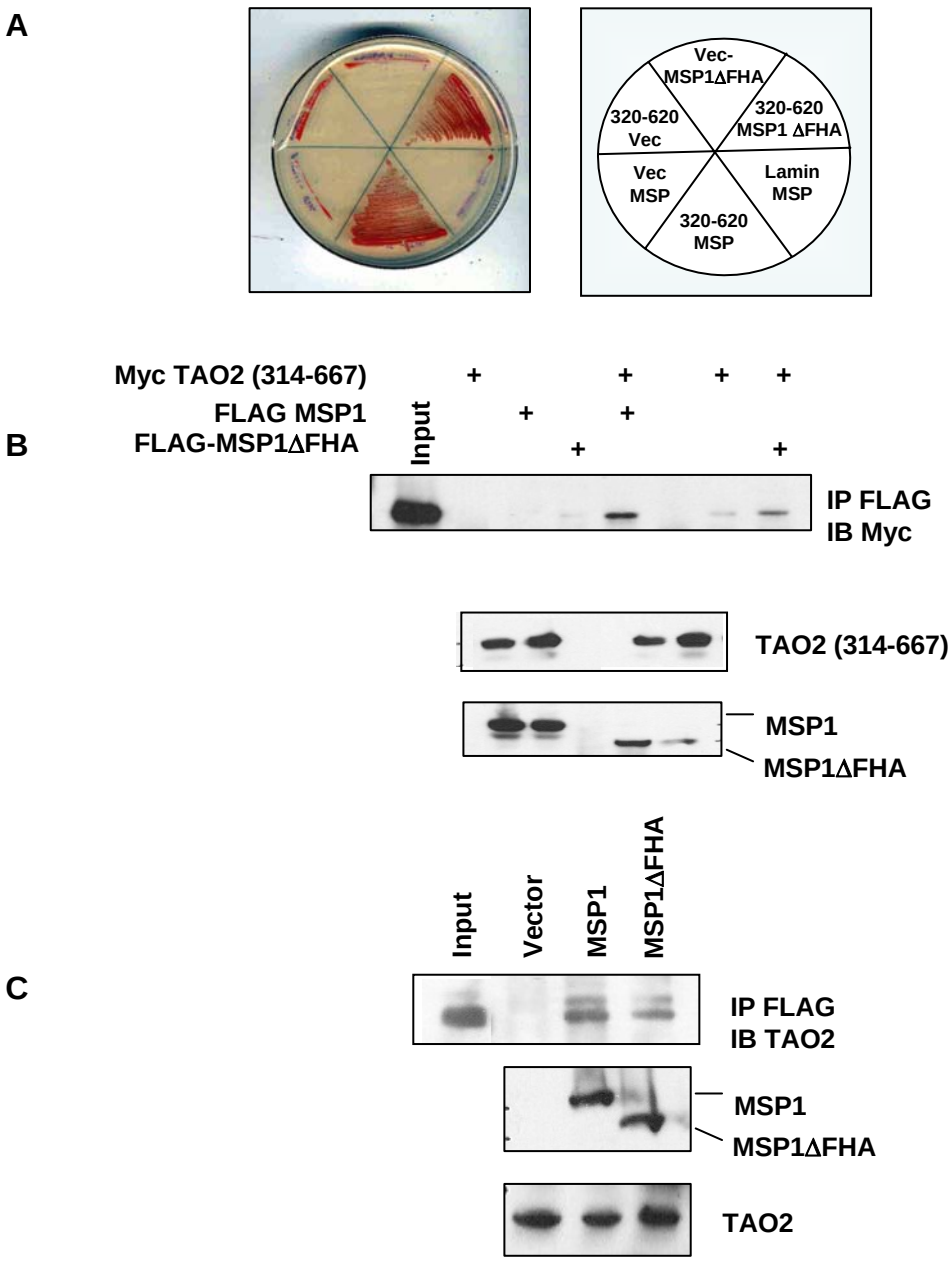

Figure 5-6. TAO2 interacts with MSP1. (A) Pairwise two-hybrid analysis of interaction between full length MSP and ΔFHA with TAO2 (320-620). (B) Over-expressed FLAG-MSP 1 constructs interact with TAO2 (314-667). (C) Endogenous TAO2 interacts with over-expressed MSP1 and ΔFHA.

CHAPTER 6. FUTURE DIRECTIONS

The TAO family of Ste20p kinases has not been studied extensively even though they were cloned nearly 10 years ago. However, recent large-scale genome-wide siRNA screens suggested that the members of the TAO family were important regulators of cellular processes such as proliferation, apoptosis (TAO3) (MacKeigan et al., 2005), vesicle trafficking (TAO1) (Pelkmans et al., 2005) and neuronal differentiation (TAO2) (Nagarajan et al., 2001). Interestingly enough, each screen identified only a member of the TAO family suggesting non-redundant roles for these protein kinases. This implies that individual TAOs carry out specific functions within the cell not shared by other TAOs. The protein kinase domains of TAOs are nearly identical and they all activate MEK3/6 in the p38 MAPK cascade. However, the C-terminal domains of these kinases share much less sequence identity and this indicates that these regions may be used to differentially interact with upstream components or substrates. The yeast-two-hybrid analysis I performed with TAO2 identified a number of proteins with seemingly diverse functions. Similar screens with fragments of TAO1 and 3 C-terminal domains would be useful to identify alternative pathways these kinases regulate.

My research identified interactions between TAO2 and heterotrimeric G proteins. The biological significance of neither the interaction nor the phosphorylation has been uncovered. The regulation of TAO2 but not TAO1 by the muscarinic-$G\alpha_o$ complex has already been elucidated (Chen et al., 2003). Studies carried out subsequently imply that TAO2 may regulate a number of $G\alpha$ family members. We observed phosphorylation of a number of $G\alpha$ subunits (except $G\alpha_q$) *in vitro* by TAO2. It would be interesting to explore these phosphorylation events in greater detail and determine their significance. We now have reagents that allow the protein

levels of TAOs to be knocked down in cells. These can now be used to ask specific questions about the role of TAOs in G protein-regulated signaling cascades, either by measuring p38 activation in response to GPCR ligands or events further upstream such as cAMP production. The interaction of TAO2 with $G_{\beta\gamma}$ subunits also implies regulation of signaling initiated by the dimer. The relative contributions of $G\alpha$ and $G_{\beta\gamma}$ on TAO2 activation needs to be resolved. A TAO2 mutant lacking the Q-x-x-E-R motif may be used to determine whether interaction with $G_{\beta\gamma}$ is necessary for specific TAO2 pathways. Cardiac hypertrophy has been shown to be regulated by p38 MAPK and MEK3 and 6 (Wang et al., 1998). Our data for TAO2 in GPCR signaling, along with observations that TAO2 protein kinase activity increases when cells are treated with GPCR agonists, supports the hypothesis that TAO2 may be important in the regulation of p38 by GPCRs. Gain- and loss of function mutants of TAO2 could be expressed via recombinant adenoviruses in cardiomyocytes induced to differentiate. We can determine if TAO2 is required for this process by monitoring well-defined parameters for differentiation (muscle-specific transcription factors, p38 activation etc).

Our studies have uncovered a potential role for all three TAO kinases in regulation of the G2/M checkpoint by activation of p38 in response to DNA damage. More importantly, we submit that TAOs may be the intermediates in the ATM/ATR activation of p38. This role for ATM/ATR has been hinted at in other studies, but components downstream of ATM/ATR have not been identified. We provide the first evidence that TAO2, and perhaps TAO1 and 3 are these mediators. The activation of TAO2 by IR is diminished in AT cells indicating that ATM is required for the activation process. Although this does not imply a direct activation, we have supporting evidence that TAO3 is phosphorylated on an SQ site in response to S-phase arrest by HU, and that TAO1 SQ/TQ phosphorylation site mutants block activation of p38 by UV. More

direct evidence is required to conclusively show that TAOs are substrates of ATM/ATR. We will transfect cells with ATM/ATR expression vectors and immunoprecipitate TAOs to observe if overexpression of these DNA damage kinases enhances TAO activity. These experiments can be done in conjunction with the expression of TAO (S/TQ) phosphorylation site mutants to demonstrate loss of phosphorylation when SQ/TQ sites are mutated. We have shown that TAO1, 2 and 3 are activated by a number of DNA damaging agents, and we pursued the UV-induced G2/M checkpoint due to the robust activation of p38 by this agent. IR and HU also induce significant activation of p38 but less so than UV. The activation of TAO1 and 2 by IR suggests that they may also be important regulators of the IR induced G2/M checkpoint. We will determine if knockdown of TAOs hampers the engagement of IR induced G2/M checkpoints, as well as G1/S and intra-S phase checkpoints caused by UV and HU. TAO2 is localized to the nucleus as assessed by immunofluorescence and cell fractionation. Treatment of cells with IR induces discrete damage foci that overlap with double-strand DNA breaks (DSB). Many proteins localize to these sites that are part of DDR. We would like to determine if TAO2 accumulates at these sites by irradiating cells and co-staining for TAOs and the DSB marker γH2A.X. We will also determine if the ATM/ATR phosphorylation sites are required for this re-distribution. Our data suggest that TAO kinases are capable of associating with one another as well as with p38. We have previously shown that TAO1 and 2 co-precipitate with MEK3 and 6 respectively. Hence, we have reason to believe that the three-tier kinase cascade is scaffolded together, either via an unknown component of perhaps the C-terminal domains of TAOs. We would like to determine the minimal binding sites on TAOs for one another as well as p38 (assuming the interaction is direct) and determine the effect of mutants in activating p38.

We have preliminary data on the ATM/ATR phosphorylation sites on TAO protein kinases. The precise site(s) and relevance in activating the checkpoint need to be demonstrated. Additionally, it is possible that TAO kinases phosphorylate one another as a means of regulating activity. Our lab has shown that WNK1 phosphorylates WNK4 on serine 332 and WNK4 phosphorylates WNK1 on a yet to be determined site (Lenertz et al., 2005). Although the biological relevance of these phosphorylations are unclear, there is evidence of interactions between WNK1 and WNK4 in regulating the membrane insertion of a number of ion channels (Xu et al., 2005). Hence, this may be a general mechanism in Ste20p related MAP3Ks and MAP4Ks. Indeed, activation via association would explain in part the multiple pathways these kinases regulate, and specificity would be determined by choice of binding partner.

As discussed in the introduction, phosphorylation of proteins is an important means of regulating activity, yet other post-translational modifications such as ubiquitination and sumoylation are also important ways in which signaling systems are modulated. It is certain that TAO kinases are under multiple modes of regulation, and determining what post-translational modifications occur in the protein (and by what conditions) will shed light on the regulation of this family of protein kinases. In the same vein, based on the results of the siRNA screens, TAOs appear to be important regulators of cell homeostasis. Hence, it will be relevant to determine if these kinases have altered signaling in disease states such as cancer.

BIBLIOGRAPHY

Aebersold, D. M., Shaul, Y. D., Yung, Y., Yarom, N., Yao, Z., Hanoch, T., and Seger, R. (2004). Extracellular signal-regulated kinase 1c (ERK1c), a novel 42-kilodalton ERK, demonstrates unique modes of regulation, localization, and function. Mol Cell Biol *24*, 10000-10015.

Andegeko, Y., Moyal, L., Mittelman, L., Tsarfaty, I., Shiloh, Y., and Rotman, G. (2001). Nuclear Retention of ATM at Sites of DNA Double Strand Breaks. J Biol Chem *276*, 38224-38230.

Aza-Blanc, P., Cooper, C. L., Wagner, K., Batalov, S., Deveraux, Q. L., and Cooke, M. P. (2003). Identification of modulators of TRAIL-induced apoptosis via RNAi-based phenotypic screening. Mol Cell *12*, 627-637.

Bakkenist, C. J., and Kastan, M. B. (2004). Initiating cellular stress responses. Cell *118*, 9-17.

Banin, S., Moyal, L., Shieh, S.-Y., Taya, Y., Anderson, C. W., Chessa, L., Smorodinsky, N. I., Prives, C., Reiss, Y., Shiloh, Y., and Ziv, Y. (1998). Enhanced Phosphorylation of p53 by ATM in Response to DNA Damage. Science *281*, 1674-1677.

Bartkova, J., Horejsi, Z., Koed, K., Kramer, A., Tort, F., Zieger, K., Guldberg, P., Sehested, M., Nesland, J. M., Lukas, C., *et al.* (2005). DNA damage response as a candidate anti-cancer barrier in early human tumorigenesis. Nature *434*, 864-870.

Bence, K., Ma, W., Kozasa, T., and Huang, X. Y. (1997). Direct stimulation of Bruton's tyrosine kinase by G(q)-protein alpha-subunit. Nature *389*, 296-299.

Benhar, M., Dalyot, I., Engelberg, D., and Levitzki, A. (2001). Enhanced ROS Production in Oncogenically Transformed Cells Potentiates c-Jun N-Terminal Kinase and p38 Mitogen-Activated Protein Kinase Activation and Sensitization to Genotoxic Stress
Mol Cell Biol *21*, 6913-6926.

Berman, K. S., Hutchison, M., Avery, L., and Cobb, M. H. (2001). kin-18, a C. elegans protein kinase involved in feeding. Gene *279*, 137-147.

Bhoumik, A., Takahashi, S., Breitweiser, W., Shiloh, Y., Jones, N., and Ronai, Z. (2005). ATM-dependent phosphorylation of ATF2 is required for the DNA damage response. Mol Cell *18*, 577-587.

Bostock, C. J., Prescott, D. M., and Kirkpatrick, J. B. (1971). An evaluation of the double thymidine block for synchronizing mammalian cells at the G1-S border. Exp Cell Res *68*, 163-168.

Brancho, D., Tanaka, N., Jaeschke, A., Ventura, J. J., Kelkar, N., Tanaka, Y., Kyuuma, M., Takeshita, T., Flavell, R. A., and Davis, R. J. (2003). Mechanism of p38 MAP kinase activation in vivo. Genes Dev *17*, 1969-1978.

Bregman, D. B., Bhattacharyya, N., and Rubin, C. S. (1989). High affinity binding protein for the regulatory subunit of cAMP-dependent protein kinase II-B. Cloning, characterization, and expression of cDNAs for rat brain P150. J Biol Chem *264*, 4648-4656.

Brown, E. J., and Baltimore, D. (2000). ATR disruption leads to chromosomal fragmentation and early embryonic lethality. Genes Dev *14*, 397-402.

Bulavin, D. V., Higashimoto, Y., Popoff, I. J., Gaarde, W. A., Basrur, V., Potapova, O., Appella, E., and Fornace, A. J., Jr. (2001). Initiation of a G2/M checkpoint after ultraviolet radiation requires p38 kinase. Nature *411*, 102-107.

Burack, W. R., and Sturgill, T. W. (1997). The activating dual phosphorylation of MAPK by MEK is nonprocessive. Biochemistry *36*, 5929-5933.

Canagarajah, B. J., Khokhlatchev, A., Cobb, M. H., and Goldsmith, E. J. (1997). Activation mechanism of the MAP kinase ERK2 by dual phosphorylation. Cell *90*, 859-869.

Chang, C. I., Xu, B. E., Akella, R., Cobb, M. H., and Goldsmith, E. J. (2002). Crystal structures of MAP kinase p38 complexed to the docking sites on its nuclear substrate MEF2A and activator MKK3b. Mol Cell *9*, 1241-1249.

Chen, B. P., Chan, D. W., Kobayashi, J., Burma, S., Asaithamby, A., Morotomi-Yano, K., Botvinick, E., Qin, J., and Chen, D. J. (2005). Cell cycle dependence of DNA-dependent protein kinase phosphorylation in response to DNA double strand breaks. J Biol Chem *280*, 14709-14715.

Chen, W., White, M. A., and Cobb, M. H. (2002). Stimulus-specific requirements for MAP3 kinases in activating the JNK pathway. J Biol Chem *277*, 49105-49110.

Chen, Z., and Cobb, M. H. (2001). Regulation of stress-responsive mitogen-activated protein (MAP) kinase pathways by TAO2. J Biol Chem *276*, 16070-16075.

Chen, Z., Gibson, T. B., Robinson, F., Silvestro, L., Pearson, G., Xu, B., Wright, A., Vanderbilt, C., and Cobb, M. H. (2001). MAP kinases. Chem Rev *101*, 2449-2476.

Chen, Z., Hutchison, M., and Cobb, M. H. (1999). Isolation of the protein kinase TAO2 and identification of its mitogen-activated protein kinase/extracellular signal-regulated kinase kinase binding domain. J Biol Chem *274*, 28803-28807.

Chen, Z., Raman, M., Chen, L., Lee, S. F., Gilman, A. G., and Cobb, M. H. (2003). TAO (thousand-and-one amino acid) protein kinases mediate signaling from carbachol to p38 mitogen-activated protein kinase and ternary complex factors. J Biol Chem *278*, 22278-22283.

Cheng, H., Kartenbeck, J., Kabsch, K., Mao, X., Marques, M., and Alonso, A. (2002). Stress kinase p38 mediates EGFR transactivation by hyperosmolar concentrations of sorbitol. J Cell Physiol *192*, 234-243.

Clapham, D. E., and Neer, E. J. (1997). G PROTEIN bg SUBUNITS. Annual Review of Pharmacology and Toxicology *37*, 167-203.

Cobb, M. H., Xu, S., Cheng, M., Ebert, D., Robbins, D., Goldsmith, E., and Robinson, M. (1996). Structural analysis of the MAP kinase ERK2 and studies of MAP kinase regulatory pathways. Adv Pharmacol *36*, 49-65.

Cohen, M. S., Zhang, C., Shokat, K. M., and Taunton, J. (2005). Structural Bioinformatics-Based Design of Selective, Irreversible Kinase Inhibitors 10.1126/science1108367. Science *308*, 1318-1321.

Colledge, M., and Scott, J. D. (1999). AKAPs: from structure to function. Trends Cell Biol *9*, 216-221.

Communal, C., Colucci, W. S., and Singh, K. (2000). p38 mitogen-activated protein kinase pathway protects adult rat ventricular myocytes against beta -adrenergic receptor-stimulated apoptosis. Evidence for Gi-dependent activation. J Biol Chem *275*, 19395-19400.

Crespo, P., Xu, N., Simonds, W. F., and Gutkind, J. S. (1994). Ras-dependent activation of MAP kinase pathway mediated by G-protein beta gamma subunits. Nature *369*, 418-420.

Crouch, M. F., and Simson, L. (1997). The G-protein G(i) regulates mitosis but not DNA synthesis in growth factor-activated fibroblasts: a role for the nuclear translocation of G(i). Faseb J *11*, 189-198.

Dan, I., Watanabe, N. M., and Kusumi, A. (2001). The Ste20 group kinases as regulators of MAP kinase cascades. Trends in Cell Biology *11*, 220-230.

Dell, E. J., Connor, J., Chen, S., Stebbins, E. G., Skiba, N. P., Mochly-Rosen, D., and Hamm, H. E. (2002). The betagamma subunit of heterotrimeric G proteins interacts with RACK1 and two other WD repeat proteins. J Biol Chem *277*, 49888-49895.

Della Rocca, G. J., Maudsley, S., Daaka, Y., Lefkowitz, R. J., and Luttrell, L. M. (1999). Pleiotropic Coupling of G Protein-coupled Receptors to the Mitogen-activated Protein Kinase Cascade. Role of focal adhesions and receptor tyrosine kinases. J Biol Chem *274*, 13978-13984.

Della Rocca, G. J., van Biesen, T., Daaka, Y., Luttrell, D. K., Luttrell, L. M., and Lefkowitz, R. J. (1997). Ras-dependent Mitogen-activated Protein Kinase Activation by G Protein-coupled Receptors. Convergence of Gi- and Gq-mediated pathways on calcium/calmodulin, Pyk2, and Src kinase. J Biol Chem *272*, 19125-19132.

Dikic, I., Tokiwa, G., Lev, S., Courtneidge, S. A., and Schlessinger, J. (1996). A role for Pyk2 and Src in linking G-protein-coupled receptors with MAP kinase activation. Nature *383*, 547-550.

Dmitrieva, N. I., Bulavin, D. V., and Burg, M. B. (2003). High NaCl causes Mre11 to leave the nucleus, disrupting DNA damage signaling and repair. Am J Physiol Renal Physiol *285*, F266-274.

Dunn, D. A. (2002). Mining the human kinome. Drug Discovery Today *7*, 1121-1123.

Durocher, D., Henckel, J., Fersht, A. R., and Jackson, S. P. (1999). The FHA domain is a modular phosphopeptide recognition motif. Mol Cell *4*, 387-394.

Durocher, D., Smerdon, S. J., Yaffe, M. B., and Jackson, S. P. (2000a). The FHA domain in DNA repair and checkpoint signaling. Cold Spring Harb Symp Quant Biol *65*, 423-431.

Durocher, D., Taylor, I. A., Sarbassova, D., Haire, L. F., Westcott, S. L., Jackson, S. P., Smerdon, S. J., and Yaffe, M. B. (2000b). The Molecular Basis of FHA Domain:Phosphopeptide Binding Specificity and Implications for Phospho-Dependent Signaling Mechanisms. Molecular Cell *6*, 1169-1182.

Elion, E. A. (2000). Pheromone response, mating and cell biology. Curr Opin Microbiol *3*, 573-581.

Eyers, P. A., Erikson, E., Chen, L. G., and Maller, J. L. (2003). A novel mechanism for activation of the protein kinase Aurora A. Curr Biol *13*, 691-697.

Faure, M., Voyno-Yasenetskaya, T. A., and Bourne, H. R. (1994). cAMP and beta gamma subunits of heterotrimeric G proteins stimulate the mitogen-activated protein kinase pathway in COS-7 cells. J Biol Chem *269*, 7851-7854.

Fischer, O. M., Hart, S., Gschwind, A., and Ullrich, A. (2003). EGFR signal transactivation in cancer cells. Biochem Soc Trans *31*, 1203-1208.

Gallego, C., Gupta, S. K., Winitz, S., Eisfelder, B. J., and Johnson, G. L. (1992). Myristoylation of the G alpha i2 polypeptide, a G protein alpha subunit, is required for its signaling and transformation functions. Proc Natl Acad Sci U S A *89*, 9695-9699.

Gavin, A.-C., Bosche, M., Krause, R., Grandi, P., Marzioch, M., Bauer, A., Schultz, J., Rick, J. M., Michon, A.-M., Cruciat, C.-M., *et al.* (2002). Functional organization of the yeast proteome by systematic analysis of protein complexes. *415*, 141-147.

Ge, B., Gram, H., Di Padova, F., Huang, B., New, L., Ulevitch, R. J., Luo, Y., and Han, J. (2002). MAPKK-independent activation of p38alpha mediated by TAB1-dependent autophosphorylation of p38alpha. Science *295*, 1291-1294.

Goldstone, S., Pavey, S., Forrest, A., Sinnamon, J., and Gabrielli, B. (2001). Cdc25-dependent activation of cyclin A/cdk2 is blocked in G2 phase arrested cells independently of ATM/ATR. Oncogene *20*, 921-932.

Gopalakrishnan, S. M., Karvinen, J., Kofron, J. L., Burns, D. J., and Warrior, U. (2002). Application of Micro Arrayed Compound Screening (microARCS) to identify inhibitors of caspase-3. J Biomol Screen *7*, 317-323.

Gorgoulis, V. G., Vassiliou, L. V., Karakaidos, P., Zacharatos, P., Kotsinas, A., Liloglou, T., Venere, M., Ditullio, R. A., Jr., Kastrinakis, N. G., Levy, B., *et al.* (2005). Activation of the DNA damage checkpoint and genomic instability in human precancerous lesions. Nature *434*, 907-913.

Hanks, S. K., Quinn, A. M., and Hunter, T. (1988). The protein kinase family: conserved features and deduced phylogeny of the catalytic domains. Science *241*, 42-52.

Hirose, Y., Katayama, M., Stokoe, D., Haas-Kogan, D. A., Berger, M. S., and Pieper, R. O. (2003). The p38 mitogen-activated protein kinase pathway links the DNA mismatch repair system to the G2 checkpoint and to resistance to chemotherapeutic DNA-methylating agents. Mol Cell Biol *23*, 8306-8315.

Hofmann, K., and Bucher, P. (1995). The FHA domain: a putative nuclear signalling domain found in protein kinases and transcription factors. Trends Biochem Sci *20*, 347-349.

Hutchison, M., Berman, K. S., and Cobb, M. H. (1998). Isolation of TAO1, a protein kinase that activates MEKs in stress-activated protein kinase cascades. J Biol Chem *273*, 28625-28632.

Jamora, C., Takizawa, P. A., Zaarour, R. F., Denesvre, C., Faulkner, D. J., and Malhotra, V. (1997). Regulation of Golgi Structure through Heterotrimeric G Proteins. Cell *91*, 617-626.

Karandikar, M., Xu, S., and Cobb, M. H. (2000). MEKK1 binds raf-1 and the ERK2 cascade components. J Biol Chem *275*, 40120-40127.

Karlseder, J., Hoke, K., Mirzoeva, O. K., Bakkenist, C., Kastan, M. B., Petrini, J. H. J., and de Lange, T. (2004). The telomeric protein TRF2 binds the ATM kinase and can inhibit the ATM-dependent DNA damage response. PLoS Biology *2*, E240.

Khokhlatchev, A. V., Canagarajah, B., Wilsbacher, J., Robinson, M., Atkinson, M., Goldsmith, E., and Cobb, M. H. (1998). Phosphorylation of the MAP kinase ERK2 promotes its homodimerization and nuclear translocation. Cell *93*, 605-615.

Knighton, D. R., Zheng, J. H., Ten Eyck, L. F., Ashford, V. A., Xuong, N. H., Taylor, S. S., and Sowadski, J. M. (1991). Crystal structure of the catalytic subunit of cyclic adenosine monophosphate-dependent protein kinase. Science *253*, 407-414.

Kolch, W. (2005). Coordinating ERK/MAPK signalling through scaffolds and inhibitors. Nat Rev Mol Cell Biol *6*, 827-837.

Kolch, W., Heidecker, G., Kochs, G., Hummel, R., Vahidi, H., Mischak, H., Finkenzeller, G., Marme, D., and Rapp, U. R. (1993). Protein kinase C alpha activates RAF-1 by direct phosphorylation. Nature *364*, 249-252.

Kozasa, T., and Gilman, A. G. (1995). Purification of Recombinant G Proteins from Sf9 Cells by Hexahistidine Tagging of Associated Subunits
10.1074/jbc.270.4.1734. J Biol Chem *270*, 1734-1741.

Kozasa, T., and Gilman, A. G. (1996). Protein kinase C phosphorylates G12 alpha and inhibits its interaction with G beta gamma. J Biol Chem *271*, 12562-12567.

Kozasa, T., Jiang, X., Hart, M. J., Sternweis, P. M., Singer, W. D., Gilman, A. G., Bollag, G., and Sternweis, P. C. (1998). p115 RhoGEF, a GTPase activating protein for Galpha12 and Galpha13. Science *280*, 2109-2111.

Kranz, J. E., Satterberg, B., and Elion, E. A. (1994). The MAP kinase Fus3 associates with and phosphorylates the upstream signaling component Ste5. Genes Dev *8*, 313-327.

Krebs, E. G., and Fischer, E. H. (1955). Phosphorylase activity of skeletal muscle extracts. J Biol Chem *216*, 113-120.

Kultz, D., and Chakravarty, D. (2001). Hyperosmolality in the form of elevated NaCl but not urea causes DNA damage in murine kidney cells. PNAS *98*, 1999-2004.

Kuma, Y., Sabio, G., Bain, J., Shpiro, N., Marquez, R., and Cuenda, A. (2005). BIRB796 Inhibits All p38 MAPK Isoforms in Vitro and in Vivo
10.1074/jbc.M414221200. J Biol Chem *280*, 19472-19479.

Kyriakis, J. M., and Avruch, J. (2001). Mammalian mitogen-activated protein kinase signal transduction pathways activated by stress and inflammation. Physiol Rev *81*, 807-869.

Laine, A., and Ronai, Z. (2005). Ubiquitin chains in the ladder of MAPK signaling. Sci STKE *2005*, re5.

Lakin, N. D., Hann, B. C., and Jackson, S. P. (1999). The ataxia-telangiectasia related protein ATR mediates DNA-dependent phosphorylation of p53. Oncogene *18*, 3989-3995.

Lee, E., Linder, M. E., and Gilman, A. G. (1994). Expression of G-protein alpha subunits in Escherichia coli. Methods Enzymol *237*, 146-164.

Lee, J.-H., and Paull, T. T. (2004). Direct Activation of the ATM Protein Kinase by the Mre11/Rad50/Nbs1 Complex. Science *304*, 93-96.

Lee, J.-H., and Paull, T. T. (2005). ATM Activation by DNA Double-Strand Breaks Through the Mre11-Rad50-Nbs1 Complex. Science *308*, 551-554.

Lee, M. S., Ogg, S., Xu, M., Parker, L. L., Donoghue, D. J., Maller, J. L., and Piwnica-Worms, H. (1992). cdc25+ encodes a protein phosphatase that dephosphorylates p34cdc2. Mol Biol Cell *3*, 73-84.

Lee, Y. S., Jang, M. S., Lee, J. S., Choi, E. J., and Kim, E. (2005). SUMO-1 represses apoptosis signal-regulating kinase 1 activation through physical interaction and not through covalent modification. EMBO Rep *6*, 949-955.

Leeuw, T., Wu, C., Schrag, J. D., Whiteway, M., Thomas, D. Y., and Leberer, E. (1998). Interaction of a G-protein beta-subunit with a conserved sequence in Ste20/PAK family protein kinases. Nature *391*, 191-195.

Lei, M., Lu, W., Meng, W., Parrini, M. C., Eck, M. J., Mayer, B. J., and Harrison, S. C. (2000). Structure of PAK1 in an autoinhibited conformation reveals a multistage activation switch. Cell *102*, 387-397.

Lenertz, L. Y., Lee, B. H., Min, X., Xu, B. E., Wedin, K., Earnest, S., Goldsmith, E. J., and Cobb, M. H. (2005). Properties of WNK1 and implications for other family members. J Biol Chem *280*, 26653-26658.

Lewis, T. S., Shapiro, P. S., and Ahn, N. G. (1998). Signal transduction through MAP kinase cascades. Adv Cancer Res *74*, 49-139.

Li, S., Armstrong, C. M., Bertin, N., Ge, H., Milstein, S., Boxem, M., Vidalain, P.-O., Han, J.-D. J., Chesneau, A., Hao, T., *et al.* (2004). A Map of the Interactome Network of the Metazoan C. elegans. Science *303*, 540-543.

Lin, D.-Y., and Shih, H.-M. (2002). Essential Role of the 58-kDa Microspherule Protein in the Modulation of Daxx-dependent Transcriptional Repression as Revealed by Nucleolar Sequestration. J Biol Chem *277*, 25446-25456.

Lindahl, T., and Nyberg, B. (1972). Rate of depurination of native deoxyribonucleic acid. Biochemistry *11*, 3610-3618.

Lounsbury, K. M., Casey, P. J., Brass, L. F., and Manning, D. R. (1991). Phosphorylation of Gz in human platelets. Selectivity and site of modification. J Biol Chem *266*, 22051-22056.

Lu, Z., Xu, S., Joazeiro, C., Cobb, M. H., and Hunter, T. (2002). The PHD domain of MEKK1 acts as an E3 ubiquitin ligase and mediates ubiquitination and degradation of ERK1/2. Mol Cell *9*, 945-956.

Lundgren, K., Walworth, N., Booher, R., Dembski, M., Kirschner, M., and Beach, D. (1991). mik1 and wee1 cooperate in the inhibitory tyrosine phosphorylation of cdc2. Cell *64*, 1111-1122.

Luttrell, L. M., Ferguson, S. S. n. G., Daaka, Y., Miller, W. E., Maudsley, S., Della Rocca, G. J., Lin, F.-T., Kawakatsu, H., Owada, K., Luttrell, D. K., *et al.* (1999). b-Arrestin-Dependent Formation of 2 Adrenergic Receptor-Src Protein Kinase Complexes. Science *283*, 655-661.

MacKeigan, J. P., Murphy, L. O., and Blenis, J. (2005). Sensitized RNAi screen of human kinases and phosphatases identifies new regulators of apoptosis and chemoresistance. *7*, 591-600.

Manganello, J. M., Huang, J. S., Kozasa, T., Voyno-Yasenetskaya, T. A., and Le Breton, G. C. (2003). Protein kinase A-mediated phosphorylation of the Galpha13 switch I region alters the Galphabetagamma13-G protein-coupled receptor complex and inhibits Rho activation. J Biol Chem *278*, 124-130.

Manke, I. A., Nguyen, A., Lim, D., Stewart, M. Q., Elia, A. E., and Yaffe, M. B. (2005). MAPKAP kinase-2 is a cell cycle checkpoint kinase that regulates the G2/M transition and S phase progression in response to UV irradiation. Mol Cell *17*, 37-48.

Manning, G., Whyte, D. B., Martinez, R., Hunter, T., and Sudarsanam, S. (2002). The protein kinase complement of the human genome. Science *298*, 1912-1934.

Marcus, S., Polverino, A., Barr, M., and Wigler, M. (1994). Complexes between STE5 and components of the pheromone-responsive mitogen-activated protein kinase module. Proc Natl Acad Sci U S A *91*, 7762-7766.

Matheny, S. A., Chen, C., Kortum, R. L., Razidlo, G. L., Lewis, R. E., and White, M. A. (2004). Ras regulates assembly of mitogenic signalling complexes through the effector protein IMP. Nature *427*, 256-260.

Matsuoka, S., Rotman, G., Ogawa, A., Shiloh, Y., Tamai, K., and Elledge, S. J. (2000). Ataxia telangiectasia-mutated phosphorylates Chk2 in vivo and in vitro. Proc Natl Acad Sci U S A *97*, 10389-10394.

Mikhailov, A., Shinohara, M., and Rieder, C. L. (2004). Topoisomerase II and histone deacetylase inhibitors delay the G2/M transition by triggering the p38 MAPK checkpoint pathway. J Cell Biol *166*, 517-526.

Mitsopoulos, C., Zihni, C., Garg, R., Ridley, A. J., and Morris, J. D. (2003). The prostate-derived sterile 20-like kinase (PSK) regulates microtubule organization and stability. J Biol Chem *278*, 18085-18091.

Moore, T. M., Garg, R., Johnson, C., Coptcoat, M. J., Ridley, A. J., and Morris, J. D. (2000). PSK, a novel STE20-like kinase derived from prostatic carcinoma that activates the c-Jun N-terminal kinase mitogen-activated protein kinase pathway and regulates actin cytoskeletal organization. J Biol Chem *275*, 4311-4322.

Morgan-Lappe, S., Woods, K. W., Li, Q., Anderson, M. G., Schurdak, M. E., Luo, Y., Giranda, V. L., Fesik, S. W., and Leverson, J. D. (2005). RNAi-based screening of the human kinome identifies Akt-cooperating kinases: a new approach to designing efficacious multitargeted kinase inhibitors.

Moriguchi, T., Urushiyama, S., Hisamoto, N., Iemura, S.-i., Uchida, S., Natsume, T., Matsumoto, K., and Shibuya, H. (2005). WNK1 Regulates Phosphorylation of Cation-Chloride-coupled Cotransporters via the STE20-related Kinases, SPAK and OSR1. J Biol Chem *280*, 42685-42693.

Mueller, P. R., Coleman, T. R., Kumagai, A., and Dunphy, W. G. (1995). Myt1: a membrane-associated inhibitory kinase that phosphorylates Cdc2 on both threonine-14 and tyrosine-15. Science *270*, 86-90.

Muller, J., Ory, S., Copeland, T., Piwnica-Worms, H., and Morrison, D. K. (2001). C-TAK1 regulates Ras signaling by phosphorylating the MAPK scaffold, KSR1. Mol Cell *8*, 983-993.

Muslin, A. J., Tanner, J. W., Allen, P. M., and Shaw, A. S. (1996). Interaction of 14-3-3 with signaling proteins is mediated by the recognition of phosphoserine. Cell *84*, 889-897.

Nagarajan, R., Svaren, J., Le, N., Araki, T., Watson, M., and Milbrandt, J. (2001). EGR2 Mutations in Inherited Neuropathies Dominant-Negatively Inhibit Myelin Gene Expression. Neuron *30*, 355-368.

O'Driscoll, M., Ruiz-Perez, V. L., Woods, C. G., Jeggo, P. A., and Goodship, J. A. (2003). A splicing mutation affecting expression of ataxia-telangiectasia and Rad3-related protein (ATR) results in Seckel syndrome. Nat Genet *33*, 497-501.

Okumura, K., Zhao, M., DePinho, R. A., Furnari, F. B., and Cavenee, W. K. (2005). From the Cover: Cellular transformation by the MSP58 oncogene is inhibited by its physical interaction with the PTEN tumor suppressor. PNAS *102*, 2703-2706.

O'Neill, T., Dwyer, A. J., Ziv, Y., Chan, D. W., Lees-Miller, S. P., Abraham, R. H., Lai, J. H., Hill, D., Shiloh, Y., Cantley, L. C., and Rathbun, G. A. (2000). Utilization of Oriented Peptide Libraries to Identify Substrate Motifs Selected by ATM. J Biol Chem *275*, 22719-22727.

Pargellis, C., Tong, L., Churchill, L., Cirillo, P. F., Gilmore, T., Graham, A. G., Grob, P. M., Hickey, E. R., Moss, N., Pav, S., and Regan, J. (2002). Inhibition of p38 MAP kinase by utilizing a novel allosteric binding site. *9*, 268-272.

Park, S. H., Zarrinpar, A., and Lim, W. A. (2003). Rewiring MAP kinase pathways using alternative scaffold assembly mechanisms. Science *299*, 1061-1064.

Parrini, M. C., Lei, M., Harrison, S. C., and Mayer, B. J. (2002). Pak1 kinase homodimers are autoinhibited in trans and dissociated upon activation by Cdc42 and Rac1. Mol Cell *9*, 73-83.

Pelkmans, L., Fava, E., Grabner, H., Hannus, M., Habermann, B., Krausz, E., and Zerial, M. (2005). Genome-wide analysis of human kinases in clathrin- and caveolae/raft-mediated endocytosis. *436*, 78-86.

Prenzel, N., Zwick, E., Daub, H., Leserer, M., Abraham, R., Wallasch, C., and Ullrich, A. (1999). EGF receptor transactivation by G-protein-coupled receptors requires metalloproteinase cleavage of proHB-EGF. Nature *402*, 884-888.

Printen, J. A., and Sprague-Jr., G. F. (1994). Protein-Protein Interactions in the Yeast Pheromone Response Pathway: Ste5p Interacts With All Members of the MAP Kinase Cascade Genetics *138*, 609-619.

Prowse, C. N., and Lew, J. (2001). Mechanism of activation of ERK2 by dual phosphorylation. J Biol Chem *276*, 99-103.

Qian, N. X., Winitz, S., and Johnson, G. L. (1993). Epitope-tagged Gq alpha subunits: expression of GTPase-deficient alpha subunits persistently stimulates phosphatidylinositol-specific phospholipase C but not mitogen-activated protein kinase activity regulated by the M1 muscarinic acetylcholine receptor. Proc Natl Acad Sci U S A *90*, 4077-4081.

Raman, M., and Cobb, M. H. (2003). MAP kinase modules: many roads home. Curr Biol *13*, R886-888.

Ren, Y., Busch, R. K., Perlaky, L., and Busch, H. (1998). The 58-kDa microspherule protein (MSP58), a nucleolar protein, interacts with nucleolar protein p120. European Journal of Biochemistry *253*, 734-742.

Robbins, D. J., and Cobb, M. H. (1992). Extracellular signal-regulated kinases 2 autophosphorylates on a subset of peptides phosphorylated in intact cells in response to insulin and nerve growth factor: analysis by peptide mapping. Mol Biol Cell *3*, 299-308.

Robbins, D. J., Zhen, E., Owaki, H., Vanderbilt, C. A., Ebert, D., Geppert, T. D., and Cobb, M. H. (1993). Regulation and properties of extracellular signal-regulated protein kinases 1 and 2 in vitro. J Biol Chem *268*, 5097-5106.

Rodbell, M. (1971). In vitro assays of adenyl cyclase. Acta Endocrinol Suppl (Copenh) *153*, 337-347.

Rual, J.-F., Venkatesan, K., Hao, T., Hirozane-Kishikawa, T., Dricot, A., Li, N., Berriz, G. F., Gibbons, F. D., Dreze, M., Ayivi-Guedehoussou, N., *et al.* (2005). Towards a proteome-scale map of the human protein-protein interaction network. *437*, 1173-1178.

Sancar, A., Lindsey-Boltz, L. A., Unsal-Kacmaz, K., and Linn, S. (2004). Molecular mechanisms of mammalian DNA repair and the DNA damage checkpoints. Annu Rev Biochem *73*, 39-85.

Sapkota, G. P., Deak, M., Kieloch, A., Morrice, N., Goodarzi, A. A., Smythe, C., Shiloh, Y., Lees-Miller, S. P., and Alessi, D. R. (2002). Ionizing radiation induces ataxia telangiectasia mutated kinase (ATM)-mediated phosphorylation of LKB1/STK11 at Thr-366. Biochem J *368*, 507-516.

Schmitt, J. M., and Stork, P. J. (2000). beta 2-adrenergic receptor activates extracellular signal-regulated kinases (ERKs) via the small G protein rap1 and the serine/threonine kinase B-Raf. J Biol Chem *275*, 25342-25350.

Schmitt, J. M., and Stork, P. J. (2002). Galpha and Gbeta gamma require distinct Src-dependent pathways to activate Rap1 and Ras. J Biol Chem *277*, 43024-43032.

Schulte, G., and Fredholm, B. B. (2003). The Gs-coupled adenosine A2b receptor recruits divergent pathways to regulate ERK1/2 and p38*. Experimental Cell Research *290*, 168-176.

Schwarz, J. K., Lovly, C. M., and Piwnica-Worms, H. (2003). Regulation of the Chk2 Protein Kinase by Oligomerization-Mediated cis- and trans-Phosphorylation
Mol Cancer Res *1*, 598-609.

She, Q.-B., Chen, N., and Dong, Z. (2000). ERKs and p38 Kinase Phosphorylate p53 Protein at Serine 15 in Response to UV Radiation. J Biol Chem *275*, 20444-20449.

She, Q. B., Ma, W. Y., and Dong, Z. (2002). Role of MAP kinases in UVB-induced phosphorylation of p53 at serine 20. Oncogene *21*, 1580-1589.

Sherr, C. J. (2004). Principles of Tumor Suppression. Cell *116*, 235-246.

Shih, M., Lin, F., Scott, J. D., Wang, H. Y., and Malbon, C. C. (1999). Dynamic complexes of beta2-adrenergic receptors with protein kinases and phosphatases and the role of gravin. J Biol Chem *274*, 1588-1595.

Shiloh, Y., Bar-Shira, A., Galanty, Y., and Ziv, Y. (1998). Cloning and expression of large mammalian cDNAs: lessons from ATM. Genet Eng (New York) *20*, 239-248.

Shimono, K., Shimono, Y., Shimokata, K., Ishiguro, N., and Takahashi, M. (2005). Microspherule Protein 1, Mi-2{beta}, and RET Finger Protein Associate in the Nucleolus and Up-regulate Ribosomal Gene Transcription. J Biol Chem *280*, 39436-39447.

Snow, B. E., Krumins, A. M., Brothers, G. M., Lee, S.-F., Wall, M. A., Chung, S., Mangion, J., Arya, S., Gilman, A. G., and Siderovski, D. P. (1998). A G protein gamma subunit-like domain shared between RGS11 and other RGS proteins specifies binding to Gbeta 5 subunits. PNAS *95*, 13307-13312.

Sobko, A., Ma, H., and Firtel, R. A. (2002). Regulated SUMOylation and ubiquitination of DdMEK1 is required for proper chemotaxis. Dev Cell *2*, 745-756.

Stelzl, U., Worm, U., Lalowski, M., Haenig, C., Brembeck, F. H., Goehler, H., Stroedicke, M., Zenkner, M., Schoenherr, A., and Koeppen, S. (2005). A Human Protein-Protein Interaction Network: A Resource for Annotating the Proteome. Cell *122*, 957-968.

Stiff, T., O'Driscoll, M., Rief, N., Iwabuchi, K., Lobrich, M., and Jeggo, P. A. (2004). ATM and DNA-PK function redundantly to phosphorylate H2AX after exposure to ionizing radiation. Cancer Res *64*, 2390-2396.

Stokes, M. P., and Michael, W. M. (2003). DNA damage-induced replication arrest in Xenopus egg extracts. J Cell Biol *163*, 245-255.

Stork, P. J., and Schmitt, J. M. (2002). Crosstalk between cAMP and MAP kinase signaling in the regulation of cell proliferation. Trends Cell Biol *12*, 258-266.

Sun, Z., Hsiao, J., Fay, D. S., and Stern, D. F. (1998). Rad53 FHA domain associated with phosphorylated Rad9 in the DNA damage checkpoint. Science *281*, 272-274.

Takekawa, M., Tatebayashi, K., and Saito, H. (2005). Conserved docking site is essential for activation of mammalian MAP kinase kinases by specific MAP kinase kinase kinases. Mol Cell *18*, 295-306.

Tanno, M., Bassi, R., Gorog, D. A., Saurin, A. T., Jiang, J., Heads, R. J., Martin, J. L., Davis, R. J., Flavell, R. A., and Marber, M. S. (2003). Diverse mechanisms of myocardial p38 mitogen-activated protein kinase activation: evidence for MKK-independent activation by a TAB1-associated mechanism contributing to injury during myocardial ischemia. Circ Res *93*, 254-261.

Tanoue, T., Adachi, M., Moriguchi, T., and Nishida, E. (2000). A conserved docking motif in MAP kinases common to substrates, activators and regulators. Nat Cell Biol *2*, 110-116.

Tassi, E., Biesova, Z., Di Fiore, P. P., Gutkind, J. S., and Wong, W. T. (1999). Human JIK, a novel member of the STE20 kinase family that inhibits JNK and is negatively regulated by epidermal growth factor. J Biol Chem *274*, 33287-33295.

Timm, T., Li, X. Y., Biernat, J., Jiao, J., Mandelkow, E., Vandekerckhove, J., and Mandelkow, E. M. (2003). MARKK, a Ste20-like kinase, activates the polarity-inducing kinase MARK/PAR-1. Embo J *22*, 5090-5101.

Tobiume, K., Matsuzawa, A., Takahashi, T., Nishitoh, H., Morita, K., Takeda, K., Minowa, O., Miyazono, K., Noda, T., and Ichijo, H. (2001). ASK1 is required for sustained activations of JNK/p38 MAP kinases and apoptosis. EMBO Rep *2*, 222-228.

Tokiwa, G., Dikic, I., Lev, S., and Schlessinger, J. (1996). Activation of Pyk2 by stress signals and coupling with JNK signaling pathway. Science *273*, 792-794.

Tosti, E., Waldbaum, L., Warshaw, G., Gross, E. A., and Ruggieri, R. (2004). The stress kinase MRK contributes to regulation of DNA damage checkpoints through a p38gamma-independent pathway. J Biol Chem *279*, 47652-47660.

Touhara, K., Hawes, B., van Biesen, T., and Lefkowitz, R. (1995). G Protein {beta}{gamma} Subunits Stimulate Phosphorylation of Shc Adapter Protein
PNAS *92*, 9284-9287.

Tournier, C., Dong, C., Turner, T. K., Jones, S. N., Flavell, R. A., and Davis, R. J. (2001). MKK7 is an essential component of the JNK signal transduction pathway activated by proinflammatory cytokines. Genes Dev *15*, 1419-1426.

Tsvetkov, L., Xu, X., Li, J., and Stern, D. F. (2003). Polo-like kinase 1 and Chk2 interact and co-localize to centrosomes and the midbody. J Biol Chem *278*, 8468-8475.

Verdun, R. E., Crabbe, L., Haggblom, C., and Karlseder, J. (2005). Functional Human Telomeres Are Recognized as DNA Damage in G2 of the Cell Cycle. Molecular Cell *20*, 551-561.

Vieth, M., Sutherland, J. J., Robertson, D. H., and Campbell, R. M. (2005). Kinomics: characterizing the therapeutically validated kinase space. Drug Discovery Today *10*, 839-846.

Vitari, A. C., Deak, M., Morrice, N. A., and Alessi, D. R. (2005). The WNK1 and WNK4 protein kinases that are mutated in Gordon's hypertension syndrome phosphorylate and activate SPAK and OSR1 protein kinases. Biochem J *391*, 17-24.

Voyno-Yasenetskaya, T. A., Faure, M. P., Ahn, N. G., and Bourne, H. R. (1996). Galpha12 and Galpha13 regulate extracellular signal-regulated kinase and c-Jun kinase pathways by different mechanisms in COS-7 cells. J Biol Chem *271*, 21081-21087.

Wang, J., Frost, J. A., Cobb, M. H., and Ross, E. M. (1999). Reciprocal signaling between heterotrimeric G proteins and the p21-stimulated protein kinase. J Biol Chem *274*, 31641-31647.

Wang, J., Tu, Y., Woodson, J., Song, X., and Ross, E. M. (1997). A GTPase-activating protein for the G protein Galphaz. Identification, purification, and mechanism of action. J Biol Chem *272*, 5732-5740.

Wang, X., McGowan, C. H., Zhao, M., He, L., Downey, J. S., Fearns, C., Wang, Y., Huang, S., and Han, J. (2000). Involvement of the MKK6-p38gamma cascade in gamma-radiation-induced cell cycle arrest. Mol Cell Biol *20*, 4543-4552.

Wang, Y., Huang, S., Sah, V. P., Ross, J., Jr., Brown, J. H., Han, J., and Chien, K. R. (1998). Cardiac muscle cell hypertrophy and apoptosis induced by distinct members of the p38 mitogen-activated protein kinase family. J Biol Chem *273*, 2161-2168.

Wetzker, R., and Bohmer, F.-D. (2003). Transactivation joins multiple tracks to the ERK/MAPK cascade. Nature Reviews Molecular Cell Biology
Nat Rev Mol Cell Biol *4*, 651-657.

Xu, B., English, J. M., Wilsbacher, J. L., Stippec, S., Goldsmith, E. J., and Cobb, M. H. (2000). WNK1, a novel mammalian serine/threonine protein kinase lacking the catalytic lysine in subdomain II. J Biol Chem *275*, 16795-16801.

Xu, B. E., Lee, B. H., Min, X., Lenertz, L., Heise, C. J., Stippec, S., Goldsmith, E. J., and Cobb, M. H. (2005). WNK1: analysis of protein kinase structure, downstream targets, and potential roles in hypertension. Cell Res *15*, 6-10.

Yamauchi, J., Nagao, M., Kaziro, Y., and Itoh, H. (1997). Activation of p38 mitogen-activated protein kinase by signaling through G protein-coupled receptors. Involvement of Gbetagamma and Galphaq/11 subunits. J Biol Chem *272*, 27771-27777.

Yan, K., and Gautam, N. (1996). A domain on the G protein beta subunit interacts with both adenylyl cyclase 2 and the muscarinic atrial potassium channel. J Biol Chem *271*, 17597-17600.

Yang, D., Tournier, C., Wysk, M., Lu, H. T., Xu, J., Davis, R. J., and Flavell, R. A. (1997). Targeted disruption of the MKK4 gene causes embryonic death, inhibition of c-Jun NH2-terminal kinase activation, and defects in AP-1 transcriptional activity. Proc Natl Acad Sci U S A *94*, 3004-3009.

Yang, S. H., Yates, P. R., Whitmarsh, A. J., Davis, R. J., and Sharrocks, A. D. (1998). The Elk-1 ETS-domain transcription factor contains a mitogen-activated protein kinase targeting motif. Mol Cell Biol *18*, 710-720.

Yoneda, T., Imaizumi, K., Oono, K., Yui, D., Gomi, F., Katayama, T., and Tohyama, M. (2001). Activation of Caspase-12, an Endoplastic Reticulum (ER) Resident Caspase, through Tumor Necrosis Factor Receptor-associated Factor 2-dependent Mechanism in Response to the ER Stress. J Biol Chem *276*, 13935-13940.

Zhang, J., Zhang, F., Ebert, D., Cobb, M. H., and Goldsmith, E. J. (1995). Activity of the MAP kinase ERK2 is controlled by a flexible surface loop. Structure *3*, 299-307.

Zhang, W., Chen, T., Wan, T., He, L., Li, N., Yuan, Z., and Cao, X. (2000). Cloning of DPK, a Novel Dendritic Cell-Derived Protein Kinase Activating the ERK1/ERK2 and JNK/SAPK Pathways. Biochemical and Biophysical Research Communications *274*, 872-879.

Zheng, B., Ma, Y. C., Ostrom, R. S., Lavoie, C., Gill, G. N., Insel, P. A., Huang, X. Y., and Farquhar, M. G. (2001). RGS-PX1, a GAP for GalphaS and sorting nexin in vesicular trafficking. Science *294*, 1939-1942.

Zhou, B. B., and Bartek, J. (2004). Targeting the checkpoint kinases: chemosensitization versus chemoprotection. Nat Rev Cancer *4*, 216-225.

Zhou, T., Raman, M., Gao, Y., Earnest, S., Chen, Z., Machius, M., Cobb, M. H., and Goldsmith, E. J. (2004). Crystal structure of the TAO2 kinase domain: activation and specificity of a Ste20p MAP3K. Structure (Camb) *12*, 1891-1900.

COPYRIGHT PERMISSION

Copyright permission was obtained for the following figures used in this dissertation.

No.	Title	Authors	Reference	Journal Figure
1	Kinomics: characterizing the therapeutically validated kinase space	Vieth et.al.	2005, Drug Disc. Today 10, (839-846)	1(B)
2	Regulation of protein kinases; controlling activity through activation segment conformation	Nolen et.al.	2004, Mol.Cell, 15 (661-675)	1(B), 2, 3
3	Targeting the checkpoint kinases: chemosensitization versus chemoprotection	Zhou and Bartek	2004, Nat.Rev.Cancer, 4 (216-225)	Box 1
4	Molecular mechanisms of mammalian DNA repair and the DNA damage checkpoints	Sancar et.al.	2004, Annu.Rev.Biochem, 73(39-85)	2
5	The protein kinase complement of the human genome	Manning et.al.	2002, Science, 298(1912-1934)	1
6	A Human Protein-Protein Interaction Network: A Resource for Annotating the Proteome	Stelzl et.al.	2005, Cell, 122(957-968)	5(A)
7	The Ste20 group kinases as regulators of MAP kinase cascades	Dan et.al.	2001, Trends in Cell Biology, 11(220-230)	2
8	Isolation of the protein kinase TAO2 and identification of its mitogen-activated protein kinase/extracellular signal-regulated kinase kinase binding domain	Chen et.al.	1999, J.Biol. Chem. 274(28803-28807)	2(A)
9	MARKK, a Ste20-like kinase, activates the polarity-inducing kinase MARK/PAR-1	Timm et.al.	2003, Embo J, 22(5090-5101)	7
10	kin-18, a C. elegans protein kinase involved in feeding	Berman et.al.	2001, Gene, 279 (137-147)	3,4
11	Sensitized RNAi screen of human kinases and phosphatases identifies new regulators of apoptosis and chemoresistance	MacKeigan et.al.	2005, Nat.Cell Biology, 7(591-600)	1(E)
12	Initiation of a G2/M checkpoint after ultraviolet radiation requires p38 kinase	Bulavin et.al.	2001, Nature, 411(102-107)	2(B)
13	MAPKAP kinase-2 is a cell cycle checkpoint kinase that regulates the G2/M transition and S phase progression in response to UV irradiation	Manke et.al.	2005, Mol.Cell, 17(37-48)	4(J,K)

VITAE

Malavika Raman was born in Madras, India, on November 16th 1976, the daughter of Saraswathi Raman and Parameshwariyer Yagna Raman. She attended school at South Island School (Hong Kong), Nower Hill High School (London, UK), the American Community School (Abu Dhabi), and Adarsh Vidyalaya Higher Secondary School (Madras, India). She received the degree of Bachelor of Pharmacy as well as a Masters in Biology from the Birla Institute of Technology and Science (Rajasthan, India) in May, 2000. In September, 2000 she entered the Graduate School of Biomedical Sciences at the University of Texas Southwestern Medical Center (Dallas, Texas). In 2001, she married Madhusudan Natarajan, Ph.D. Their dog, Puli, adopted them in October 2004.

Permanent Address: Old Number 63 (New Number 3), Luz Avenue
Mylapore, Chennai, Tamil Nadu 600004
India